69-13,914

HAVENS, Jerry Arnold, 1939-
THERMAL DECOMPOSITION OF WOOD.

The University of Oklahoma, Ph.D., 1969
Engineering, chemical

University Microfilms, A XEROX Company, Ann Arbor, Michigan

Downloaded from SHAREOK. Persistent Handle URL: https://hdl.handle.net/11244/2554

THE UNIVERSITY OF OKLAHOMA

GRADUATE COLLEGE

THERMAL DECOMPOSITION OF WOOD

A DISSERTATION

SUBMITTED TO THE GRADUATE FACULTY

in partial fulfillment of the requirements for the

degree of

DOCTOR OF PHILOSOPHY

by

JERRY ARNOLD HAVENS

Norman, Oklahoma

1969

THERMAL DECOMPOSITION OF WOOD

APPROVED BY

C. M. Sliepcevich

Harold V. Hunsaker

F. M. Townsend

J. Reed Welker

DISSERTATION COMMITTEE

ABSTRACT

A mathematical model developed for computer solution of heat transfer problems involving change of phase heat effects has been applied to the prediction of transient temperature distributions and volatile product evolution rates in decomposing wood specimens. For use in the model, the "energy capacity" of dry wood, which includes both sensible heat and decomposition heat effects, has been measured using a differential scanning calorimetric technique. The "energy capacity" data for thermal decomposition of dry pine and oak woods in nitrogen show that the net internal heat effect due to decomposition is endothermic.

The decomposition heat effect, as evidenced in the "energy capacity" curves, shows striking correlation with thermal gravimetric and differential thermal gravimetric data which were measured in this study. Thermal gravimetric analyses were made with heating rates varying from 20°C/min to 160°C/min and the results indicate that for such rates the application of a heat transfer-thermal decomposition model which neglects dependence on rate of heating is defensible.

The thermal conductivity was expressed as a function of local density, which in turn was specified as a function of temperature by using thermal gravimetric data and assuming constancy of the wood specimen's exterior dimensions during the heating-decomposition process.

A fast-response electrical heater was designed to allow accurate specification of a constant heat flux boundary condition at the surface of a wood test specimen. Using this heater, wood specimens were heated and partially decomposed while temperature profiles in the test specimen were measured with fine wire thermocouples. These temperature profiles, along with measurements of the weight loss of the heated specimen, were in satisfactory agreement with results predicted by the mathematical model.

ACKNOWLEDGEMENTS

Without the assistance of a number of people this research could not have been successfully completed. Among those who have contributed to this work I would like to express my sincere gratitude to the following persons:

Dr. C. M. Sliepcevich, George Lynn Cross Research Professor of Engineering, for his direction and support.

Dr. J. R. Welker, Associate Director of the Flame Dynamics Laboratory, for his assistance and constructive criticism in the overall program.

Dr. H. V. Huneke, Professor of Mathematics; Dr. F. M. Townsend, Associate Professor of Chemical Engineering; and Dr. J. E. Francis, Assistant Professor of Aerospace and Mechanical Engineering; for their service on my graduate committee.

Dr. H. T. Hashemi and Mr. Harold Bradbury for their invaluable advice and assistance in the formulation and solution of the mathematical model.

My fellow graduate students, Mr. Dwight Pfenning and Dr. Ameer Koohyar, for listening to my problems.

I am grateful to the Continental Oil Company, the Union Carbide Company, and the University of Oklahoma Research Institute for providing financial assistance.

I also appreciate the efforts of Mrs. Joyce Meyer, Mrs. Ruth Hogan, and Miss Connie Ellender in the preparation of the manuscript.

Finally, I wish to thank my parents, whose many sacrifices have been largely responsible for the opportunities I have had to continue my formal education, and my wife and son for waiting patiently for me to complete this study.

Jerry A. Havens

TABLE OF CONTENTS

	Page
LIST OF TABLES	ix
LIST OF ILLUSTRATIONS	x
Chapter	
I. INTRODUCTION	1
II. STATEMENT OF PROBLEM AND REVIEW OF PREVIOUS WORK	5
Internal Decomposition Heat Effects	8
Kinetics of Decomposition	18
Measurement of Weight Loss of a Specimen Heated in a Constant Temperature Environment	19
Measurement of Weight Loss of a Specimen Exposed to an Increasing Temperature Environment	27
Measurement of Pressure Changes in a Closed Chamber Due to Formation of Gaseous Decomposition Products	37
Measurement of Temperature in an Externally Heated Specimen	38
Measurement of Heat of Decomposition	43
Transient Heat Balance Methods	43
Differential Thermal Analysis Methods	50
Thermal and Physical Properties	69
Specific Heat	70
Density	72
Thermal Conductivity	74
Effect of Moisture Content	86
Effect of Diathermancy	87
Effect of Internal Convection and Secondary Pyrolysis	88

Page

III. EVALUATION OF AVAILABLE THERMAL ANALYSIS METHODS 94

Differential Thermal Analysis. 95
Thermal Gravimetric Analysis 131

IV. THE PROPOSED MATHEMATICAL MODEL 142

V. PROCEDURE AND RESULTS 154

Measurement of "Energy Capacity" vs Temperature Relationship of Wood Using Differential Scanning Calorimetry 154
Measurement of Weight Loss and Rate of Weight Loss of Wood as a Function of Temperature Using Thermal Gravimetric Analysis 180
Specification of Thermal Conductivity as a Function of Temperature and Decomposition History. 191
Experimental Test for Model Validation . . 214

VI. DISCUSSION OF RESULTS 246

VII. SUMMARY AND CONCLUSIONS 262

LITERATURE CITED 265

LIST OF TABLES

Table		Page
II-1.	Activation Energies for Weight Loss of Wood Samples by Thermal Degradation . . .	21
II-2.	Activation Energy of Decomposition of Wood and its Major Components	25
II-3.	Activation Energies for Untreated Ponderosa Pine Samples	26
II-4.	Summary of Robert's and Clough's Data on Thermal Decomposition of Wood	27
II-5.	Kinetic Parameters of Pyrolysis From Dynamic Thermogravimetry	33
II-6.	Activation Energies and Rates of Heat Evolution	42
II-7.	Results of Carbonization of Wood at 275°C According to Klason	46
II-8.	Carbonization Tests on 45 mm ID Wood Rods .	57
II-9.	Carbonization Tests on 20 mm ID Wood Rods .	58
II-10.	Thermal Conductivity Values for Wood Reported by Griffiths and Kaye	82
II-11.	Estimates of Magnitude of Internal Convection Heat Effect in Decomposing Cellulosic Material by Blackshear and Murty	92
V-1.	Ferromagnetic Calibration Standards	182
V-2.	Thermal Diffusivity of Pine Samples-Oil Bath Temperature = 197°C	210
V-3.	Thermal Diffusivity of Pine Samples-Oil Bath Temperature = 97°C	210

LIST OF ILLUSTRATIONS

Figure		Page
II-1.	Computed and Measured Central Temperature-Time Curves	11
II-2.	Kinetics of Weight Loss Plots for Wood, α-Cellulose, and Lignin	32
II-3.	Weight Loss vs Temperature of Beech Sawdust in Vacuum at Different Heating Rates	35
II-4.	Rate of Heat Evolution for Oak Wood . . .	41
II-5.	Heat Generation Rate and Temperature vs Time in Pine Cylinder (r = 11.2 mm) with Surrounding Temperature = 80°C . .	51
II-6.	Heat Generation Rate and Temperature vs Time in Pine Cylinder (r = 11.2 mm) with Surrounding Temperature = 300°C . .	51
II-7.	Measured Temperature in 45 mm ID Pine Sample and Compensation Cylinder at Different Radii	54
II-8.	Net Energy Delivered to Carbonization Cylinder and Mean Temperature for 45 mm ID Pine Sample	54
II-9.	Differential Thermal Analysis of α-Cellulose	60
II-10.	DTA and TGA Results for (A) "Ash-Free" and (B) "Pure" Cellulose in Air	64
II-11.	DTA and TGA Results for (A) "Ash-Free" and (B) "Pure" Cellulose in Nitrogen . .	65
II-12.	Photograph of Wood Showing Non-Isotropicity and Non-Homogeneity	71

Figure		Page
II-13.	Specific Heat C and Mean Specific Heat C_M for Charcoal as a Function of Temperature	73
II-14.	Experimental Apparatus Used by Blackshear and Murty	75
II-15.	Density Distribution as a Function of Time and Radius of Cellulose Cylinder . .	76
II-16.	Density vs Temperature Plots for Decomposing α-Cellulose Cylinder with Radial Position as Parameter	77
II-17.	Schematic of End-Grain Pattern of Ash Board Showing Location of Test Specimens	80
III-1.	Comparison of Sample Temperature, Reference Temperature, and Differential Temperature Curves in Differential Thermal Analysis	97
III-2a.	Typical DTA Configuration	101
III-2b.	Idealized DTA Recording of an Endothermic Transition	101
III-3.	Schematic Diagrams of "Dynamic Difference Calorimetry" Type Cells Manufactured by Du Pont	111
III-4.	Typical Calibration Curve of Du Pont Differential Scanning Calorimeter	113
III-5.	Block Diagram of Perkin-Elmer Differential Scanning Calorimeter	115
III-6.	Analog Representation of Adiabatic and Isothermal Calorimeters	119
III-7.	Schematic Diagram of Differential Isothermal Calorimetry Setup	121
III-8.	Typical Temperature-Heat Flow Relationship	126
III-9.	Block Diagram of Sample Holder with Temperature Feedback	129

Figure		Page
III-10.	Schematic of Perkin Elmer TGS-1 Thermobalance	136
III-11.	Schematic of TGS-1 Temperature Calibration System	140
III-12.	Typical TGS-1 Temperature Calibration Run	140
IV-1.	A Mesh Region (i,j) and Its Adjacent Mesh Points	146
V-1.	Photograph of Differential Scanning Calorimeter	156
V-2.	Typical Specific Heat Determination, Molten Linear Polyethylene, 405-485°K, Scanning Rate = 20°C/min	164
V-3.	Relation Between Programmed and Actual Temperatures in Perkin-Elmer DSC-1B Instrument	164
V-4.	Temperature Calibration of DSC-1B Differential Scanning Calorimeter . . .	166
V-5.	Purge Gas Flow Pattern in Differential Scanning Calorimeter Sample Head	171
V-6.	Specific Heat Calibration of DSC-1B . . .	175
V-7.	"Energy Capacity" of Pine Wood as a Function of Temperature in Nitrogen Atmosphere	176
V-8.	"Energy Capacity" of Oak Wood as a Function of Temperature in Nitrogen Atmosphere	179
V-9.	Photograph of Thermobalance	181
V-10.	Per Cent of Original Dry Weight Remaining as Solid Material vs Temperature for Pine in Nitrogen Atmosphere	186
V-11.	Per Cent of Original Dry Weight Remaining as Solid Material vs Temperature for Oak in Nitrogen Atmosphere	187

Figure Page

V-12. Temperature Calibration of TGS-1 Thermobalance at Different Heating Rates 188

V-13. Effect of Rate of Heating on Kinetics of Weight Loss of Dry Pine Wood in Nitrogen Atmosphere 189

V-14. Effect of Rate of Heating on Kinetics of Weight Loss of Dry Oak Wood in Nitrogen Atmosphere 190

V-15. Rate of Weight Loss of Dry Pine Wood in Nitrogen as a Function of Temperature 192

V-16. Rate of Weight Loss of Dry Oak Wood in Nitrogen as a Function of Temperature 193

V-17. Quotient of Thermal Conductivity and Density for Wood and Charcoal 197

V-18. Estimated Thermal Conductivity of Wood as a Function of Temperature and Decomposition History 199

V-19. Thermal Conductivity vs Density for Charcoal 201

V-20. Schematic Diagram of Thermal Diffusivity Apparatus 206

V-21. Example Plot of Y vs t From Thermal Diffusivity Data 209

V-22. Schematic of Resistance Wire Heater and Wood Cylinder 217

V-23. Photograph of Resistance Wire Heater With and Without Wood Sample in Place. . 218

V-24. Temperature Dependence of Electrical Resistance of Tophet A 80-20 Nickel-Chromium Wire 219

V-25. Schematic of Section of Cylindrical Symmetry of Center Test Specimen 225

Figure		Page
V-26.	Photograph of Cross Section of Pine Test Cylinder After Completion of Run. .	236
V-27.	Effective Thermal Conductivity vs Temperature Relationship Giving Satisfactory Agreement Between Predicted and Measured Temperatures . .	238
V-28.	Comparison of Predicted and Measured Temperature Profiles	239
V-29.	Comparison of Measured and Predicted Temperature vs Time at Two Radial Positions for Eight Minute Run	241
V-30.	Comparison of Measured and Predicted Temperature vs Time at Two Radial Positions for Six Minute Run	242
V-31.	Comparison of Measured and Predicted Temperature vs Time at Two Radial Positions for Four Minute Run	243
V-32.	Measured vs Predicted Weight Loss of Pine Test Section	244
VI-1.	"Energy Capacity" of Pine Wood as a Function of Temperature in Nitrogen Atmosphere Showing Sensible Heat and Decomposition Heat Effect Regions . . .	247
VI-2.	Comparison of Decomposition Heat Effect With Rate of Weight Loss of Pine Wood as a Function of Temperature	250
VI-3.	"Energy Capacity" of Oak Wood as a Function of Temperature in Nitrogen Atmosphere Showing Estimated Sensible Heat and Decomposition Heat Effect Regions	253
VI-4.	Comparison of Decomposition Heat Effect With Rate of Weight Loss of Oak Wood as a Function of Temperature	254

THERMAL DECOMPOSITION OF WOOD

CHAPTER I

INTRODUCTION

There is a general class of transient, multidimensional heat transfer problems, involving heterogeneous, non-isotropic media with strongly temperature dependent thermal properties and simultaneous phase change and/or chemical reaction, which is of great practical importance. Examples of current interest include ablative cooling systems (as in rocket re-entry nose cones), seasonal or artificial freezing and thawing of soils, cooling of large castings or forgings during which crystalline transformations occur, and thermal decomposition of solids during the process of ignition and combustion. The mathematical modeling of such problems is difficult. There is very little information in most cases about the heat effects resulting from the phase change or chemical reaction processes and the dependence of thermal properties on temperature. Even when this information is available, there remains the considerable problem of inclusion of this information in a mathematical form which allows solution.

The thermal decomposition and ensuing ignition and combustion of solid materials has been the subject of intense study at the Flame Dynamics Laboratory of the University of Oklahoma during the past five years. A variety of materials has been studied, including wood, cloth, and plastics. The present work was undertaken to provide badly needed information about the heat transfer behavior of such materials. The mathematical modeling of heat conduction in wood is a problem which falls into the general class described above. Wood was chosen for these initial studies for several reasons. It is readily available, cheap, and has a wide range of thermal and physical properties. Of particular interest is the wide variation in density, upon which thermal properties are strongly dependent. Wood is also non-homogeneous and non-isotropic, and it undergoes a rather complicated decomposition process upon reaching sufficiently high temperature[1].

Despite these complexities, significant progress can be made toward understanding heat transfer and thermal decomposition in wood by investigation of individual areas about which very little is known. One such area is that of heat and weight loss effects which occur as a result of thermal decomposition of the solid. These

[1]Goos (24) has listed 213 compounds which have been identified as molecular "debris" resulting from the thermal decomposition of wood.

effects are important for two reasons. First, the decomposition heat effects must be known if the temperature history of the solid is to be obtained. Secondly, it is the decomposition products which actually ignite when the necessary conditions are met; therefore, knowledge of their rate of formation and resulting concentrations in the region adjacent to the solid specimen may be important in predicting ignition.

A survey of the literature revealed that relatively few studies have been made concerning the internal thermal decomposition heat effects in wood. In general, the results of such studies have shown considerable variation and disagreement. The survey indicated that presently available differential thermal analysis and thermal gravimetric analysis techniques could provide some of this information. Therefore, a thorough evaluation of thermal analysis instrumentation was carried out. This evaluation resulted in the acquisition of a complete thermal analysis system manufactured by the Perkin-Elmer Company, U.S.A., including both differential scanning calorimetry and thermal gravimetric analysis equipment.

In order to attack the overall heat transfer problem successfully, data from thermal analysis studies must be obtained in a form which can be used in a mathematical model which can be solved. A numerical technique has been previously developed at the University of Oklahoma (26)

which can predict the temperature-time relationship in a two dimensional media undergoing phase change if the thermal and physical properties are known. Thus, a major objective of this work was to obtain information about thermal properties and decomposition heat effects in wood, using thermal analysis equipment, in a form which could be used in the previously developed numerical technique.

A further objective was to define and carry out an experiment in which a wood specimen could be heated and partially decomposed in such a way that boundary conditions could be specified with sufficient confidence to allow meaningful comparison between measured and theoretically predicted results.

CHAPTER II

STATEMENT OF PROBLEM AND REVIEW OF PREVIOUS WORK

When a wood specimen is subjected to heat from any source under conditions which result in the internal energy of any portion of the specimen rising above some minimum level, the wood begins to undergo a decomposition process. This decomposition process results in the production of volatile materials which are capable of supporting combustion. If certain necessary conditions are satisfied, these decomposition products can be ignited, either by an independent source of energy or simply by reaching a state of auto-excitation that results in spontaneous ignition.

Several conditions have to be satisfied before an ignition process will take place. There must be a sufficient heat absorption by the wood specimen to cause it to undergo thermal decomposition, which produces the necessary "fuel". There must be sufficient oxygen present and means by which the "fuel" can mix with that oxygen. The concentration of this fuel-oxygen mixture must be within the flammable limits, and the fuel-oxygen mixture must be in a sufficiently "energized" state.

A complete understanding of the phenomenon of wood-ignition depends not only on the properties of the specimen but also on the conditions affecting the behavior of the volatile decomposition products after they have left the immediate vicinity of the specimen. Simultaneous consideration of all of these factors results in an extremely complex problem. However, the problem can be divided into smaller parts which can be studied individually, and the results of these studies will then hopefully lend a better understanding to the overall problem.

Thus the problem to be considered herein is the characterization of the heat transfer and thermal decomposition behavior of the solid source of decomposition products. The behavior of the gaseous decomposition products which are produced will not be considered directly. A model of the thermal decomposition behavior of the solid source is needed to predict when and how the volatile decomposition products (the "fuel") are produced.

However, a description of the heat transfer and thermal decomposition behavior of the solid is still a very complex problem. The problem of predicting heat transfer behavior in any solid which simultaneously undergoes thermal degradation or decomposition, although occuring quite frequently (for examples other than that considered in this work, witness the widespread interest in solid

propellant rocket motors and ablation-controlled heat removal systems), is not completely understood.

Consider a wood specimen which is exposed to heat from an external source. The heat which is transferred to the specimen may be by a combined radiative-convective-conductive mechanism. In order to encompass all of the known effects which may have a direct bearing on the decomposition behavior of the specimen it is necessary to have information concerning the importance and effect of the following factors:

1. The heat and mass transfer boundary conditions at the surface of the specimen must be known.

2. The thermal and physical properties such as thermal conductivity, density, and heat capacity of the material must be known as a function of temperature and decomposition history.

3. The effect of internal heat generation or absorption resulting from the decomposition process must be known as a function of temperature and decomposition history.

4. If the heat transfer to the specimen has an appreciable radiative component, the degree of diathermancy (free passage) of the specimen to radiation of that spectral distribution must be known.

5. The effect of moisture.

6. The effect of the non-homogeneity and non-isotropicity of the wood specimen.

7. The effect of heat transfer by internal convection due to the flow of decomposition products from their location of formation to the specimen surface must be known, as well as the effect of any additional, or secondary, chemical transformations which may occur in the interstices of the specimen during this flow process.

The primary objective of this work was a study of the internal thermal decomposition heat effects in wood and the formulation of a mathematical model which includes such heat effects. However, any attempt to test the validity of such a model experimentally requires consideration of all of the factors listed above. Therefore, the review of previous work included any additional information which would be helpful in the design of a model validation experiment.

Internal Decomposition Heat Effects

Mathematical modeling of the temperature history in wood subjected to heating by an external source has most often been based on treatment of the wood as an inert, homogeneous, isotropic heat transfer medium with constant and uniform thermal properties. However, a few investigators have attempted inclusion of internal decomposition heat effects in their mathematical model. Bamford, Crank, and

Malan (3), in their classical study of the ignition of wood slabs contacted on both faces by flame, were probably the first to do so. Assuming one dimensional heat flow, isotropicity and homogeneity of the wood, and constant and uniform thermal and physical properties, they employed the one-dimensional heat conduction equation with a heat source term included:

$$K \frac{\partial^2 T}{\partial x^2} = \rho C \frac{\partial T}{\partial t} + Q \frac{\partial w}{\partial t} \qquad \text{(II-1)}$$

where K = thermal conductivity ($cal/cm^2 sec\,^\circ C/cm$)

ρ = density (gm/cm^3)

C = heat capacity ($cal/gm\,^\circ C$)

Q = heat of decomposition (cal/gm)

w = weight of volatile or reactable constituents in the wood (gm/cm^3)

They then formulated boundary conditions representing combined convective and radiative heating of the solid surface and solved the resulting initial value problem with an electrical analog technique.

The heat source term $Q\,\partial w/\partial t$, as used by Bamford, et al., assumes the applicability of a constant heat of reaction; that is, a heat evolution per unit volume or weight of "decomposable" material, which is independent of temperature (and time) during the course of the heating

process. The value of Q used by Bamford, Crank and Malan was obtained as follows. They placed a thermocouple in the center of a wood slab which was positioned in contact with a flame, and they measured the magnitude of the comparatively sudden rise in temperature at the center of the specimen which, as shown in Figure II-1, began at about 600°K. Then, assuming that this sudden rise of temperature ΔT is due solely to the total available heat of decomposition, and that no heat is conducted away, a heat balance based on a unit volume gives

$$C\rho\ \Delta T = Q\ W_o \qquad \text{(II-2)}$$

where C = heat capacity (cal/gm °C)

ρ = density (gm/cm^3)

ΔT = the magnitude of the sudden temperature rise (°C)

W_o = initial weight of volatile products (gm/cm^3)

Q = heat of decomposition (cal/gm)

Equation (II-2) was used to solve for Q, utilizing literature reported values of the heat capacity C and density ρ, and a value for W_o obtained by weighing the charcoal produced when a known weight of wood was decomposed completely in the absence of air. They reported a value of Q, thus determined, of 86 cal/gm (exothermic) which was

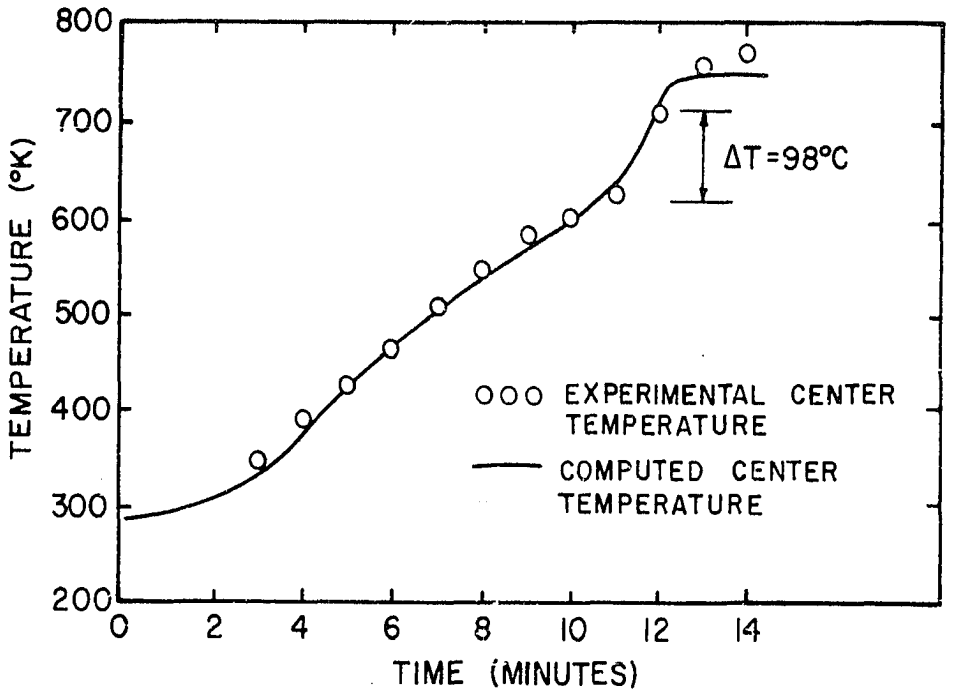


Figure II-1. Computed and Measured Central Temperature-Time Curves (3).

claimed to agree satisfactorily with a value (not given) computed by taking the difference between heats of combustion of the wood and its decomposition products.

The quantity $\partial w/\partial t$, which represents the rate of weight change of the "decomposable" components per unit volume was assumed to be describable by a first-order kinetic expression,

$$\frac{\partial w}{\partial t} = kw \qquad \text{(II-3)}$$

where w is the weight of the "decomposable" components per unit volume at time t. The rate constant k was assumed to be temperature dependent in the Arrhenius sense;

$$k = k_o e^{-E/RT} \qquad \text{(II-4)}$$

where k = specific rate constant (sec^{-1})

k_o = frequency factor (sec^{-1})

E = "pseudo" activation energy (cal/gm mole)

T = absolute temperature ($^\circ K$)

A single "equivalent" reaction was assumed so that mean values of E and k_o could be used. The values of E and k_o were obtained by a trial and error process. Values for E and k_o were assumed (according to Bamford, et al., approximate values were obtained by rough measurement of the

rate of decomposition of wood at various temperatures, but no details were given) and were corrected until a temperature vs time curve for the center of the slab, obtained by numerical solution of Equation (II-1), agreed satisfactorily with the experimentally determined curve shown in Figure II-1.

The final values used by Bamford, Crank, and Malan for parameters in Equation (II-1) were:

$$\rho = 0.60 \text{ gm/cm}^3$$

$$C = 0.55 \text{ cal/gm } ^\circ\text{C}$$

$$Q = 86 \text{ cal/gm}$$

$$W_o = 0.375 \text{ gm/cm}^3$$

$$k_o = 5.3 \times 10^8 \text{ sec}^{-1}$$

$$E = 33{,}160 \text{ cal/gm mole}$$

The accuracy and applicability of these values for the activation energy and frequency factors are open to considerable question on several accounts.

1. Their determination depends directly on having accurate values of density and heat capacity and assumes that these values remain constant.

2. In the determination of Q, temperature gradients in the sample are neglected, or in other words, no conduction effects were considered in determining the magnitude of the temperature effect due to decomposition.

3. The measurement of Q assumes the decomposition and the resulting heat effect to occur over a very narrow temperature range (occuring around 430°C), and that no appreciable heat effects are present at other temperatures.

4. The values of E and k_o may be questioned on the basis of the accuracy of the numerical technique used to solve the equation as well as on the applicability of the mathematical model. If one studies the technique used (which was a rather imaginative and sophisticated technique in 1940) one sees that there are good reasons to doubt the accuracy of the solution[1].

5. The value of W_o, which is determined by weighing of the residue, is reported by other investigators to be dependent on the conditions of heating (14), and to some extent, on the rate of heating.

Nevertheless, the values reported for Q, k_o, E, and W_o by Bamford, et al., have been used by several authors as the basis for further study. Weatherford, et al., (77) have presented results of a long term study of wood ignition based largely on numerically calculated solutions to Equation (II-1). They used Bamford, Crank, and Malan's reported values of Q, W_o, E, and k_o. They stated that only a slight difference (less than 10%) was found between numerical

[1] Weatherford, et al., (77) have presented numerical solutions of Bamford, Crank, and Malan's model using the same values for the parameters involved. They question the formers' numerical results.

solutions of the model when the heat generation term was included or deleted.

Concerning Weatherford's results, a brief look at the heat source term proposed by Bamford, et al., is informative. It has been stated that the heat of reaction term Q was measured by determining the magnitude of the temperature increase at the center of the sample when the center temperature was approximately 600°K. The sudden rise in temperature around 600°K indicated that the maximum heat effect occurred when the wood reached that temperature. Thus, in order for the proposed model to be applicable, the maximum value of the heat generation term should occur at or around a temperature of 600°K. Using Bamford, et al.'s reported values of Q, k_o, and E, and letting $w = W_o$ (corresponding to its maximum), one calculates:

$$\begin{aligned} & Q\, k_o \exp(-E/RT)\, W_o \\ &= (86)\ (5.3 \times 10^8) \exp[(-33{,}160)/ \\ &\quad (1.97)\ (600)]\ (0.375) \\ &= 0.012 \text{ cal/cm}^3\text{sec} \end{aligned}$$

By considering a heat balance on a unit volume of wood with a uniform heat source of 0.012 cal/cm^3sec, and assuming no heat conducted in or out:

$$\text{Heat generated (per cm}^3) = \text{accumulation of heat (per cm}^3)$$

$$= \rho C \frac{dT}{dt}$$

Thus: $0.012 \text{ cal/cm}^3\text{sec} = (0.60 \text{ gm/cm}^3)(0.55 \text{ cal/gm °C}) \cdot \frac{dT}{dt}$

and $\frac{dT}{dt} = (0.012)/(0.60)(0.55) = 0.037°\text{C/sec}$

or $\simeq 2°\text{C/min}$

Since the rate of increase of temperature at a given position in a solid due to heat being transferred by conduction alone is proportional to the temperature gradient at the given position, $\partial T/\partial x$, the contribution of the heat source term will be of more or less importance in determining the actual temperature history of the material as the magnitude of the purely conductive effects is varied. Thus in the case of the heating of materials by exposure to high incident radiant energies, such as those resulting from thermal radiation from nuclear explosions, the purely conductive effects may be sufficiently large to negate the effect of internal heat generation rates on the heat transfer characteristics. Obviously then, for some rates of external heat application, the temperature history of the material calculated from Equation (II-1) will not be significantly different from that calculated from an otherwise similar equation which does not include internal heat generation effects. It is suggested that for this reason Weatherford's results did not show the internal heat generation effects to be very important, when calculated using the model of Equation (II-1).

With reference to the model proposed by Bamford, et al., it is also informative to look at the effect of slight changes in the values of the parameter E, the "pseudo-activation energy." For example, a change in the value of E from 33,160 cal/gm mole to 30,000 cal/gm mole (roughly 10%) results in a predicted heat release of 0.171 $cal/cm^3 sec$ at 600°K, or an increase by a factor of more than 14. Thus the accuracy of the predicted values (assuming the applicability of the model) is strongly dependent on the value of the activation energy used.

This strong effect of the value of pseudo-activation energy on the result of the solution of a similar model, which also includes the effect of diathermancy, has been shown by Lawrence (41). He solved the equation

$$K \frac{\partial^2 T}{\partial x^2} + \gamma H e^{-\gamma x} = \rho C \frac{\partial T}{\partial t} + Q \frac{\partial w}{\partial t} \qquad \text{(II-5)}$$

where γ = Lambert's law attenuation constant (cm^{-1})

H = absorbed and transmitted flux at surface ($cal/cm^2 sec$)

and the other terms are as defined in Equation (II-1). He stated that for the assumed values (from Bamford, Crank, and Malan) of the other parameters, the effect of the term $Q\ \partial w/dt$ was negligible for activation energies greater than 35,000 cal/gm mole but that it became important when the activation energy was decreased to 25,000 cal/gm mole.

A large number of other experimental studies have been carried out in attempts to characterize accurately cellulose and wood internal decomposition kinetics and heat effects and these will be discussed in the following sections.

Kinetics of Decomposition

A major portion of the work done to date has been based on the assumption of validity of a first-order kinetic model described by Equations (II-3) and (II-4). Several methods have been used to determine the values of the heat of reaction Q, pseudo-activation energy E, and frequency factor k_o for use in Equation (II-1) to describe the pyrolytic-decomposition of wood. Bamford, Crank, and Malan's work has been described. The determination of the activation energy and frequency factor necessary to characterize the rate of decomposition, or kinetics of weight loss, has received the most attention. The methods used for this determination fall into the following broad classes:

1. The measurement of weight loss of a specimen heated in a constant temperature environment

2. The measurement of weight loss of a specimen exposed to an increasing temperature environment

3. The measurement of pressure changes in a closed chamber due to formation of gaseous products

4. The measurement of temperatures in a specimen exposed to external heating under controlled conditions, using said temperature to solve the heat conduction equation

with a source term of the form of Equation (II-1) for values of the activation energy and "pre-exponential factor" (the product of the heat of reaction and frequency factor, $Q\ k_o$).

Measurement of Weight Loss of a Specimen Heated in a Constant Temperature Environment: If the kinetics of the thermal decomposition of wood are assumed to be describable as a first order reaction, then the rate of change of weight of "decomposable" material can be represented by the relations:

$$\partial w/\partial t = kw \qquad \text{(II-3)}$$

and

$$k = k_o e^{-E/RT} \qquad \text{(II-4)}$$

where w = weight of "decomposable" material (gm/cm^3)

t = time (sec)

T = absolute temperature ($^\circ K$)

k = decomposition rate constant (sec^{-1})

k_o = frequency factor (sec^{-1})

E = activation energy (cal/gm mole)

R = ideal gas law constant (cal/gm mole$^\circ$K)

Rearrangement and integration of Equation (II-3) with respect to t, assuming constancy of K, gives

$$\ln w = kt + \ln w_o$$

where w_o = initial weight of "decomposable" material (gm/cm^3)

Thus if the logarithm of the weight of remaining "decomposable" material is plotted versus time, a straight line should result whose slope is equal to the specific rate constant k. If Equation (II-4) is rearranged by taking the logarithm of both sides of the equation, the result is

$$\ln k = -E/RT + \ln k_o$$

so that if values of ln k determined for different temperatures are plotted vs 1/T, the value of the activation energy can be determined from the slope, -E/R, of the resultant straight line, and the value of the frequency factor can be obtained from the intercept.

Stamm (65) used this method to correlate data on the weight loss of wood measured by himself and by McClean (45) and Mitchell, et al. (48). He calculated the activation energy and frequency factor for the weight loss of pine, fir, and spruce samples of sizes ranging from 1 x 1 x 6 inches to 1/16 x 1 x 5 7/8 inches, and of Douglas fir sawdust and its components. Samples were heated in an oven or under the surface of a molten metal, at constant temperatures ranging from 93.5°C to 300°C. Heating times ranged from 1 minute to 2.4 years!

Stamm also determined activation energies for the rate of decomposition of the major wood components, α cellulose, lignin, and hemi-cellulose. A summary of his data is shown in Table II-1. In these studies some of the samples

TABLE II-1

ACTIVATION ENERGIES FOR WEIGHT LOSS OF WOOD SAMPLES BY THERMAL DEGRADATION (Stamm (65))

Material	Heating Condition	Time Range	Temperature Range (°C)	Frequency Factor (sec^{-1})	Activation Energy (kcal/gm mole)
Southern and white pine, Sitka spruce, Douglas fir sticks, and Sitka spruce veneer*	Oven	1 hr-2.4 yr.	94-250	5.1×10^{11}	29.5
	Under molten metal	1 min-6 days	167-300	2.3×10^{11}	29.8
Douglas fir sawdust	Oven	16 hr-64 days	110-220	1.9×10^{9}	25.0
α-cellulose from Douglas fir	Oven	16 hr-64 days	110-220	4.8×10^{9}	26.0
Hemicellulose from Douglas fir	Oven	2 hr-64 days	110-220	3.6×10^{10}	26.7
Lignin from Douglas Fir	Oven	16 hr-64 days	110-220	1.4×10^{10}	23.0

*The values for these different types of samples were said to be approximately the same; the value reported is an average.

were heated in an oven so that the surfaces of the specimen were subjected to oxidation while for others oxidation was not present. The weights were determined by intermittant removal of the samples from the heater and weighing; thus for heating times short enough that uniform temperature was not established early in the process, the results would be dependent on the sizes and geometry of the specimens. "Residual weight" as used by Stamm refers to weight of sample remaining, not "decomposables."

McNaughton (46), in a similar study, reported weight loss data for kiln-dried hard maple motor wedges, 1/8 by 1/4 by 3 inches, heated for periods ranging from 16 days to 1,050 days at the temperatures of 107 to 150°C. His measurements result in predicted values of the frequency factor and activation energy of 1.2×10^{10} sec^{-1} and 33.1 kcal/gm mole°C respectively.

Akita (1) also investigated the isothermal decomposition of wood at temperatures ranging from 150°C to 400°C. He stated that the rate of decomposition was slow below 200°C but became rapid at temperatures above 270°C. At the higher temperatures, the decomposition rate in the presence of air was measured by continuous weighing with a spring balance. Measurements were made at pressures from atmospheric down to 2 mm Hg. absolute. The samples were contained in a pyrex tube immersed in a constant temperature, molten metal bath. The change in

length of the spring due to change in weight was recorded photographically or measured with the aid of a microscope.

Since wood is composed of a variety of constituents, Akita postulated that the rate of isothermal decomposition should follow an equation of the type

$$\frac{dN}{dt} = \sum_i k_i (N_{\infty i} - N_i) \qquad \text{(II-6)}$$

where N = total number of moles of gas evolved at time t

N_i = number of moles of gas evolved at time t, by i^{th} constituent

$N_{\infty i}$ = number of moles of gas evolved at time ∞, by i^{th} constituent

k_i = specific rate constant for i^{th} constituent (sec^{-1})

He further postulated that since wood is essentially composed of cellulose, lignin, and hemicellulose, the results for wood should be adequately described by three such terms. He found that hemicellulose decomposed fastest and cellulose slowest. Data for cellulose and lignin were said to fit a first order kinetic model with the rate computed on the basis of <u>decomposable</u> material. However, he reported that an apparent change of mechanism of cellulose decomposition occurred at a temperature of approximately 340°C, resulting in two different activation energies above and below this

temperature. Arrhenius activation energies were reported as in Table II-2.

This apparent alteration in kinetic behavior of cellulose at some "threshold temperature" led Martin (47) to suggest that the specific rate constant k could be represented by a combination of the rates of two "elementary" reactions as

$$-\frac{dw}{dt} = (k_1 + k_2)w = (k_{o1}e^{-E_1/RT} + k_{o2}e^{-E_2/RT})w \qquad \text{(II-7)}$$

He assumed that at low temperatures (below the "threshold temperature") k_1 would predominate, while at temperatures above the "threshold temperature," k_2 would predominate.

Tang (67), using a constant temperature thermogravimetric technique, found similar kinetic behavior for pine samples with a reported threshold temperature of 330°C for some specimen shapes, while for other specimen shapes a single activation energy was found to characterize the decomposition over the entire temperature range studied (300°C-385°C). Tang used an American Instrument Company "Thermograv" balance in this work. The activation energies computed from these measurements are shown in Table II-3.[2] In later papers (68,69) Tang stated that these results were questionable, due to excessive weight loss (as much as 35%) during

[2]Tang stated that the dual activation energy for the larger specimens was due to excessive temperature gradients and the effects of thickness on the diffusion of the products from the center of the specimen.

TABLE II-2

ACTIVATION ENERGY OF DECOMPOSITION OF WOOD AND ITS MAJOR COMPONENTS (AKITA (1))

Material	Temperature Range (°C)	Activation Energy (kcal/gm mole)
Lignin	270-400	26.0
Hemicellulose	270-400	17.0
Cellulose	270-340	36.0
Cellulose	340-370	24.0
Wood (Japanese Cypress)*	270-340	26.0 (average)
	340-370	23.0 (average)

*Wood specimens were 25 x 15 x 1.2 mm.

TABLE II-3

ACTIVATION ENERGIES FOR UNTREATED
PONDEROSA PINE SAMPLES (TANG (67))

Geometry of Specimen	Thickness of Specimen (cm)	Activation Energy (kcal/gm mole) Below 330°C	Above 330°C
veneers	0.013	45.6	45.6
	0.028	44.9	44.9
	0.318	37.8	37.8
dowels	0.635	44.1	44.1
	0.952	41.1	28.5
	1.270	40.7	28.7

the preheating period, in which the sample was approaching the specified constant temperature.

Measurement of Weight Loss of a Specimen Exposed to an Increasing Temperature Environment: Roberts and Clough (53) made continuous weight measurements of oven-dried beech cylinders (2 cm x 15 cm, weighing approximately 25 grams) exposed to increasing heating rates in a cylindrical muffle furnace. The temperature of the furnace increased at approximately 10°C/min to a preset control temperature maintained to within 5°C. The measurements were made in a flowing nitrogen atmosphere. Five thermocouples were also inserted along small holes drilled parallel to the axes of the cylinders. The weight of the specimen was recorded at 30 second intervals until five minutes after the decomposed specimen had reached constant weight. The data from 5 runs are summarized in Table II-4.

TABLE II-4

SUMMARY OF ROBERT'S AND CLOUGH'S DATA ON THERMAL DECOMPOSITION OF WOOD (53)

	Experiment Number				
	1	2	3	4	5
Maximum temperature achieved by specimen (°C)	445	353	505	394	282
$\frac{\text{Final Weight}}{\text{Initial Weight}} \times 100$ (%)	30.9	52.5	28.0	39.9	78.6
Maximum rate of weight loss (mg/sec)	92	26	193	40	8
Surface area of specimen (cm^2)	97	88	88	88	85

The data were used to determine the frequency factor k_o and the activation energy E in the following expression:

$$\frac{-dw}{dt} = k_o\ (w-w')\ \exp\ (-E/RT)$$

where w = weight of specimen at time t (gm)

w' = final weight of specimen (gm)

For the first four experiments, good agreement between experimental and calculated weight vs time curves was obtained with values of E = 15 kcal/gm mole and k_o = 9.1 x 10^4 min^{-1}, while for experiment No. 5 better agreement was obtained with k_o = 2.6 x 10^9 min^{-1} and E = 25 kcal/gm-mole. They suggested that this difference was due to different decomposition mechanisms above and below 300°C.

Several workers have studied the kinetics of wood decomposition, or pyrolysis, by a technique known as dynamic thermogravimetry. In this method a continuous measurement of the sample weight (usually a very small sample, 10-100 mg, is used) is made while the sample is being heated at a linear rate. The method has several advantages over the static gravimetric technique (where the sample is maintained at a constant temperature). Considerably less data are required than in the static method. Furthermore, if the sample undergoes any appreciable reaction (or weight loss) during the period required to bring the temperature to the desired level in the static

method, the results are often questionable (See preceding discussion of Tang's work).

Several methods have been used for the determination of the kinetics of a thermal decomposition process from dynamic thermogravimetric data. The most widely used is probably that of Freeman and Carroll (68). For a development of this method the kinetic model of wood pyrolysis is postulated as:

$$\frac{-dw}{dt} = kw^n \qquad \text{(II-8)}$$

where w = amount of decomposable material at time t (gm/cm^3)

k = specific rate constant (sec^{-1})

n = order of reaction

Assuming Arrhenius temperature dependence of the rate constant,

$$k = k_o e^{-E/RT} \qquad \text{(II-9)}$$

where the terms are as defined earlier.

Solving for k in Equation (II-8) and substituting from Equation (II-9) gives

$$k_o e^{-E/RT} = -\frac{dw/dt}{w^n} \qquad \text{(II-10)}$$

Taking the logarithm of both sides of Equation (II-10),

$$\ln k_o - E/RT = \ln (-dw/dt) - n \ln w \qquad \text{(II-11)}$$

Differentiating with respect to T and rearranging then gives

$$\frac{E dT}{RT^2} = \frac{d \ln (-dw/dt)}{dT} - n \frac{d \ln w}{dT} \qquad \text{(II-12)}$$

Integrating over a finite temperature range ΔT, we have

$$-\frac{E}{R} \Delta(T^{-1}) = \Delta \ln \left(-\frac{dw}{dt}\right) - n \Delta(\ln w) \qquad \text{(II-13)}$$

Dividing through by $\Delta(\ln w)$ gives

$$-\frac{\frac{E}{R} \Delta(T^{-1})}{\Delta(\ln w)} = \frac{\Delta \ln (-dw/dt)}{\Delta(\ln w)} - n \qquad \text{(II-14)}$$

Thus if $\frac{\Delta(T^{-1})}{\Delta(\log w)}$ is plotted vs $\frac{\Delta[\log (-dw/dt)]}{\Delta(\log w)}$

a straight line of slope - E/2.303 (R) and intercept n should be obtained.

Tang (66) investigated the use of this difference method for determining the kinetic parameters of weight loss of ponderosa pine samples 0.14 mm thick and 100 mg initial weight heated under vacuum. The primary reason for using the difference method was to determine the reaction order n. Tang's results generally substantiated the assumption of pseudo first order kinetics. However the plot of

$$\frac{\Delta[\log\ (-dw/dt)]}{\Delta(\log\ w)} \text{ vs. } \frac{\Delta(T^{-1})}{\Delta(\log\ w)}$$

reflected a large scatter of data for the portion of the plot representing the initial stages of decomposition, and the data in this portion did not fall on the straight line with the points representing higher temperatures. Tang attributed this scatter to two factors:

1. The initial (low temperature) decomposition proceeds via a different mechanism from that of the high temperature decomposition process and/or.

2. Experimental error in weight loss data in the low temperature stage, when the weight loss is very small.

Tang stated that when the difference data for these initial stages was plotted assuming pseudo zero-order reaction, a good fit of the data was obtained.

In order to alleviate the problem of the amplification of errors by the difference method, Tang (66) made pseudo-first order plots directly from the rate data using experimentally determined values of dw/dt and the relation

$$\frac{dw}{dt} = k_o e^{-E/RT_w}$$

Such a plot is shown in Figure II-2. The activation energies and frequency factors for pine wood, α-cellulose, and lignin thus determined are shown in Table II-5.

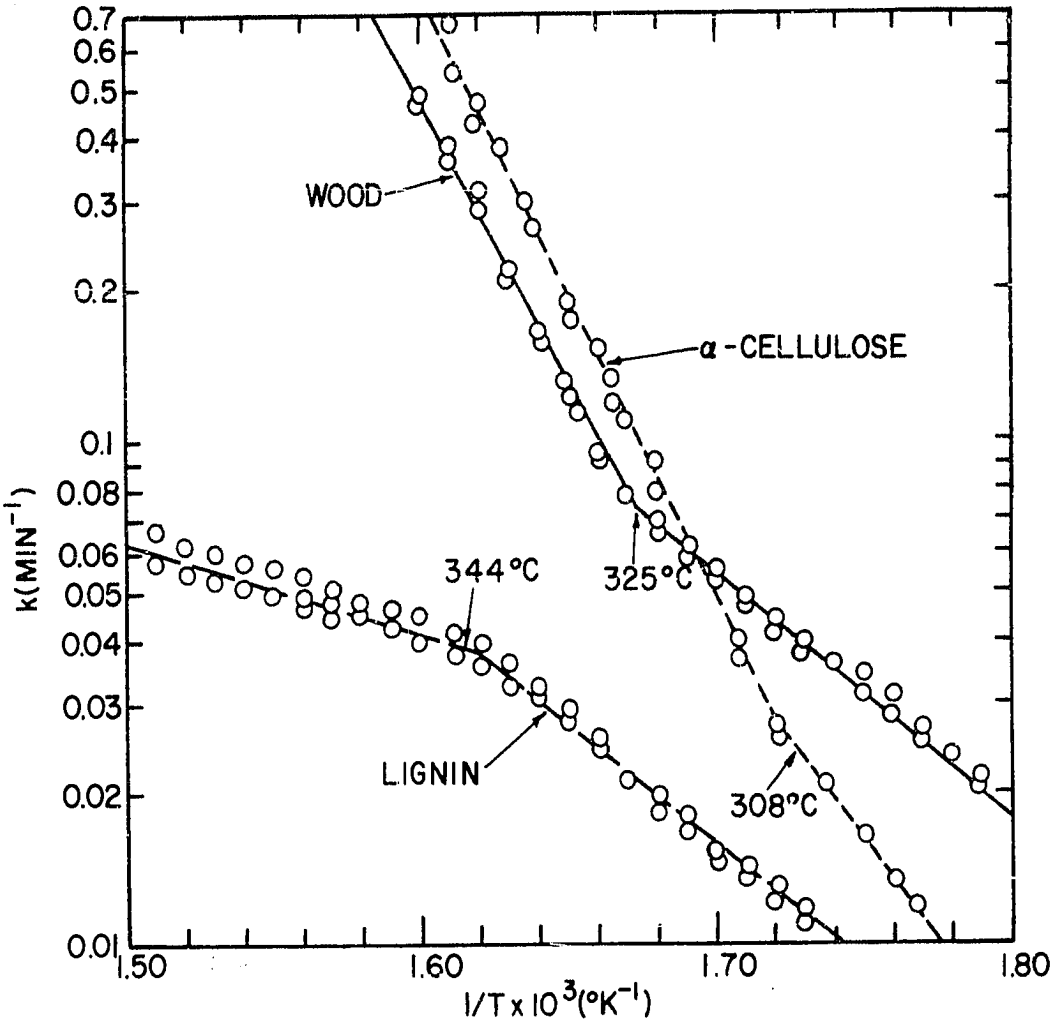


Figure II-2. Kinetics of Weight Loss Plots for Wood, α-Cellulose, and Lignin (66).

TABLE II-5

KINETIC PARAMETERS OF PYROLYSIS FROM
DYNAMIC THERMOGRAVIMETRY (TANG (66))

Material	First Stage			Second Stage		
	T(°C)	k_{01} (min^{-1})	E_1 (kcal/gm mole)	T(°C)	k_{02} (min^{-1})	E_2 (kcal/gm mole)
Pine wood	280-325	1.98×10^{7}	23	325-350	3.92×10^{18}	54
α-cellulose	240-308	3.85×10^{11}	35	308-360	2.37×10^{19}	54
Lignin	280-344	9.86×10^{5}	21	344-435	5.6×10^{10}	9

*For 100 mg samples in vacuum (0.3 mm Hg absolute).

Note that the results show that the activation energies for cellulose and wood are lower in the low temperature range than in the high temperature range, in direct contrast to the earlier results of Tang determined from static thermogravimetric analysis and those of Akita for Japanese cypress. The data here can be represented by an equation as suggested by Martin (see Equation II-7).

Heinrich and Kaesche-Krischer (29) used dynamic thermogravimetry to study the weight loss kinetics of beech sawdust (samples were approximately 20 mg) subjected to linearly increasing temperature rates of 1, 2, 3, 4, and 12°C per minute in a vacuum. The samples were dried by exposure to vacuum (10^{-2}TORR) for several hours before making measurements. As shown in Figure II-3, up to a temperature of 200°C essentially no weight loss occurred, but weight loss became rapid above about 250°C and continued to approximately 400°C. The weight loss at completion totaled about 83% at all heating rates tested although there was a noticeable shift of the weight loss curve toward higher temperatures with higher heating rates. Such behavior could be caused by thermal lag, since the sample temperature does not follow the heater temperature as well for higher heating rates, or it may be due to an actual dependence of the decomposition kinetics on the heating rate, or both. It would be expected that time dependency might be rather important at such low

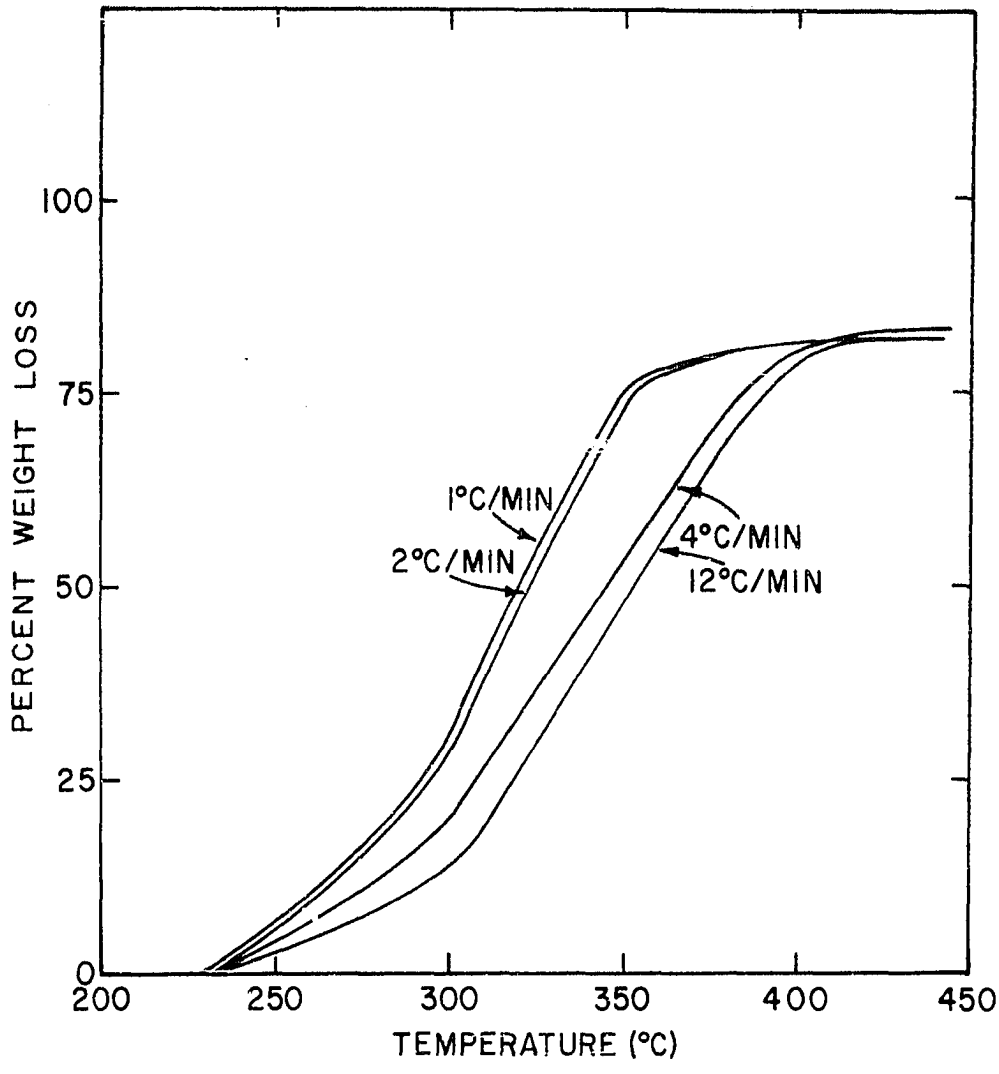


Figure II-3. Weight Loss vs Temperature of Beech Sawdust in Vacuum at Different Heating Rates (29).

heating rates. However this question was not discussed, the results were only noted.

The results of Heinrich and Kaesche-Krischer's experiments were also presented in the form of rate of weight loss curves vs temperature, obtained by taking the slope of the weight loss curve and plotting vs temperature. For beech sawdust, three distinct maxima in the rate of weight loss curve were found at approximately 260°C, 280°C, and 330°C. Rate of weight loss curves were presented for a heating rate of 1°C/min only, since the response capability of the recording instrument was said to be insufficient to allow resolution of the temperature-weight loss curve accurately enough at the higher rates. This lack of resolution capability casts further doubt on the meaning of the observed shift of the weight loss curve at the higher heating rates, suggesting that the shift to the right at higher heating rates may have been an instrumental artifact.

Heinrich and Kaesche-Krischer concluded that since separate maxima could be distinguished in the rate of weight loss vs temperature curve, the decomposition mechanism could not be treated as a pseudo, first order process. They also stated that these three observed maxima were not well enough separated to allow treatment of each as a first order reaction individually.

Measurement of the Pressure Changes in a Closed Chamber Due to Formation of Gaseous Decomposition Products: Wright and Hayward (82) studied the rate of decomposition of western red cedar and western hemlock cubes which were suddenly introduced into a nitrogen atmosphere maintained at high temperature. The reaction vessel was a Hevi-Duty retort furnace of about 60 liters capacity heated by electrical resistance elements. The furnace temperature was regulated automatically. The samples, cut in the shape of cubes, ranged from 3 mm to 19 mm (edge dimension). The samples were oven dried for at least 24 hours before being used.

The decomposition process was followed by measuring the increase in pressure in the chamber due to the liberation of gases from the sample. A diaphragm manometer was made by cementing an S. R. -4 strain gage to the center of the surface of a steel diaphragm in the retort lid. Deflection of the diaphragm under pressure altered the resistance of the strain gage. The output of the strain gage transducer was recorded ona Brush Oscillograph. A calibration curve was made by comparing recordings so obtained with measured values of the pressure obtained from a manometer. Values of the pressure at various times were expressed as a percentage of the final pressure (100 P/P^{∞}). Thus values of 100 $(1-P/P^{\infty})$ were assumed to correspond to the percentage of the original wood undecomposed at any instant. By trial,

it was found that plots of $[100\ (1-P/P^{\infty})]^{\frac{1}{2}}$ vs time were substantially straight lines. Wright and Hayward then concluded that the kinetics of decomposition of the cubes was ½ order.

The variation of the rate constant in the resulting expression,

$$100\ \frac{dP/P^{\infty}}{dt} = k\ (100\ (1-P/P^{\infty})^{\frac{1}{2}} \qquad \text{(II-15)}$$

with specimen size and oven temperature was then studied. It was found that the rate constant for the cubes was directly proportional to the specific surface (external surface area per unit weight of wood) and the temperature.

Additional experiments showed that for the same types of wood cut into the shape of discs, the data indicated that the kinetics were zero order.

Measurement of Temperature in an Externally Heated Specimen: Bowes (10) studied the rate of heat evolution and activation energies for oak, iroko, western red cedar, African mahogany, beech, and American whitewood. Raspings of the wood were packed into a tube supported in an electric furnace. Air, preheated to near the furnace temperature, was forced through the specimen at a constant rate while the furnace was heated from room temperature at constant electrical power. The temperature at the center of the specimen was measured with a thermocouple. The temperature-time records were used, with corrections for heat transfer

between the specimen and its surroundings, to calculate the net rate of heat evolution at a series of temperatures during spontaneous heating, which occurred in the range 200-300°C. The calculations are discussed in the following.

It was assumed that the net rate of heat evolution, q, in a unit volume with thermal capacity C surrounding the thermocouple could be expressed by the relation

$$\frac{q}{C} = \frac{q_e - q'}{C} = \frac{dT_s}{dt} + \frac{hA}{C}(T_f - T_s) \qquad \text{(II-16)}$$

where q_e = actual rate of heat evolution in the unit volume considered, at time t (cal/sec)

q' = rate of heat loss from the unit volume at time t (cal/sec)

T_s = temperature of specimen in the unit volume at time t (°C)

T_f = furnace temperature at time t (°C)

C = thermal capacity of unit volume (cal/°C)

h = a heat transfer coefficient (cal/cm^{2}sec °C)

A = boundary area of unit volume considered (cm^2)

A value of the quantity $\frac{hA}{C}$ was estimated by solving Equation (II-16) when an inert material was used (dry sand) using measured values of T_f, T_s, and dT_s/dt. Using values of hA/C thus obtained, the quantity q/C was calculated at

a series of temperatures. This value was multiplied by the specific heat of wood, assumed to be 0.34 cal/gm °C. The results for oak are shown in Figure II-4. Similar plots were reported for the other woods. Considerable differences in the predicted rates of heat evolution were indicated.

Bowes then assumed that the heat of decomposition q is constant in the temperature range studied. Thus, if the reaction kinetics were assumed first order, the activation energy could be calculated from the rates of heat evolution q_1 and q_2 at temperatures T_1 and T_2, respectively, as follows:

$$E = 2.303\ R\ \frac{\log q_2 - \log q_1}{1/T_1 - 1/T_2} \qquad \text{(II-17)}$$

where R is the ideal gas constant = 1.97 cal/g-mole°K. For this purpose, it was assumed that the rate of heat loss in the volatile reaction products and loss to the thermocouple was at all times small in comparison to the true evolution rate q_e; thus

$$q \approx q_e$$

Values of the activation energies thus determined are shown in Table II-6, along with the exothermic heat evolution rate for the various woods computed for a temperature of 250°C.

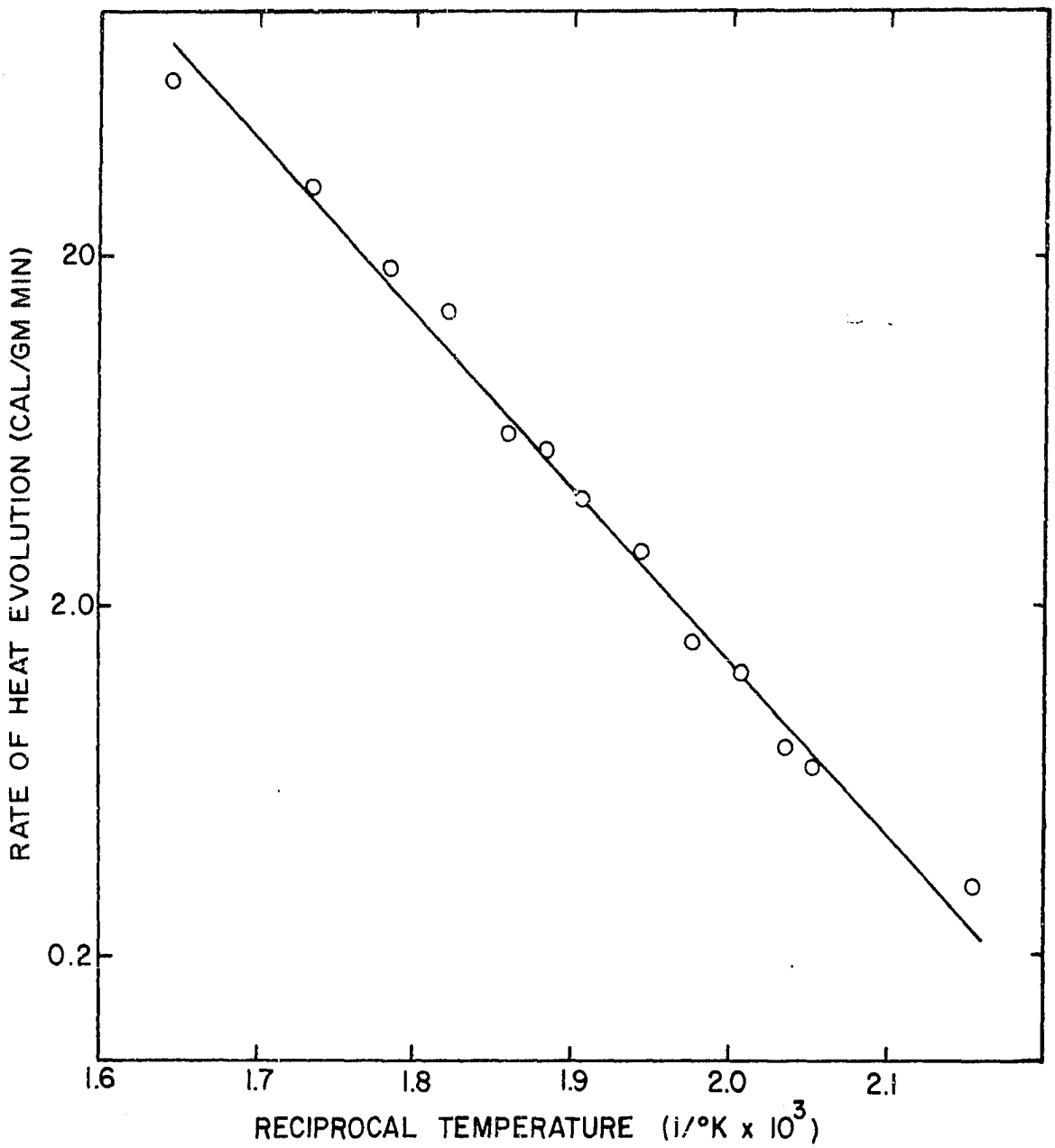


Figure II-4. Rate of Heat Evolution for Oak Wood (10).

TABLE II-6

ACTIVATION ENERGIES AND RATES
OF HEAT EVOLUTION (BOWES (10))

Specimen	E (kcal/gm mole)	q (cal/gm min) at 250°C
Oak	23.2	4.1
Iroko	33.0	3.9
Western red cedar	31.0	3.2
African mahogany	31.5	2.7
Beech	28.8	2.6
American whitewood	25.2	2.5

It should be noted that whatever the merit of the approach may have been, the results are probably not descriptive of the internal decomposition heat effects in wood. In fact the thermal effects measured were probably due to various types of oxidation and combustion reactions resulting from the presence of the air being forced through the cylinder containing the specimen.

Bowes and Townshend (11), studying the ignition of combustible dusts on hot surfaces utilizing the thermal explosion theory of Semenov (22), determined the activation energy E, and "pre-exponential" factor Qk_o, for beech sawdust in the form of layers on a hot surface. They reported values of 26.5 kcal/gm mole and 9.40×10^8 cal/cm^3 for E and

Qk_o respectively, for sawdust whose particle size was 18-120 British Standard Sieve, and 29 kcal/gm mole and 1.16×10^{10} cal/cm^3·sec for E and Qk_o respectively for finer particle sizes (<120 B.S. Sieve).

Measurement of Heat of Decomposition

Several investigators have devised other experiments for measuring the amount of heat generated or absorbed due to decomposition in a specimen of wood or cellulose which is being externally heated. Basically the approaches involve either (a) solution of a transient balance heat equation or (b) differential thermal analysis techniques.

Transient Heat Balance Methods: Akita (1) estimated the internal heat generation due to slow thermal decomposition of wood below 200°C utilizing experimentally measured transient temperatures. The temperature in the center of a sphere of wood heated from the outside surface in the absence of air was measured by a thermocouple. The equation for heat conduction with homogeneous generation of heat described by the relation

$$Q\ dw/dt = Qk\ (w - w_\infty)$$

where w = weight of reactant at time t (gm/cm^3)

k = rate constant (sec^{-1})

w_∞ = final weight of reactant at time ∞ (gm/cm^3)

was solved using values for the rate constant from Akita's own previous weight loss studies. An approximate solution gives

$$T_o = T_a + \frac{2QN_\infty}{C\rho} \sum_{n=1}^{\infty} (-1)^n \frac{a^2k}{\alpha\pi^2n^2 - a^2k}\left[\exp \frac{\alpha\pi^2n^2t}{a^2} - \exp(-\alpha t)\right] \qquad \text{(II-18)}$$

where T_a = Surface temperature (or temperature of heating medium) (°C)

T_o = temperature at the center of the sphere of radius a (°C)

Q = heat generated (cal/gm decomposed)

C = specific heat (cal/gm°C)

ρ = density (gm/cm^3)

k = rate constant (sec^{-1})

α = thermal diffusivity (cm^2/sec)

Equation (II-18) was fitted to the experimental data for Japanese cypress by adjusting Q, the only unknown. The best fit gave 32 cal/gm (exothermic). The rate of heat generation was reported to be approximately 6 cal/gm min.

Klason (34) made a series of tests of carbonization both of cellulose and of wood of various species. The tests were made in an upright cylindrical copper retort, 100 mm in diameter and 320 mm in height. Thermocouple temperature measurements were made of the wood in the center of the retort. The final retort temperature in the experiments was 400°C, and this temperature was maintained until decomposition product generation had ceased. The test times

varied between 7 and 10 hours. A typical temperature-time variation at the center of the sample is shown below for a test with pine wood.

TIME (hours)	1	2	3	4	5	6	7	8	9
TEMP (°C)	133	216	287	316	342	364	379	386	400

Klason estimated the quantities and calorific values of all products obtained in the carbonization. The total heat of reaction or decomposition was obtained by subtracting the sum of the product calorific values from the calorific value of the original material. For purposes of this calculation, Klason assumed the reaction to take place at 275°C. Typical results, along with intermediate values used in the calculation, are shown in Table II-7. The calculated heat liberation (or heat generated internally) is approximately 6% of the woods' heat of combustion. By heat of combustion, Klason means the gross calorific value. Notice that the calculation of the heat liberated, or heat of reaction, involves the subtraction of two nearly equal numbers so that the result is very sensitive to error or variation in either of the two numbers from which it is derived.

Klason's results have been used by Browne and Brenden (14) in their determination of the heat of combustion of the volatile pyrolysis products of fire-retardent treated pine wood. If wood samples are first partly pyrolyzed

TABLE II-7

RESULTS OF CARBONIZATION OF WOOD AT 275°C ACCORDING TO KLASON (34). (DATA REPRESENTS 1 KILOGRAM OF DRY TEST MATERIAL.)

	Pine	Spruce	Birch	Beech
Test Material				
Heat of Combustion (kcal)	5070	4910	4910	4790
Heat Absorbed (kcal)	93.3	93.3	93.3	93.3
Total (kcal)	5163.3	5003.3	5003.3	4883.3
Carbonization Products				
Heat of Combustion (kcal)	4605.9	4547.2	4470.4	4322.5
Heat Absorbed (kcal)	241.1	233.0	243.6	254.3
Total (kcal)	4847.0	4780.2	4714.0	4567.8
Heat Liberated (or generated internally) (kcal)	316.3	223.1	289.3	315.5

and then the resultant char and volatile products are burned to carbon dioxide and water, the total heat resulting from the thermal decomposition of the wood is:

$$\Delta H_c(\text{Wood}) = \Delta H_c(\text{Char}) + \Delta H_c(\text{Volatiles}) + \Delta H(\text{Pyrolysis})$$

where ΔH_c = heat of combustion

Based on Klason's results, Browne and Brenden assumed the $\Delta H(\text{Pyrolysis})$ term to be sufficiently small to be neglected. They used the remaining equation to determine $\Delta H_c(\text{Volatiles})$, the heat of combustion of the volatile products, after determining $\Delta H_c(\text{Wood})$ and $\Delta H_c(\text{Char})$ by bomb calorimetry.

The work of Roberts and Clough has been mentioned earlier. From temperature measurements made with thermocouples at different radii in the wood cylinders studied (2 cm x 15 cm, heated in a cylindrical muffle furnace) they estimated values of the heat generated internally as follows. They wrote a heat balance on a cylindrical element within the specimen as net heat transferred across the surface + heat generated within the element = accumulation of heat within the element. They stated that the first and third of these terms were calculated from the measured temperature distribution, while values for the second were obtained by fitting a value for q, the heat of reaction. For the high temperature range (above a maximum temperature achieved in the sample of 300°C) good agreement with experimental measurements was obtained with q = 55-75 cal/gm, while at lower temperatures

a value of 280 cal/gm was obtained (exothermic).

Widell (79) also made a series of tests involving the measurement of the temperature distribution in wood specimens which were heated externally. These measurements were then used in conjunction with the differential equation for unsteady state heat conduction in an infinitely long, homogeneous, isotropic cylinder to make computations of the internal heat generation rates. Most of the tests utilized 45 mm OD by 150 mm long wood rods sheathed in a brass cylinder. Resistance wire was wound around the brass cylinder for external heating. The temperature of the cylinder wall was determined by a thermocouple screwed to it. The brass cylinder was sunk in a container filled with silica gel at the beginning of a run and was heated to the temperature fixed for the test. The test rod, with thermocouples in place, was then inserted in the cylinder. At the beginning temperature readings were taken every minute, later every two minutes, and toward the end of the test every five minutes.

Tests were carried out with cylinder wall temperatures of 80, 300, and 550°C for samples of pine, spruce, birch, and asp. In the case of 300°C and 550°C cylindrical wall temperatures the wood temperature rose above the cylinder wall temperature, indicating exothermic heat effects. Quite marked differences in these temperature curves were found for different woods.

Widell utilized the differential heat conduction equation for a cylindrical body with an internal heat source and one dimensional heat transfer in the form:

$$\frac{\partial T}{\partial t} = \alpha\left(\frac{\partial^2 T}{\partial r^2} + \frac{1}{r} \cdot \frac{\partial T}{\partial r}\right) + \frac{1}{C\rho} \cdot Q \qquad \text{(II-19)}$$

where T = temperature (°C)

t = time (sec)

r = radius of cylinder (cm)

α = thermal diffusivity (cm^2/sec)

K = thermal conductivity ($cal/cm^2 sec°C/cm$)

C = heat capacity ($cal/gm°C$)

ρ = density (gm/cm^3)

Q = heat generated per unit of volume and unit of time ($cal/cm^3 sec$)

By plotting T as a function of the radius for different times, Widell determined $\partial T/\partial r$. From plots of these values as a function of the radius at the same times he determined $\frac{\partial^2 T}{\partial r^2}$. He then determined $\partial T/\partial t$ from graphs of T vs time at different values of the radial distance from the center of the specimen. Using values of K, C, α, and ρ, which he measured or obtained from the literature, he then calculated the value of the heat source term from Equation (II-19), rearranged:

$$\frac{Q}{K} = \frac{1}{\alpha} \cdot \frac{\partial T}{\partial t} - \left(\frac{\partial^2 T}{\partial r^2} + \frac{1}{r}\frac{\partial T}{\partial r}\right) \qquad \text{(II-20)}$$

Since the carbonization product gases depart at high temperature, the computed heat generation rate, Q, represents the difference between the heat generated and the enthalpy increase of the departing gases.

Figure II-5 and II-6 shows the results of such a computation for the 11.2 mm radius position in a 45 mm test rod of pine with surrounding (cylinder) temperature of 80°C and 300°C respectively. For the case of 80°C surrounding temperature, the entire curve lies in the endothermic region. For the case of 300°C surrounding temperature the endothermic effect is maximum at a temperature of 125°C and then decreases until the net effect appears exothermic at a temperature of approximately 250°C. Thereafter, the exothermic effect assumes a fairly constant value of 90 cal/gm hr based on initial dry sample weight.

Differential Thermal Analysis Methods: Relatively few studies of the thermal decomposition of wood using differential thermal analysis (DTA, see Chapter III for description and theory of this method) have been made. One early investigation which utilized a differential thermal analysis technique was that of Widell (79). His work was a rather detailed study, actually involving two independent experimental approaches, of which the first has been discussed in the preceding section.

In the second approach, the wood specimen was a cylindrical rod 150 mm in length and 45 mm in outside diameter (some 20 mm OD samples were also studied), with a

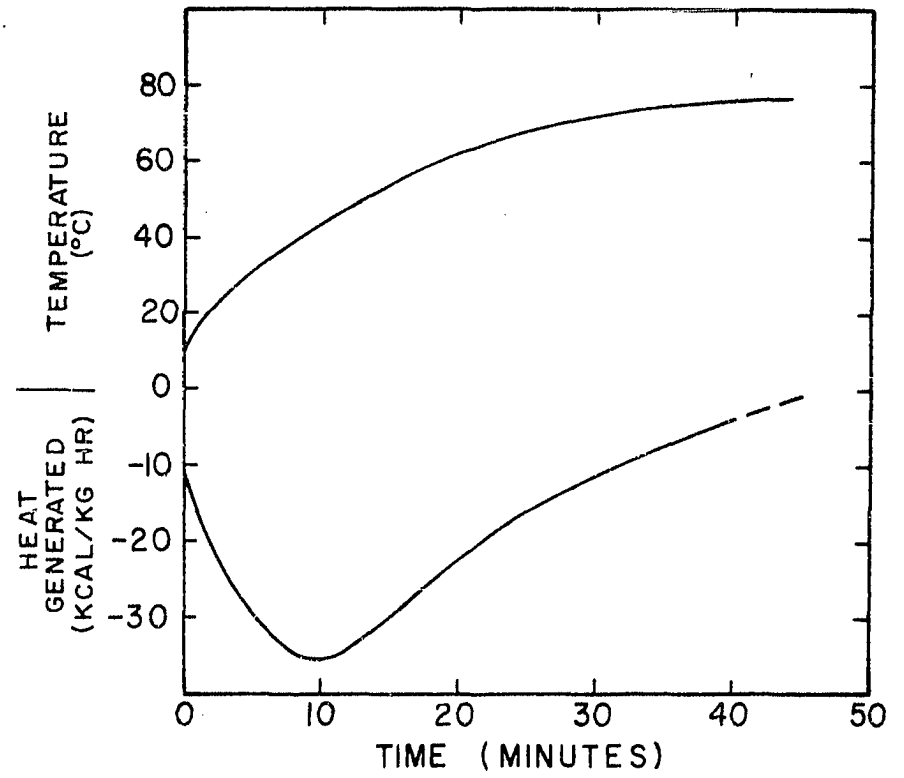


Figure II-5. Heat Generation Rate and Temperature vs Time in Pine Cylinder (r = 11.2 mm) with Surrounding Temperature = 80°C (79).

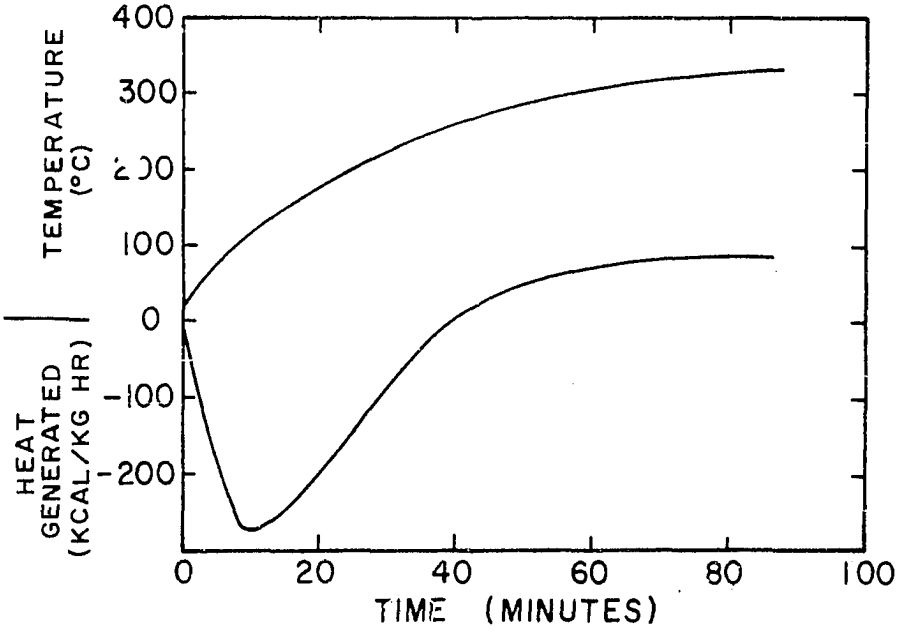


Figure II-6. Heat Generation Rate and Temperature vs Time in Pine Cylinder (r = 11.2 mm) with Surrounding Temperature = 300°C (79).

hole 20 mm in diameter through its longitudinal axis. An electrical resistance heater was inserted in the hole in the specimen so that a snug fit was obtained. The heating element extended past both ends of the specimen. Chromel-alumel thermocouples were placed at various locations in the test specimen, normally at distances of 10, 13.5, and 17 mm from the axis of the 45 mm diameter cylinder (the locations of the thermocouples in the 20 mm OD test specimens were not given). The test specimen with its internal heater was enclosed in a brass cylinder provided with stainless steel end covers. Chromel-alumel thermocouples were also placed in the center of the heating element and on the outside surface of the brass cylinder. The cylinder with the test specimen was placed in a cylindrical container 300 mm in diameter and the container was filled with silica gel. To avoid the problem of having to determine the heat losses from the test cylinder to and through the surrounding silica gel, an identically constructed compensation cylinder provided with electrical heater and thermocouples for surface temperature measurement was placed in an identical 300 mm diameter container packed with silica gel. The electrical energy delivered to the two heaters was measured by voltmeters and ammeters. During a test a constant power level to the carbonization cylinder was maintained, while the power to the compensation cylinder was regulated in such a way that the surface temperature of the two cylinders was kept equal throughout the experiment. Thus, the heat losses

from the two cylinders were assumed equal. The power to the carbonization cylinder was normally maintained at either 35 or 50 watts. A run was started by switching on the power to the carbonization cylinder. At the outset the power output to the compensation cylinder necessary to maintain its surface temperature equal to that of the carbonization cylinder was low due to the initially low values of the carbonization cylinder surface temperature. As this temperature rose, the output power to the compensation cylinder had to be increased and at some time actually became higher than the power to the carbonization cylinder. Widell stated that this effect was due to exothermic decomposition effects in the wood specimen. An example of the temperature course in an experiment with pine wood is shown in Figure II-7. Curves 3 and 4 are the surface temperatures of the compensation and carbonization cylinders resepctively. Note the good agreement in the surface temperature measurements, indicating that the power to the compensation cylinder was correctly regulated.

Figure II-8 shows the net power delivered to the carbonization in the same test, i.e. the energy delivered to the carbonization cylinder less the energy to the compensation cylinder, as a function of time. Also shown is a plot of the mean temperature, determined by graphical integration of the measured temperatures as a function of radius and

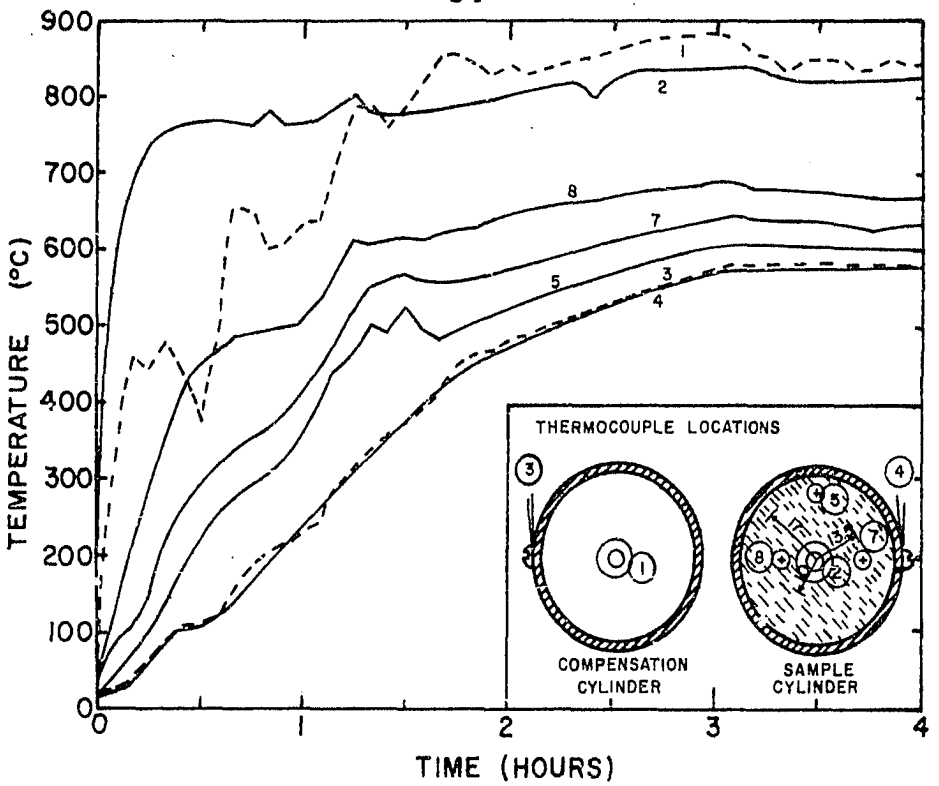


Figure II-7. Measured Temperatures in 45 mm ID Pine Sample and Compensation Cylinder at Different Radii (79).

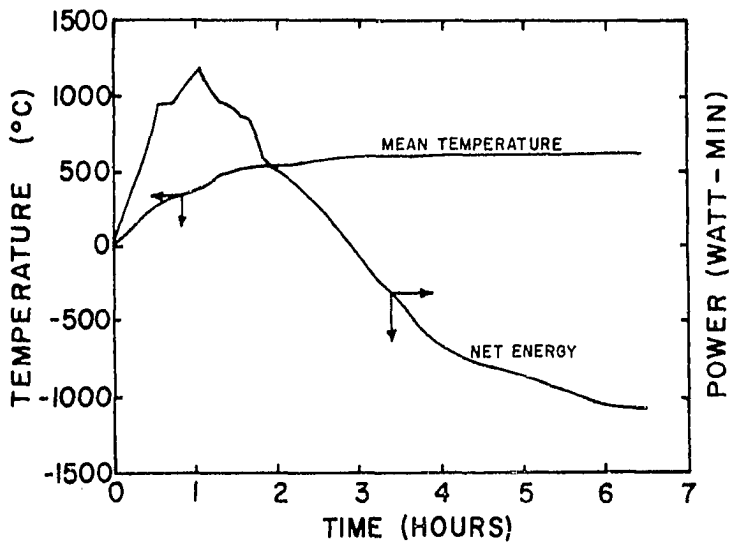


Figure II-8. Net Energy Delivered to Carbonization Cylinder and Mean Temperature for 45 mm ID Pine Sample (79).

dividing by the cross-sectional area of the cylinder. The curve has a maximum at 1 hr 5 minutes, or at a mean temperature of 400°C. The amount of net energy is then 17.3 kcal corresponding to 136 cal/gm weighed material or 150 cal/gm moistureless material. After this peak is passed, the net energy decreases, presumably due to the onset of exothermic heat effects in the specimen. It must be remembered that the net energy curve also reflects the sensible heat effects in the specimen. If no reaction or phase change heat effects were present, if heat capacity of the material were constant with temperature, and if changes in shape of the temperature profile in the specimen were neglected, a horizontal curve in the net energy plot would indicate that no endothermic or exothermic heat effects were taking place. Widell thus stated that after approximately 6.5 hrs, exothermic heat effects had ceased. At this time the total net energy (net area under the curve) is 15.5 kcal. Therefore the material had given a surplus of heat of 122 cal/gm of weighed material or 134 cal/gm moistureless material during its carbonization. In the run illustrated the initial specimen weight was 126.7 grams and the inital moisture content was 11.4 grams. Assuming the water left as vapor at 100°C and was initially at 19°C at the beginning of the test, the heat consumed by the moisture would be 620 cal/gm. Widell corrected for this effect and stated that dry pine material should

show a surplus of heat under the same test conditions of 196 cal/gm.

Several runs with pine and beech rods 45 mm in diameter were made. Table II-8 summarizes the data from four such tests. Note that there is considerable variation in the values of surplus heat of carbonization (exothermic-endothermic-sensible heat effects) as a function of time but that there is good agreement on a value of approximately 200 cal/gm of surplus heat for the entire carbonization process.

The results of the series of tests made with 20 mm pine rods internally heated are summarized in Table II-9. Note that the maximum values of the energy delivered during the endothermic portion are in the range of 200 to 350 cal/gm dry material. This range is considerably higher than the approximately 80 cal/gm required in the tests with 45 mm rods. Note also that no surplus heat was generated in the 20 mm ID rods. Widell suggested that these differences were due to the effect of the large difference in temperature gradients in the rods of different sizes.[3]

A study with 20 mm pine rods was also made of the effect of different heating rates (by stepwise varying the power delivered to the carbonization cylinder),

---

[3]This discrepancy points out the difficulty of absolute explanation of the results since the temperature distribution in the sample varies so much with change in size and configuration of the sample.

TABLE II-8

CARBONIZATION TESTS ON 45 mm ID WOOD RODS
(WIDELL (79))

	Test No.			
	32	34	35	33
Test Material	pine	pine	pine	beech
Duration of Test (hr)	6	6	6.5	6.25
Weight of Specimen (dry) (gm)	113.6	109.0	115.3	156.9
Weight of charcoal residue (%)	26.9	27.0	28.0	25.5
Maximum Net Energy Rate to Carbonization Cylinder (cal/gm)	75	72	89	70
Surplus Heat Generated Computed on Dry Weight Basis at				
time = 2 hours (cal/gm)	17	6	-2	41
3 hours (cal/gm)	131	101	72	128
4 hours (cal/gm)	100	174	143	172
5 hours (cal/gm)	199	196	169	179
6 hours (cal/gm)	200	201	192	181

TABLE II-9

CARBONIZATION TESTS ON 20 mm ID PINE RODS
(WIDELL (79))

	Test No.			
	36	37	38	39
Duration of Test (hr)	4.75	5.6	5	3
Weight of Specimen (dry) (gm)	17.43	17.78	18.33	20.17
Weight of Charcoal Residue (%)	29.90	25.00	22.10	31.00
Maximum Net Energy Rate to Carbonization Cylinder (cal/gm)	256	251	346	346
Surplus Heat Generated (cal/gm)	0	0	0	0

Widell stated that these tests showed that the exothermic heat generation is not confined to the temperature range 300-400°C, but with sufficiently rapid heating it can be displaced to higher temperatures. This effect is characteristic of differential thermal analysis results (61,78).

Widell stated that a weakness of this technique was that the amounts of energy liberated during carbonization are obtained from the difference between numbers that are of almost equal magnitude so that accuracy is relatively poor. In addition, the specification of equal heat losses from the carbonization and compensation cylinders may be very difficult to attain experimentally. For example, at high temperatures the effect of radiative loss differences due to differences in cylinder surface characteristics may be quite a problem. (This effect is discussed further in Chapter V, with reference to difficulties encountered in the present work).

Tang and Neill (69) estimated the heats of pyrolysis and of combustion of α-cellulose using differential thermal analysis. The sample and reference material (Al_2O_3) were placed in sealed pyrex capsules for the heat of pyrolysis measurement. A typical DTA recording is shown in Figure II-9. The area under the curve was determined by graphical integration and was used to calculate the heat released or absorbed from the relation:

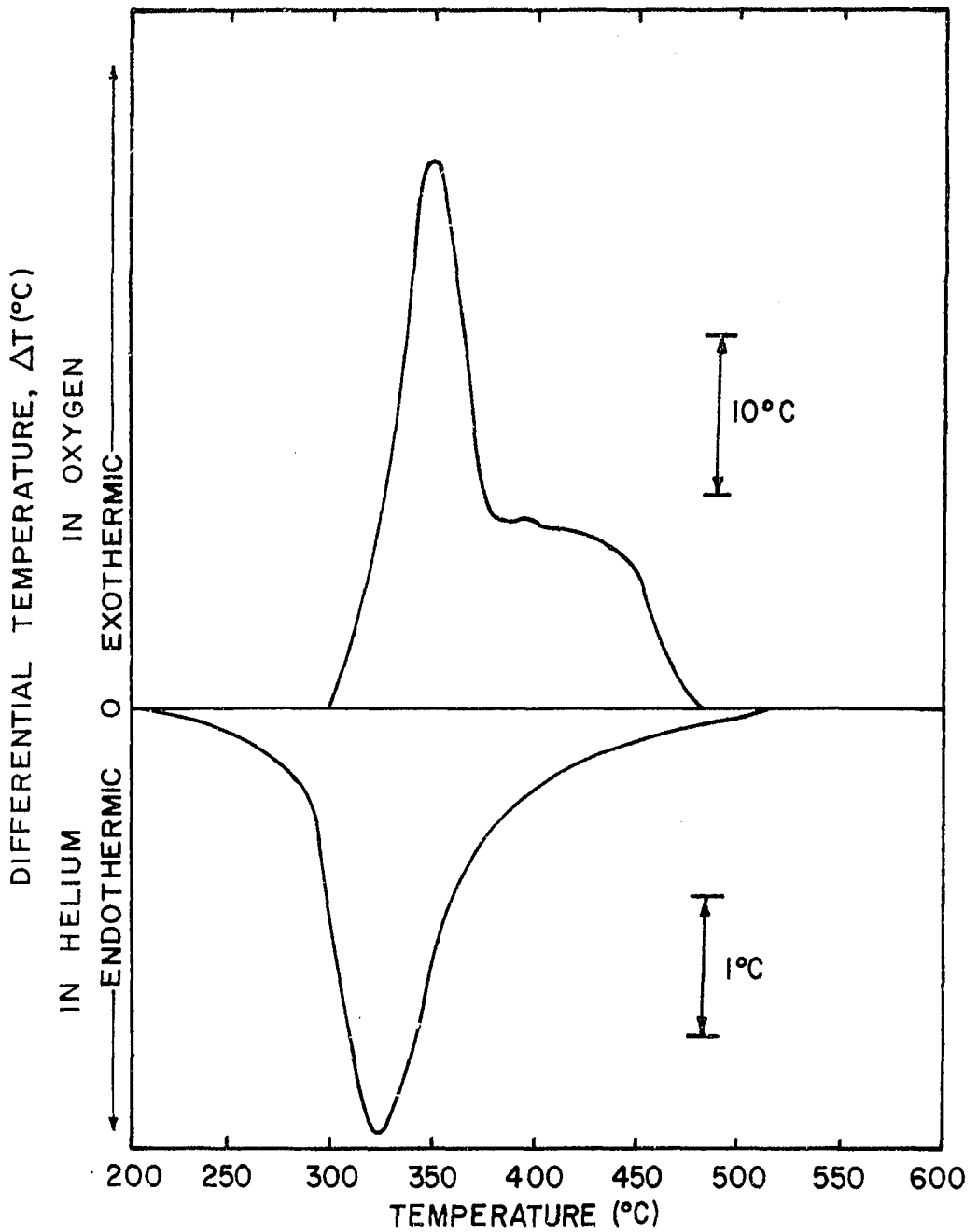


Figure II-9. Differential Thermal Analysis of α-Cellulose (69).

$$(\Delta H)_s = \frac{A_s m_k}{A_k m_s} (\Delta H)_k \qquad \text{(II-21)}^4$$

where $(\Delta H)_s$ = heat of reaction (pyrolysis) of sample (cal/gm)

$(\Delta H)_k$ = known heat of transformation of calibration standard (cal/gm)

m_s, m_k = weight of sample and calibration standard respectively (gm)

A_s, A_k = integrated area under DTA curves for sample and calibration standard respectively (cm^2)

The heating rate was 12°C/min for all DTA determinations. The heat of pyrolysis determined from runs made in a flowing helium atmosphere was calculated to be 88 ± 3.6 cal/gm (endothermic).

Tang and Neill also measured the heat of combustion of α-cellulose by differential thermal analysis in a flowing oxygen atmosphere. The heat of vaporization of ammonium chloride in a flowing nitrogen atmosphere was used in Equation (II-21) to determine the heat of combustion. The value of

$$\frac{m_k (\Delta H)_k}{A_k} = 2.2 \ \frac{\text{cal}}{\text{cm}^2} \quad \text{for } NH_4Cl$$

---

[4] See Chapter III for derivation of this equation.

where $(\Delta H)_k$ = 39.6 kcal/gm mole or 740 cal/gm was used. This calculation resulted in heats of combustion of cellulose which were about 12% lower than a value of 4030 cal/gram determined by oxygen-bomb calorimetry.

The reasons why results determined in this manner by differential thermal analysis may be seriously questioned will be discussed in a later section on thermal analyses techniques. However, at this point, it is interesting to note the work done by Broido (13). Broido investigated "pure" cellulose (an α-cellulose paper containing 2.5% carbon black, density = 0.67 gm/cm^3, 0.54 millimeters thick, ash content = 15%) and "ash free" cellulose (Schleicher and Schuell No. 589 white ribbon analytical filter paper, ash content <0.01%) by differential thermal analysis and thermogravimetric analysis. The apparatus used for both the DTA and TGA studies was reportedly the instrument at the Forest Products Laboratory used by Tang and Neill (69). For the DTA experiments about 5 grams of shredded paper were placed in a sample tube so as to surround completely the thermocouple. The reference tube was packed to an equal depth with aluminum oxide. The experiments were carried out in both flowing nitrogen and air. These gases entered the tube through a glass sleeve at a point slightly above the level of the sample and discharged from the top of the tube. Typical resulting TGA and DTA

recordings are shown in Figure II-10 for measurements in air and in Figure II-11 for measurements in nitrogen. Note that Broido's results indicate the heat effect of cellulose decomposition in an inert atmosphere (nitrogen) to be endothermic over part of the temperature range of 100°C to 500°C and exothermic over part of the range. Also the endothermic and exothermic effects are of comparable magnitude. This result is in direct contrast to the totally endothermic behavior of cellulose in helium presented by Tang and Neill. One must keep in mind that there were probably some small differences in composition of these samples and that the sample handling procedure was considerably different. However, the central question is, which behavior, if either, is actually descriptive of the internal decomposition heat effects which take place when cellulose is externally heated?

Several other studies have been made of the thermal decomposition of wood by means of differential thermal analysis. In most of these studies no attempt was made to determine heat effects quantitatively; however, the qualitative DTA results were reported to be indicative of the character of the heat effect (exothermic or endothermic), and to some extent, of its magnitude.

Arseneau (2) used differential thermal analysis equipment built by himself to study the thermal breakdown of balsam fir filings and their components in air when

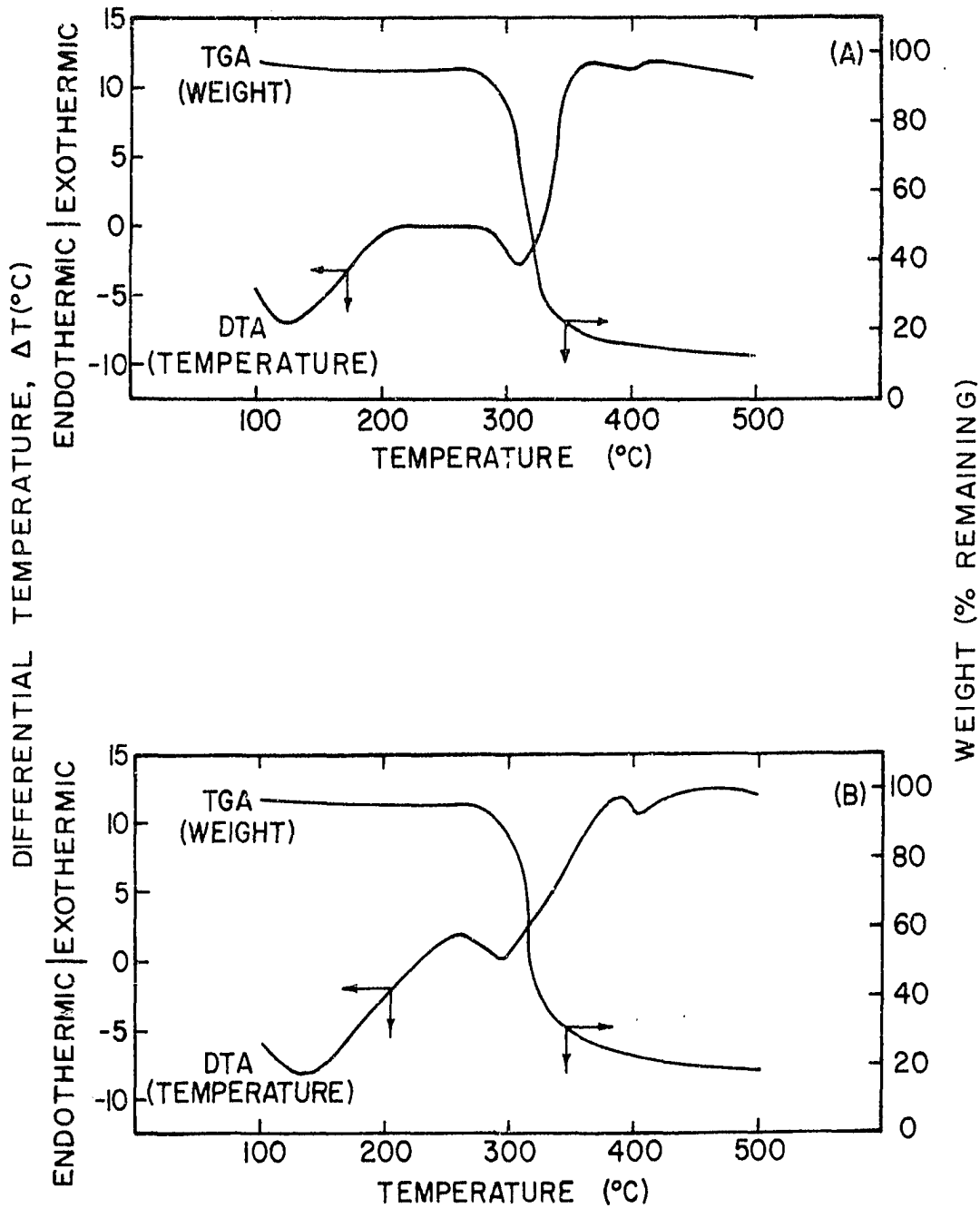


Figure II-10. DTA and TGA Results for (A) "Ash-Free" and (B) "Pure" Cellulose in Air (13).

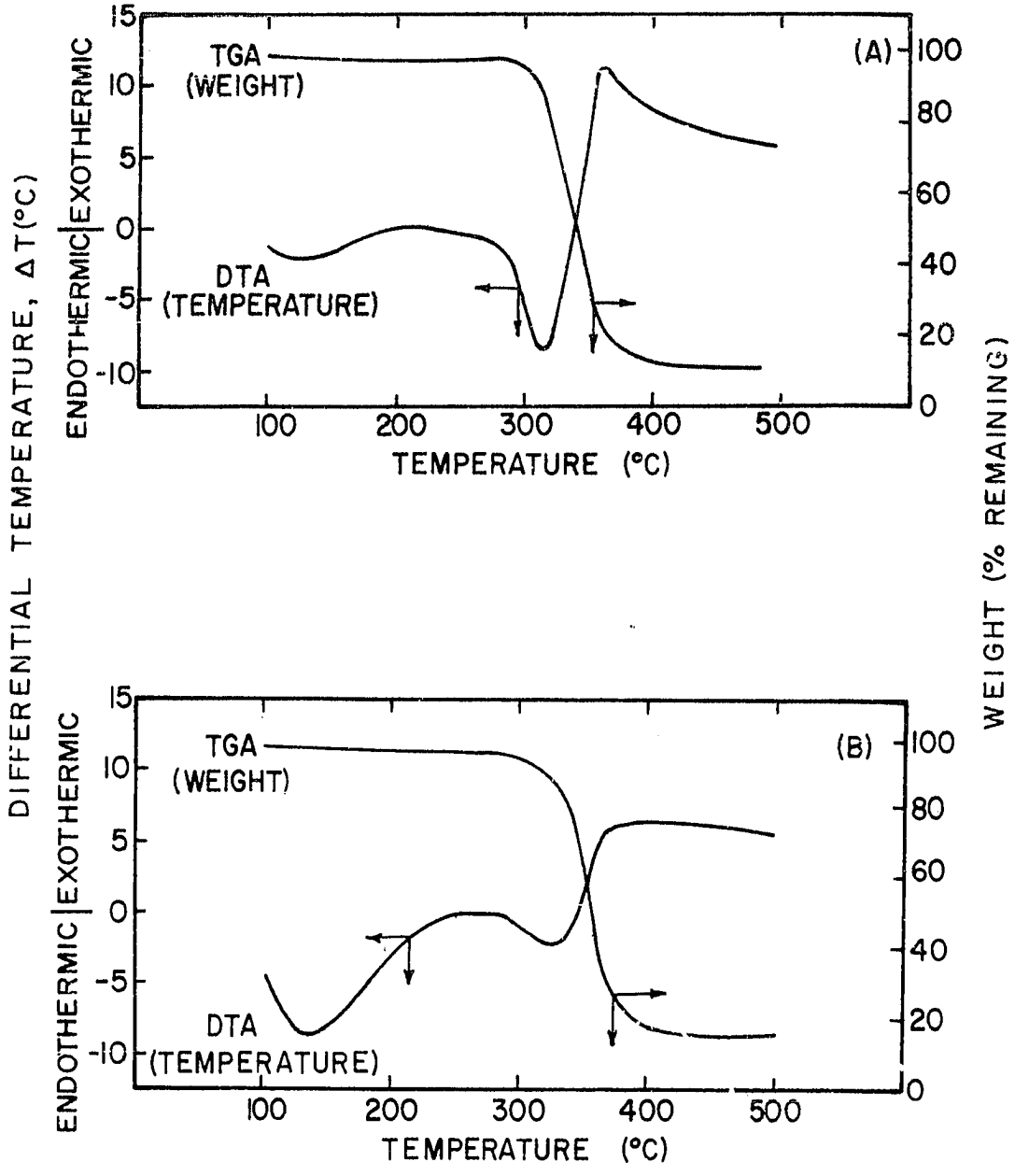


Figure II-11. DTA and TGA Results for (A) "Ash-Free" and (B) "Pure" Cellulose in Nitrogen (13).

heated from 50°C to 420°C at a heating rate of 5.8°C per minute. He concluded that the decomposition effect in air was endothermic up to a temperature of 270°C and exothermic for higher temperatures. A further conclusion was that the thermogram (plot of ΔT vs T or time) for balsam fir is simply a composite of the individual thermograms of its components with little or no interaction.

A similar study by Sergeeva and Vaivads (59) on birchwood indicated that pyrolysis was accompanied by considerable interaction between its components.

Domansky and Rendos (18) made differential thermal analysis measurements on pine, beech, alder, poplar, oak, and white beech sawdust (the size of the individual particles was less than 0.3 mm) in air. Measurements were also made on cellulose, hemicellulose, and lignin from each of these wood types. All samples were dried at 100°C for 5 hours before running. The sample size was not given but the heating rate was in all cases 10°C/min. The thermograms of the different wood types were all found to have the same qualitative character, exhibiting three distinctly separate regions. In the range from 100°C up to 170°C a large endotherm was apparent. A temperature range in which the decomposition became exothermic began at about 215°C and this exotherm exhibited a maximum at about 270°C. At temperatures above 350°C little or no heat effect was observed. In agreement with Arseneau, Domanski and Rendos

also concluded that a mixture of cellulose, hemicellulose, and lignin, in which these components are present in the same proportion as in wood, behaves thermally as wood.

Heinrich and Krischer (29) made DTA measurements on beech, pine, and spruce cylinders 37 mm long and 25 mm in diameter in nitrogen. The samples were dried at 105°C (length of drying period was not reported) before running. In all cases the rate of temperature rise was 1°C/min. They concluded that for all the woods tested no exothermic reactions occur in an inert atmosphere below 250°C, but they found evidence of exothermic effects exhibited by two separate peaks in the ΔT vs T curve at temperatures of about 270°C and 330°C. Their results were said to be in qualitative agreement with their studies of the same woods by thermal gravimetric techniques, the results of which have been discussed in an earlier section.

Iskhakov (30) studied the thermal decomposition of wood using differential thermal analysis, and found considerably different results at different rates of heating (2.2, 10, and 16°C/min). He also found strong dependence of the results on the atmosphere in which the analysis was carried out (hydrogen and nitrogen).

Tyulpanov (72) studied the thermal decomposition of finely ground birchwood heated in nitrogen. Using cold traps, he condensed the volatile decomposition products for subsequent analysis. The amount of the various decomposition

products was said to be reasonably independent of the heating rate. He stated the belief that wood decomposition could not be described kinetically as a single-component process.

Sanderman and Augustin (57) studied the thermal decomposition of wood and its three major constituents; cellulose, hemicellulose, and lignin, as well as several mono- and polysaccharides. The DTA equipment was built by them. Experiments were carried out in flowing nitrogen, flowing air, and with restricted air supply, at a heating rate of 7°C/min. The wood samples were in the form of sawdust. In the case of spruce and beech wood decomposing in a flowing nitrogen atmosphere, the decomposition was found to be endothermic up to a temperature of 250°C, with two separate exothermic peaks occuring at approximately 350°C and 410°C. The behavior in a limited air supply (achieved by starting a run with air in the small chamber, but without allowing additional air to reach the sample) was essentially the same as in the case of the flowing nitrogen atmosphere, except for the appearance of two small exothermic peaks at approximately 240°C and 300°C.

Keylworth and Christoph (32) used a DTA apparatus of their own design to study the thermal decomposition of wood with and without treatment with fire-retardant salts. Using a calibration procedure similar to that used by Tang (68) they measured the heat evolved in the thermal decomposition of these materials in air. They obtained a value

of 4500 cal/gm for untreated beech, which is in fair agreement with a value of 4000 cal/gm for the heat of combustion of wood obtained by bomb calorimetry. No studies of wood decomposition in inert atmospheres were made although some were planned for a later date.

Thermal and Physical Properties

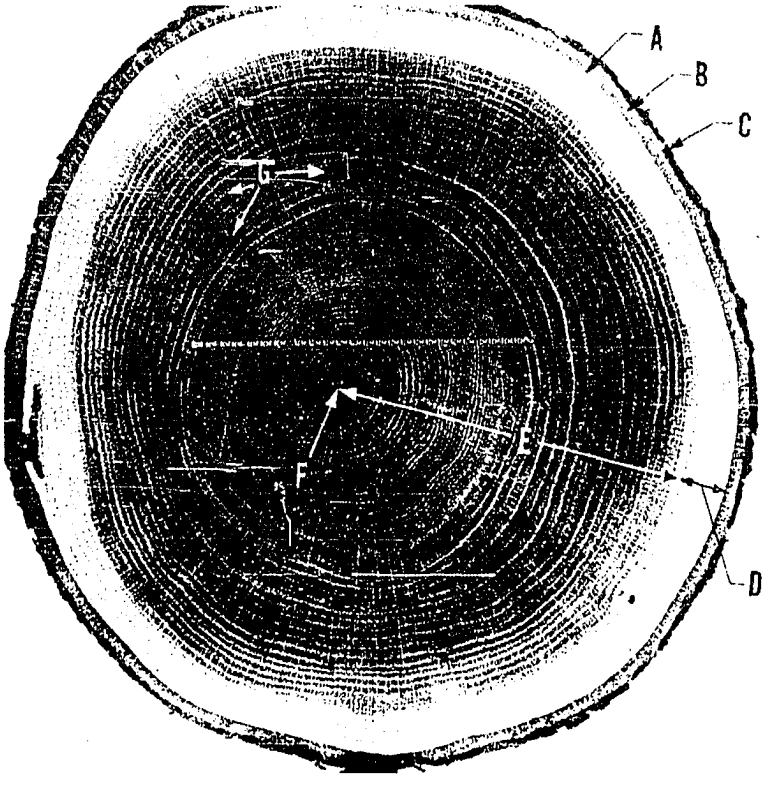
Prediction of the transient temperature distribution in a wood specimen requires knowledge of several properties. Specification of density, heat capacity, and thermal conductivity is required as a function of temperature and decomposition history. Little information is available in this area with the exception of that which can be gained about density variations by analysis of the weight loss studies, particularly the dynamic thermogravimetric studies which have been discussed earlier. Some work has been done to define the temperature dependence of heat capacity of non-decomposing wood, and several studies have been made of thermal conductivity of wood at temperatures below 100°C. Some of this information is useful in fixing "ballpark" estimates and checking experimental results; the more important studies are outlined in the following sections.

As is well known, wood is quite non-homogeneous and non-isotropic. In addition to the non-isotropicity due to the directional grain structure, both non-homogeneity and non-isotropicity result from variable growth rate. The most obvious result of variable growth rate is evidenced by

the difference between springwood and summerwood as shown by the light and dark rings in the photograph of Figure II-12. Additional deviations from uniformity of structure in a given wood species is evidenced by the difference between sapwood (the light colored layer in the photograph of Figure II-12, which carries the sap from roots to leaves), and heartwood (the darker, inner portion of the trunk, consisting of inactive, non-growing material). Also the presence of wood rays, which connect the various layers from pith (the central core) to the bark for storage and transfer of nutrients, result in still more non-uniformity. Additional complicating factors are introduced if the specimen contains knots, checks, or compression wood. However, in Grade 1 lumber, which is relatively free of these latter characteristics, the effects of non-homogeneity and non-isotropicity due to wood rays, growth rings, sapwood vs heartwood content, and the directional grain structure are the important variables which must be known in order to completely specify the thermal properties of dry wood.

Specific Heat

Several studies have been made of the specific heat of wood, both in the dry and wet states, at temperatures below the decomposition threshold. Dunlap (19) is the major reference on the subject. He measured the specific heat of small cylinders (about 6 grams) of oven-dry wood in the temperature range 0°C to 106°C, using a modified Bunsen's ice



A - Cambium Layer
B - Inner Bark
C - Outer Bark
D - Sapwood
E - Heartwood
F - Pith
G - Wood Rays

Figure II-12. Photograph of Wood Showing Non-Isotropicity and Non-Homogeneity.

calorimeter. He reported that the specific heat of 20 species ranging in density from 0.23 to 1.10 gm/cm^3 could be reasonably described by the linear relation:

$$C = 0.266 + 0.00116\ T \qquad \text{(II-22)}$$

where C = specific heat (cal/gm°C)

T = temperature (°C)

He also reported that there was no significant difference between specific heat of heartwood and sapwood of the same species, that geographic origin did not appear to markedly influence the specific heat, and that there appeared to be no significant difference between the different wood species studied.

Kollman (35) studied the specific heat of wood containing free moisture. He proposed an expression for the specific heat of wet wood as follows:

$$\bar{C}_x = (x)\ (C_w) + (1-x)\ \bar{C}$$

where $\bar{C}_x$ = mean specific heat of moist wood (cal/gm°C)

x = moisture content as a fraction of net weight

C_w = specific heat of water (cal/gm°C)

$\bar{C}$ = specific heat of oven-dry wood (cal/gm°C)

Widell (79) presented the relation shown in Figure II-13 for the specific heat and mean specific heat of charcoal.

Density

The local density variation of a wood specimen

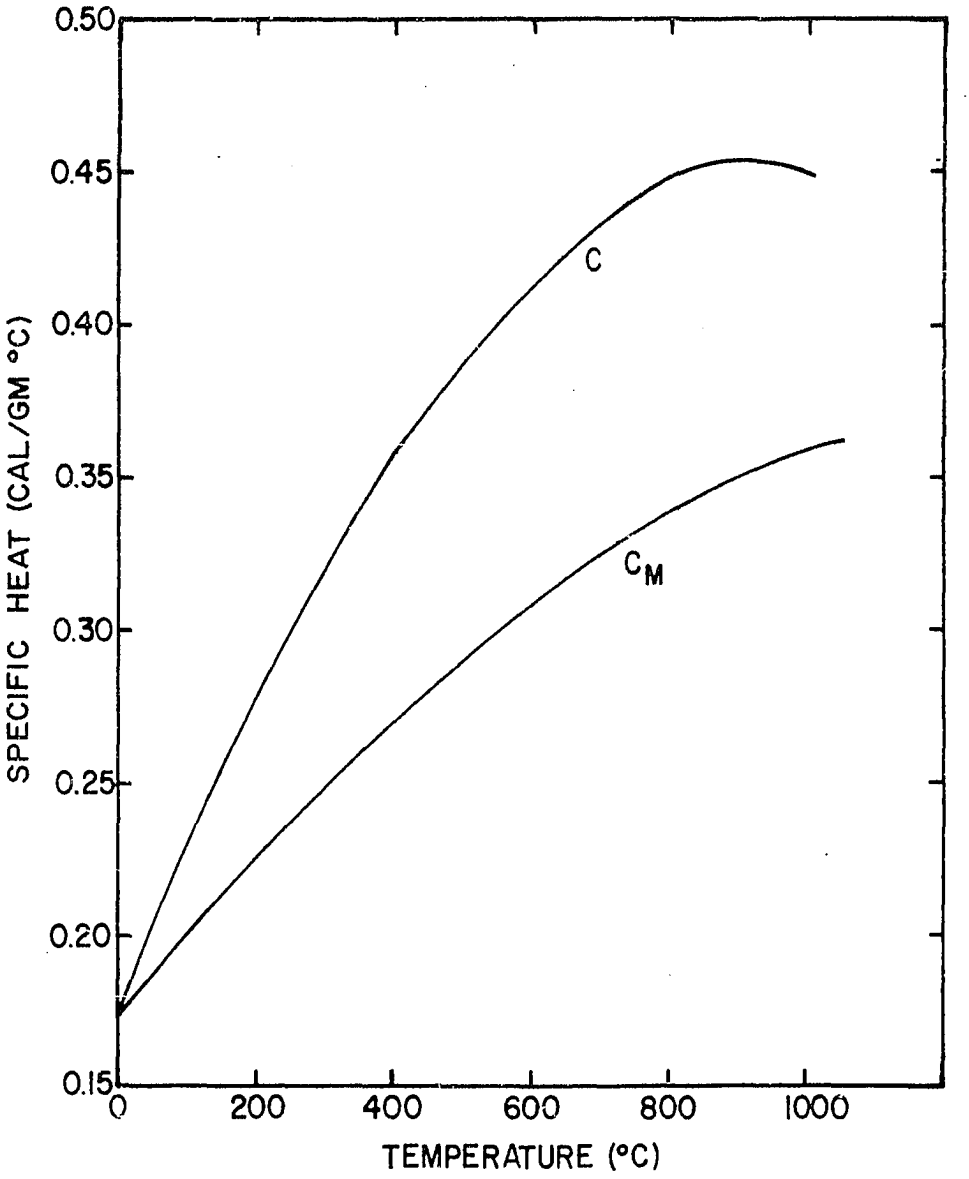


Figure II-13. Specific Heat C and Mean Specific Heat C_M for Charcoal as a Function of Temperature (79).

during decomposition can be obtained from thermogravimetric data if the specimen is assumed to retain its original size and exterior boundaries. The validity of such an assumption of course depends on the duration and extent of decomposition but is probably good during the pre-ignition process in most cases since the material may ignite before the charring zone has penetrated deeply.

Blackshear and Murty (8) measured density variations in externally heated, compressed cellulose cylinders using an x-ray technique. A diagram of their apparatus is shown in Figure II-14. A typical density distribution as a function of time and radius of the cylinder is shown in Figure II-15. From thermocouple temperature measurements, they were also able to specify the temperature in the decomposing cylinder as a function of time and radius. By combining the two results they plotted density versus temperature with radius as a parameter as shown in Figure II-16. The similarity of Figure II-16 to plots obtained from dynamic thermogravimetry is striking (compare with Figure II-3).

Thermal Conductivity

In contrast with heat capacity and density, the thermal conductivity of wood is known to be strongly direction-dependent and is affected not only by local non-homogeneity, but also directly by density variation within the specimen.

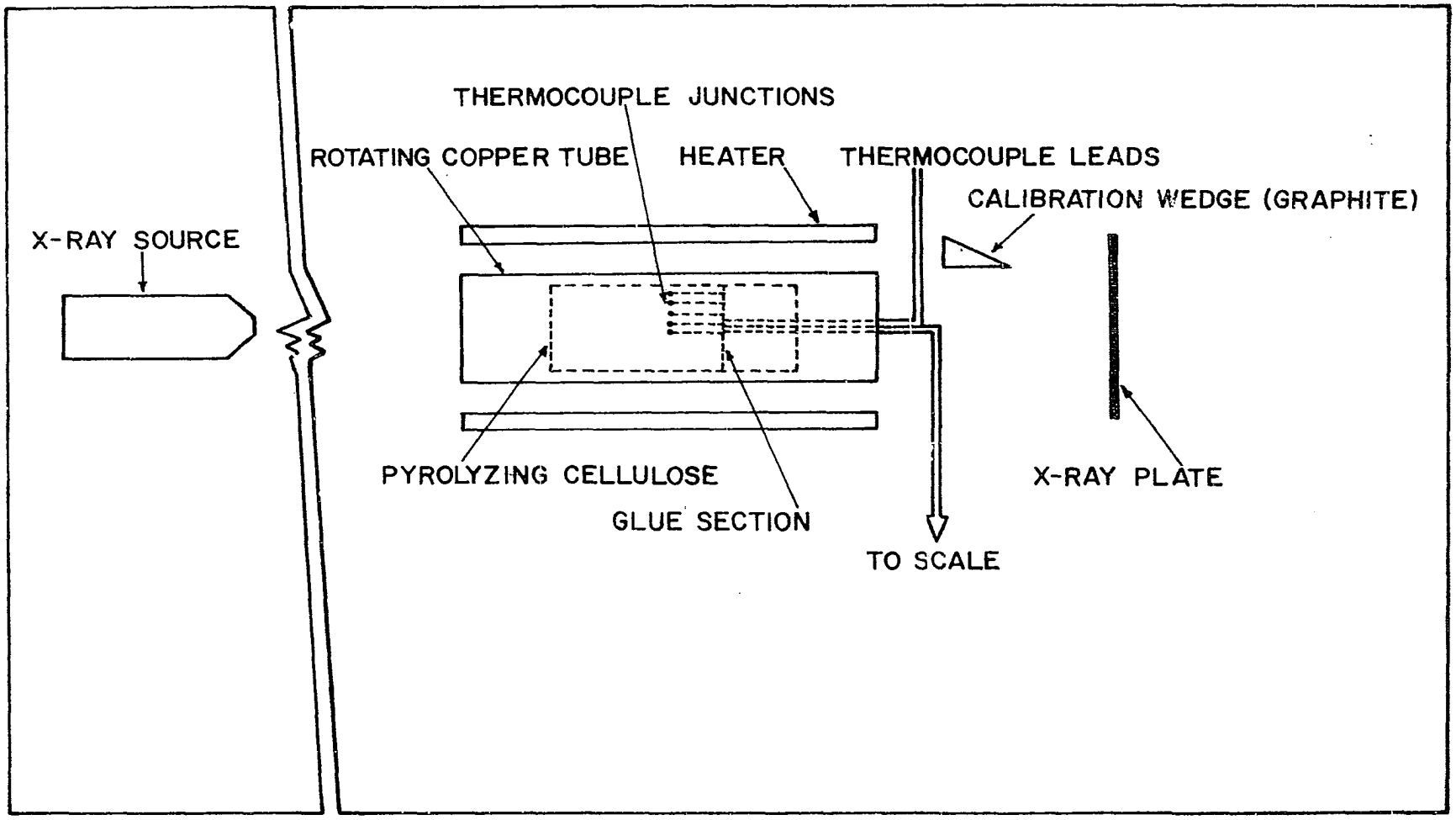


Figure II-14. Experimental Apparatus Used by Blackshear and Murty (8).

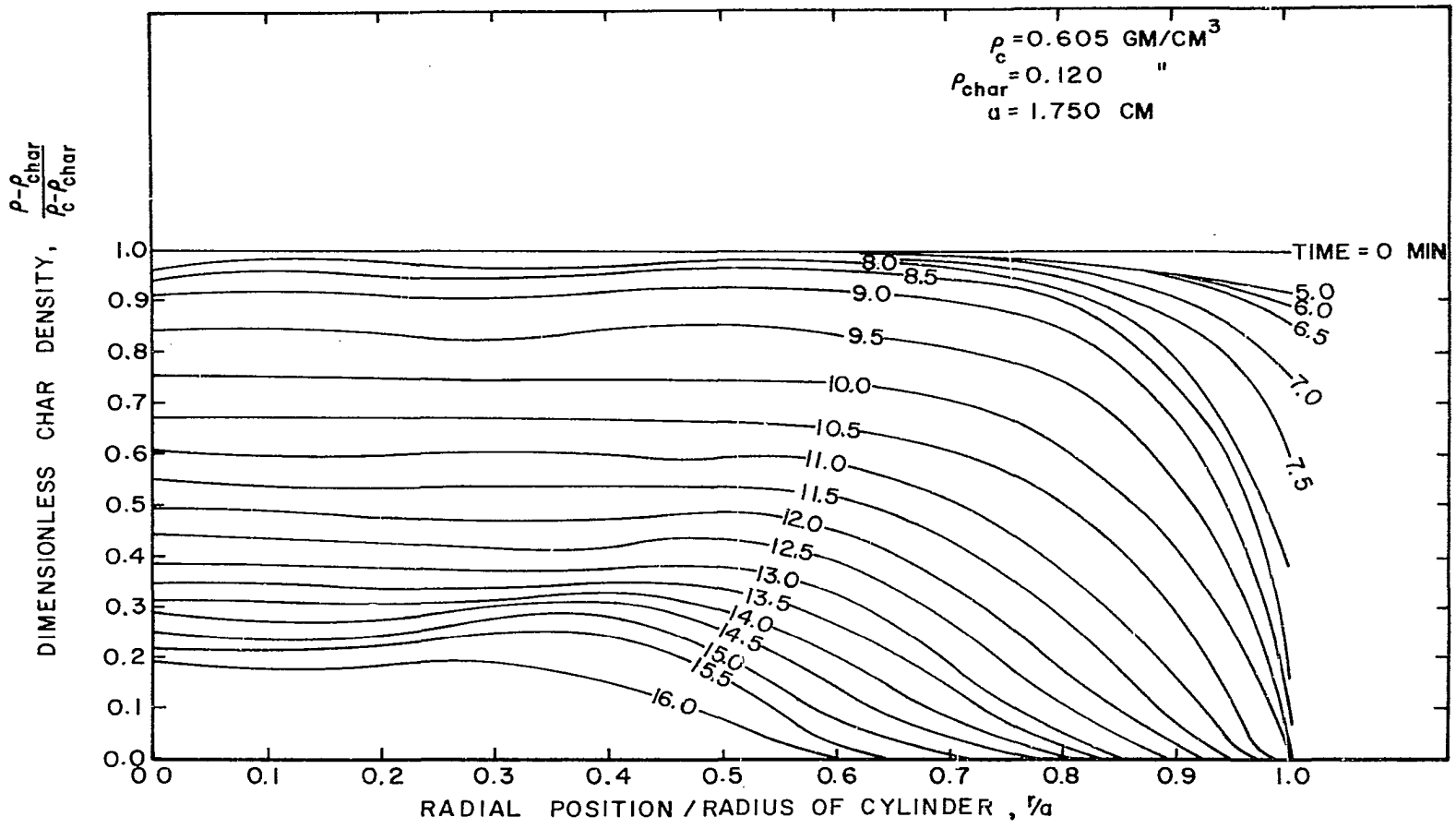


Figure II-15. Density Distribution as a Function of Time and Radius of Cellulose Cylinder (From Blackshear and Murty (8)).

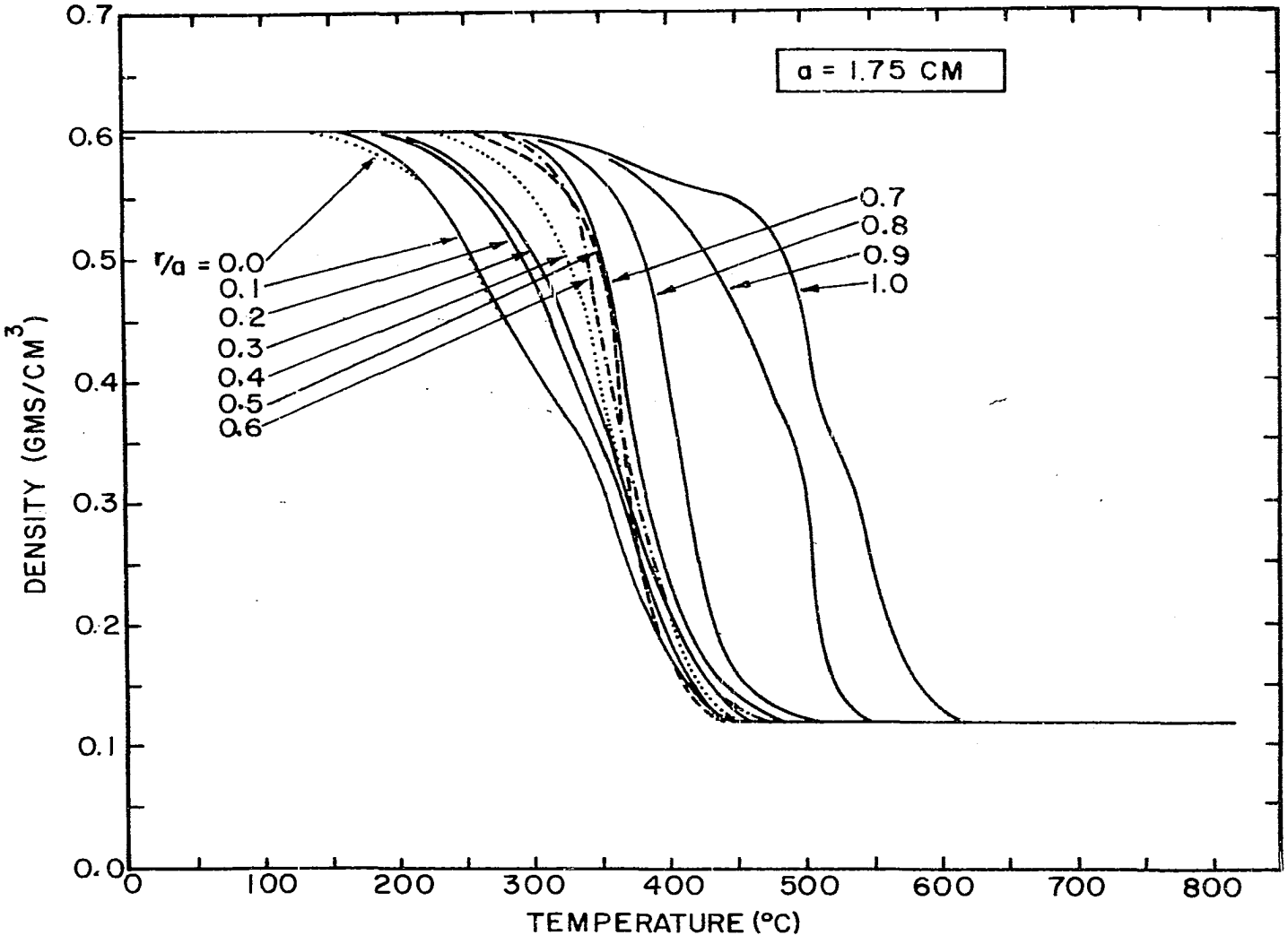


Figure II-16. Density vs Temperature Plots for Decomposing α-Cellulose Cylinder with Radial Position as Parameter (8).

To this author's knowledge, the previous studies of thermal conductivity of wood have been restricted to measurements at temperatures below 100°C, and almost no work has appeared in the literature concerning the dependence of thermal conductivity on temperature and/or decomposition history.

Before one can proceed to specify thermal conductivity of a wood specimen, it is necessary to know the effect, or by some means to eliminate the need for consideration, of the following factors:

1. Variation between thermal conductivity of summerwood and springwood.

2. Variation of thermal conductivity with density (for a given species).

3. Variation between thermal conductivity of sapwood and heartwood

4. Variation of thermal conductivity with direction due to orientation in the grain structure.

5. Variation of thermal conductivity of wood with moisture content.

Several studies have been made on thermal conductivity of wood which shed considerable light on these questions.

It should be stated here that all measurements and experiments performed in the present work were on dried wood (zero free water content); therefore, the effect of moisture was not a problem and will not be discussed, except to note where it has been studied for the benefit of the

reader who may desire such information.

Griffiths and Kaye (25) studied the effect on thermal conductivity of wood structure, direction of heat flow, and moisture content, in eight species. With reference to the directional dependence, they defined three approximately perpendicular axes of reference in a wood specimen:

1. Parallel to the grain, or wood fibers
2. Across the grain (perpendicular to fiber length) and radial to the annual growth rings
3. Across the grain (perpendicular to fiber length) and tangential to the annual growth rings.

Figure II-17 illustrates the appearance of the annual rings in a specimen of ash. Samples were cut from the positions indicated in the figure. For instance, a circle indicates that a disc, 1 3/4 inches in diameter, was cut from the position shown. The flow of heat in the thermal conductivity measurement, of course, took place at right angles to the disc. The rectangles indicate such a disc in section. In this way samples were obtained which permitted the determination of thermal conductivity with heat flow along any one of the principal axes defined above. In addition, samples were taken in the same manner but from a location where the growth rings were very close in order to determine the effect of grain density. In these "close grain" samples, the direction of heat flow with reference to the principal axes is denoted by:

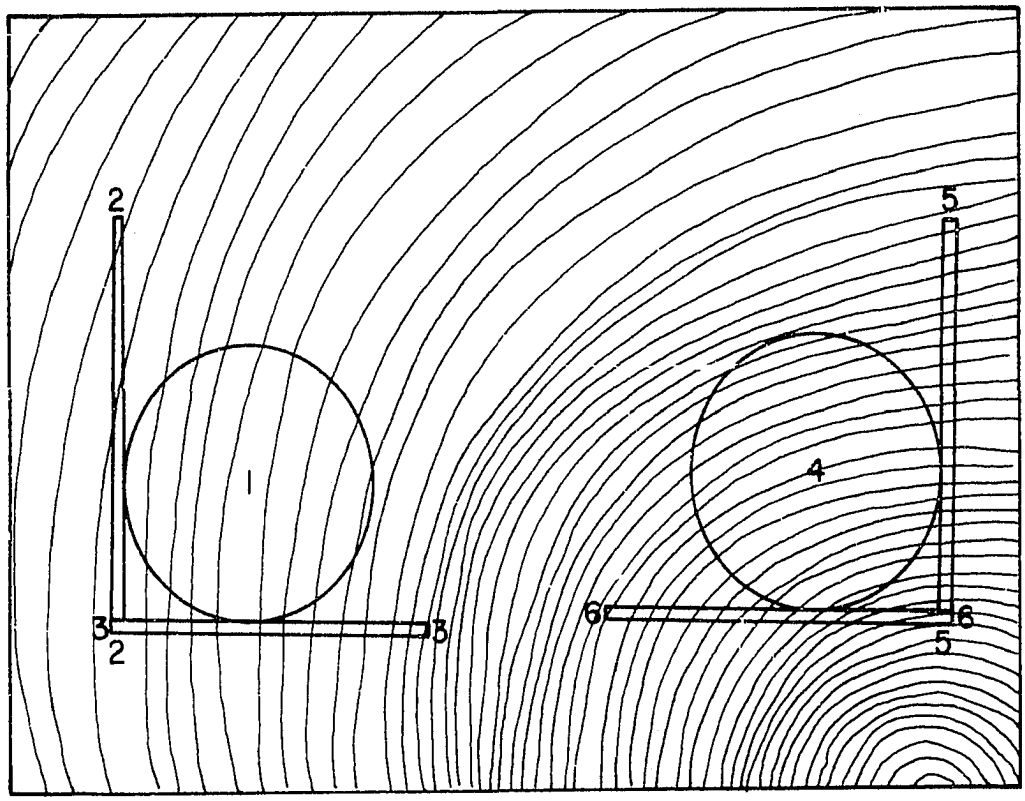


Figure II-17. Schematic of End Grain Pattern of Ash Board Showing Location of Test Specimens (25).

4. corresponding to (1) above

5. corresponding to (2) above

6. corresponding to (3) above.

Griffith and Kaye's results of thermal conductivity measurements of the eight types of wood, by the hot-plate method, are shown in Table II-10. The temperature drop across the test specimen varied from 3° to 20°C in different tests. Although all samples tested contained appreciable amounts of moisture, the data serve to show the effect of direction of heat flow on the thermal conductivity. Griffith and Kaye concluded that the longitudinal conductivity is roughly twice that of either transverse conductivity, and that the radial conductivity is approximately 5 to 10% greater than the tangential conductivity. They stated that the higher longitudinal conductivity was due to the virtually unbroken heat flow path in that direction as contrasted to either transverse direction. They believed the slightly higher conductivity observed in the radial direction over the tangential direction was due to the radially directed wood rays, which provided an easy path for flow in the radial direction but obstructed heat flow in the tangential direction. It should be noted that the moisture content, which has a rather strong effect on conductivity, was not constant throughout and that there are exceptions to the statement of higher conductivity in the radial direction than in the tangential direction (see ash). Thus, one may properly question if a significant difference in the two transverse

TABLE II-10

THERMAL CONDUCTIVITY VALUES FOR WOOD
REPORTED BY GRIFFITHS AND KAYE (25)

Species	Density (gm/cm^3)	Position	Thermal Conductivity* ($cal/cm^2 sec °C/cm$)
Ash	0.74	1	0.000365
	0.74	2	0.000369
	0.74	3	0.000714
	0.74	4	0.000464
	0.74	5	0.000416
	0.74	6	0.000754
Mahogany	0.70	1	0.000391
	0.70	2	0.000351
	0.70	3	0.000701
	0.70	4	0.000416
	0.70	5	0.000387
	0.70	6	0.000776
Spruce	0.41	1	0.000341
	0.41	2	0.000264
	0.41	3	0.000550
	0.41	4	0.000242
	0.41	5	0.000237
	0.41	6	0.000509
Walnut	0.65	1	0.000346
	0.65	2	0.000326
	0.65	3	0.000794
Teak	0.72	2	0.000314
	0.72	5	0.000341

*Mean Sample Temperature = 20°C.

directions is shown by the data. In any case it appears small.

Rowley (55) stated that over 100 tests on 14 species of wood by the U.S. Forest Products Laboratory in 1929 led to the following conclusions:

1. Thermal conductivity varies approximately as a linear function of density in any given species.

2. Somewhat greater conductivity may be expected tangential to the growth rings, than radially, in species with strongly marked annual rings.

3. No consideration need be given to the position of annual rings in species of uniform grain.

4. Thermal conductivity varies substantially as a linear function of moisture content if the latter is expressed in terms of weight per unit volume of wood.

Note that Rowley's observation that tangential conductivity is somewhat higher than radial conductivity in wood with strongly marked annual rings conflicts with that of Griffiths and Kaye. Also, Rowley states that where the growth rings are not evident, no difference could be found. Thus, there seems to be further indication that the difference is very small, if significant at all.

Wangaard (75,76) studied the effect on thermal conductivity in 40 tree species of density, moisture content, direction of heat flow, and chemical composition (resin content, etc.) using the hot plate method, and he compared his results with those of Rowley. All tests were made with

approximately a 25°C drop across the specimen and a mean temperature of 28°C. Wangaard's comparison of Rowley's data with his own gave an average difference of only 0.86%, which was not statistically significant. He concluded:

1. A high correlation existed between heat conductivity and density and moisture content in wood below the fibersaturation point. (He presented an alignment chart to show the relationship between conductivity and these two variables).

2. Radial conductivity was found to exceed tangential conductivity in the hardwoods (these have strong grain structure) by a small but significant amount. This difference may be attributed to the influence of the radially oriented wood rays. The ray volume in the softwoods is so small that the difference in conductivity in the radial and tangential directions is insignificant.

3. The type, size, and arrangement of the longitudinal cells in wood, at least insofar as they are contrasted in the structure of hardwoods as compared with softwoods, had no appreciable effect upon the transverse conductivity of heat.

4. Pecularities in gross structure or chemical composition of the wood of individual species appeared to exercise little or no influence upon thermal conductivity, other than that due to the resultant change in density.

MacLean (44) reported thermal conductivity values for 32 species of wood, comprising both hardwoods and

softwoods. The primary variables studied were density, moisture content, proportion of springwood and summerwood, and direction of heat flow. The measurements were made with a temperature drop of 22 to 28°C between the two faces of the sample. The average temperature of the test specimens was about 30°C. His results showed that the thermal conductivity of oven-dry wood could be correlated with density by the linear relation:

$$K = 0.00478\ \rho + 0.000568$$

where K = Thermal conductivity ($cal/cm^2 sec°C/cm$)

ρ = Density of wood (gm/cm^3)

The intercept, $K = 0.000568$ $cal/cm^2 sec°C/cm$, at zero density, is the approximate conductivity of air at the average temperature of the specimen. The maximum deviation of the experimentally determined thermal conductivity of 18 different species in 84 tests on oven-dry wood was 8.4% with an average absolute deviation for all determinations of 2.9%. Included in the 84 tests were samples with varying amounts of sapwood and heartwood. MacLean also tested Douglas fir specimens to compare conductivity in the radial and tangential directions. He found no pronounced differences although there appeared to be a tendency for higher conductivity in the tangential direction. He also stated that there probably would be no important difference in conductivity for these two directions. MacLean's data was in general agreement with other investigators in showing the conductivity in the

longitudinal directions was about 2 1/4 to 2 3/4 times the conductivity in either of the transverse directions.

Effect of Moisture Content

Wood absorbs moisture from the surrounding air. When the wood is heated that moisture will have an effect on the heat transfer characteristics of the specimen and on the wood decomposition process. Very little work has been done to determine its exact effect although it obviously will act as an additional heat sink. Thus, its vaporization heat requirement could be an important factor in determining the transient temperature history of a wood specimen.

As has been discussed in the previous section, some studies have been made to determine the effect of absorbed moisture on the thermal conductivity of wood at temperatures well below 100°C. No work has been done (to this author's knowledge) to include the effect of heat of vaporization or transfer of heat due to moisture migration in heat transfer models. Some authors (8) have suggested that as the surface of a specimen heats up, the moisture immediately below the surface may vaporize and migrate further into the wood where it recondenses and thus acts as a vaporization heat sink repeatedly. However this mechanism has not been proven.

Most of the work done on moisture migration in heated wood samples has been for the purpose of obtaining information important to the design of wood-drying facilities, and as such, has not included any effects on wood decomposition.

Suggestions have also been made that the presence of free moisture may actually alter the decomposition mechanism and the products which are formed as a result of the decomposition.

In short, very little is known about the exact effect and importance of free moisture in a wood specimen on that specimen's behavior when it is subjected to an external heat flux of sufficient intensity to cause thermal decomposition.

Effect of Diathermancy

If any solid material is exposed to thermal radiation, some of that radiation will penetrate the surface of the specimen only to be absorbed in the interior. The extent of that penetration will depend on the properties of the solid material and the spectral distribution of the thermal radiation.

Most heat transfer models which have been proposed for wood decomposition-ignition-combustion studies have assumed the wood specimen to be opaque, so that all incident thermal radiation is absorbed or reflected at the surface and subsequent transfer of heat to the wood specimen's interior is by conduction only.

The effect of diathermancy (free passage of heat rays) can have a pronounced effect on the temperature distribution in an irradiated solid. It is quite possible that in a diathermanous, inert material, which is being heated by external thermal radiation and which is losing

heat from its surface, a temperature maximum may occur in the specimen interior.

Williams (80), in a Ph.D. thesis on damage initiation in organic materials exposed to high intensity thermal radiation, studied the effect of the spectral distribution of the incident radiation on diathermancy in plastics and wood. He concluded that oven-dried birch and pine samples are effectively opaque to radiation emitted from a black body at 2000°K or below, where the major portion of the radiation has a wavelength in the infrared region. However, for higher "effective black body temperature" sources, the spectral distribution is shifted more into the shorter wavelength region and diathermancy can become an important factor.

Effect of Internal Convection and Secondary Pyrolysis

When a wood specimen begins to decompose due to application of heat, the decomposition products must pass from their location of origin to the surface of the specimen in order to escape. Usually, these decomposition products, whose temperature is initially close to the solid temperature at the location and time of their origin, must pass through a region of higher temperature before reaching the surface. Thus heat exchange can occur from the hot solid to these decomposition products, resulting in a lower solid temperature near the surface than might otherwise be

expected.

In addition, there is the possibility that the products of the primary pyrolysis of the wood, when contacting these higher temperature regions, may further decompose or react with the solid or other absorbed gases and thus further alter the heat absorption-transfer behavior of the specimen.

In studies of thermal degradation of cellulosic materials, it has almost always been assumed that these modes of energy transport are negligible in comparison with the conductive mode of heat transfer. To this author's knowledge, the only work done to establish the importance of these effects is that of Blackshear and Murty (8).

Blackshear and Murty assumed a model consisting of a solid matrix that remains inert while an entrained active material within the matrix is gasified, wherein the gasified material and the inert matrix are in thermal equilibrium. They arrived at the following set of equations for a plane one-dimensional system in which the pyrolysis or gasification process is describable kinetically as a first order process.

$$\frac{\partial}{\partial T}(\rho h) = \frac{\partial}{\partial x} K \frac{\partial T}{\partial x} + C_g W_g \frac{\partial T}{\partial x} + \rho_g^\circ (C_g T + H_r)$$

$$\rho_g^\circ = \frac{\partial W_g}{\partial x} \qquad \text{(II-24)}$$

$$\rho^\circ = \rho_g^\circ = -(\rho - \rho_m)(k_o e^{-E/RT}) = -\rho_g k_o e^{-E/RT}$$

where ρ_g = density of active, or gasifiable material (gm/cm^3)

ρ_m = density of inert matrix (gm/cm^3)

ρ = density = $\rho_g + \rho_m$ (gm/cm^3)

ρ° = rate of change of density with time ($gm/cm^3 sec$)

k_o = frequency factor (sec^{-1})

K = effective thermal conductivity (here assumed to be that of the solid matrix) ($cal/cm^2 sec°C/cm$)

C_g = specific heat of the gaseous materials (assumed constant) ($cal/gm°C$)

h = enthalpy of local gaseous and solid components (cal/gm)

T = temperature (°C)

H_r = heat of pyrolysis or reaction (cal/gm)

W_g = mass flow rate of gasified material per unit of cross section ($gm/sec\ cm^2$)

This model makes provision for energy transport by conduction, internal convection, and primary decomposition heat effects. It neglects secondary pyrolytic or reaction heat effects in the outflowing gases in the char layer.

When the characteristic length is ℓ, the ratio of the convection term ($C_g\ W_g\ \partial T/\partial x$) to the conduction term ($\partial/\partial x\ K\ \partial T/\partial x$) becomes

$$\frac{\text{energy flux by convection}}{\text{energy flux by conduction}} = \frac{C_g\ W_g}{K} \qquad \text{(II-25)}$$

which has the form of a "modified" Peclet number, where $C_g W_g$ refers to the gaseous material and K refers to the solid matrix. Thus if $C_g W_g \ell/K << 1$, Blackshear and Murty suggested that the convective effects can be neglected in comparison with the conduction effects.

Blackshear and Murty assumed that after a time

$$t = \frac{\rho C L^2}{K}$$

where ρ = density (gm/cm^3)

C = heat capacity ($cal/gm°C$)

K = thermal conductivity ($cal/cm^2 sec°C/cm$)

L = thickness of specimen (cm)

the characteristic length of a burning specimen should be its thickness L. They then suggested that a criterion for the neglect of the convection term in Equation (II-24) for $t \geq \rho C L^2/K$ would be a lower limit on the value of $W_g C_g L/K$, specifically

$$W_g C_g L/K < 0.1$$

The data most readily available for examining the magnitude of this "Peclet number" is the value W_g at the specimen's surface. Using data they obtained by measuring mass loss rates of vertical cylinders 5 cm in length burning in room air and data obtained from Bamford, Crank, and Malan (3) and Roberts and Clough (53), Blackshear and Murty presented the results in Table II-11, where the value of W_g at the surface of the specimen is denoted by $\dot{m}''$.

TABLE II-11

ESTIMATES OF MAGNITUDE OF INTERNAL CONVECTION HEAT EFFECT IN DECOMPOSING CELLULOSIC MATERIAL BY BLACKSHEAR AND MURTY (8)

Source	Remarks	L (cm)	K (cal/cm sec°C)	C_g (cal/gm°C)	$\dot{m}''^2$ (gm/cm^{2}sec)	$\frac{\dot{m}''C_gL}{K}$
Blackshear and Murty (8)	$\dot{m}''$ = maximum value measured after $t = \rho C_g L^2/K$	0.667	16×10^{-4}	0.27	11.8×10^{-4}	0.133
		0.687			11.69	0.135
	L = radius of cylinder	0.696			9.26	0.109
	K obtained from measured values of thermal diffusivity and density, and an assumed specific heat for the solid $C = 0.55\ C_g$: estimated	0.762			10.30	0.133
		0.909			8.14	0.125
		1.016			8.56	0.146
		1.028			8.91	0.155
		1.048			8.80	0.156
		1.175			9.16	0.181
		1.206			8.28	0.169
		1.276			6.70	0.144
		1.479			8.05	0.200
		1.606			7.86	0.214
		1.619			8.34	0.228
		1.835			6.28	0.194
		3.225			5.84	0.320
Bamford, Crank, Malan (3)	$\dot{m}''$: taken from Table 1, ref. (3)	0.555	2.7×10^{-4}	0.27	6.96×10^{-4}	0.380
		1.035			5.08	0.521
	$\dot{m}'' = L/t \times 0.375$	1.270			7.92	1.001
	L = 1/2 thickness of specimen	1.035			5.88	0.602
	t = total heating and burning time	1.585			4.50	0.715
		1.900			4.16	0.792
	K taken from ref. (3) C_g estimated	2.070			3.37	0.700
Ref. (3) Table 3	Data for 5 cm thick specimen of Columbian pine heated radiantly on one side $\dot{m}'' =$ (final depth of char/ total time) 0.375	0.435	2.7×10^{-4}	0.27	13.5×10^{-4}	0.635
		0.50			11.6	0.370
		0.83			10.35	0.860
		0.75			9.90	0.745
		5.0			5.47	2.74
Roberts and Clough Ref. (53)	Data from Table 1 of ref. (53) $\dot{m}''$ measured directly L = radius K and C_g estimated	0.5	2.7×10^{-4}	0.27	81.0×10^{-4}	8.1
		0.5			25.0	2.5
		0.5			170.0	11.0
		0.5			30.0	3.0
		0.5			7.6	0.76

It is seen that in no case is the Peclet number less than 0.1; therefore Blackshear and Murty concluded that neglect of the convection term in a heat balance equation such as Equation (II-24) could cause a misrepresentation of the heat flux near the surface of the specimen. It is important to note that this analysis applies only after sufficient time has passed to allow specification of the characteristic length as the sample thickness, and that for shorter times the magnitude of the computed Peclet number will result in a predicted convective contribution which is probably too high.

CHAPTER III

EVALUATION OF AVAILABLE THERMAL ANALYSIS METHODS

The initial task of this research was to review the thermal analysis methods which were available for determining heat absorption (or generation) effects and weight loss behavior of solid materials during heating and to evaluate their applicability to the study of thermal decomposition of wood.

Literally thousands of articles and several handbooks have been written concerning general application of differential thermal analysis and thermal gravimetric analysis. The text "Handbook of Differential Thermal Analysis" by Smothers and Chiang (61) alone gives a listing of over 4200 published articles prior to 1966 and the number may have doubled by now. Similar literature coverage exists concerning applications of thermal gravimetric analysis. However, the applications of these methods to problems as complex as the thermal decomposition of wood have been relatively few. For this reason a detailed evaluation of the possibility of using differential thermal analysis and thermal gravimetric analysis techniques for studies on thermal decomposition of wood had to be made before the instrumentation for this investigation could be specified.

Differential Thermal Analysis

The differential thermal analysis technique, hereafter called DTA, is based on measurement of the difference of internal energies, or heat contents, between an inert (*i.e. no internal heat generation or absorption effects*) reference material and the sample material, when both are heated in a similar thermal environment. The technique which is most often used involves measuring the temperature difference between the inert (reference) material and the material under study (usually utilizing a differential thermocouple) as the two materials are simultaneously exposed to a thermal environment which produces a linear temperature increase of the reference material.

This type of measurement has most often been accomplished experimentally by placing the reference material and sample in separate, but identical, chambers or wells in a metal heating block (or, less frequently, some other type of heat sink such as a fluid bath) such that the sample and reference materials are located symmetrically with respect to a heating element. Each chamber contains an identical temperature measuring device (usually a thermocouple). Ideally, the inert material is chosen so as to have, as nearly as possible, the same thermal and physical properties (particularly density, heat capacity, and thermal conductivity) as the material being studied.

To illustrate this commonly used technique, consider a hypothetical pair of materials, identical in all

respects except that at a prescribed temperature T_1, one of the materials, which we shall call the sample, undergoes a solid-solid phase transition which is endothermic in nature. Further assume the thermal properties of the sample are the same before and after the transition. Consider the graph of temperature vs time for the reference material as in Figure III-1. Assuming the heat input rate to be constant and the thermal properties to be temperature independent for the reference material, a straight line will result, as shown by Curve A. However, if the sample is exposed to this same thermal environment, the temperature of the sample will progress identically with that of the reference until the temperature T_1 is reached, at which time, due to the absorption of heat by the endothermic phase transition, the sample temperature will become lower than the reference material. After the phase transition is complete the sample temperature will return again to equality with the reference material temperature, as shown by curve B in Figure III-1. If the difference in temperature, $\Delta T = T_s - T_r$, between the sample and reference materials is plotted vs time (or reference material temperature) for this case, the result appears as in curve C in Figure III-1. It is seen that the differential curve exhibits a more pronounced peak than the sample temperature curve. This increased "resolution" of an endothermic (or exothermic) transition is one of the advantages of the DTA technique.

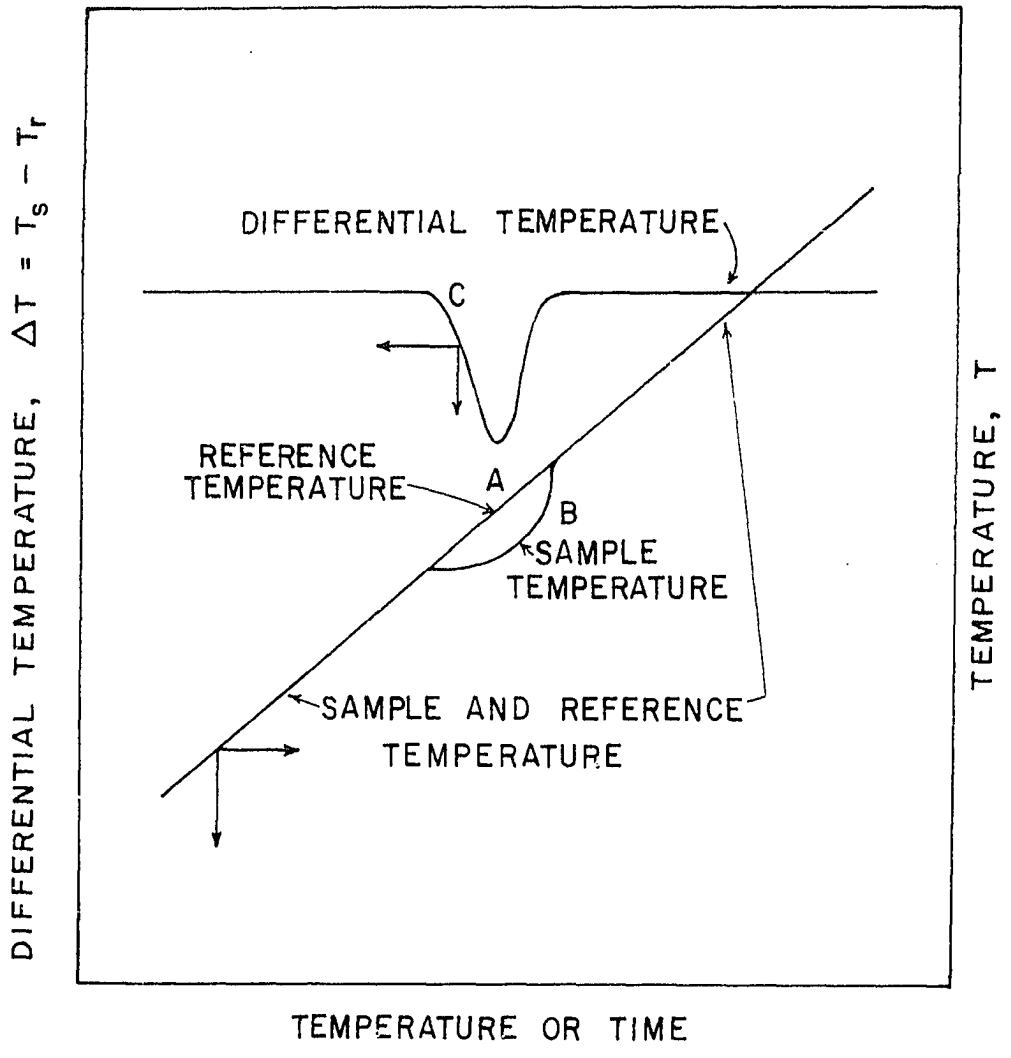


Figure III-1. Comparison of Sample Temperature, Reference Temperature, and Differential Temperature Curves in Differential Thermal Analysis.

The number, shape, and position of the various endothermic and/or exothermic "peaks" on such a record, normally called a "thermogram," may be used as a means for the qualitative identification of the material under study. In addition, since the magnitude of the differential temperature observed, and hence the area under the differential temperature curve, is directly dependent on the magnitude of the heat effect, the curves can theoretically be used to determine heats of transition quantitatively.

However, the proverbial gap between "theoretically" and "practically" is quite prominent in this application. An analysis of the technique described above suggests that the shape of the DTA curve is dependent on two general types of variables (61); (A) instrumental factors and (B) sample characteristics. These may be detailed as follows:

(A) Instrumental Factors

1. Furnace atmosphere
2. Furnace size and shape
3. Sample holder material
4. Sample holder geometry
5. Wire and junction size of thermocouples
6. Furnace heating rate
7. Speed and response of recording instrument
8. Thermocouple location in sample

(B) Sample Characteristics

1. Particle size
2. Thermal conductivity
3. Heat capacity
4. Packing density
5. Swelling or shrinkage of sample
6. Amount of sample
7. Effect of diluent
8. Degree of crystallinity

The importance of these variables and a description of their effect is discussed thoroughly in the literature (61,78); even a cursory discussion of each here would be rather lengthy. Therefore, the approach will be to single out those factors which are important in this study and discuss them as they appear.

The net effect of the dependence of DTA results on so many factors is that DTA curves measured in the manner described above are not very reproducible from one apparatus to another, or for that matter, even on the same instrument. For this reason, there has been much consideration given to the standardization of DTA instruments and procedures, but no such standardization appears to be forthcoming at the present time. Smothers and Chiang (61) describe approximately 20 DTA instruments presently on the market in this country and overseas, and their descriptions indicate considerable variation in the instrumental factors listed above.

Since one of the purposes of this work was to determine the magnitude of the internal decomposition, or pyrolysis, heat effects in wood which is being heated externally by means of a differential thermal analysis technique, the use of DTA methods for making quantitative determinations was of primary interest.

Many arguments, both pro and con, have been presented for the use of DTA in measuring heat generation or absorption effects quantitatively, and a great amount of work has been carried out concerning the theoretical interpretation of DTA data. An abbreviated discussion of the more important of these theories follows.

The most widely used theory for quantitative DTA is due to Speil (63). Consider a DTA configuration as shown in Figure III-2a. As has been outlined in the preceding section, the idealized recording of an endothermic sample transition by such an apparatus should appear as in Figure III-2b. As the temperature of the sample and reference material reaches the neighborhood of the transition temperature T_1, the sample temperature begins to lag behind the reference material temperature (point a). This temperature lag, indicated by $\Delta T = T_{sample} - T_{reference}$, increases until the rate of heat absorption by the sample due to the sample transformation is balanced by the increased rate of heat transfer to the sample well from the heated block, at point b. After point b is passed, the rate of heat absorption by the sample becomes smaller than the rate of heat transfer from the

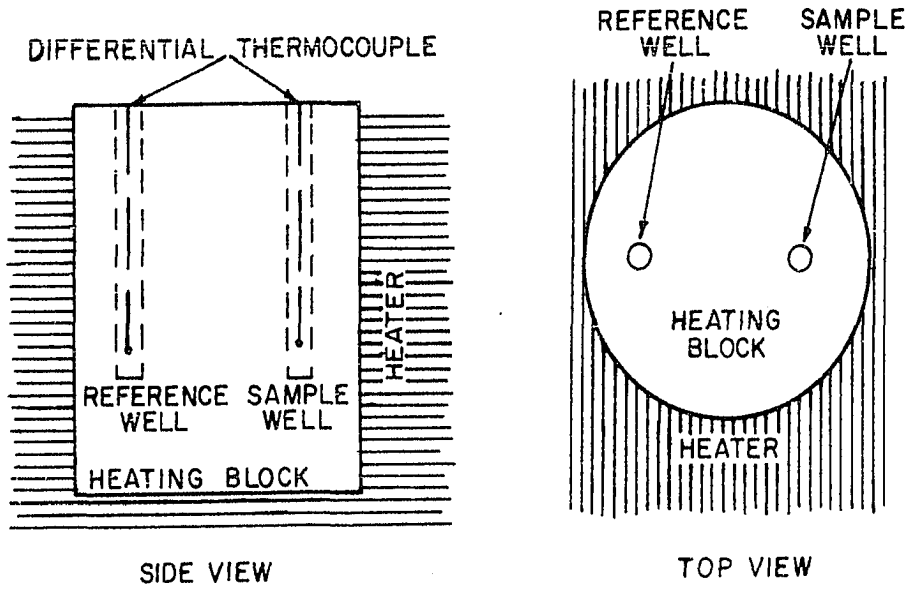


Figure III-2a. Typical DTA Configuration.

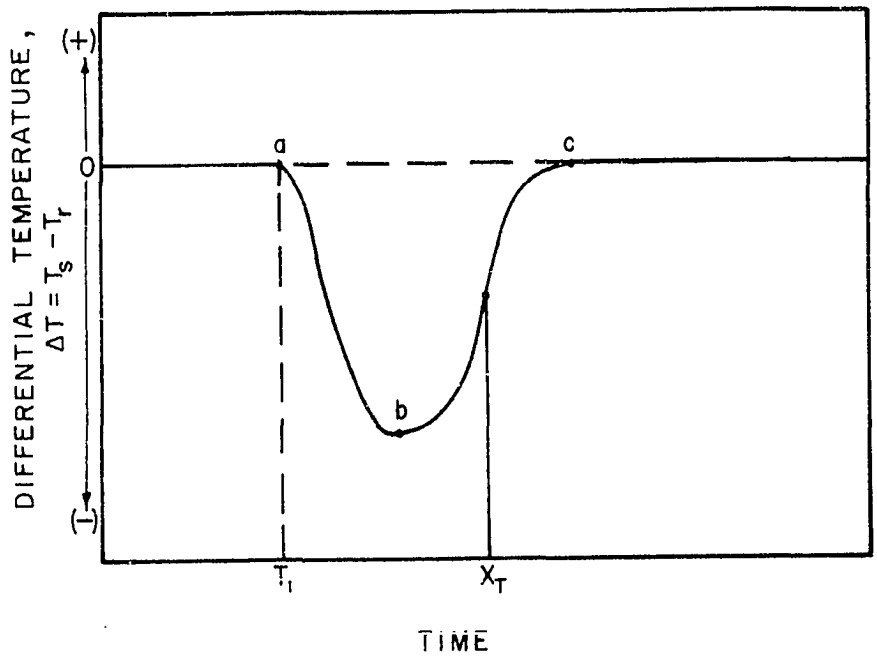


Figure III-2b. Idealized DTA Recording of an Endothermic Transition.

block into the sample so that the magnitude of ΔT begins to diminish. At some point x, between b and c, the transition is complete, and the differential temperature returns to zero at c.

If the sample temperature is assumed uniform, a heat balance (at any point in time, say x_t) on the sample gives

$$gh_s (T_w - T_s) + m_s \frac{dE_s}{dt} = m_s c_s \frac{dT_s}{dt} \qquad \text{(III-1)}$$

where the terms from left to right represent heat transferred to the sample from the heating block, the heat absorbed in the sample due to the phase change, and the accumulation of heat in the sample, respectively.

A similar heat balance on the reference material gives

$$gh_r(T_w - T_r) = m_r c_r \frac{dT_r}{dt} \qquad \text{(III-2)}$$

where: t = time (sec)

m_s = mass of sample (gm)

m_r = mass of reference material (gm)

dE_s = the increment of heat absorbed due to the endothermic transition by the sample in time dt (cal/gm)

g = geometrical shape constant (normally the same for reference and sample) (cm^2)

h_r = heat transfer coefficient between heating block wall and reference material (assumed constant) (cal/cm^2 sec °C)

T_w = temperature of heating block wall in sample and reference wells (°C)

T_r = temperature of reference (°C)

T_s = temperature of sample (°C)

c_r = sensible heat capacity of reference material (assumed constant) (cal/gm °C)

c_s = sensible heat capacity of sample (assumed constant) (cal/gm °C)

Letting

$$c_r = c_s + \delta_c \qquad \text{(III-3)}$$

$$h_r = h_s + \delta_h$$

$$m_s = m_r$$

and subtracting Equation (III-2) from Equation (III-1) gives

$$m_s \frac{dE_s}{dt} + gh_s (T_r - T_s) - g\delta_h (T_w - T_r) = \qquad \text{(III-4)}$$

$$m_s \left[c_s \frac{dT_s}{dt} - c_s \frac{dT_r}{dt} - \delta_c \frac{dT_r}{dt} \right]$$

Assuming the terms containing δ_c and δ_h are negligible compared to the other terms,

$$m_s \frac{dE_s}{dt} - gh_s \Delta T = m_s c_s \frac{d(\Delta T)}{dt} \qquad \text{(III-5)}$$

where $$\Delta T = T_s - T_r$$

Integrating between points a and c in the curve shown in

Figure III-2b, and assuming m_s, c_s, g and h_s constant,

$$m_s \int_a^c \frac{dE_s}{dt}\,dt = m_s c_s \int_a^c \frac{d(\Delta T)}{dt} + gh_s \int_a^c \Delta T\,dt \qquad \text{(III-6)}$$

$$= m_s c_s\, \Delta T\Big]_a^c + gh_s \int_a^c \Delta T\,dt$$

However, $\Delta T\Big]_a^c = 0\text{-}0 = 0$, since the curve is assumed to have returned to the original baseline. Thus

$$\Delta E_s = \frac{gh_s}{m_s} \int_a^c \Delta T\,dt \qquad \text{(III-7)}$$

Speil's treatment has been extended by Vold (74) to include the effect of heat transfer from the sample and reference to the surroundings (other than the block, for example, to include end effects) and the effect of heat transfer between the reference and sample. However, in any of the equipment now available commercially, these effects can probably be considered negligible contributions to the end result. In any case, the determination of the heat transfer coefficients representing these modes of transfer would be extremely difficult. Soule (62) derived a result similar to Equation (III-7) based on the transient heat conduction equation.

By far the largest part of the quantitative DTA measurements have been based on a mathematical model similar to Equation (III-7) of Speil. Therefore it is worthwhile to consider the validity of the assumptions which are inherent in such a model.

1. The thermal and physical properties (heat capacity, density, thermal conductivity and mass) are assumed to be the same, or very nearly so, for the sample and reference material.
2. The effect of differences in heat losses from the sample and reference material are neglected.
3. The geometrical factor is assumed to be the same for sample and reference.
4. The coefficients of heat transfer between the heating block wall and the sample and reference are assumed equal, and constant.
5. The mass of the sample is assumed to remain constant.
6. The temperatures of the sample and reference material are assumed uniform (i.e., no temperature gradients exist in the sample or reference.

Assumption (1) can be approximated by judicious choice of reference material, or by using a diluent. In the use of a diluent, the sample material is mixed with inert material in small proportions so that the resulting mixture will have a heat capacity, thermal conductivity, and density

similar to the pure reference material. The effect of using such a diluent on the resolution of heat effects has been studied by Barrall and Rogers (4).

Boersma (9) has shown that the heat conducted away from small samples through the thermocouple wires can be large enough to have a considerable effect on the area of the peak obtained. Hauser (27) and Vassallo and Harden (73) have also studied the effect of thermocouple wire and bead size, and have made recommendations on the sizes to be used in DTA work.

At temperatures where radiation heat transfer becomes important, differences in emission and absorption characteristics between sample and reference will result in differences in heat losses, even when temperatures are equal. The importance of this effect can be quite pronounced; in fact it has been used as a basis for determination of emissivities of materials by thermal analysis (54).

Assumption (3) appears to be justified, since in most DTA equipment great care is taken to insure that the sample and reference materials are located symmetrically with respect to the heating element so that the geometric constants for the sample and reference are identical. Kronig and Snoodijk (38) made mathematical calculations of the geometrical shape constant for use in Equation (III-7) for various types of specimen holders.

The assumption of constant and equal heat transfer coefficients between the heating block wall and the sample, and between the heating block wall and the reference material, has not been studied to this author's knowledge. Obviously, theoretical prediction of this value would prove very difficult, if not impossible. Normally, as will be discussed later, this problem is avoided by experimentally determining an overall calibration constant which includes this unknown heat transfer coefficient.

Assumption (5) restricts usage of the method ideally to applications where the sample does not decompose or undergo any type of weight change, or if weight change does occur, to applications where the weight (or mass) is known as a function of time (or temperature).

Assumption (6) is most often justified by making the amount of reference material and sample as small as possible so as to minimize thermal gradients. Commercially available instruments presently utilize samples weighing less than 20 mg, and are capable of analysis of a sample as small as 1 mg (61, 78).

In practice, the coefficient of the integral in Equation (III-7) is usually measured experimentally using a material of known weight and heat of transition to calculate ψ in the equation

$$m_s \Delta E_s = \psi \int_a^c \Delta T \, dt \qquad \text{(III-7a)}$$

Wittels (81) found the area under the DTA curve resulting from the decomposition of calcite according to the reaction

$$C_aCO_3 + \text{Heat} \rightarrow C_aO + CO_2$$

to be a linear function of the amount of sample, which he suggested as validation of the assumption of constancy of the factor ψ in Equation (III-7a).

Several other investigators have discussed the determination of phase transition heat effects based on measurement of ψ by calibration of the apparatus with materials having accurately known heats of transition. Kracek (37) determined calibration constants for his apparatus using the known heats of fusion of benzoic acid, silver nitrate, sodium nitrate, and potassium nitrate. Other workers using this technique include Berg, et al., (7), Kulp and Trites (40), Sabatier (56), and Barshad (6). Attempts at measuring heats of pyrolysis and combustion of wood using this procedure have been made by Tang (69) and Keylworth and Christoph (32).

In cases where the assumptions underlying the development of Speil's equation are reasonably approximated, the results of various authors appear to be in fair agreement (within ± 20% or so). It should be noted that most of the studies have been made to determine pure phase change heat effects. For example, melting of benzoic acid is a commonly cited determination. It has been used widely as a reference material for standardization of DTA instruments. However, there has been sufficient disagreement between investigators

to cause considerable doubt as to the confidence which can be placed in quantitative measurements made in the preceding manner.

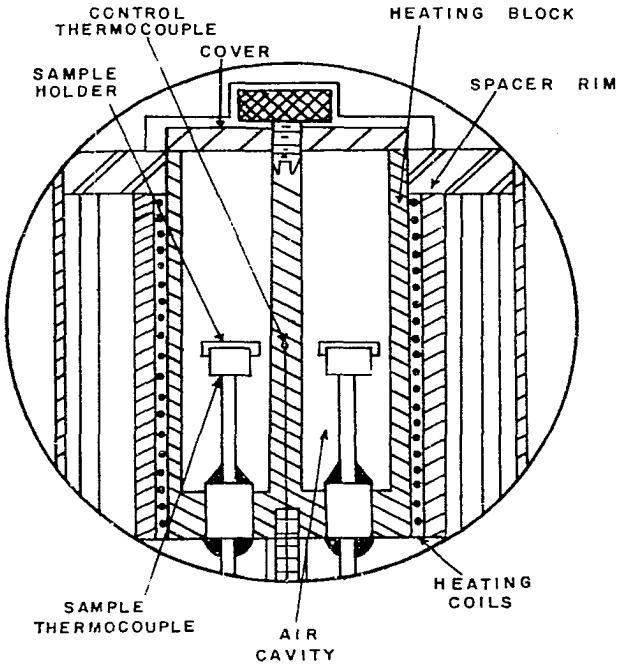
Furthermore, when the heat effect which is of interest occurs with an evolution of gaseous material and a change in physical and thermal properties, the application of such a method becomes more questionable. Boersma (9) and Schwiete and Ziegler (58) stated that thermal effects indicated by thermocouples embedded in powdered samples, in the usual DTA method, are limited by the small amount of powder immediately surrounding the thermocouple junction. Also, the thermal effects as registered by the thermocouple are influenced by changes in the thermal conductivity between the powder and thermocouple bead, which is changed when the individual particles are rearranged and changed due to thermal decomposition. This problem led Schwiete and Ziegler and Boersma to introduce the so-called Dynamic Difference Calorimetry method (58), in which the sample and reference materials are contained in separate identical closed metal crucibles, through the walls of which all heat exchange between the furnace and reference or sample occurs. The thermocouple junctions are placed in the thickened crucible bottoms, so that the enthalpy difference of the crucibles and their contents is the quantity sought. Since the heat flow path from the sample (usually in the form of a thin layer in the crucible) is more easily reproduced, it is claimed that much of the variation in results obtained from what we shall call the

"Standard DTA Method" (utilizing direct thermocouple-sample contact) is overcome.

The cross section of a calorimeter cell produced by the du Pont Company utilizing the design suggested by Boersma and Schwiete and Ziegler is shown in Figure III-3. Holders for sample and reference materials are located in separate air cavities in a heating block. A resistance heating element is wound around the block. Chromel-alumel thermocouples are welded to the bottoms of the sample and reference holders. The isolation of the sample and reference holders by the air cavity provides high resistance to heat transfer so that when the sample undergoes transition or reaction, the heat effect is retained by the sample and holder. The resulting ΔE_s value obtained from the peak area is claimed to be essentially independent of sample size, specific heat, and packing density.

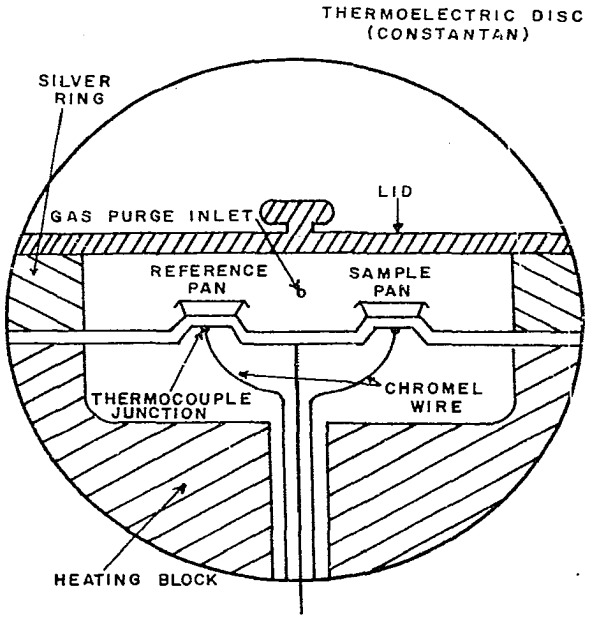
This calorimetry cell has however recently been replaced by du Pont with a new design which is marketed under the trade name "Differential Scanning Calorimeter Cell." The cross section of the cell is shown in Figure III-3. The cell design incorporates a thermoelectric disc consisting of a constantan plate with raised platforms for placement of sample and reference in shallow, 6.6 mm diameter aluminum pans. A chromel wire is welded at the center of each platform, providing a thermocouple junction in direct contact with the bottom of each pan for measurement of temperature difference. In addition, an alumel wire is welded at the

DU PONT BOERSMA-TYPE
DIFFERENTIAL CALORIMETRY CELL



CELL CROSS-SECTION

DU PONT DIFFERENTIAL
SCANNING CALORIMETRY CELL



CELL CROSS-SECTION

Figure III-3. Schematic Diagrams of "Dynamic Difference Calorimetry" Type Cells Manufactured by Du Pont.

center of the sample platform (not shown in sketch) providing a chromel-alumel thermocouple junction for determining the temperature of the sample pan. The constantan disc serves a dual function as: 1) the major path of heat transfer from the block to the sample and reference and 2) an integral part of the temperature measuring thermocouples.

In either of the du Pont cells, a calorimetric determination is made from the relation:

$$\Delta E_s\,(\text{mcal/mg}) = E \cdot \frac{A\ \Delta T_s\ T_s}{ma}$$

where E = calibration coefficient (mcal/°C·min)

A = peak area (cm^2)

ΔT_s = Recorder Y-axis sensitivity (°C/cm)

T_s = Recorder X-axis sensitivity (°C/cm)

m = sample mass (mg)

a = heating rate (°C/min)

This relation is of the same form as Equation (III-7), and can be derived by application of Speil's theory. The calibration constant E is determined, as has been discussed previously, by calibration with a transition of accurately known heat effect. Due to changes in the relative importance of the conductive and radiative heat transfer contributions to the differential temperature measurement, the calibration coefficient E is quite temperature dependent. A typical calibration curve determined with several metals with accurately known heats of fusion is shown in Figure III-4.

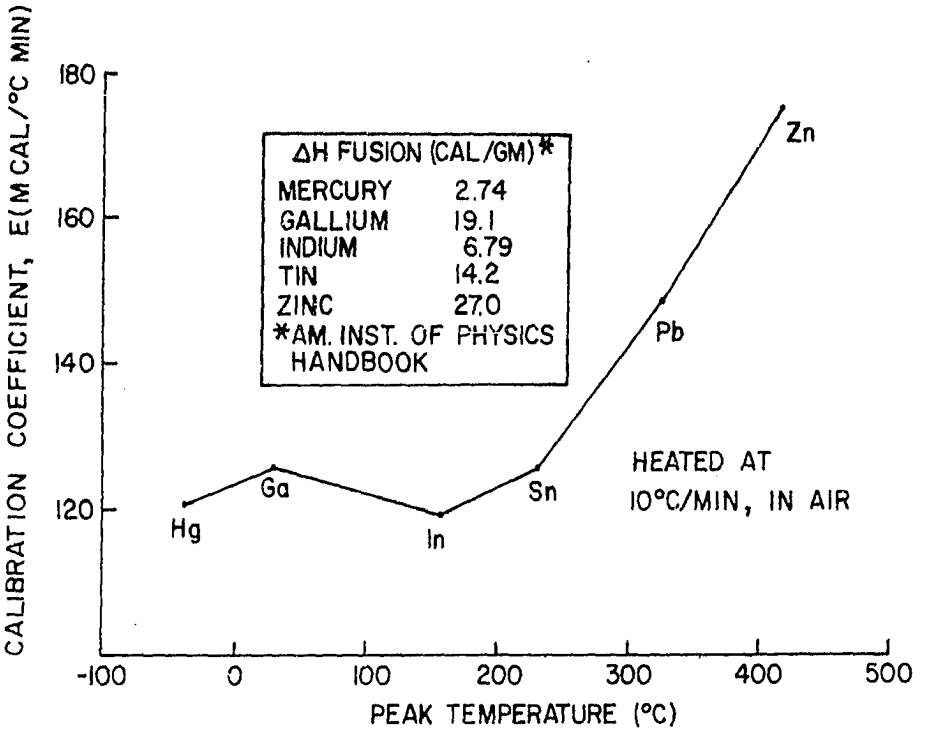


Figure III-4. Typical Calibration Curve of Du Pont Differential Scanning Calorimeter.

A differential thermal analysis instrument which operates in a different manner from those discussed before has been recently introduced by the Perkin-Elmer Company, also under the trade name "Differential Scanning Calorimeter." The method of operation is similar to the "Dynamic Difference Calorimetry" method of Boersma in that the sample and reference materials (an empty holder can be used as reference if desired) are placed in small metal holders in whose bases are imbedded temperature measurement devices (platinum resistance elements are used instead of the usual thermocouples). However, unlike "Dynamic Difference Calorimetry" or "Standard DTA," separate platinum resistance heating elements are imbedded in the bottom of the sample and reference holders so that heat to the two sides can be independently controlled. The method of operation, then, is to maintain the sample and reference holders at the same temperature by adjusting the electrical power dissipated in each holder in the required manner. Power can be increased to the sample side while being reduced to the other side or vice versa.

A block diagram of the instrument is shown in Figure III-5. The maintenance of equality of temperature of the sample and reference holders is accomplished by a differential temperature control loop. Signals representing the sample and reference holder temperatures, as measured by the platinum resistance thermometers, are fed

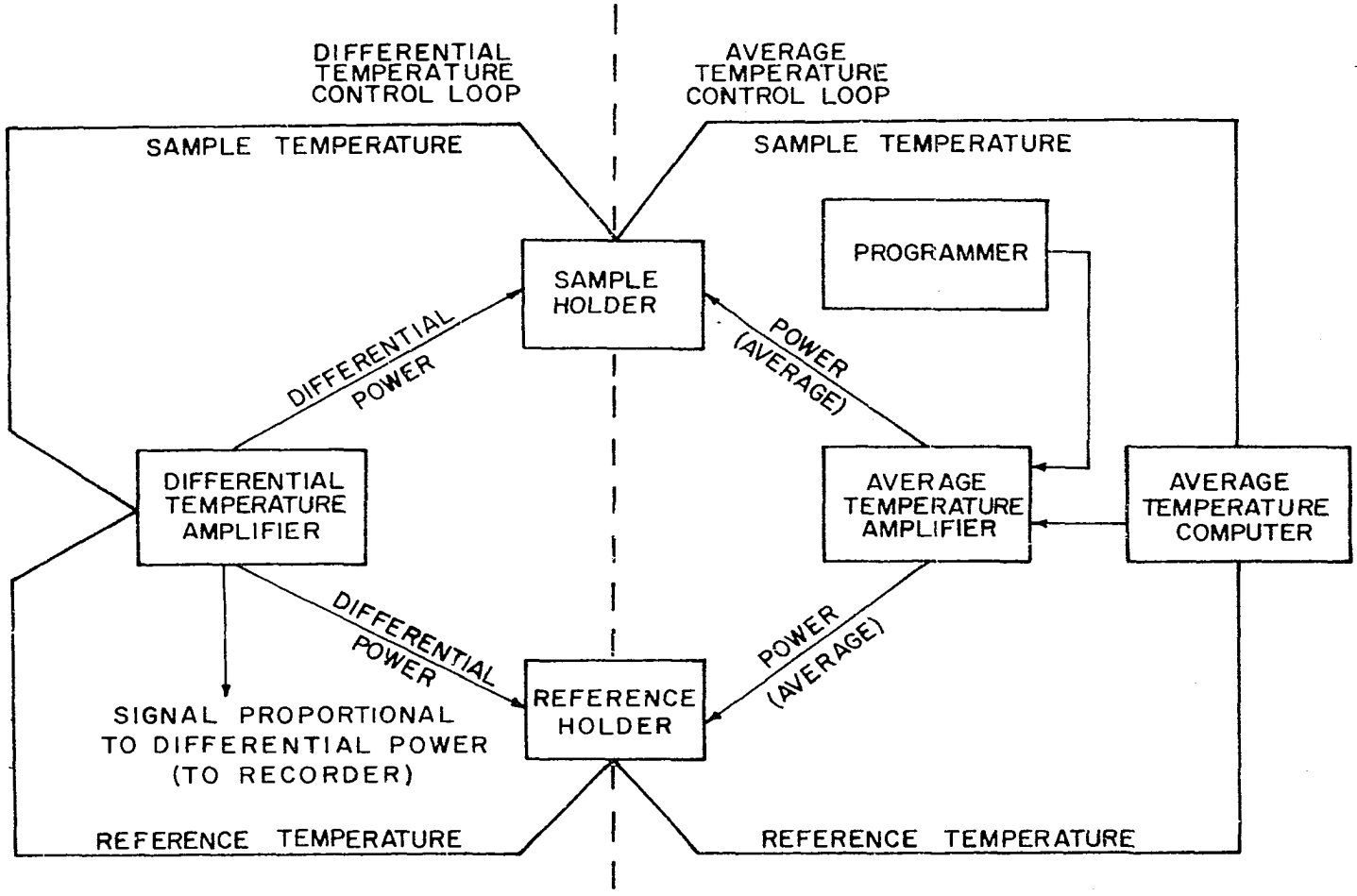


Figure III-5. Block Diagram of Perkin-Elmer Differential Scanning Calorimeter.

to a differential temperature amplifier via a comparator circuit, which determines whether the reference holder or sample holder temperature is greater. The differential temperature amplifier output is then used via a feedback circuit to adjust the differential power increment into the reference and sample holders in the direction and magnitude necessary to correct any temperature difference between them. A signal proportional to this differential power is also transmitted to a potentiometric recorder giving a recording from which differential power versus time can be obtained. The area under a peak, then, is claimed to be directly proportional to the heat energy absorbed or liberated by the sample.

In a separate control loop, a programmer provides a linearly increasing electrical signal that is proportional to the desired sample temperature rise rate. This programmer signal is compared with a signal received from the platinum resistance thermometers imbedded in the sample and reference holders via an average temperature computer. The error signal is used, via feedback, to effect a linearly increasing sample holder-reference holder temperature.

In order to make a judgment as to the desirability of one or the other of the aforementioned methods of differential thermal analysis for studies on the thermal decomposition of wood, it is helpful to regress a moment and look into the possible approaches that may be used to obtain

enthalpy or heat content information from a sample material. The discussion which follows is largely drawn from O'Neil's paper (50) although the underlying principles and reasoning are well-established.

There are two basic approaches to the extraction of enthalpy, or heat content data:

1. Adiabatic Calorimetry, in which the enthalpy or heat content of a sample is a predetermined and reproducible function of time, while the sample temperature is the dependent, measured variable.

2. Isothermal Calorimetry, in which the temperature of the sample is the independent, reproducible variable while the heat content is the dependent, measured variable.

Adiabatic calorimetry has much to recommend it; the most important advantage is the relative ease with which it is usually accomplished. It is a relatively simple matter to increase the heat content of a large thermal mass in a reproducible manner while measuring its temperature, while it is usually considerably more difficult to generate reproducible temperature programs and to measure variable heat flow rates. However, the isothermal calorimetric method is fundamentally superior to the adiabatic method in most instances. The advantage of the isothermal method is that the independent variable (temperature) is an intensive parameter while the measured, dependent, variable (heat content) is an extensive parameter. This advantage is explained in the following discussion.

The distinction between adiabatic and isothermal calorimetry can be illustrated by means of electrical circuit analogs. In the analog circuits, voltage represents temperature (the intensive parameter) and current represents heat flow rate (the extensive parameter). The passive thermal circuit elements, resistance to heat flow and thermal capacity, are analogous to electrical resistance and capacitance respectively. In an electrical circuit an ideal voltage source, by definition, has a resistance of zero, while an ideal current source has an infinite resistance. The thermal analog of a current source is a device which generates heat at a rate independent of its own temperature, such as an electrical resistance heater. The thermal analog of a voltage source is more difficult to realize; it is a temperature source, capable of delivering or absorbing heat at any rate without changing its temperature. Most thermal systems can be represented diagrammatically by a suitable combination of these ideal elements (temperature sources, heat sources, heat flow resistances, and thermal capacity).

In Figure III-6a a sample is shown totally enclosed by a sample holder, to which it is coupled by a resistance R_o (R_o will obviously depend on the area and degree of contact, and the medium separating the sample and sample holder). The sample holder is supported inside an enclosure which is assumed to be at ambient temperature T_A, and the resistance to heat flow between the enclosure and the sample holder is R_T. An equivalent thermal circuit is shown in Figure III-6b.

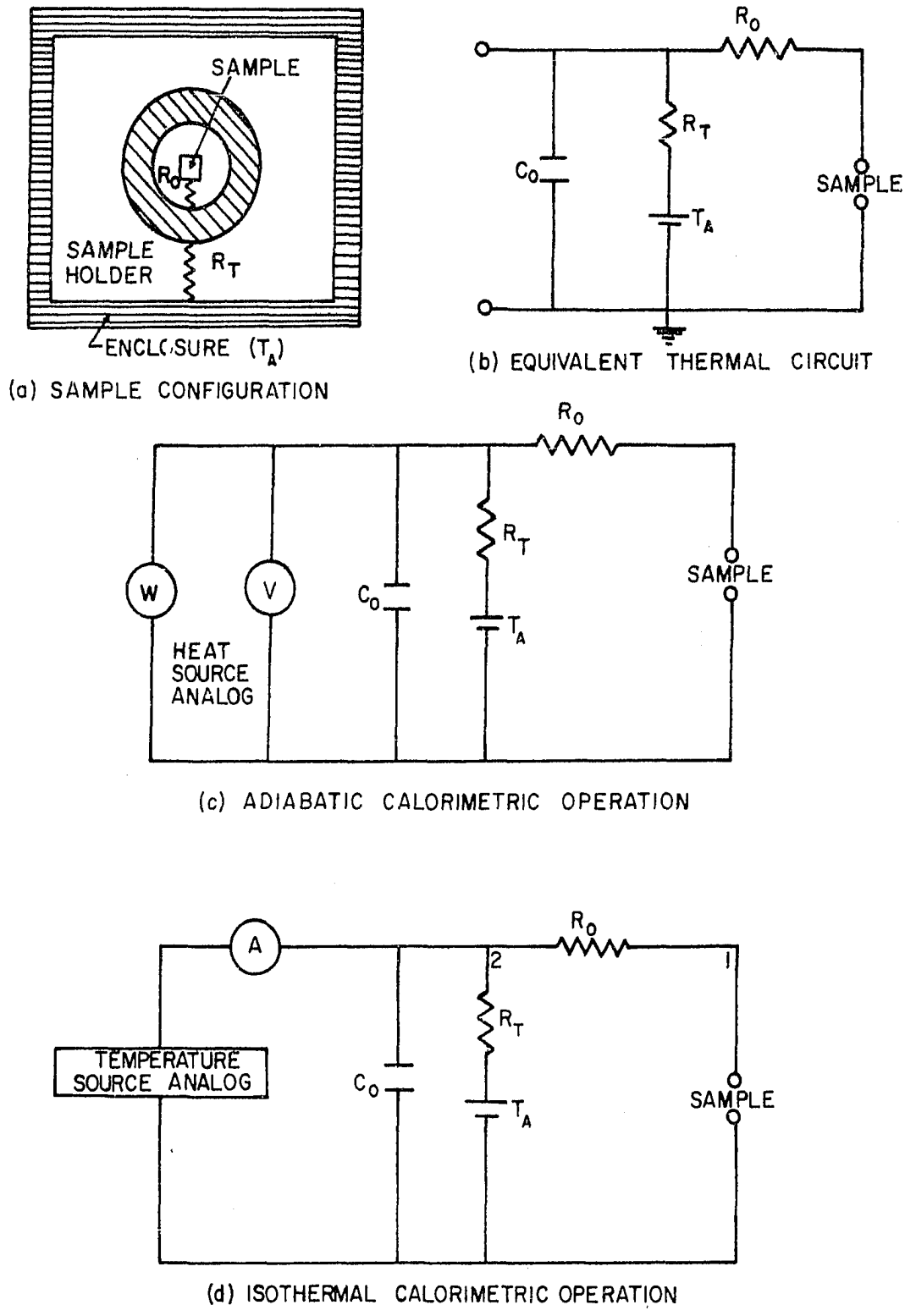


Figure III-6. Analog Representation of Adiabatic and Isothermal Calorimeters.

C_o represents the total thermal capacity of the sample holder, and the sample itself is represented by the pair of terminals so marked. Either adiabatic or isothermal calorimetry may be accomplished with this system by suitable usage of temperature and/or heat sources and associated measuring devices. For adiabatic operation, the sample holder is connected to a heat flow source shunted by a temperature measuring device (a temperature measuring device can be thought of as sort of a "thermal voltmeter") as shown in Figure III-6c. For isothermal calorimetry, a temperature source in series with a heat flow rate measuring device (a "thermal ammeter") is used as shown in Figure III-6d.

In either the adiabatic or the isothermal calorimetry system the heat flow through R_o cannot be distinguished from the heat flow through R_T to the enclosure. Since the heat flow through R_o is the desired quantity, this problem has to be overcome. An obvious solution in the case of isothermal calorimetry is differential operation, in which two identical sample holders are supplied from the same temperature source, as in Figure III-7. In this configuration, the heat flow rate into (or out of) the reference holder (either empty, or containing an inert reference material if desired) is subtracted continuously from the heat flow rate into the sample holder. The heat flow rate through R_T is determined only by the temperature source T_p and the environment temperature T_A, which are the same for both holders. Thus if R_T is made the same for both holders, this

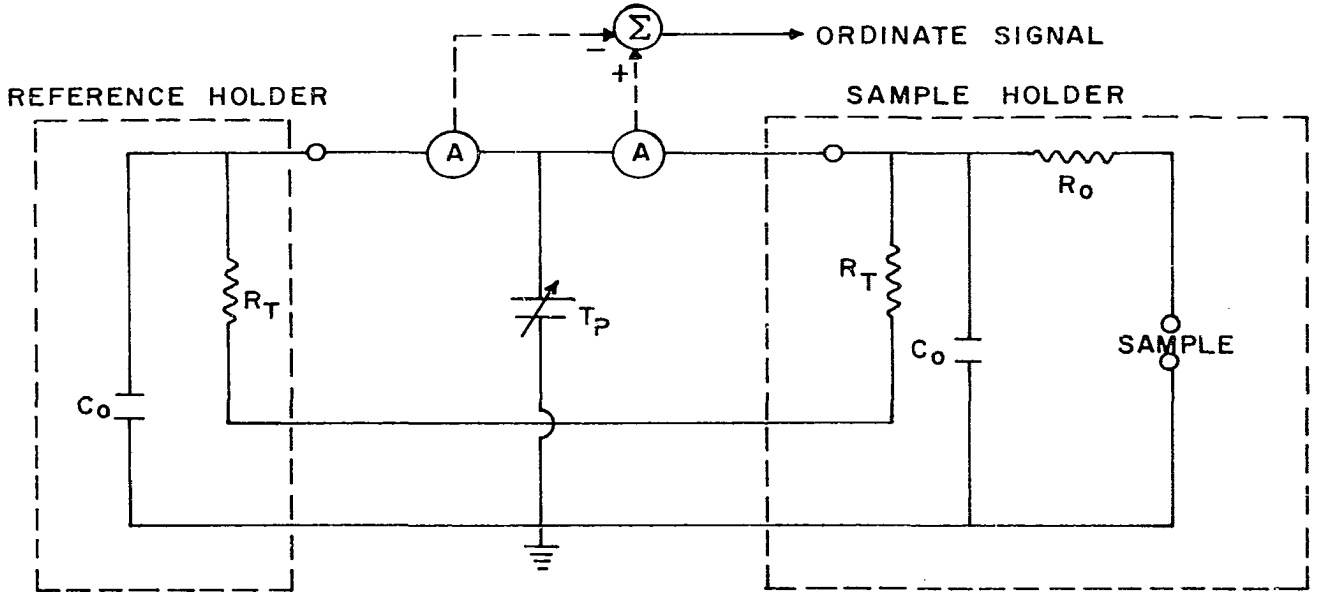


Figure III-7. Schematic Diagram of Differential Isothermal Calorimetry Setup.

differential heat flow rate is equal to the heat flow rate into (or out of) the sample.

However, in adiabatic calorimetry, the heat flow rate through R_T cannot be cancelled out by differential operation since the sample and reference temperature are not equal. This problem is a direct consequence of using an extensive parameter as the independent variable. The only alternative is to make R_T so large as to allow a negligible heat flow or to make the ambient temperature equal to the sample holder temperature throughout the analysis. Such an adiabatic calorimeter has several distinct disadvantages. Without ambient temperature control, the large thermal resistance that is required results in a large thermal time constant, with resultant low resolution capability. With ambient temperature control one is back to the problem of generating reproducible temperatures of the environment which requires further sophistication. Realization of this requirement can be very difficult depending on the ambient temperature behavior which must be effected.

Adiabatic calorimeters have reached a high degree of perfection, within the basic limitations discussed above, and the literature abounds with suggested designs and applications. For the purposes of the work done herein, however, the low resolution capability of such methods makes them inapplicable.

Most of the routine differential thermal analysis and scanning calorimetry is done with a class of instruments in which the flow of heat to the sample is not measured "directly," as it is in true isothermal or adiabatic calorimetry. In such instruments, the sample holder is coupled to a source of heat through a thermal resistance. The temperature difference across this resistance is measured, and from this data the heat flow rate is calculated. Such instruments are usually of the differential type utilizing a reference sample holder to correct approximately for heat transfer to the ambient. The differential arrangement requires that the resistances to heat flow be the same for the reference and sample sides. If the differential arrangement is not used, the resistance must be known in order to calculate the heat flow rate. Such factors as the constancy of the coupling resistance, the presence of radiation as well as convective heat transfer, and variation in sample holder geometry or heat loss characteristics from run to run must be resolved. The "standard DTA" apparatus as well as the "Dynamic Difference Calorimetry" instruments (for example, the du Pont "Scanning Calorimeter") fall into this category. The lack of reproducibility of quantitative heat effect measurements with the "standard DTA" instruments is doubtless due in large part to the problem of reproducing the contact resistance between the sample (or reference) and the temperature measuring element. In either of these methods, neither

the temperature nor the heat flow rate to the sample or reference materials is the same when a heat generation effect is occurring in the sample. Therefore neither represents a good approach to isothermal calorimetry or adiabatic calorimetry. The popularity of the methods is due partly to their ease of implementation but also to a fair extent, in this author's opinion, to a lack of understanding of their limitations.

The above discussion suggests that isothermal scanning calorimetry, if it can be accomplished, is superior in some important respects to techniques of the adiabatic type or of the "Standard DTA" or "Dynamic Difference Calorimetry" type. One means of approaching the performance of a true isothermal scanning calorimeter is by the use of proportional-feedback temperature control, and this is the method used in the Perkin-Elmer instrument discussed earlier.

Consider a sample holder with a heat flow source coupled closely to it; for example, the holders in the Perkin-Elmer instrument with their imbedded platinum resistance heaters. The temperature of the sample holder, T_S (assumed for this analysis to be a uniform temperature, so that a lumped parameter model can be employed), is determined by the heat flow rate Q, into the sample holder, and the thermal resistance between the sample holder and the environment, R_T. The environment temperature is T_A. The functional relationship of T_S and Q is non-linear in general since heat transfer can occur by combined radiation, conduction, and

convection. Such a relationship might appear as in Figure III-8 where Q is the abscissa, T_s is the ordinate, and R_T is the small signal thermal resistance between the sample holder and the environment.

To determine the response of the sample holder temperature to a sudden heat flow rate, such as would result from a sample exotherm, consider the analog circuit of Figure III-6d and let ΔQ_s be the increment of heat generated by the sample. Writing a heat balance at point 1;

$$\frac{T_s - T_{sample}}{R_o} + Q_s = 0 \qquad \text{(III-8)}$$

A current balance at point 2 gives.

$$\frac{T_s - T_A}{R_T} + C_o \frac{dT_s}{dt} + \frac{T_s - T_{sample}}{R_o} = 0 \qquad \text{(III-9)}$$

therefore,

$$\frac{T_s - T_A}{R_T} + C_o \frac{dT_s}{dt} = Q_s \qquad \text{(III-10)}$$

Initially, $Q_s = 0$ and $T_s = T_A$, and the above equation reduces at time $t = 0$ to

$$T_s - T_A = 0 \qquad \text{(III-11)}$$

Subtracting Equation (III-11) from Equation (III-10) and letting $T_s - T_A = \Delta T_s$ gives

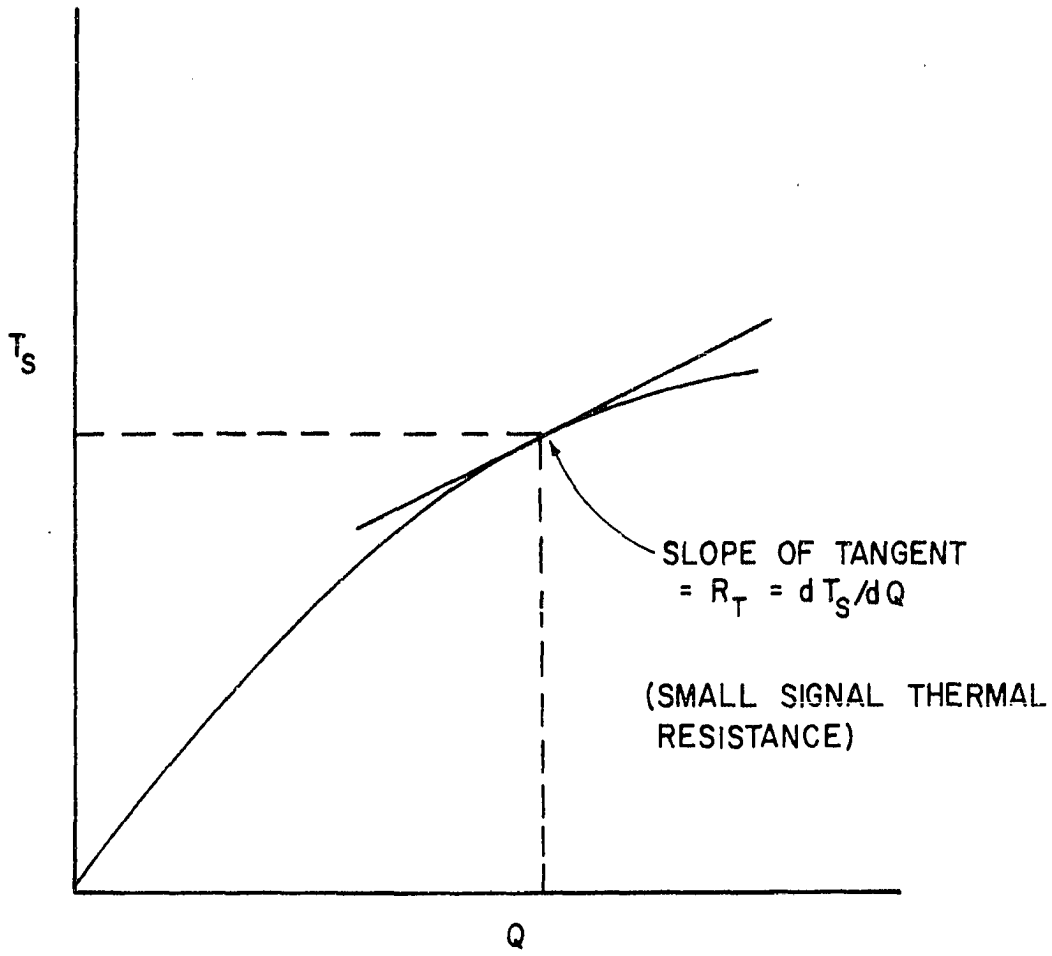


Figure III-8. Typical Temperature-Heat Flow Relationship.

$$\frac{d\Delta T_s}{dt} + \frac{\Delta T_s}{C_o R_T} = \frac{Q_s}{C_o} \qquad \text{(III-12)}$$

Taking the Laplace transform of both sides of Equation (III-12) and rearranging gives

$$\frac{\Delta T_s(S)}{Q_s(S)} = \frac{1}{C_o}\left(\frac{1}{S + 1/C_o R_T}\right) \qquad \text{(III-13)}$$

If Q_s were a step function, the response in sample holder temperature would then be:

$$\Delta T_s(t) = Q_s R_T \left[1 - e^{-t/R_T C_o}\right] \qquad \text{(III-14)}$$

For a time variable heat flow rate Q, the integral of $\Delta T_s(t)$ is just the integral of Q_s with respect to time, multiplied by a calibration factor R_T or,

$$\int \Delta T_s(t)\,dt = R_T \int Q_s(t)\,dt \qquad \text{(III-15)}$$

which is of course the same form which has been derived earlier from DTA theory. This system (without feedback temperature control) describes the dynamic behavior of a system such as the du Pont Scanning Calorimeter. Note that since the relation between T_s and Q_s is nonlinear, the small signal thermal resistance, R_T, will be temperature dependent. This dependency is vividly evident in the calibration curve for the duPont instrument as shown in Figure III-4. Also note that all heat flow (input) signals are modified by a first-order filtering time constant $R_T C_o$. The magnitude of this time constant is

of course a measure of the calorimeter's ability to resolve a transient heat effect in the sample.

Now assume that the sample holder temperature, T_s, is measured and compared with a linearly increasing signal which is proportional to a desired temperature program T_p. Assume also that the difference between these two temperatures is amplified and used via a feedback path to control the input heat flow rate Q to the sample holder. A block diagram of such a system is shown in Figure III-9.

Referring to Figure III-9, it can be shown that the response in sample temperature ΔT_s to a change in heat input ΔQ_s is described by the transfer function

$$\frac{\Delta T_s(S)}{\Delta Q_s(S)} = \frac{R_T/(1+KR_T)}{(R_T C_o/1+KR_T)S + 1} \qquad \text{(III-16)}$$

The transient response of ΔT_s is then given by

$$\Delta T_s(t) = \mathcal{L}^{-1}\left[\Delta Q_s(S)\ \frac{R_T/(1+KR_T)}{(R_T C_o/1+KR_T)S + 1}\right] \qquad \text{(III-17)}$$

where $\mathcal{L}^{-1}$ denotes the inverse LaPlace transform. For example, if $\Delta Q_s(t)$ is a unit impulse,

$$\Delta T_s(t) = R_T/(1+KR_T)\ \exp\left[-\frac{t(1+KR_T)}{R_T C_o}\right] \qquad \text{(III-18)}$$

Thus, as the amplifier gain K is increased, the response of $\Delta T_s(t)$ to sample heat inputs tends to zero, that is,

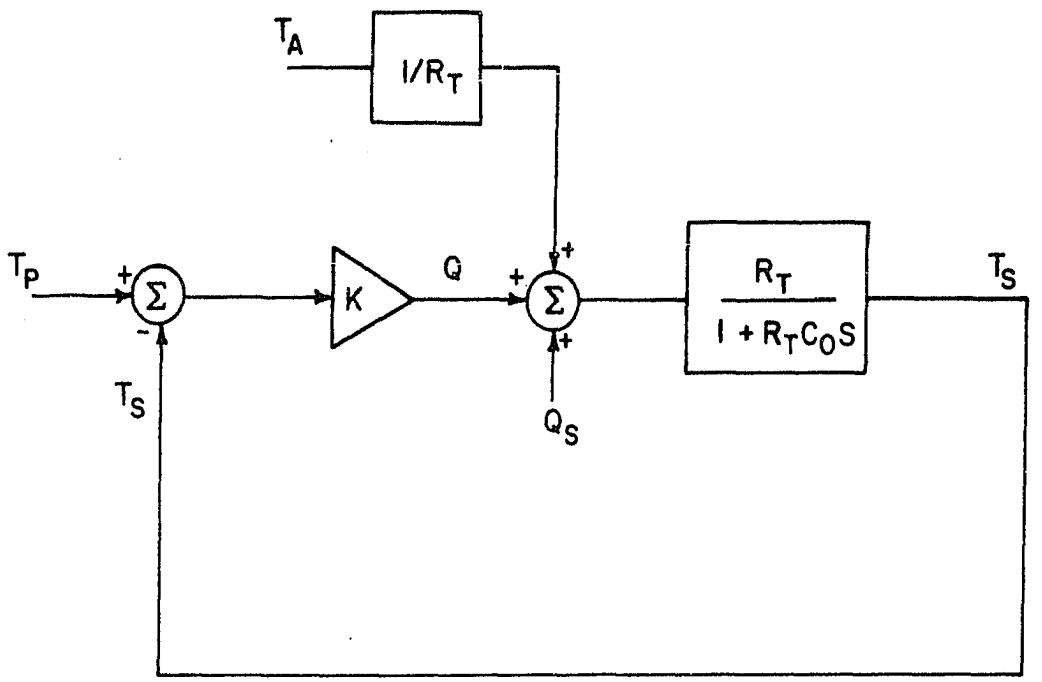


Figure III-9. Block Diagram of Sample Holder with Temperature Feedback.

the change in sample holder temperature due to heat inputs from the sample becomes negligibly small. Also, the system time constant is now

$$\tau = \frac{R_T C_o}{1+KR_T} \qquad \text{(III-19)}$$

and the speed of response is thereby improved by increasing K. Also, the heat flow Q supplied to the holder compensates accurately for the heat flow from the sample itself, Q_s. For example, it can be shown that the response of ΔQ to a unit impulse change in ΔQ_s is given by

$$\Delta Q(t) = KR_T/(1+KR_T) \exp\left[-\frac{t(1+KR_T)}{R_T C_o}\right] \qquad \text{(III-20)}$$

which tends to 1 for high values of K.

These effects can be summarized as follows:

1. The time constant given by Equation (III-19) approaches zero for large values of the gain. Therefore, since this time constant is a measure of the instrument's capability to resolve a time varying sample heat input, the resolution of the instrument is markedly improved by the addition of feedback control.

2. Equation (III-20) shows that for high gains, essentially all of the sample heat flow rate is supplied by the feedback circuit. One can, therefore, measure and record Q as a function of time and treat it as Q_s vs time. This substitution corresponds to placing a "thermal ammeter" in series with a temperature source as shown in the diagram

of the isothermal calorimeter in Figure III-6d.

As before, the heat flow through R_o is indistinguishable from that through R_T. However, this problem can again be overcome by using two identical holders which operate at the same temperature. One can then cancel the component of Q due to losses through R_T by measuring the difference between the two total heat flow rates to the holders.

Thermal Gravimetric Analysis

In thermal gravimetric analysis (hereafter TGA), the change in weight of a sample is measured as a function of increasing temperature or, as in isothermal TGA, as a function of time. The basic requirements are a precision balance and a furnace which can be programmed so as to maintain a constant temperature or to effect a controlled temperature rise; usually a linear increase in temperature is desired. The results of a TGA run may be presented as a weight vs temperature (or time) curve or as a rate of weight loss vs temperature (or time) curve; the latter is usually referred to as a differential thermo-gravimetric (DTG) curve. The DTG curve offers certain advantages over the TGA curve especially when it is desired to compare the results with those obtained by differential thermal analysis. DTG curves can be obtained from conventional TGA curves by graphical differentiation but the process is time consuming and graphical differentiation techniques are not generally

known for their high accuracy. A better method is to differentiate electronically the signal from a TGA run and to plot the DTG curve out directly. Commercial instrumentation with this capability is available.

As with DTA results, the shape of the TGA or DTG curve is influenced, to a greater or lesser extent, by several factors (78), some of the more critical ones being:

1. Heating rate
2. Furnace design
3. Method of measurement of temperature of sample
4. Sample size and form
5. The atmosphere in which the analysis is made
6. Dynamic response of weighing mechanism, recording mechanism, and temperature sensor.

As with DTA equipment, a large variety of instruments are available over a wide cost range. Coats and Redfern (17) have presented a list of requirements which should be met by a good thermal gravimetric analyzer. These include:

1. Continuous recording of the weight change of the sample as a function of temperature or time

2. Reproducibility of sample heating rate and, if possible, linearity of the sample temperature increase

3. Uniformity of the temperature in the hot zone

4. Provision for variation in heating rate, isothermal operation and controlled atmosphere or vacuum operation

5. Elimination of physical effects occurring during an analysis (radiation, convection currents, heat-up of balance mechanism, and magnetic effects caused by furnace winding) which alter the weighing mechanism performance.

6. Provision of as accurate sample temperature measurement as possible.

7. Sufficient balance sensitivity to allow use of small samples (1 mg or less).

Requirements 1, 4, and 7 are met reasonably by most commercially available thermal gravimetric analysis instruments (78) although there appear to this author to be considerable differences in the response speed capability of the different type balances, which might be important if high rates of heating are desired or if accurate resolution of fast weight changes is desired.

Since requirements 2, 3, 5 and 6 all have to do with the design of the heating system and temperature measurement, it seems fair to say that the real problems in the usage of TGA result from the uncertainties due to the heating of the sample and not to the weighing process itself.

There are numerous, widely different types of furnace or sample heater designs available; to review them here would be prohibitive, but the following assessment is generally true for most of the instruments now available.

1. Reproducibility of <u>furnace</u> heating rate (not necessarily sample heating rate) is probably very good

(say to within ± 2% of temperature range) in the more expensive instruments ($5000 class).

2. Uniformity of temperature of heating zone appears, on the basis of furnace design, to be widely different for different types of instruments. Most of the furnaces are electrical resistance wire wound elements which are designed to enclose the sample partially. Obviously the size of the furnace and the sample enclosure space should be minimized to allow high heating rates and provide for greater uniformity of the sample heating zone.

3. Temperature measurement is almost always made by using a thermoelectric sensing element (thermocouple, thermistor, or resistance thermometer) either in contact with the sample, or more frequently, very close to the sample. If the element contacts the sample, one has the problem of its effect on the weight measurement, if not, the interpretation of the difference between the temperature registered by the sensing element and the true sample temperature is a problem. Furthermore, the dynamic response of the temperature measuring element is important.

4. Wide variation in furnace-to-balance mechanism proximity in available instruments appears to exist. It seems obvious that the further removed the furnace is from the balance mechanism, especially if baffling or other means to prevent convection currents in the balance mechanism location are employed, the less interaction would occur.

However, some instruments insert the balance beam directly into the furnace, as is the case with the du Pont Thermal Gravimetric Analyzer. This arrangement does not appear to this author to be a good design. In fact, the following statement is quoted from a Cahn Electro-balance instruction manual of September 1, 1965.

" . . . The universal experience of other microbalance builders has been that even a minute amount of stray heat radiation can cause significant error, especially when it falls unsymmetrically on the two halves of the balance beam. . . . It seems extremely courageous to insert deliberately one half of a balance beam into a furnace, whose temperature not only varies but may vary as much as 1000°C during a run."

The Perkin-Elmer company has recently (Dec., 1967) introduced a thermal gravimetric analysis instrument called the TGS-1 Thermobalance which can be used in conjunction with its Differential Scanning Calorimeter. This instrument incorporates several new design concepts which, in this author's opinion, offer considerable advantages. The instrument utilizes the Cahn "RG" Recording Electronic Microbalance with the addition of a radically new furnace design which fits closely around the sample container inside a glass weighing enclosure. A schematic diagram of the system is shown in Figure III-10. The electrobalance is based on the null-balance principle. When the sample weight changes,

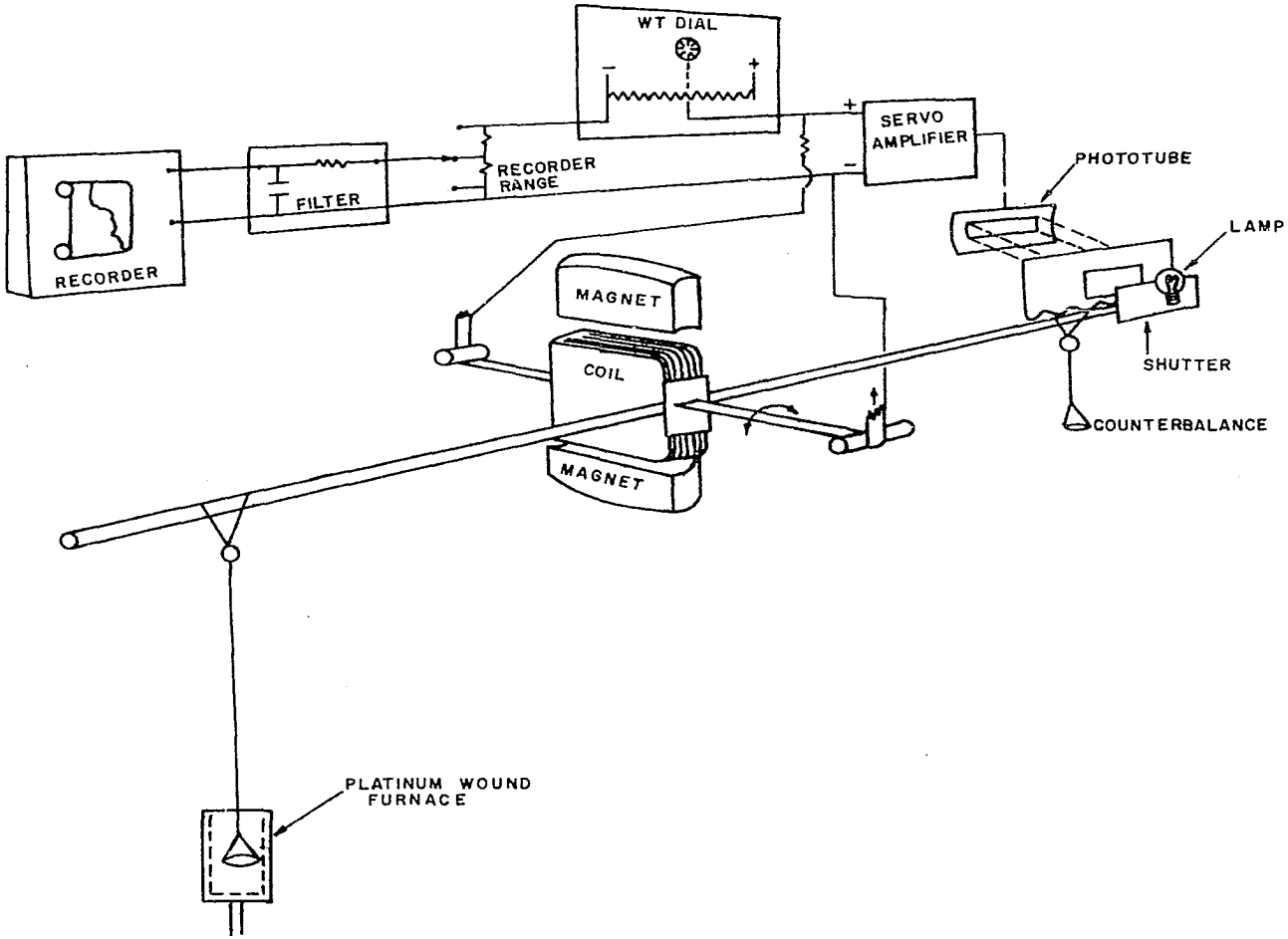


Figure III-10. Schematic of Perkin Elmer TGS-1 Thermobalance.

the beam tends to deflect in the corresponding direction. The flag mounted on the opposite end of the beam is thus moved, changing the amount of light admitted to the phototube, thus changing the phototube output current. This phototube current is amplified in a servo-amplifier and applied to a coil attached to the beam, which is suspended in a magnetic field. The current in the coil acts like a D.C. motor, exerting a force on the beam to restore it to the original balance position. This change in electromagnetic force is proportional to the change in weight, and the relation can be established by calibration with standard weights. The restoring force is so powerful and fast that the beam appears visually to be locked in place.

It is obvious that the beam cannot be returned to exactly the original position after a weight change since some offset is required to cause the added current to flow through the coil. The ratio of the offset which would occur without feedback to that which occurs with the servo operating is the servo loop gain G, and is greater than 1000 according to the manufacturer. Since the dynamic response of the beam, as measured by its time constant, is also speeded up by a factor which is a function of the servo loop gain G, the system's response time is much faster than an identical no-feedback balance, being on the order of a few milliseconds.

The samples are placed in small aluminum or platinum pans approximately 0.38 cm in diameter and 0.13 cm deep. The pan is suspended from the balance beam on a hangdown wire into the micro-furnace which consists of a 6-mil platinum wire wound on a 0.95 cm outside diameter, 1.25 cm long aluminum oxide cylinder. The bottom of the cylinder is closed and joined to a 0.16 cm aluminum oxide tube through which the heating wire passes to the external lead wires. The inside diameter of the furnace is approximately 0.76 cm so that when the sample is hanging in the center of the furnace, the distance from the sample to the furnace wall is less than 2 millimeters.

The furnace resistance wire acts as both heater and temperature sensor. In the temperature sensing mode, it forms one side of a bridge circuit, the other side being driven by the output voltage from the program potentiometer in the Differential Scanning Calorimeter control unit. An error signal is thus developed and fed to an amplifier. In the heating mode, the amplifier output is connected to the heater by means of a silicon-controlled rectifier that delivers 60 cycle power pulses necessary to correct the temperature error.

The extremely low thermal mass of the furnace allows rapid temperature rise. The instrument is capable of a heating rate of 160°C/min, considerably faster than any other instrument on the market, to this author's knowledge. The

furnace is positioned more than 17 cm below the balance beam, and a baffle arrangement to minimize convection currents is used between the furnace and balance beam. The result is that the balance accuracy is virtually unaffected by furnace temperatures of 1000°C. Another important feature is that when the system is purged with a desired gas the flow can be directed into the center hangdown tube and out the bottom of the sample hangdown tube, thus sweeping any decomposition products away from the balance mechanism.

Furthermore, a new method of temperature calibration has been utilized. The calibration is based on the use of reversible magnetic transition in ferromagnetic alloys. In this method, small samples of several ferromagnetic elements and alloys are placed in the sample pan. A magnet is positioned around the sample hangdown tube at a level below the sample, as shown in Figure III-11. Thus the ferromagnetic samples exert a downward component of magnetic force on the sample pan. This force will be registered as an apparent weight. However, as the furnace temperature is programmed upward, each of the ferromagnetic materials loses its ferromagnetism at a highly repeatable temperature called the Curie point. As the ferromagnetic force components of each sample go to zero, an apparent weight loss is recorded. Figure III-12 shows a typical calibration run using four such standards. Thus a calibration can be made of the

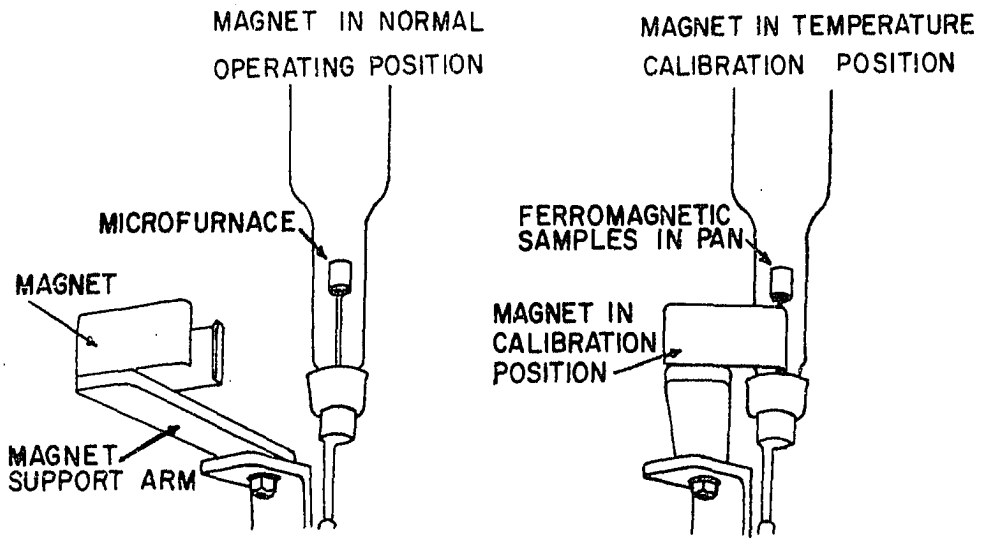


Figure III-11. Schematic of TGS-1 Temperature Calibration System.

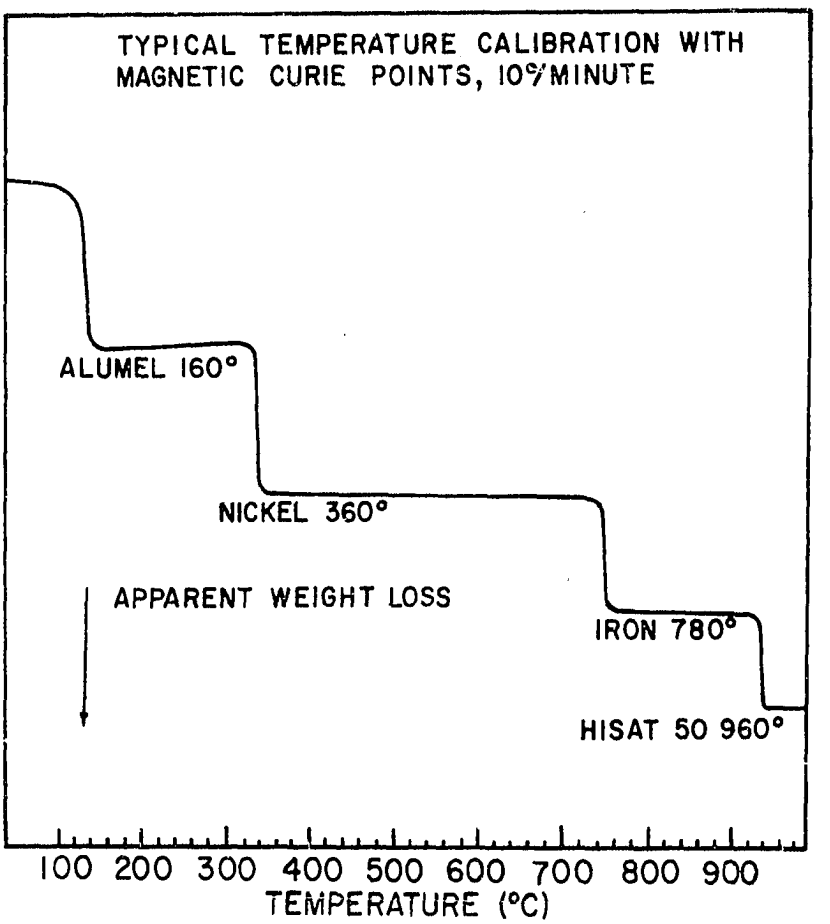


Figure III-12. Typical TGS-1 Temperature Calibration Run.

temperature of the metal samples inside the sample pan vs the digital programmer readout, which is thought to be a much better indication of sample temperature than has been achieved previously.

CHAPTER IV

THE PROPOSED MATHEMATICAL MODEL

The analysis of heat conduction in a combustible material requires the solution of the unsteady state transport equations for a heterogeneous medium in which phase changes and chemical reactions are occuring. The objective of the mathematical approach in this thesis was to formulate a model of the heat transfer and accompanying thermal decomposition of wood, which includes the effects of heat sinks and/or sources resulting directly from the thermal decomposition of the solid. The models which have been previously proposed have, to this author's knowledge, all been based on an approach similar to that of Bamford, Crank, and Malan (3). Such models have been based on the equation for heat transfer in an inert, homogeneous, isotropic medium with constant and uniform thermal and physical properties, which has been modified by addition of a term to include a heat generation (or absorption) source of the form

$$Q \frac{\partial w}{\partial t}$$

where Q = heat generated (or absorbed) per unit weight of solid material decomposed (cal/gm)

$\frac{\partial w}{\partial t}$ = local rate of decomposition, expressed as rate of weight loss of solid per unit time (gm/cm^3 sec)

In all previous treatments a constant value has been assumed for Q, the heat generation or absorption per unit weight decomposed, and by far the largest part of the studies have used a value for Q of 86 cal/gm (exothermic) proposed by Bamford, Crank, and Malan. The kinetics of the decomposition process have almost always been assumed to be described by a first order kinetic model of the form

$$\frac{\partial w}{\partial t} = kw = k_o e^{-E/RT} w$$

where w = local weight of decomposable material per unit volume (gm/cm^3)

k = rate constant (sec^{-1})

k_o = frequency factor (sec^{-1})

E = activation energy for decomposition (cal/gm mole)

R = ideal gas law constant (cal/gm mole °C)

T = absolute temperature (°K)

The uncertainties associated with such an approach and the variation in suggested values of parameters for use in this model have been discussed earlier. Of course,

even this model necessitates a numerical solution since the partial differential equations are nonlinear and presently available analytical solution methods are not applicable. The common practice in such a case is to write a discrete approximation of the differential equation; however there still remains the problem of guaranteeing that the solutions to the difference equations thus obtained are stable and that they converge to the correct values (52).

In this work a different approach is used. The method was developed and its validity was established by Hashemi (26). In this method, the region of interest is divided into a set of cells of finite dimension, and a heat balance is written on each cell. In this way the requirement of heat balance for each cell can be guaranteed even though the rate of heat transfer at the boundary of each cell is approximate. Thereby, the problem in obtaining a consistent set of difference equations is avoided.

To illustrate the procedure for setting up such a set of difference equations, consider a two dimensional region in which a network of mesh points has been developed by the intersection of N_x lines parallel to the x-axis and and Ny lines parallel to the y-axis. Let the intersection of the i^{th} line parallel to the x-axis and j^{th} line parallel to the y-axis (the point x_i, y_j) be a mesh point, denoted as (i,j). Let the distance between mesh points (i,j) and (i-1, j) be h_i, $1 \leq i \leq N_x$, and the distance between mesh

points (i,j) and (i,j-1) be k_j, $1 \leq j \leq N_y$. Let the rectangle defined by lines $x_i - \frac{1}{2} h_i$, $x_i + \frac{1}{2} h_{i+1}$, $y_j - \frac{1}{2} k_j$, and $y_j + \frac{1}{2} k_{j+1}$ be the mesh region (i,j). Figure IV-1 shows one such mesh region and its adjacent mesh points.

Assume that for a two dimensional locally isotropic medium the heat fluxes in the x and y directions obey Fourier's Law and are given by

$$j_x = - K \frac{\partial T}{\partial x} \approx - \frac{T(x+\Delta x, y) - T(x,y)}{R\Delta x}$$

and

$$j_y = - K \frac{\partial T}{\partial y} \approx - \frac{T(x, y+\Delta y) - T(x,y)}{R\Delta y} \qquad \text{(IV-1)}$$

where j_x, j_y = heat fluxes in x and y directions, respectively (cal/cm^2 sec)

K = thermal conductivity ($cal/cm^2 sec °C/cm$)

T = temperature (°C)

$R = \frac{1}{K}$, the thermal resistivity (cm sec °C/cal)

Let the temperature T at a mesh point (i,j) be $T_{i,j}$ and the average value of the thermal resistivity R and the internal energy E for a mesh region (i,j) be $R_{i,j}$ and $E_{i,j}$ respectively. Let the average values of $R_{i,j}$ and $E_{i,j}$ be those obtained at the temperature $T_{i,j}$ of the mesh point (i,j).

Let the rates at which heat is transferred by conduction into the mesh region (i,j) through sides 1,2,3 and 4 (see Figure IV-1) be q_1, q_2, q_3, and q_4, respectively.

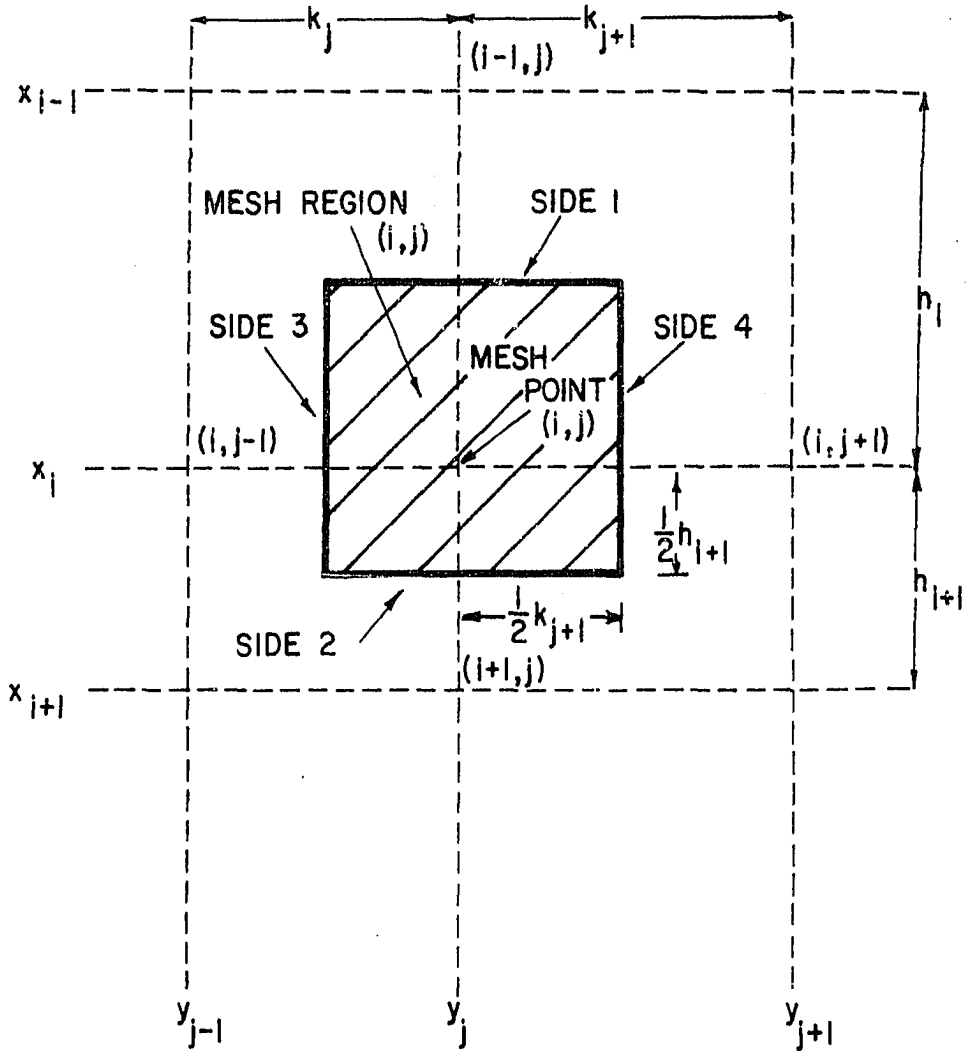


Figure IV-1. A Mesh Region (i,j) and Its Adjacent Mesh Points.

Then the heat balance around a mesh region (i,j) is

$$(q_1 - q_2) + (q_3 - q_4) = \Delta V_{i,j} \frac{dEi,j}{dt} \quad \text{(IV-2)}$$

where $\Delta V_{i,j}$ is the volume of the mesh region (i,j) and is given by

$$\Delta V_{i,j} = \Delta z \ (\tfrac{1}{2} h_i + \tfrac{1}{2} h_{i+1})(\tfrac{1}{2} h_j + \tfrac{1}{2} h_{j+1}) \quad \text{(IV-3)}$$

where Δz = the thickness of the region

q_1, q_2, q_3, and q_4 can be approximated with the aid of Equation (IV-1) to obtain

$$q_1 = -\tfrac{1}{2} \Delta z \ (k_j + k_{j+1})(T_{i,j} - T_{i-1,j})/[\tfrac{1}{2} h_i \ (R_{i,j} + R_{i-1,j})]$$

$$q_2 = -\tfrac{1}{2} \Delta z \ (k_j + k_{j+1})(T_{i+1,j} - T_{i,j})/[\tfrac{1}{2} h_{i+1} \ (R_{i,j} + R_{i+1,j})]$$

$$q_3 = -\tfrac{1}{2} \Delta z \ (h_i + h_{i+1})(T_{i,j} - T_{i,j-1})/[\tfrac{1}{2} k_j \ (R_{i,j} + R_{i,j-1})]$$

$$q_4 = -\tfrac{1}{2} \Delta z \ (h_i + h_{i+1})(T_{i,j+1} - T_{i,j})/[\tfrac{1}{2} k_{j+1} (R_{i,j} + R_{i,j+1})]$$

(IV-4)

Equations (IV-4), when substituted in Equation (IV-2) result in the desired difference equations. However, it is helpful to write the resulting difference equation in terms

of dimensionless variables. To this end let

$$u_{i,j} = (T_{i,j} - T_1)/(T_2 - T_1)$$

$$r_{i,j} = \tfrac{1}{2} K_o R_{i,j}$$

$$e_{i,j} = E_{i,j}/[C_o(T_2 - T_1)]$$

$$\tau = K_o t/(C_o h^2)$$

$$c_i = 2h^2/h_i (h_i + h_{i+1})$$

$$c_j = 2h^2/k_j (k_j + k_{j+1})$$

$$b_i = 2h^2/h_{i+1}(h_i + h_{i+1})$$

$$b_j = 2h^2/k_{j+1}(k_j + k_{j+1}) \qquad \text{(IV-5)}$$

Substituting Equations (IV-4) into Equation (IV-2), rearranging, and dividing by $K_o (T_2 - T_1)\Delta V_{i,j}/h^2$ gives

$$\frac{-c_i u_{i-1,j}}{r_{i,j} + r_{i-1,j}} + \left[\frac{c_i}{r_{i,j} + r_{i-1,j}} + \frac{b_i}{r_{i,j} + r_{i+1,j}}\right] u_{i,j}$$

$$- \frac{b_i u_{i+1,j}}{r_{i,j} + r_{i+1,j}} - \frac{c_j u_{i,j-1}}{r_{i,j} + r_{i,j-1}} + \left[\frac{c_j}{r_{i,j} + r_{i,j-1}}\right.$$

$$\left. + \frac{b_j}{r_{i,j} + r_{i,j+1}}\right] u_{i,j} - \frac{b_j u_{i,j+1}}{r_{i,j} + r_{i,j+1}} + de_{i,j}/d\tau = 0$$

(IV-6)

where u = dimensionless temperature, $\frac{T - T_2}{T_2 - T_1}$

r = dimensionless thermal resistivity ($\frac{1}{2} K_o/K$)

K_o = reference state thermal conductivity (cal/cm^2 sec $^\circ C/cm$)

$E_{i,j}$ = internal energy (including sensible and decomposition heats) (cal/cm^3)

$e_{i,j}$ = dimensionless internal energy

C_o = reference state specific heat (cal/cm^3 $^\circ C$)

τ = dimensionless time

h = a geometrical scaling factor (cm)

c_i, c_j = dimensionless geometrical factors

b_i, b_j = dimensionless geometrical factors

For each mesh point at which the dimensionless temperature $u_{i,j}$ is unknown one obtains one equation such as Equation (IV-6). For N mesh points one then has a set of N simultaneous equations to be solved for N unknowns.

The nonlinearity of the problem of heat conduction accompanied by decomposition is due to the strongly non-linear relation between $e_{i,j}$ and $u_{i,j}$, particularly in the range of temperatures where thermal decomposition occurs. If the internal energy $e_{i,j}$ which includes decomposition and sensible heat effects is assumed to be an explicit function of temperature only, and not a function of the rate of change

of temperature (in other words, if it is assumed to be independent of the rate of heating), one can write

$$\frac{de_{i,j}}{d\tau} = \frac{de_{i,j}}{du} \frac{du_{i,j}}{d\tau} = \varphi_{i,j} \frac{du_{i,j}}{d\tau} \qquad \text{(IV-7)}$$

where $\varphi_{i,j}$ can be thought of as an "energy capacity," analogous to specific heat in inert materials, but including decomposition and phase change heat effects in the proposed application. (The problem of specification of this "energy capacity" will be considered in Chapter V.)

Utilizing the relation given by Equation (IV-7), the N simultaneous equations (Equation (IV-6)) for the N unknown values of $u_{i,j}$ can be expressed in matrix notation as

$$\Phi \frac{dU(\tau)}{d\tau} + (H + V)U(\tau) = S(\tau) \qquad \text{(IV-8)}$$

where Φ = a NxN diagonal matrix whose entries are the values of $\varphi_{i,j}$

U = an N-dimensional vector whose entries are the unknown values of $u_{i,j}$

S = an N-dimensional source vector whose entries are zero when the mesh region (i,j) is not adjacent to the boundary, and contain information related to boundary conditions when the mesh region (i,j) is adjacent to the boundary

H and V are real NxN matrices with positive diagonal entries and non-positive off-diagonal entries, and both H and V have at most three non-zero entries per row. If one orders the mesh points by rows, i.e. from left to right, top to bottom, then H is the direct sum of tridiagonal matrices, i.e.

$$H = \begin{bmatrix} H_1 & & \\ & H_2 & \\ & & \ddots \\ & & & H_{N_x} \end{bmatrix}$$

where H_i, $1 \le i \le N_x$ are tridiagonal matrices whose diagonal entries are $[c_i/(r_{i,j} + r_{i-1,j}) + b_i/(r_{i,j} + r_{i+1,j})]$ and the off diagonal entries are $- c_i/(r_{i,j} + r_{i-1,j})$ and $- b_i/(r_{i,j} + r_{i+1,j})$. If instead, the mesh points are ordered by columns, i.e. from top to bottom, left to right, then V is the direct sum of tridiagonal matrices V_j, $1 \le j \le N_y$, i.e.

$$V = \begin{bmatrix} V_1 & & \\ & V_2 & \\ & & \ddots \\ & & & V_{N_y} \end{bmatrix}$$

where V_j, $1 \le j \le N_y$ are tridiagonal matrices whose diagonal entries are $[c_j/(r_{i,j} + r_{i,j-1}) + b_j/(r_{i,j} + r_{i,j+1})]$ and the off-diagonal entries are $- c_j/(r_{i,j} + r_{i,j-1})$ and $- b_j/(r_{i,j} + r_{i,j+1})$.

Equation (IV-7) is applicable to all mesh regions of interest, including the mesh regions adjacent to the boundary surface. For example, if side 1 of a mesh region (i,j) is insulated then one sets $r_{i-1,j} = \infty$ (in practice a very large number, say 10^6 would be used). If, instead, the temperature on side 1 of mesh region (i,j)(i.e. $u_{i-1,j}$) is prescribed, then one sets $r_{i-1,j} = 0$ and moves the expression $c_i u_{i-1,j}/r_{i,j}$ to the right hand side of Equation (IV-6). Obviously one can use a similar method to specify a prescribed temperature on any other side or more than one side of any mesh region.

All natural boundary conditions fall into two categories; (a) the heat flux at the boundary is prescribed, or (b) the environment temperature is prescribed. When the heat flux is prescribed the thermal resistivity of the external region is set equal to infinity and the prescribed value(s) of q_i, $1 \leq i \leq 4$, after being divided by $K_o (T_2 - T_1)\Delta V_{i,j}/h^2$ is added to the right hand side of Equation (IV-6). When the temperature of the environment is prescribed the value of thermal resistivity of the external mesh region is set equal to the heat transfer resistance at the boundary. When this resistance is zero, the boundary temperature is equal to the environment temperature.

Computer programs for solution of the temperature distribution in the region of interest [i.e. the solution of the system of first order, differential equations (IV-7)]

have been developed by Hashemi (26). The numerical procedure is based on a variant of the Peaceman-Rachford alternating direction, implicit, iterative method.

Thus if one can specify the "energy capacity" $de_{i,j}/du = \varphi_{i,j} = f(u)$ (which includes heat effects due to decomposition as well as sensible heat effects) and the thermal conductivity K(u), transient temperature distributions satisfying Equation (IV-7) can be computed.

Furthermore, if the weight loss behavior of wood as a function of temperature can be specified, step-wise integration of that weight vs temperature relation can be carried out (during the computer solution for the temperature distribution) to predict the transient weight loss behavior of a large wood specimen. Since the weight loss of the specimen is due to the decomposition of the solid, resulting in formation of combustible gaseous materials, one can thus specify the rate of "fuel" generation by a heated wood specimen. Obviously, such a capability would be extremely valuable in explaining the ignition phenomena of wood.

The above development is applicable if the Cartesian coordinates x and y are replaced by any other pair of orthogonal coordinates. The only change is in the coefficients c_i, b_i, c_j and b_j (26).

CHAPTER V

PROCEDURE AND RESULTS

The work covered herein can be conveniently subdivided into four areas: (a) differential scanning calorimetry studies; (b) kinetics of weight loss studies using thermal gravimetric techniques; (c) estimation of thermal conductivity as a function of temperature and decomposition history; and (d) experimental validation of the transient temperature distributions and decomposition product generation rates predicted by the proposed model.

Measurement of "Energy Capacity" vs Temperature Relationship of Wood Using Differential Scanning Calorimetry

The principles of differential scanning calorimetry as performed with the Perkin-Elmer DSC-1B instrument have been outlined in Chapter III. On the basis of the evaluation of the probable success of the different thermal analysis methods in application to the study of wood decomposition, it was decided to use a Perkin-Elmer DSC-1B

Differential Scanning Calorimeter in this work. A photograph of the calorimeter is shown in Figure V-1.

Reference to the proposed heat transfer model description in Chapter IV shows that the heat effects due to decomposition need not necessarily be separated from the sensible heat effects for use in such a model. In fact, it is desirable to measure the total heat effect lumped together, if it can be used in such form, since the necessary number of parameters to be specified is reduced and the problem of interaction of errors in the specification of such parameters is minimized.

Thus the approach was to try to measure the "energy capacity" of wood, which lumps together all of the heat effects due to sensible heat and heat generated or absorbed due to thermal decomposition, as a function of temperature, over a range sufficient to allow usage of such information in the proposed model. This is a rather far reaching extension of the use of the instrument beyond its normal application. In fact, the measurement of specific heat or heat capacity of materials which do not undergo degradation or reaction, by such methods, although theoretically possible with "standard DTA" techniques, has only become a practical undertaking with the advent of the "Dynamic Difference Calorimetry" and "Differential Scanning Calorimetry" techniques. Furthermore, their use for measurement of the energy capacity of a solid material

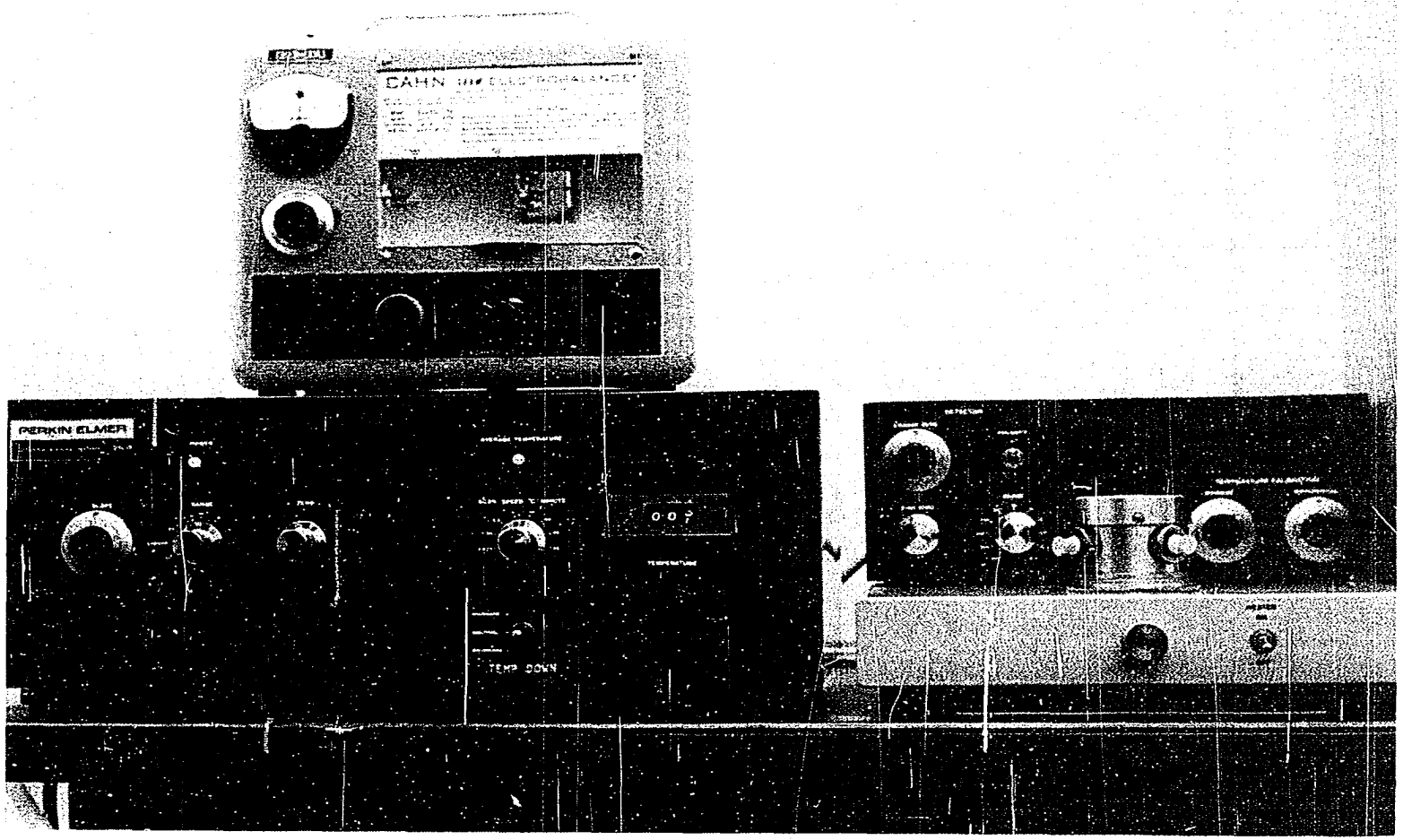


Figure V-1. Photograph of Differential Scanning Calorimeter.

including both sensible and decomposition heat effects has not appeared, to this author's knowledge.

First consider the measurement of specific heat or heat capacity of an inert material with the Perkin-Elmer DSC-1B. This measurement is an extension of one of the basic functions of the calorimeter, which is to measure the amount of heat required to raise the temperature of a sample at a predetermined rate. It has been established in Chapter III, that within the limitations involved, the ordinate read out of the DSC-1B represents the difference in dissipated electrical power required to maintain the sample holder (and its sample) at the same temperature as the reference holder, while both sample and reference holder temperatures are increasing at a prescribed linear rate. This differential power requirement is dependent on three primary factors:

1. The heat capacity difference between the sample and reference holders.

2. The additional heat capacity of the sample (consider using an empty reference holder).

3. The differences in heat losses from the sample holder and reference holder.

Consider an empty reference holder and a sample holder containing a sample of some inert material. Let both holders be maintained at a steady state temperature $T = T_{sample} = T_{sample\ holder} = T_{reference\ holder}$. In order

to maintain this temperature, heat must be supplied to make up for the heat lost from the two holders. These heat losses may occur by conduction, convection (natural or forced), and radiation, or a combination thereof. It is obvious that if the heat losses from the two sides are to be the same regardless of the steady state temperature T, then the following conditions must be met.

1. The Newtonian heat transfer coefficient must be identical for both sides.

2. The surface area of the holders which is exposed to the environment must be equal.

3. The radiative surface properties of the two sides must be the same (if the sample "sees" the external environment, this would include the surface properties of the sample).

It is practically impossible to achieve such absolute equality, since oxidation of the holders and other surface phenomena which affect the radiative heat transfer characteristics cannot be easily controlled, and even the absolute maintenance of equality in conduction-convection heat losses is difficult. If one causes the temperature T to rise, but still maintains the temperature of the two sides equal, the heat capacity differences between reference holder and sample holder-sample also affect the differential power input required. However, the increment of differential power required to offset the additional heat capacity of the sample itself during a run is the desired value. This increment may be

obtained by running a "no sample" baseline, then running a sample under the same conditions and determining the differential power required by the sample by difference. In order to carry out this measurement, the heat losses from the two sides must be identical during the sample and no-sample runs, independent of the contents of the sample holder. This requirement can be accomplished by covering the reference and sample holders with snug-fitting covers that can be reproducibly placed. Since the radiation and convection heat losses occur principally from the exterior of the holders, a covered holder will have the same surface heat losses, regardless of its contents, if the contents of the sample are completely enclosed.

The equality of heat losses during the sample and no-sample run can be checked on the instrument by simply allowing the recorder pen to reach its equilibrium position during isothermal operation at the beginning and end of the sample and no-sample runs. Since the covered holders have the same heat losses regardless of the content of the holders, and since the differential power read out at isothermal equilibrium depends only on such differential heat losses, the reading at isothermal equilibrium for both the sample and no sample runs serve as a check on the reproducibility of the differential heat losses for the two runs.

This check on the reproducibility of heat losses from run to run is extremely important and without it

there is no assurance that the increment of differential power corresponding to the heat capacity of the sample can be determined by difference. It should be noted that one tends to disregard the importance and the difficulty of reproducing these heat losses. It is no simple task to maintain the holders at exactly the same temperature with exactly the same heat losses (this requirement is in fact one of the inherent difficulties in isothermal calorimetry and has been discussed earlier in Chapter III). The maintenance of equal temperatures reproducibly is not too difficult since the feedback element functions to make any temperature corrections necessary by adjusting the heat to the holders. What can be very difficult is to maintain the heat losses equal from run to run. For instance, consider two stainless steel sample holders that are heated at 20°C/min from 100°C to 500°C. If during this heating process any surface effects occur, such as oxidation or condensation, the radiative heat transfer characteristics of the holders will be changed. Thus if the run is repeated at 20°C/min from 100°C to 500°C, the heat losses from the two holders will not be the same as they were in the first run. Likewise, the positioning of the caps on the holders must be reproduced exactly and any purging gas flow through the instrument must be reproduced exactly if the heat losses are to be reproduced.

To illustrate the problem, consider the individual magnitudes of the three primary factors which contribute to the differential power input required to maintain the sample holder-sample and reference holder at the same temperatures while scanning at 20°C/min.

The difference in heat capacity of the holders themselves is very small since their dimensions and mass can be made essentially identical. Furthermore this difference, if it exists, does not change appreciably from run to run. The magnitude of the differential power input increment which must be supplied to offset the addition of the heat capacity of the sample can be determined easily from the sample mass, estimates of its specific heat, and the rate of temperature rise. Suppose the sample weighs 10 mg (about the maximum size sample of milled pine wood that can be contained in the holder without compression) and that its specific heat is 0.35 cal/gm °C. Then the differential heat that must be supplied to offset the effect of sample heat capacity is

$$\frac{dq}{dt} = 10 \text{ mg } (0.35 \text{ mcal/mg } ^\circ\text{C}) \left(\frac{0.333^\circ\text{C}}{\text{sec}}\right)$$

$$= 1.166 \text{ mcal/sec}$$

Now consider the difference in heat emitted by radiation which will occur from a sample holder at 400°C with an overall outside surface area of 1 cm^2 (the actual sample

holder with cover has a slightly larger surface area) when the effective emissivity of the surface changes by 0.1 (a change which can easily result from oxidation of the surface or condensation of materials onto the holder surfaces):

$$\Delta\left(\frac{dq}{dt}\right) = 0.1\ \sigma\ A\ T^4$$

where σ = Stephan-Boltzmann constant (1355×10^{-12} mcal/sec cm^2 °K^4)

A = surface area of holder (cm^2)

T = temperature of holder (°K)

Thus

$$\Delta\left(\frac{dq}{dt}\right) = 0.1\ (1355 \times 10^{-12})(1)(673)^4$$

$$\cong 27 \text{ mcal/sec}$$

a value 23 times greater than the differential power input due to sample heat capacity. Fortunately, if the sample holders are properly conditioned the differences resulting from such changes from run to run with inert samples are not large enough to be important. Thus one can run a "no-sample" and a sample run from say 100°C to 200°C, checking the isothermal heat losses at both 100°C and 200°C, and use the two measurements to determine the heat capacity of the sample from the relation

$$C = \frac{dq/dt}{m \cdot dT/dt} \qquad (V\text{-}1)$$

where C = heat capacity of sample (cal/gm°C)

dq/dt = differential heat input into sample, determined by difference (cal/sec)

dT/dt = scan speed (°C/sec)

m = mass of sample (gm)

A typical specific heat determination on molten linear polyethylene, taken from the manufacturer's literature, is shown in Figure V-2. The quantity dq/dt is found by measuring the distance between the no sample base line and the sample curve at the desired temperature and by multiplying this distance by a calibration constant obtained by calibrating the instrument with a material which undergoes an accurately known thermal transition. In the DSC-1B this power calibration is normally made using the heat of fusion of indium (melting point $\cong$ 156.2°C). Ideally this calibration constant should not be a function of temperature since we are not relying on a temperature measurement to arrive at the heat flow rate (see discussion in Chapter III). The manufacturer suggests that the use of the calibration factor determined from the heat of fusion of indium, over the entire range of the instrument (0-500°C) in determinations of specific heat, should not cause errors greater than 5% normally. The error that does exist in using this constant

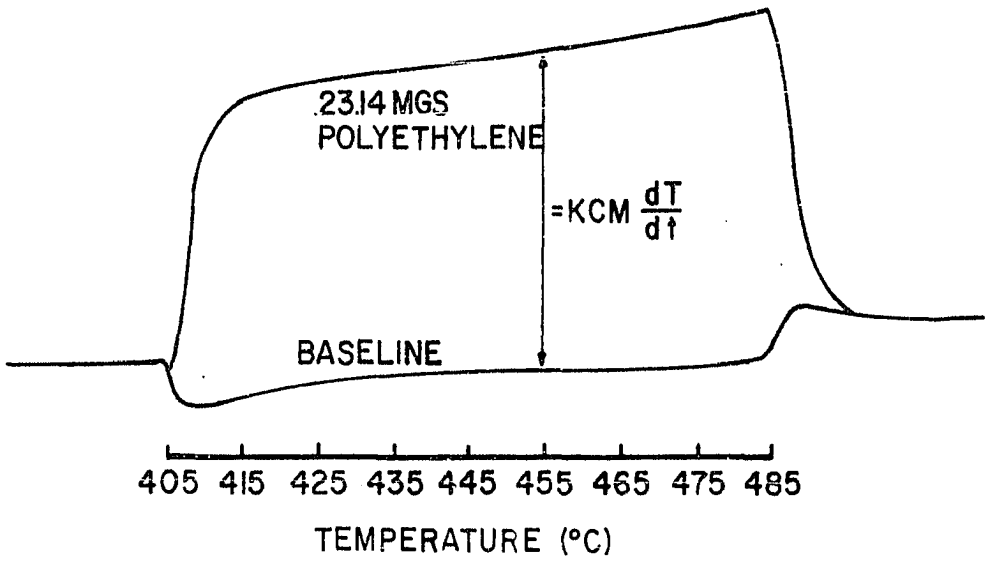


Figure V-2. Typical Specific Heat Determination, Molten Linear Polyethylene, 405-485°K, Scanning Rate = 20°C/Min (71).

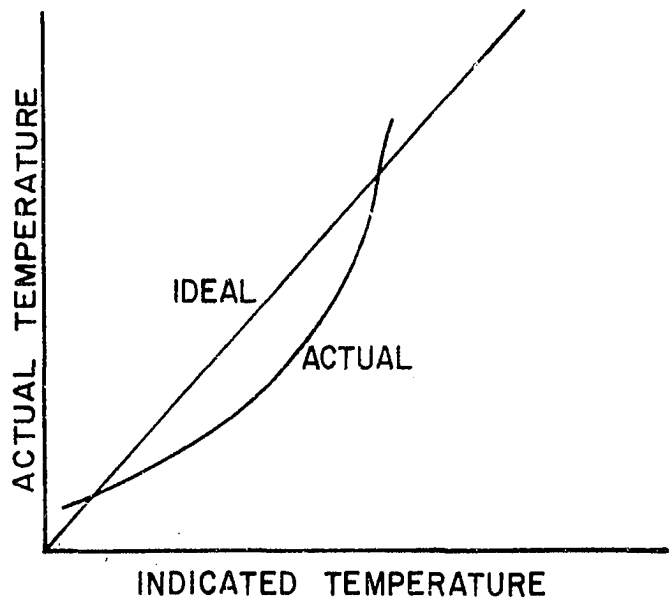


Figure V-3. Relation Between Programmed and Actual Temperatures in Perkin-Elmer DSC-1B Instrument.

to determine the specific heat of an unknown sample by use of Equation (V-1) results from the inherent non-linearity of the temperature programmer. Due to some unavoidable non-linearity in the control circuitry and to the inherent non-linearity of the platinum resistance temperature sensing elements, the temperature rise of the sample and reference holders is not truly linear but takes the shape shown in Figure V-3. A temperature calibration must be carried out to relate the digital programmer output reading, which is linear, to the actual sample holder-reference holder temperature. This calibration is done by observing the differential power input peak which occurs during heat of fusion of several, accurately defined, standard materials and by plotting those actual transition temperatures vs the ideal programmer output. In this study the temperature calibration was made using the melting points of indium (156.2°C), tin (231.9°C), lead (327.3°C), and zinc (419.5°C). The manufacturer states that if the instrument is calibrated so that the actual melting point temperatures of indium and lead agree with the programmer output, the maximum error which will exist anywhere in the range 0-500°C is 7°C. The non-linearity of the temperature calibration of the DSC-1B instrument used in this study was somewhat worse than this. A calibration curve using the four standards cited above is shown in Figure V-4. This calibration was made at a programmer rate of 20°C/minute, but note that due to the non-linearity, the actual temperature

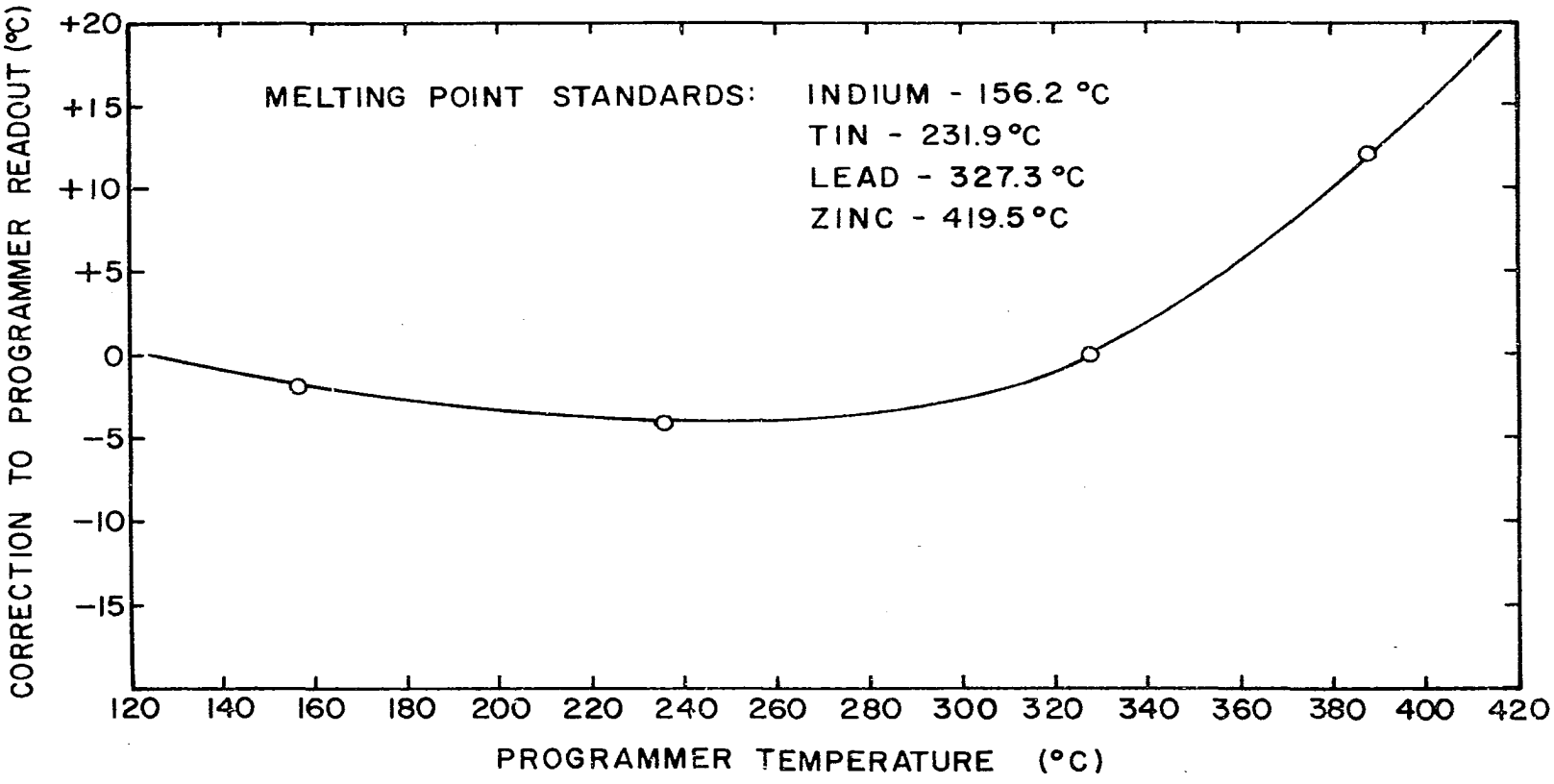


Figure V-4. Temperature Calibration of DSC-1 Differential Scanning Calorimeter.

rise rate is slightly less than this value in the lower portion (up to about 260°C) and greater than this in the high portion (above 260°C). Thus the use of a value of $\frac{dT}{dt}$ = 20°C/min in Equation (V-1) will result in an error which may be as high as 10% at some temperatures.

This problem can be eliminated by performing a specific heat type power calibration of the instrument. In this method, one measures the deflection of the instrument readout from a no-sample base line when running an inert sample whose heat capacity as a function of temperature is very accurately known. This deflection, y', is equal to

$$y' = \frac{1}{K} \cdot \frac{dT}{dt} \cdot C' \cdot m'$$

where y' = pen deflection with standard material (cm)

K = calibration constant (cal/sec cm)

$\frac{dT}{dt}$ = rate of temperature rise (°C/sec)

C' = heat capacity of standard (cal/gm °C)

m' = mass of standard material (gm)

Likewise the deflection y, obtained with the sample, is equal to

$$y = \frac{1}{K} \cdot \frac{dT}{dt} \cdot C \cdot m$$

where y = pen deflection with sample (cm)

K, dT/dt as above

C = heat capacity of sample (cal/gm °C)

m = mass of sample (gm)

Thus the unknown heat capacity C can be found from the relation

$$C = \frac{y\ m'}{y'\ m} C'$$

and the result is not affected by the non-linearity of the temperature program.

The standard material for such a specific heat calibration is a small sapphire (Al_2O_3) disc of accurately known mass. The heat capacity of sapphire is known to an accuracy of at least 4 decimal places throughout the temperature range 0-1200°K (76). If this method is used, three runs are required; one with empty holders, one with a sapphire standard, and one with the unknown sample.

Now consider the application of the method to the measurement of the energy capacity of wood, which includes decomposition heat effects. Obviously, the mass of the sample will decrease as the decomposition proceeds and the decomposition products will leave the sample holder in the gaseous form. If the decomposition products can be removed from the holders without affecting the outside radiative transfer properties of the surfaces of the holders or holder covers, the heat losses from the holders themselves will remain the same as if no material was in the holder, as in the case of an inert material. The decomposition products can be allowed to escape the holder by punching a very small hole in the sample holder cover. However, the sample must not "see" through this hole in the sample holder cover

since this would allow the sample surface characteristics (which change with time) to affect the radiative heat losses. This can be prevented by placing a small, loose fitting, metal disc on top of the sample which allows exit of the decomposition products but does not allow any of the sample to "see" through the hole in the sample holder cover. This procedure will result in reproducibility of heat losses if the decomposition products do not recondense on the sample holder or sample holder exterior, or on the enclosure which "sees" the sample holder. This problem has plagued the application of the DSC instrument, as well as the other types of instruments discussed previously, in studies involving thermal decomposition. The condensation of materials inside the sample head must be prevented if the differential heat losses are to be controlled.

This condensation problem was encountered when the instrument was first used for study of the decomposition of wood. The decomposition products formed spots and films on the sample holder and its cover, causing changes in surface heat transfer characteristics that resulted in differential power input differences between the no-sample and sample runs of as much as 100 times the magnitude of the heat capacity of non-decomposing wood. After several approaches were tried, the problem was finally eliminated to a sufficient degree by simply redirecting the inert purge gas (dry nitrogen) through a different path in the

sample head and by increasing its flow rate from the manufacturer's suggested value of 40 ml/min to approximately 100 ml/min. The direction of purge gas flow in normal usage of the instrument is as shown in Figure V-5a. Note that in the manufacturer's design the purge gas must change its direction of flow 180°; the area where this change of direction takes place is directly above the sample and reference holders. Thus the purge gas does not effectively sweep the decomposition products away, and contamination of the exterior surfaces of the holders results. By bringing the purge gas in at the same location, but moving its outlet path to a level corresponding to, or higher than, the holders, a much more effective sweeping action is realized. This desired flow path was simply accomplished by opening one of the ports on the side of the calorimeter cover, which are provided for introduction of materials into the sample head with a hypodermic syringe, and allowing the purge gas to exit there (Figure V-5b). By a combination of flow redirection and a substantial increase in the purging rate (the rate of 100 ml/min was about the maximum which did not result in excessively noisy readout) the desired measurements were possible. However, a considerable number of runs were made before the final operating conditions were established, and even then the exact reproduction of heat losses in the no-sample and sample runs was achieved only two or three times, although

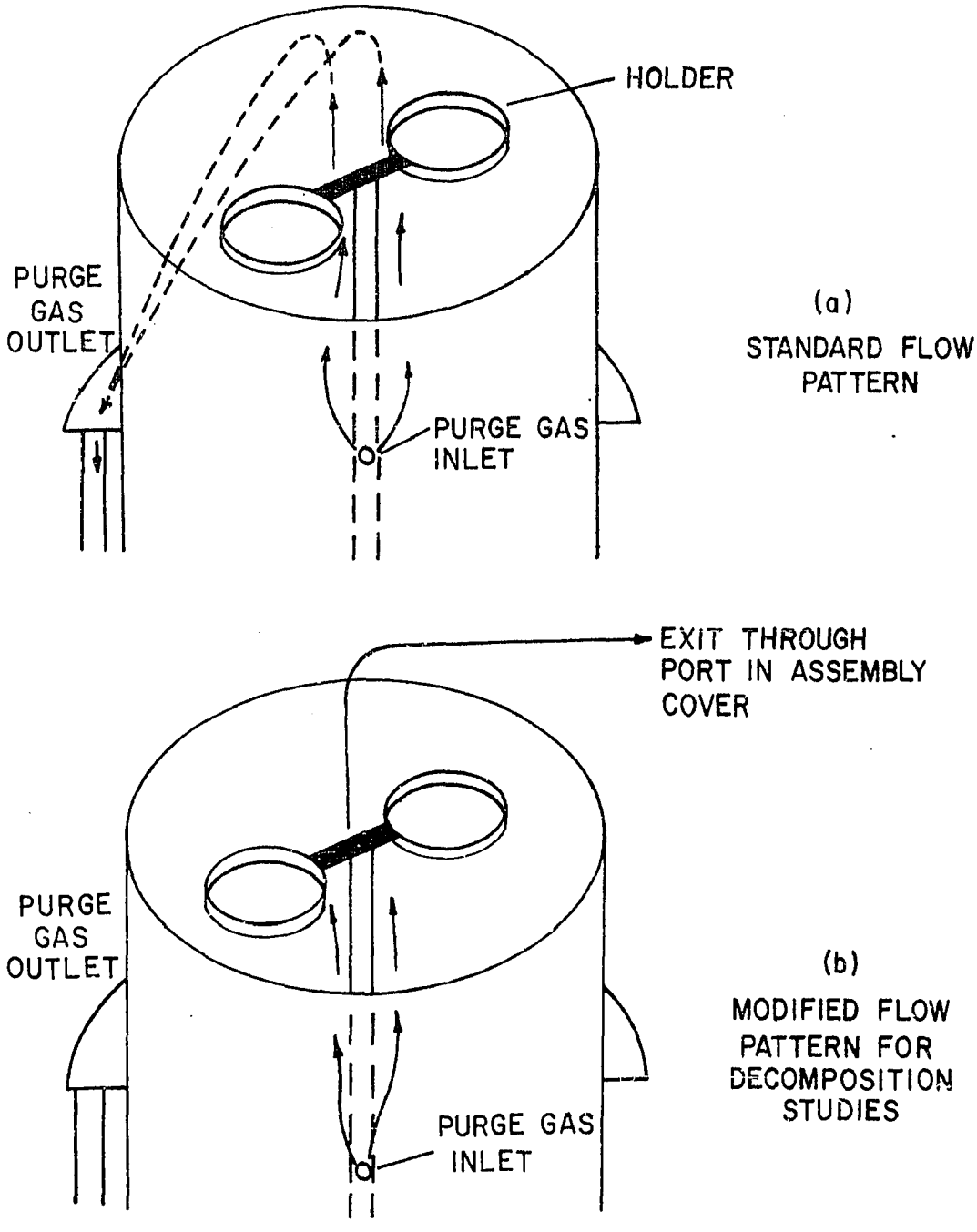


Figure V-5. Purge Gas Flow Pattern in Differential Scanning Calorimeter Sample Head.

reproduction to within less than 10% of the magnitude of sample heat capacity could be made repeatedly.

All calorimetric runs reported in this study were made at a nominal scanning rate of 20°C/min. Faster scanning rates (the next higher rate available is 40°C/min) caused greater difficulty in reproduction of the heat losses between no-sample and sample runs. Slower scanning rates did not result in large enough differential heat input due to energy capacity of the sample to afford the desired accuracy. (Remember that this portion of the differential power input is proportional to the scan speed as well as the mass of the sample remaining.)

All calorimetric runs were made using dry nitrogen as the purge gas. Thus, a basic assumption underlying the use of data so obtained, in the proposed heat transfer model, is that in a large wood specimen the decomposition process occurs internally in the absence of oxygen. Oxygen will of course be present near the surface of such specimens in normal situations, and its presence may be important (due to heat effects resulting from gas phase and gas-solid oxidative reactions) at or near the surface. The proposed model, in its present form, does not include heat effects due to gas-phase reactions. Therefore, in order to establish its validity in description of internal heat effects, all experiments on thermal decomposition of wood were carried out in a dry nitrogen atmosphere.

The desired form of data input for the mathematical model is the "energy capacity" (cal/cm^3 °C). If the assumption is made in the model that the sample dimensions do not change, the energy capacity of the wood per unit volume can be obtained for any sample if the initial density is known and the energy capacity is known in calories per °C per original unit of weight. The pen deflection, y, can be combined with the instrument power calibration, K, to get the instantaneous heat absorbed by the sample dq/dt. This value can then be substituted in the relation:

$$\frac{dE_s}{dT}\left(\frac{\text{cal}}{\text{original wt °C}}\right) = \frac{K \cdot y}{m \cdot dT/dt} = \frac{dq/dt\ (\text{cal/sec})}{m \cdot dT/dt}$$

where E_s = energy content of sample (cal/gm) (based on original wt)

K = instrument power calibration constant (cal/sec cm)

m = original wt of wood sample (gm)

T = temperature (°C)

y = pen deflection (cm)

The quantity dE_s/dT can then be used to calculate the energy capacity in calories per °C per unit volume of wood throughout the heating and decomposition process by multiplying by the initial dry density of the wood.

The instrument power calibration was carried out using a sapphire specific heat standard. However, due to

the time involved in making the determinations and the inherent difficulty in reproducing the heat losses from run to run, a sapphire run was not made each time a wood sample was run. Instead, a sapphire specific heat calibration run was made with the instrument at the beginning of the study and a frequent check was made on the constancy of the calibration by running a heat of fusion power calibration on indium. Figure V-6 shows a plot of the power factor, determined using the sapphire standard, as a function of temperature for the range of interest. This factor was calculated from the relation

$$K = \frac{20 \cdot C' \cdot m'}{y}$$

where y = deflection from "no sample" base line (cm)

C' = heat capacity of sapphire (cal/gm °C)

m' = mass of sapphire standard (gm)

Since the temperature program was very reproducible the use of the above factor for calculation of the energy capacity of the wood sample from the relation

$$\frac{dE_s}{dT} = \frac{K \cdot y}{20 \cdot m}$$

in effect cancels out the error due to assuming the scan rate to be exactly 20°C/min.

Figure V-7 shows the results of runs made on dry pine wood in a dry nitrogen atmosphere as a function of temperature from 100°C to 450°C. The samples were prepared by

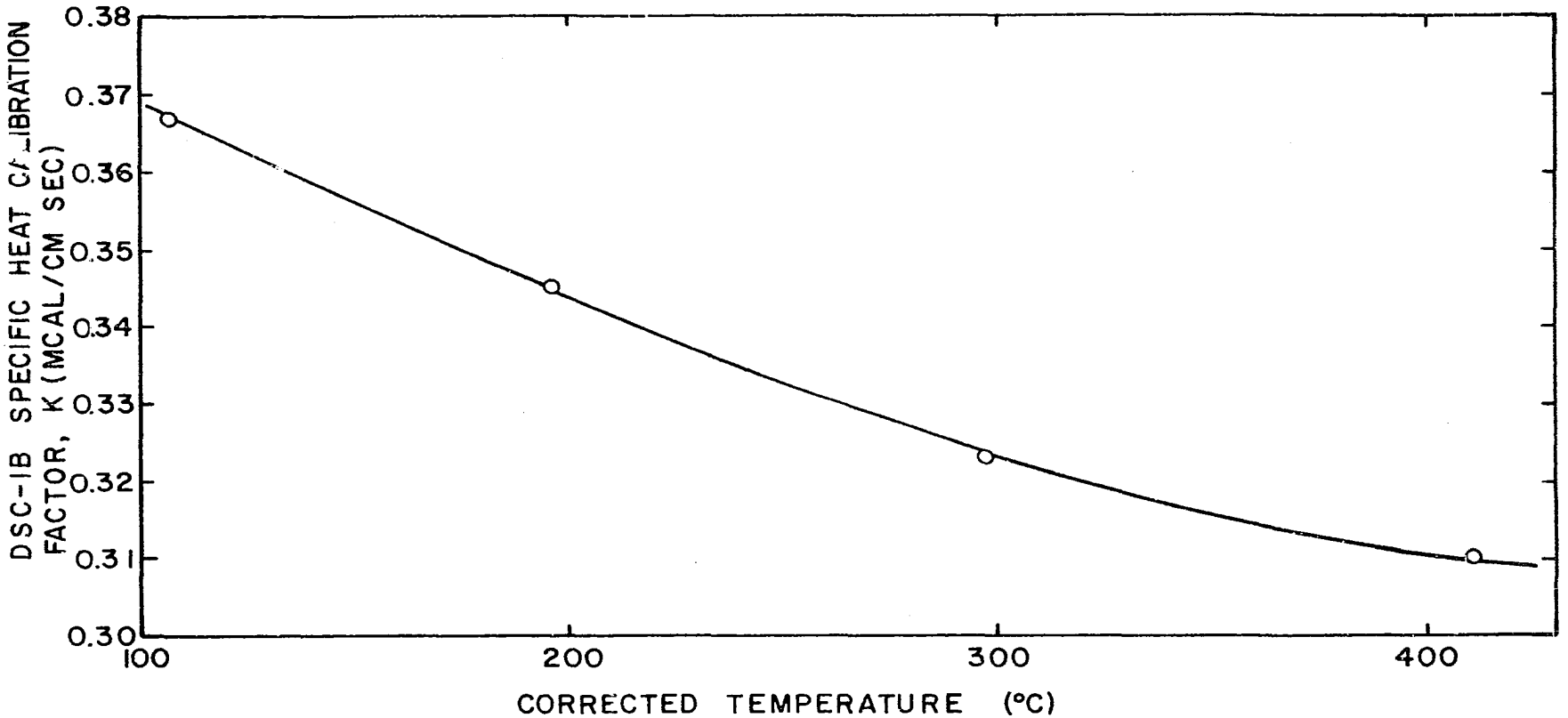


Figure V-6. Specific Heat Calibration of DSC-1B.

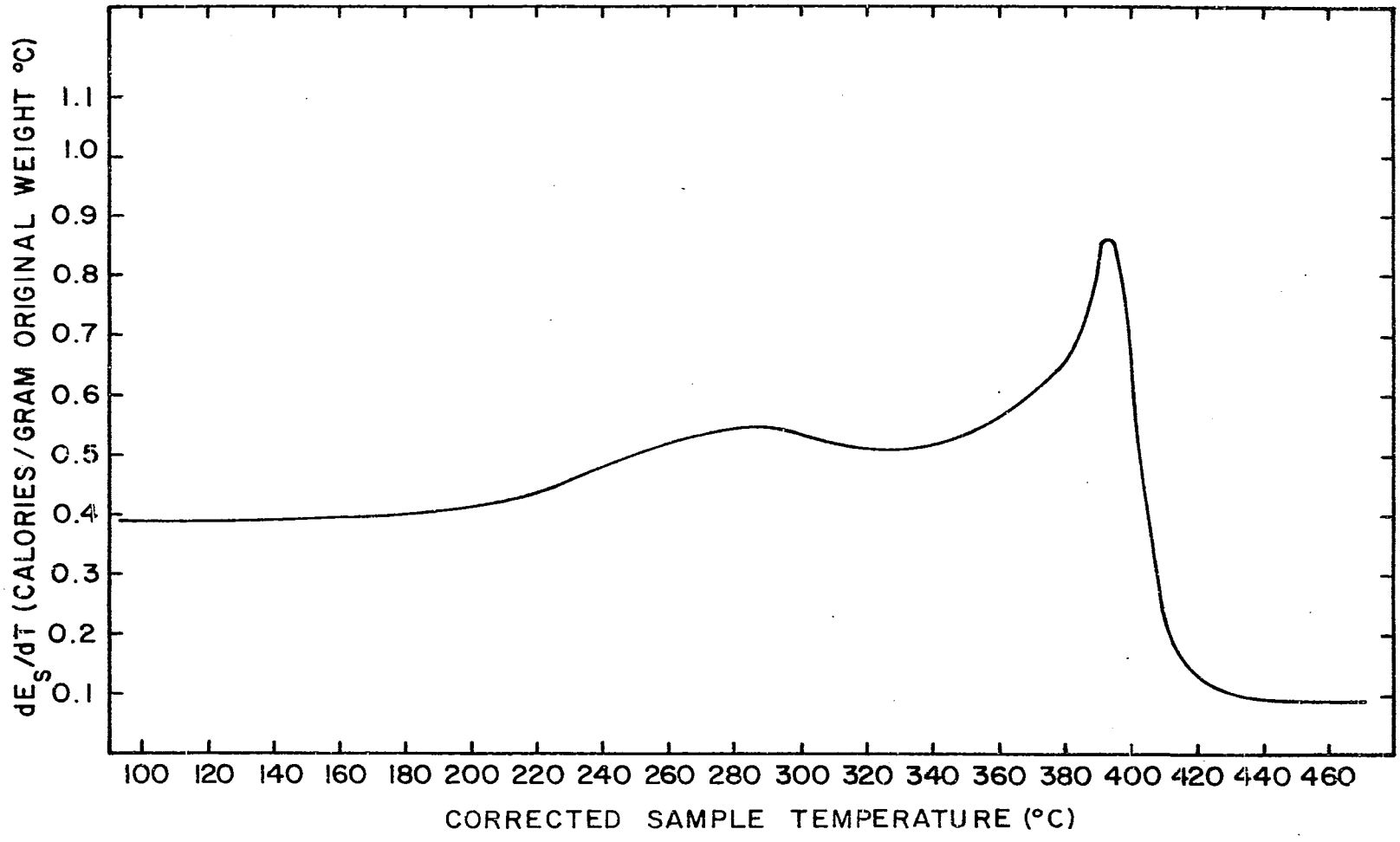


Figure V-7. "Energy Capacity" of Pine Wood as a Function of Temperature in Nitrogen Atmosphere (Based on Original, Non-Decomposed Weight).

grinding white pine chips in a Wiley intermediate model laboratory mill. The fraction passing a 40-mesh screen was used for analysis. The weight of samples was on the order of 10 milligrams. The samples were dried in the instrument by raising their temperature to 150°C and maintaining that temperature (by operating the instrument in the isothermal mode) for about 3 minutes, before beginning a run.

The measurements were made in two parts; first, a measurement of the energy capacity of wood from 100°C to 230°C was made and then a separate measurement was made from 230°C to 450°C. This two-step procedure was necessary to allow reproduction of heat losses from no-sample to sample runs. Generally, reproducibility of heat losses is easier for short temperature scans. To obtain a check on the isothermal heat losses at the beginning and end of a run, no internal heat effect should occur at these end temperatures. Since the highest temperature which could be reached before decomposition heat effects became evident was 230°C, it was used as the upper bound for the lower temperature portion. This bound was determined by a trial and error process. Likewise the upper temperature range had to extend far enough to get an isothermal heat loss check at the upper end temperature which meant that the second scan had to be made to a temperature at which no appreciable decomposition heat

effects were occurring. For decomposition of pine in nitrogen, the decomposition process is essentially complete at a temperature of about 410°C. It is important to note that this temperature was not known with any certainty before this work was begun. Since the instruments operating temperature limit is 500°C, the measurement could not have been made in this manner if the decomposition were still proceeding at 500°C. The belief that the instrument's temperature range was sufficient to cover the area of interest was formed partly from suggestions in the literature and partly from the decomposition weight loss studies of previous investigators which have been discussed in Chapter II.

Figure V-8 shows a similarly prepared plot of the results obtained from calorimetric runs on milled oak samples.

The reproducibility of the location of the large peak for both types of wood was extremely good, to within about ± 2°C for more than 20 runs. The problem of location of base line (that is, the establishment of the heat loss contribution to the differential power input) caused some scatter in the data from different runs. Approximately 10 runs were made on pine and 6 runs on oak in which the reproduction of the base line was within 10%. In these runs a base line correction was made to account for slight differences in the isothermal heat loss checks. However, at least two pine runs were made which required no such correction, and the line for the pine data is drawn through those points.

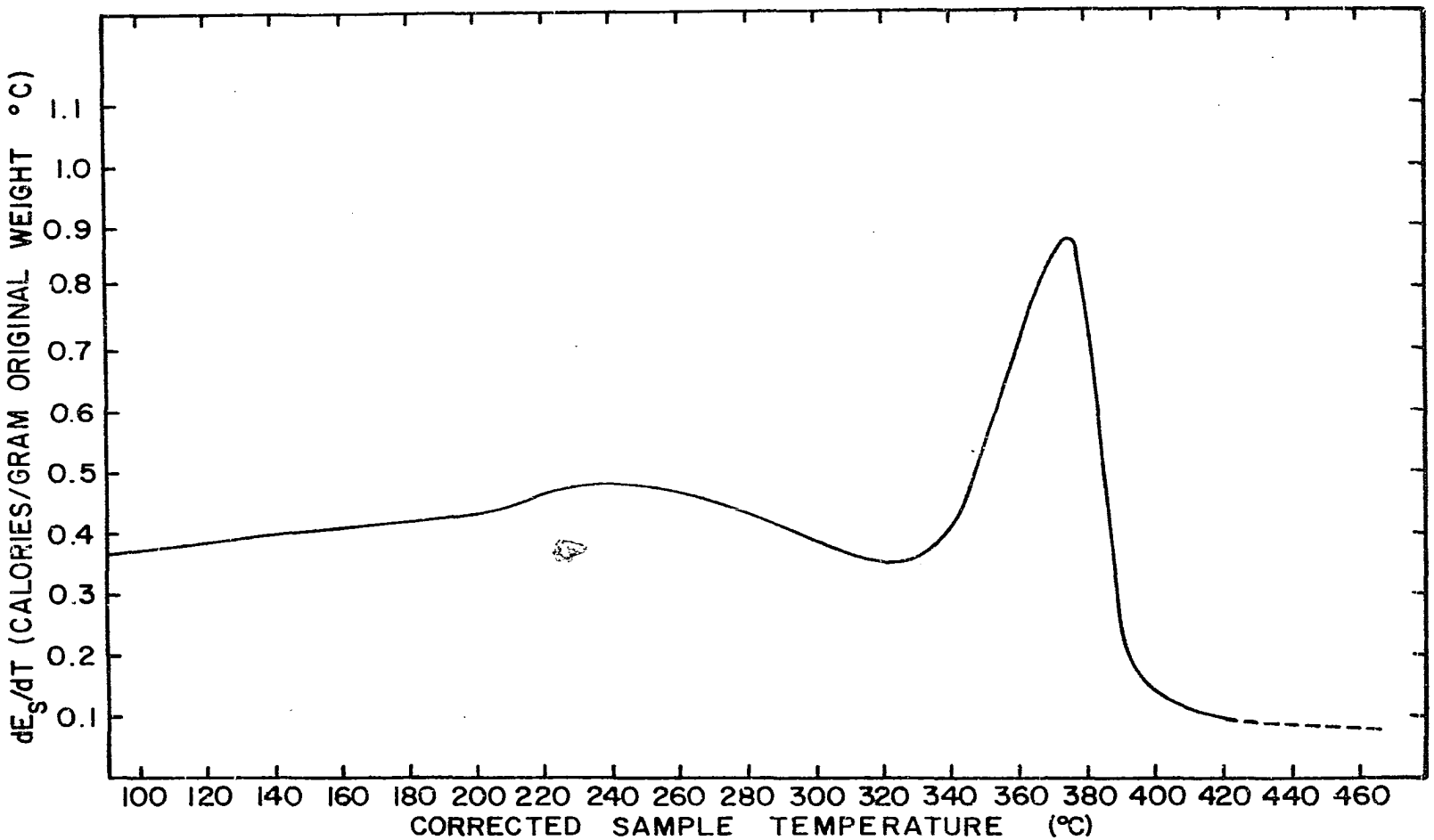


Figure V-8. "Energy Capacity" of Oak Wood as a Function of Temperature in Nitrogen Atmosphere (Based on Original, Non-Decomposed Sample Weight).

The results of these two pine runs were identical to within about 5% over the entire range.

Measurements of Weight Loss and Rate of Weight Loss of Wood as a Function of Temperature using Thermal Gravimetric Analysis

The instrument used in this portion of the study was a Perkin-Elmer TGS-1 Thermobalance which has been described in Chapter III. A photograph of the instrument is shown in Figure V-9.

The analyses were carried out on milled white pine and oak samples from the same lot as used in the calorimetry studies discussed in the preceding section.

The temperature calibration of the instrument was carried out using the Curie point ferromagnetic standards as discussed in Chapter III. The magnetic standards are supplied by the manufacturer in wire form. Table V-1 lists the ferromagnetic standard materials supplied, along with their respective Curie point transition temperatures.

The temperature calibration of the TGS-1 Thermobalance involves determining a calibration curve relating the digital readout of the temperature programmer with the observed Curie point transitions, which are a measurement of the temperature of material in the sample pan. Since a calibration curve of dial reading vs these observed transition temperatures involves interpolation between the temperatures shown in Table V-1, one must use a sufficient

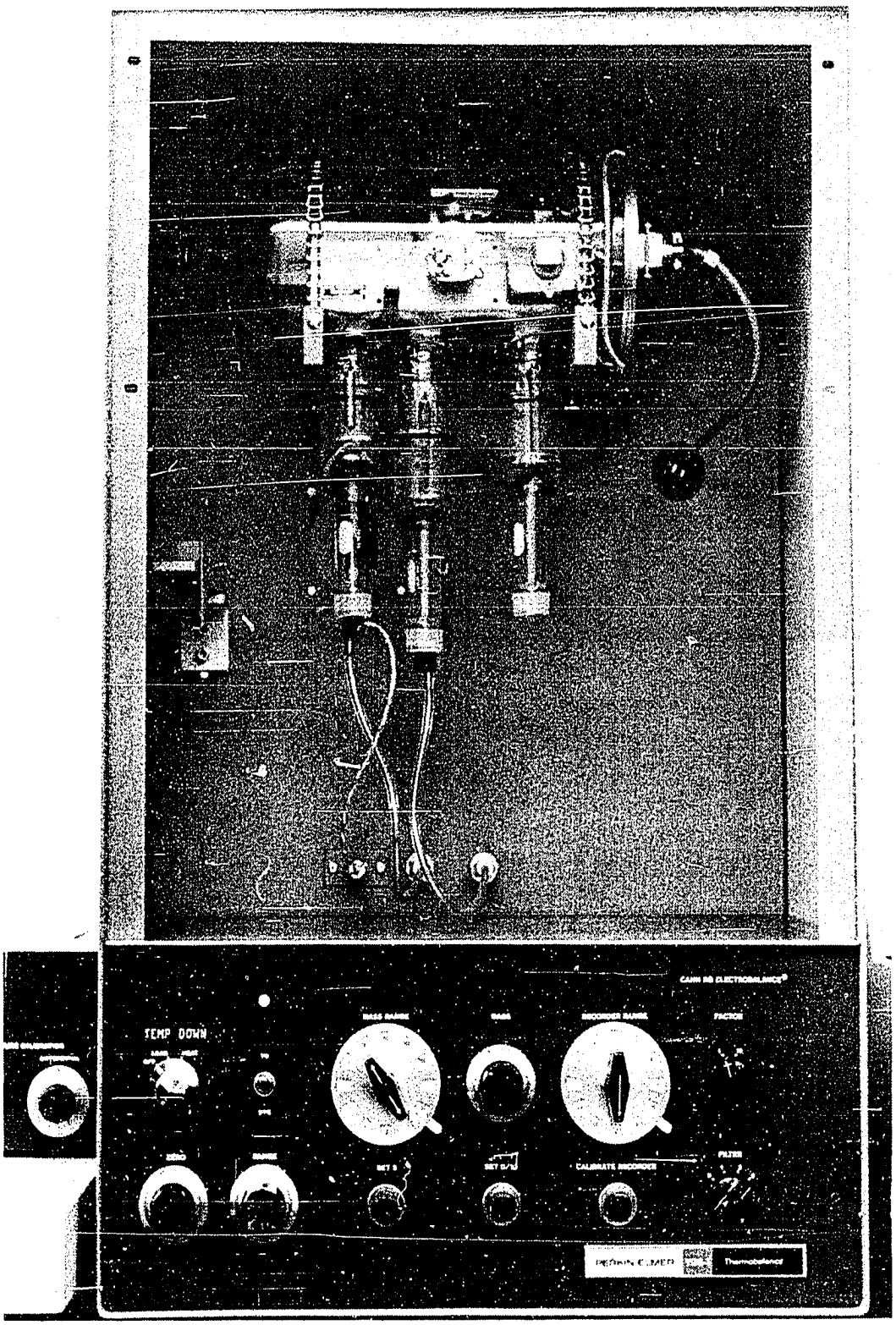


Figure V-9. Photograph of Thermobalance.

TABLE V-1

FERROMAGNETIC CALIBRATION STANDARDS

Metal	Curie Point Temperature (°C)
Monel	65
Alumel	158
Nickel	358
Mumetal	390
Nicoseal	445
Perkalloy	598
Iron	786
Hi-Sat 50	994

number of points to define the shape of this calibration curve over the temperature range of interest. Ideally one would hope for a nearly linear temperature increase for two reasons; first, interpolation becomes more certain between the Curie point temperatures, and secondly, a linear temperature increase greatly simplifies the application of many of the kinetic models which can be used for characterizing the weight loss behavior. The manufacturer's operating manual suggests that the calibration can be made so that the error in assuming linearity of the sample temperature rise rate (for a nominal scan speed of 20°C/min) will not be greater than

± 10°C over the entire range of the instrument (0-1000°C). This claim was not found to be the case; no matter how the calibration controls were set, there appeared to be a much greater degree of non-linearity. After a number of trial calibration runs were made, it was finally decided to use a sample analysis range of 0-600°C and calibrate so as to achieve the maximum degree of linearity over this range. Alumel, nickel, nicoseal and perkalloy magnetic standards were used.

The magnetic standards were cut to a size of approximately 2 milligrams each (knowledge of the exact weight is not necessary) and placed in a sample pan. The pan was then filled with powdered Al_2O_3 which served a dual purpose. It provides a large increase in the inertia of the pan and its contents, which minimizes swinging of the sample pan into the furnace walls (which of course introduces spurious peaks in the output recording). It also provides some insulating effect, which probably more nearly approximates the heat transfer characteristics of a pan containing a wood sample than does a pan which is empty except for the small magnetic standards. In order to make the conditions of a temperature calibration run and a sample run as nearly identical as possible, a loose-fitting aluminum disc was placed on top of the sample pan. This disc-cover, although it allows the wood decomposition products to escape the pan in a sample run, provides a much better reproduction of heat loss

characteristics, and thus of temperature, between the calibration and sample runs than would result if the samples were heated in uncovered pans. Also, this arrangement more closely approximates the conditions under which the calorimetric measurements were made. All weight loss studies were made in a flowing dry nitrogen atmosphere. To insure that the glass weighing mechanism did not contain any air, the outlet was connected to a vacuum pump through a two-way valve. Before each temperature calibration run or sample run was made, the system was evacuated to a pressure of less than 1 inch of mercury and then was purged with dry nitrogen. This vacuum-purge cycle was repeated three times, after which the dry nitrogen purge rate was set at 40 ml/min (standard conditions), and the run (temperature calibration or wood sample) was made.

Since the ferromagnetic-to-paramagnetic transition of the standards is essentially reversible, a calibration scan can be repeated several times to check the reproducibility of the programmer. The dial reading at which the Curie point transitions occurred was found to be reproducible to within ± 4°C generally. Before each run of a wood sample was made a set of the above four magnetic standards was scanned at the desired heating rate three separate times to insure that the programmer was reproducible. After such a temperature calibration run was made, the sample pan was then filled with a milled pine sample, (initial dry sample

weight was about 2 milligrams), covered in the same manner as for the temperature calibration run, and it was scanned at the same nominal heating rate. Then a separate pine sample was run to check the reproducibility of the wood decomposition results. The process was then repeated with two milled oak samples (approximately 4 milligram dry sample weight). The results of such a pair of runs on milled pine at a nominal scan rate of 20°C/min are shown in Figure V-10 where the data are presented as percent of original dry weight vs corrected temperature. Note that the wood sample results were extremely reproducible.

Figure V-11 shows the results of milled oak samples run at a nominal scan rate of 20°C/min with the data presentation in the same manner as before.

To study the effect of rate of heating, wood samples were run at higher nominal scan rates of 40°C/min, 80°C/min and 160°C/min. A separate temperature calibration was made for each rate so that the temperature of the sample could be estimated as closely as possible. Figure V-12 shows typical corrections to the programmer which had to be made at each heating rate. Figures V-13 and V-14 show the results of runs made at 40°C/min, 80°C/min, and 160°C/min, respectively, on pine and oak (the 20°C/min run results are included for comparison). Two separate runs were made with each wood type and heating rate to demonstrate reproducibility.

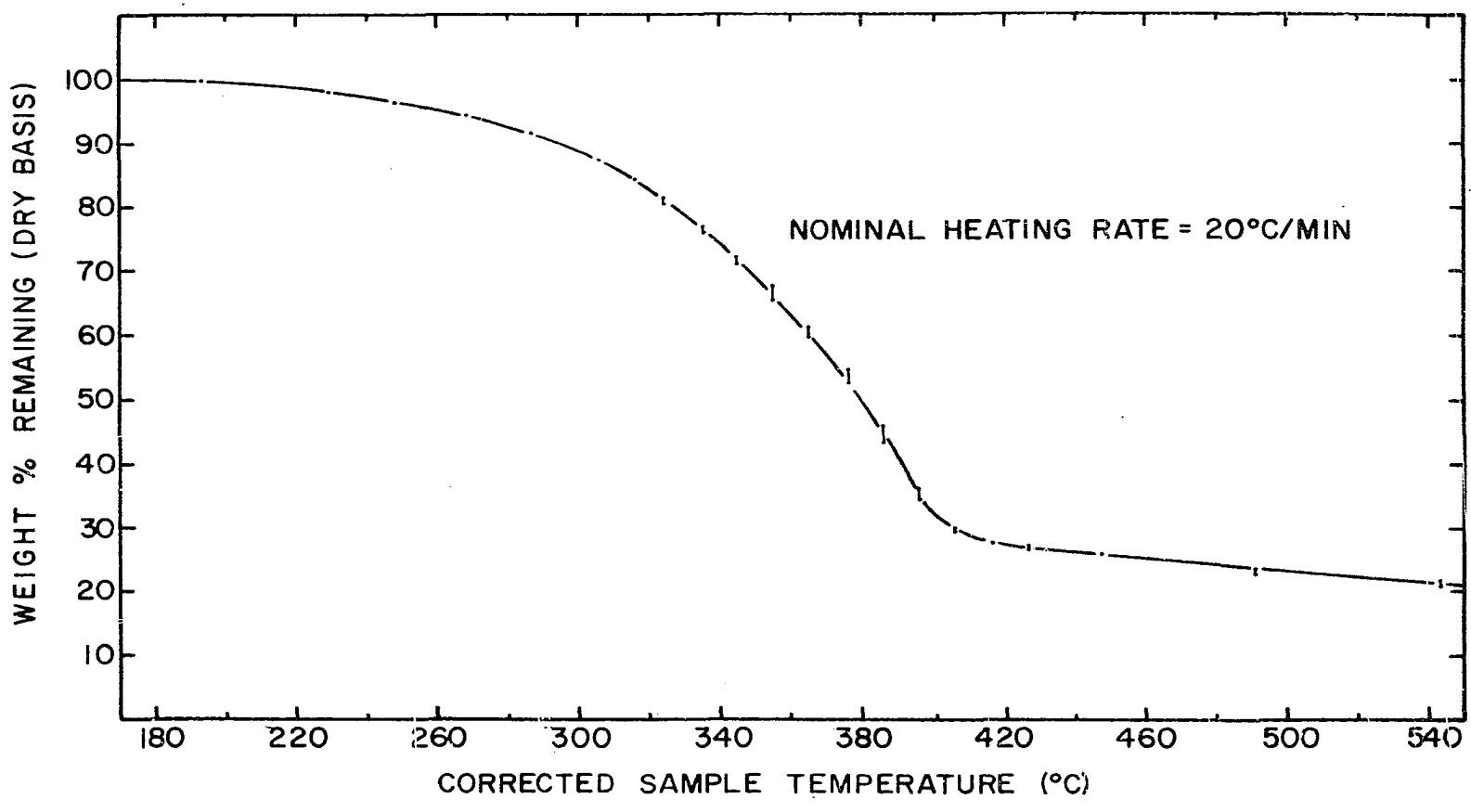


Figure V-10. Per Cent of Original Dry Weight Remaining as Solid Material vs Temperature for Pine in Nitrogen Atmosphere.

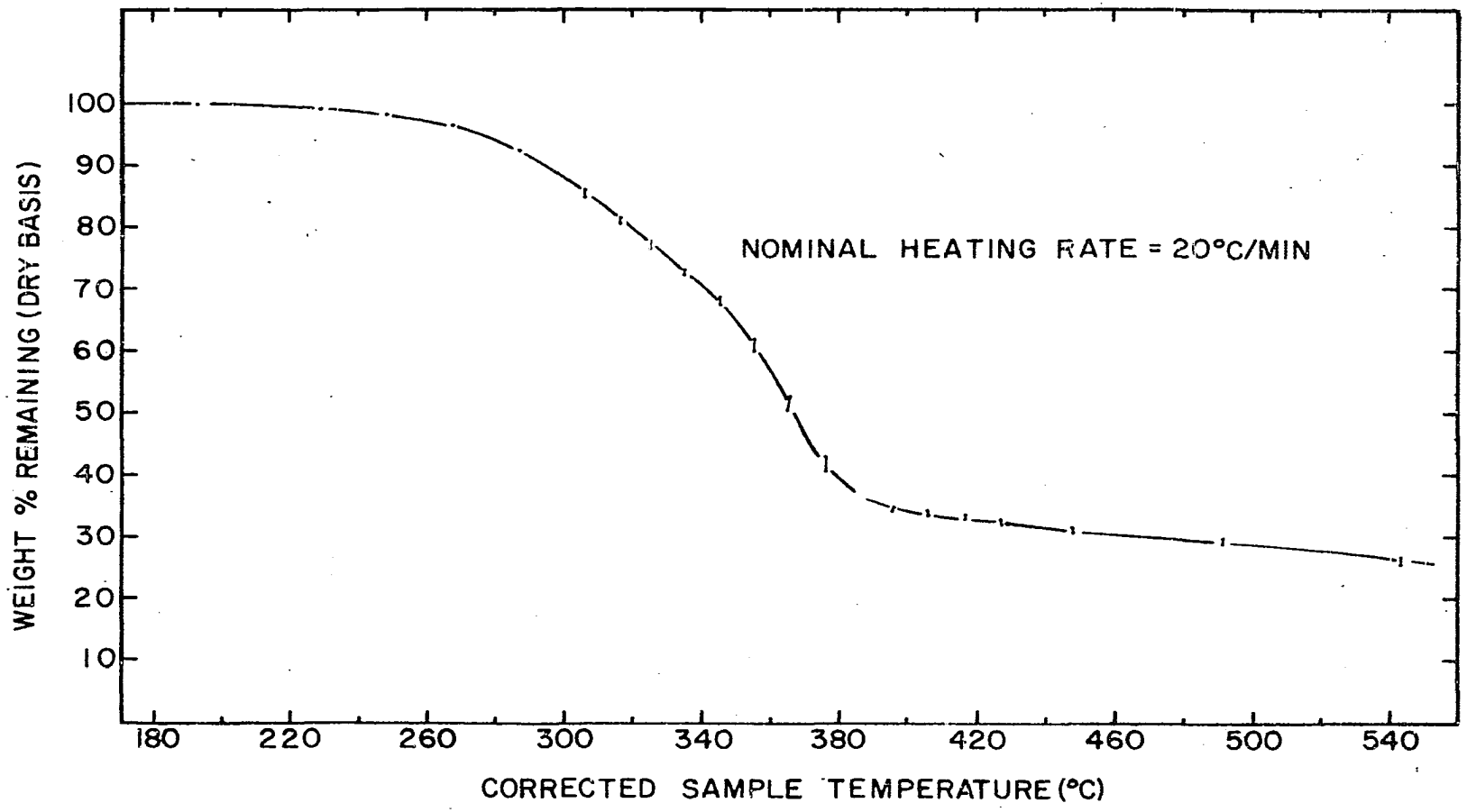


Figure V-11. Per Cent of Original Dry Weight Remaining as Solid Material vs Temperature for Oak in Nitrogen Atmosphere.

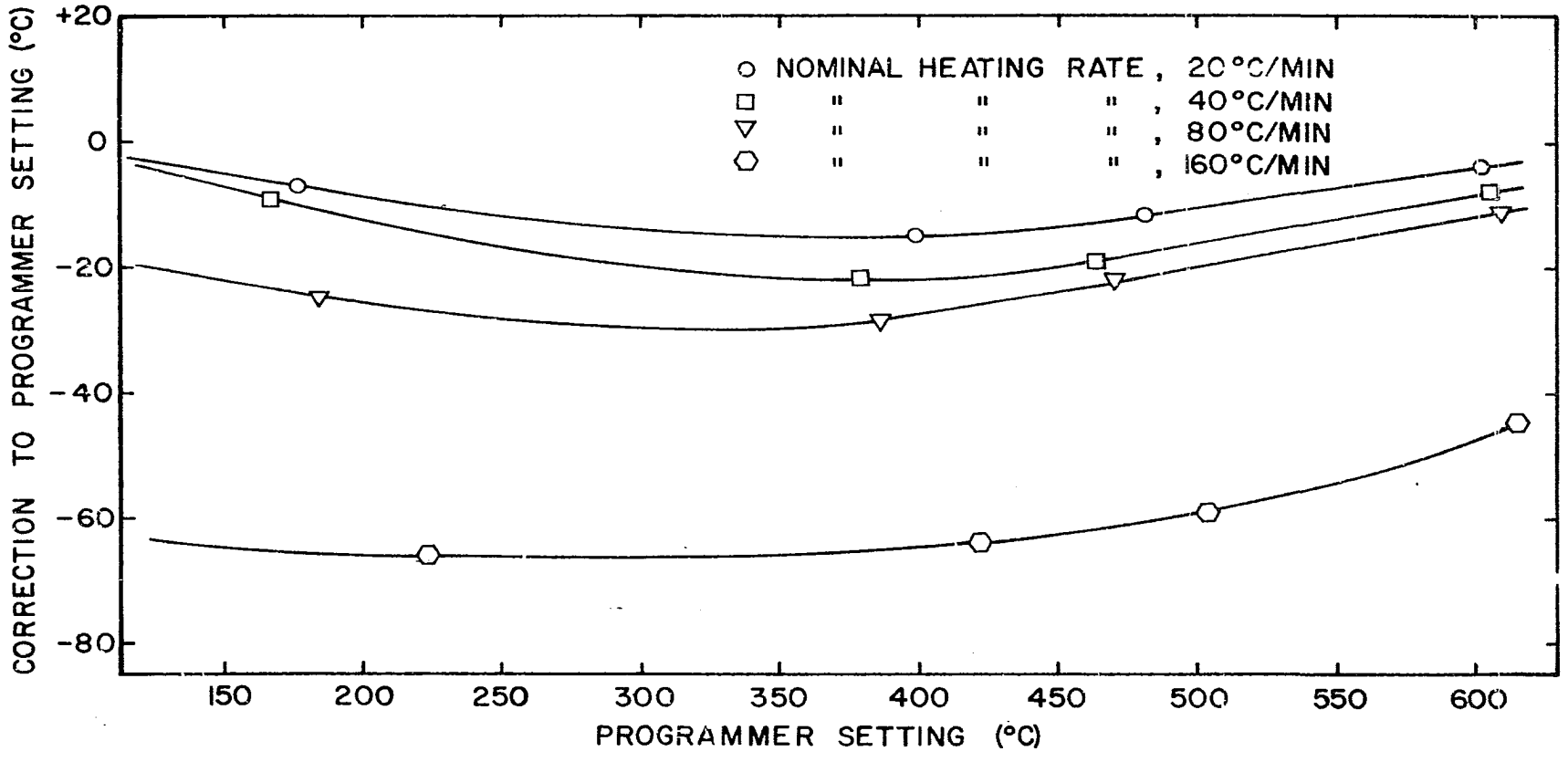


Figure V-12. Temperature Calibration of TGS-1 Thermobalance at Different Heating Rates.

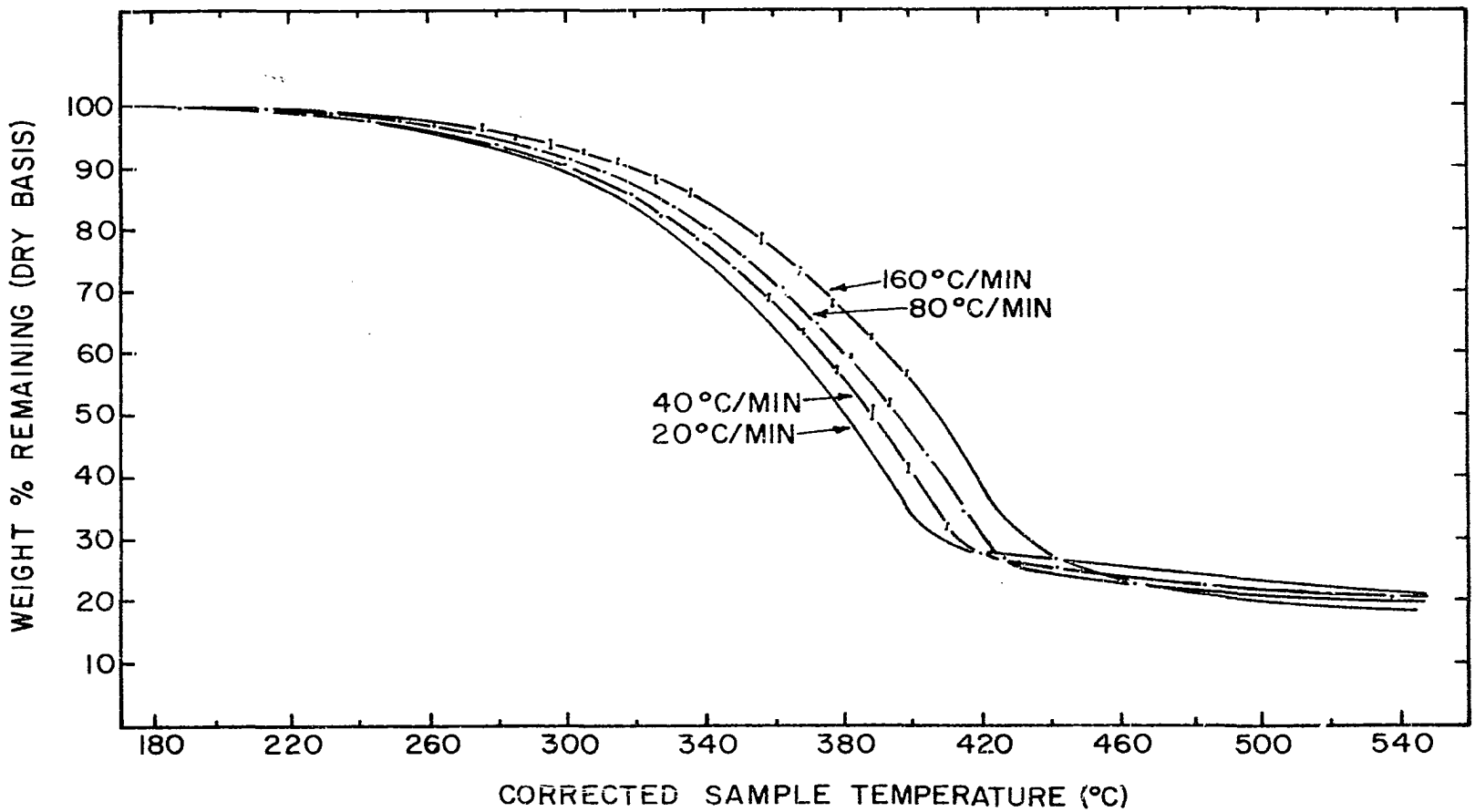


Figure V-13. Effect of Rate of Heating on Kinetics of Weight Loss of Dry Pine Wood in Nitrogen Atmosphere.

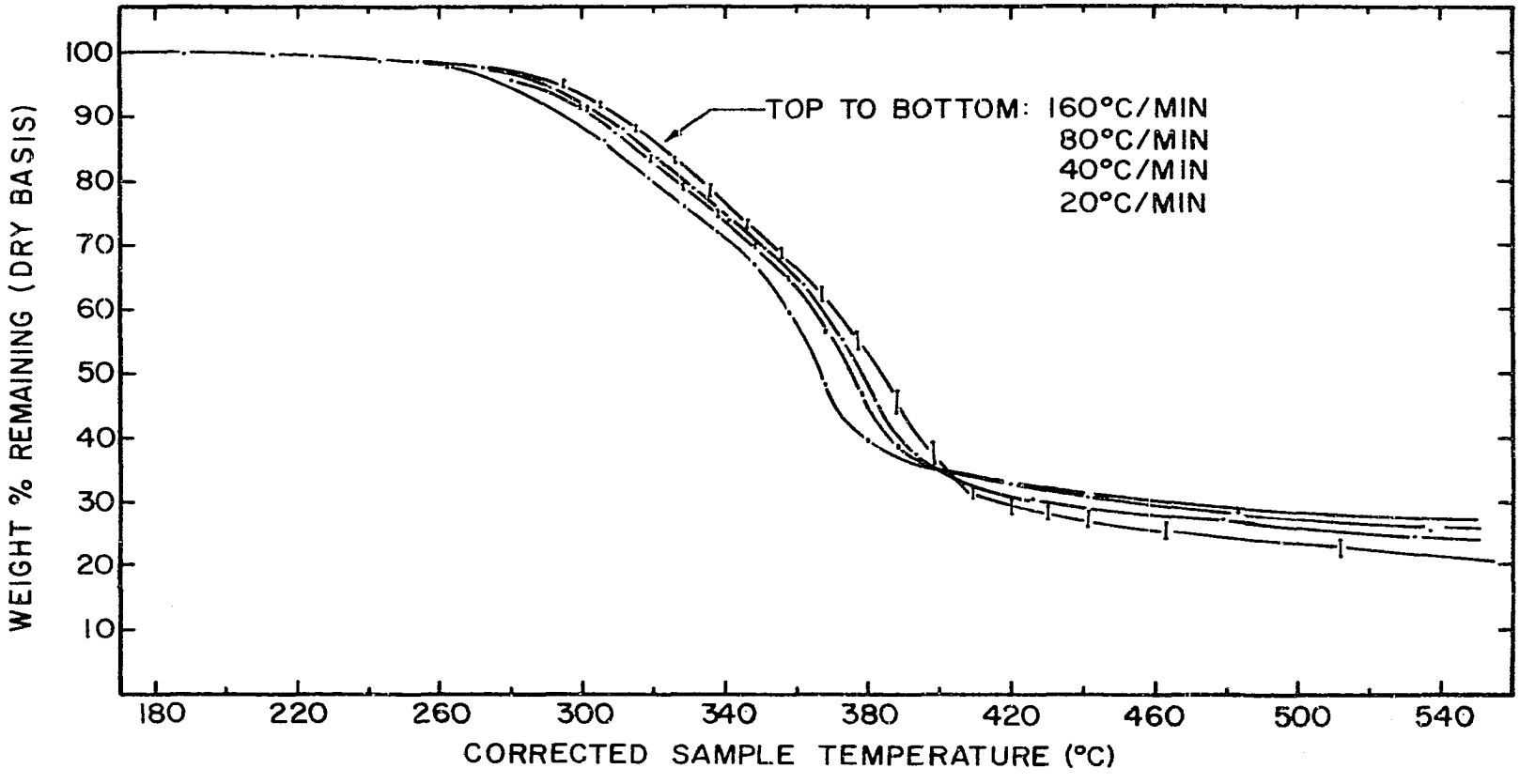


Figure V-14. Effect of Rate of Heating on Kinetics of Weight Loss of Dry Oak Wood in Nitrogen Atmosphere.

In addition, for more direct comparison with the scanning calorimetry results, differential thermal gravimetric runs were also made on pine and oak at a nominal heating rate of 20°C/min. The temperature calibration for these runs was carried out in the same manner as for the thermal gravimetric runs. Figures V-15 and V-16 show the results for pine and oak respectively, where the data are presented as percent (of original weight) loss per degree centigrade vs corrected temperature. Again, for each wood type two runs were made to check reproducibility, and the results show that the reproducibility was extremely good.

Specification of Thermal Conductivity of Wood as a Function of Temperature and Decomposition History

For a single wood specimen the density can be considered uniform and constant prior to onset of thermal decomposition (at about 200°C). The specimen can be sawed so as to specify the direction of grain relative to the desired heat flow direction; for example, a cylinder can easily be cut from a board so that the grain direction is parallel to the cylinder axis. For such a cylindrical configuration, one needs only to specify the thermal conductivity as a function of temperature in the transverse direction (assuming radial transverse and tangential transverse conductivities are equal, see Chapter II for discussion) if experimental conditions are designed to allow

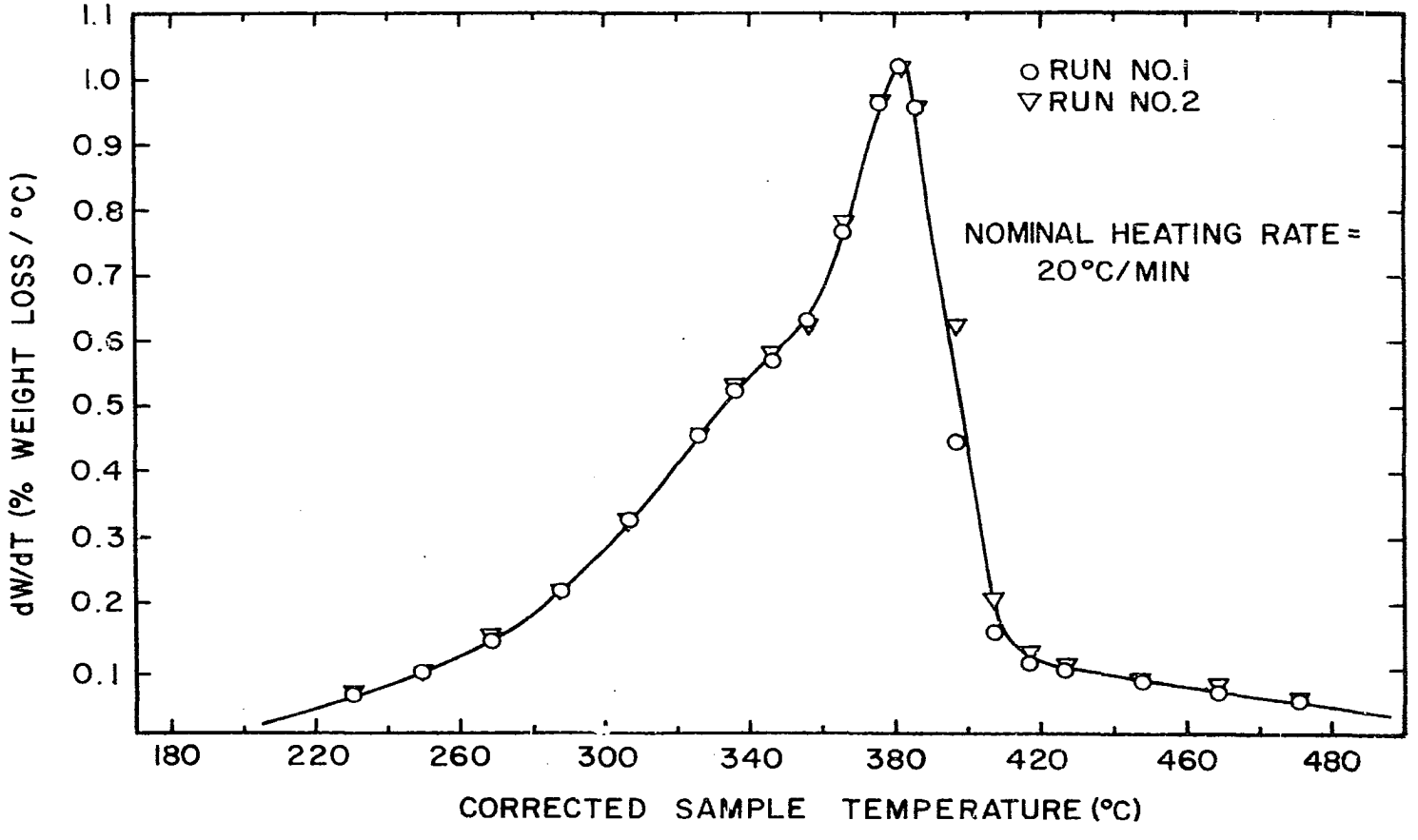


Figure V-15. Rate of Weight Loss of Dry Pine Wood in Nitrogen as a Function of Temperature (Expressed as Per Cent (of Original Weight) Loss per Degree Centigrade).

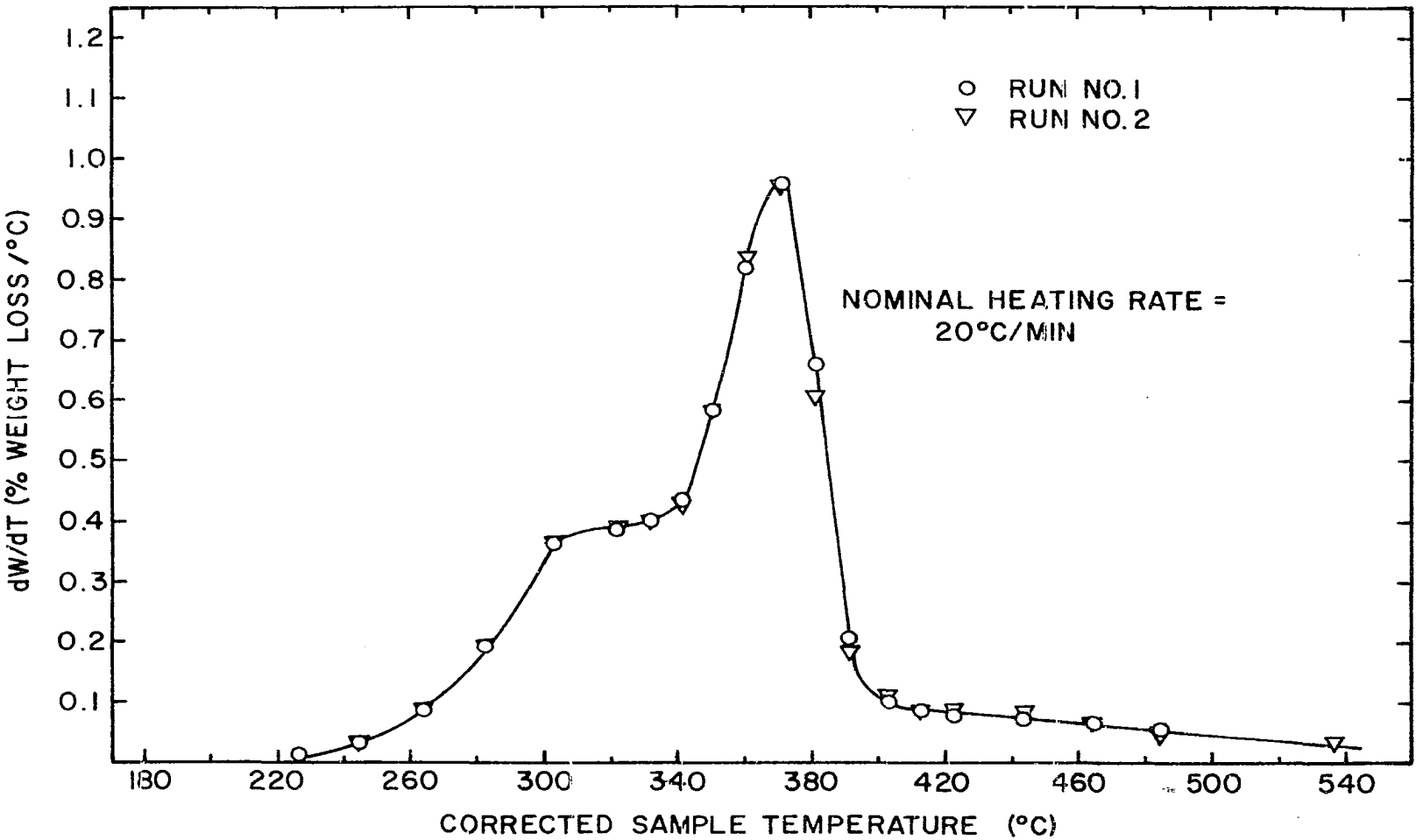


Figure V-16. Rate of Weight Loss of Dry Oak Wood in Nitrogen as a Function of Temperature (Expressed as Per Cent (of Original Weight) Loss per Degree Centigrade).

only radial, one dimensional heat conduction. Such an experimental arrangement was used in this work and is described in a later section; however, it suffices here to say that the problem can be practically reduced for such an experimental arrangement to one of specifying the transverse (perpendicular to the grain direction) conductivity as a function of temperature and thermal decomposition history.

As discussed in Chapter II, there is a considerable amount of information available concerning the thermal conductivity of wood, and correlations which have been shown to be reasonably valid are available for specification of the transverse thermal conductivity as a function of density. These data are strictly applicable only at temperatures similar to those obtained in the course of their measurement, generally under 100°C. The exact dependence on temperature of the thermal conductivity of wood has received no systematic study, to this author's knowledge. Furthermore, such a specification by experimental measurement is not an easy task, and it would require very careful design of an apparatus having greater capabilities than those presently available.

Therefore, it was decided that in the present work the thermal conductivity input to the proposed model would rely primarily on correlations available in the literature although some brief studies were made, using apparatus which was available at this laboratory, to provide some

check on the data used from the literature.

Samples which were used in the model-validation experiments to be discussed later were taken from a 2 x 8 white Ponderosa pine board. The density varied from about 0.48 gm/cm^3 to about 0.52 gm/cm^3 with location in the board (variations of this magnitude in density of wood taken from different locations in the same board are not uncommon, based on this and prior experience at this laboratory.) Assuming an average dry-density of 0.50 gm/cm^3 the thermal conductivity can be predicted using McLean's (44) correlation as follows:

$$K = 0.00478\ (0.50) + 0.000568$$
$$= 0.00296\ cal/cm^2\ sec\ °C/cm$$

Neglecting, as a first estimate, the effect of temperature (the value of 0.00296 cal/cm^2 sec °C/cm is for a temperature of approximately 30°C), this value can be used to describe the transverse thermal conductivity of the samples at temperatures below those where decomposition begins to occur.

At temperatures above the decomposition threshold, it was assumed that the thermal conductivity was a much stronger function of density (resulting from the increased porosity of the specimen due to loss of volatilized materials) than of temperature. Thus, if the remaining partially decomposed material had the same <u>composition</u> as the original wood, its thermal conductivity could be estimated from

thermal conductivity-density correlations, provided its density dependence on temperature was known throughout the decomposition process. Furthermore, a review of the literature revealed that for very low density materials such as wood, matted hair, matted silk fibers, flax, and other density-similar materials the thermal conductivity does not vary greatly with the type of solid material but depends more directly on the density of the material. This observation suggests that the change in composition of the wood during its thermal decomposition should not strongly affect its thermal conductivity except in relation to its reduced density (excluding temperature effects). Widell (79) presented the data in Figure V-17 showing the quotient of thermal conductivity and density for wood and charcoal as a function of temperature, which seems to support this assumption.

Therefore, since the thermal decomposition weight loss behavior had been measured in the course of this work, and since the model which is employed assumes no change in overall dimension of the wood specimen being heated, the density as a function of temperature can be specified throughout the decomposition process. One has then only to multiply the original density of the sample by the percent weight remaining as determined from Figure V-10 to specify <u>local</u> density as a function of temperature.

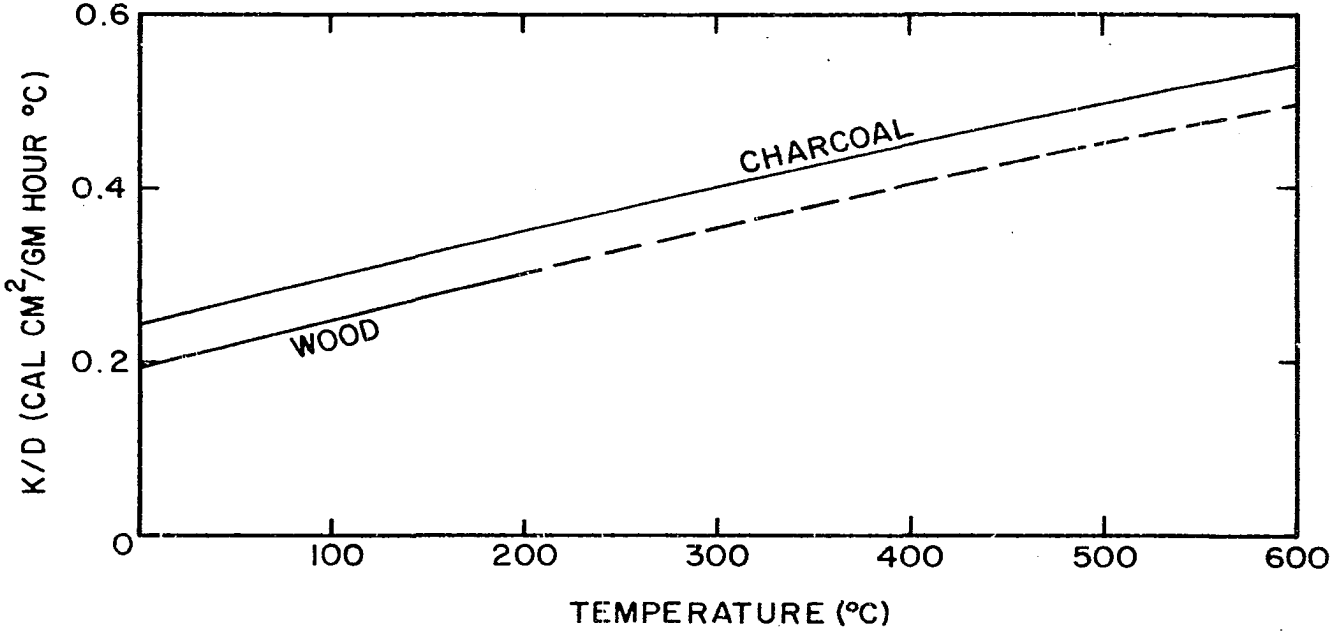


Figure V-17. Quotient of Thermal Conductivity and Density for Wood and Charcoal (79).

It has been shown that the thermal conductivity of dry wood is a reasonably linear function of its density. Thus, the thermal conductivity can be represented by the relation

$$K = 0.00478\ \rho + 0.000568$$

where K = thermal conductivity (cal/cm^2 sec °C/cm)

ρ = density of wood (gm/cm^3)

On the basis of the above assumptions, the thermal conductivity during the thermal decomposition process can be represented by the relation

$$K = 0.00478\ \rho_o\ f + 0.000568$$

where ρ_o = original density of bone dry wood specimen (gm/cm^3)

f = fraction of weight remaining at temperature T, from thermogravimetric data.

Using values of f obtained from Figure V-10, the relation of thermal conductivity to temperature was extended through the decomposition temperature range as shown in Figure V-18. For higher temperatures, the value of K was assumed to remain constant and equal to that calculated for the highest fraction of weight loss. For actual use as input data for machine computations, this thermal conductivity vs temperature relation was approximated by three straight line segments as shown by the dotted lines in

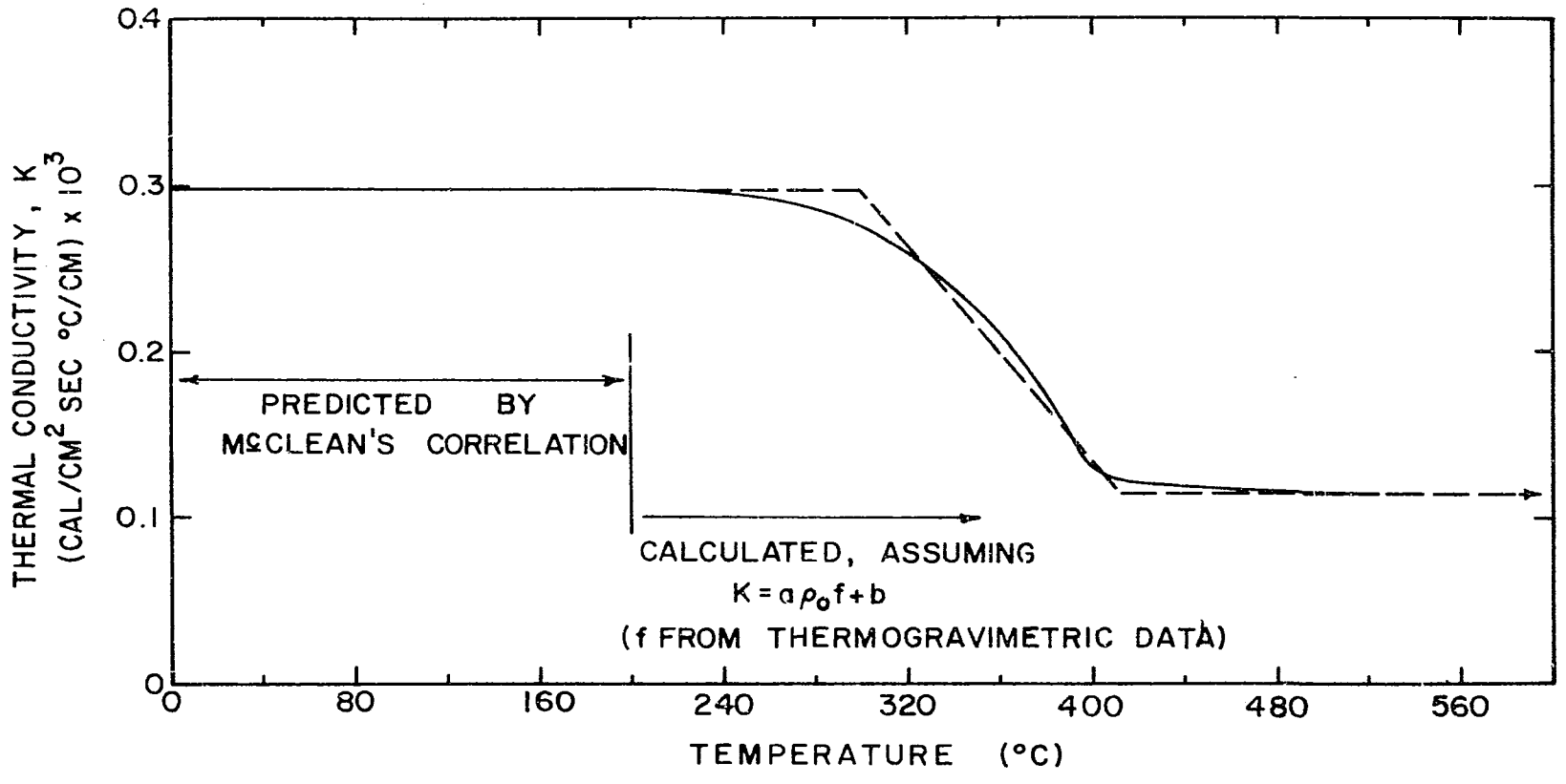


Figure V-18. Estimated Thermal Conductivity of Wood as a Function of Temperature and Decomposition History.

Figure V-18. It is interesting to note that the value of 0.000112 cal/cm^2 sec °C/cm predicted for the completely charred region is in agreement with a value of 0.000114 cal/cm^2 sec °C/cm obtained by extrapolation of data on conductivity of charcoal as a function of density (at 25°C) taken from the Handbook of Chemistry and Physics (45th Edition) as shown in Figure V-19.

It should be emphasized that the above estimation of thermal conductivity does not include any direct effect of temperature; that is, it amounts to specifying the thermal conductivity as a function only of density, which in turn is a function of temperature.

It was also decided to make some measurements of the thermal conductivity of wood in this laboratory to provide checks on the values predicted by the conductivity-density correlations of Waangard and McLean. Because of the difficulties involved in making such measurements by the steady state hot-plate method (which was the method used in all of the previous investigations cited in Chapter II), it was decided to measure the thermal conductivity of wood below its decomposition temperature range by means of a transient method which has been shown by Chung and Jackson (16) to be applicable to low thermal conductivity materials. This method has been used previously at this laboratory by Koohyar (36) with reasonably good results. The method is based on experimental determination of the

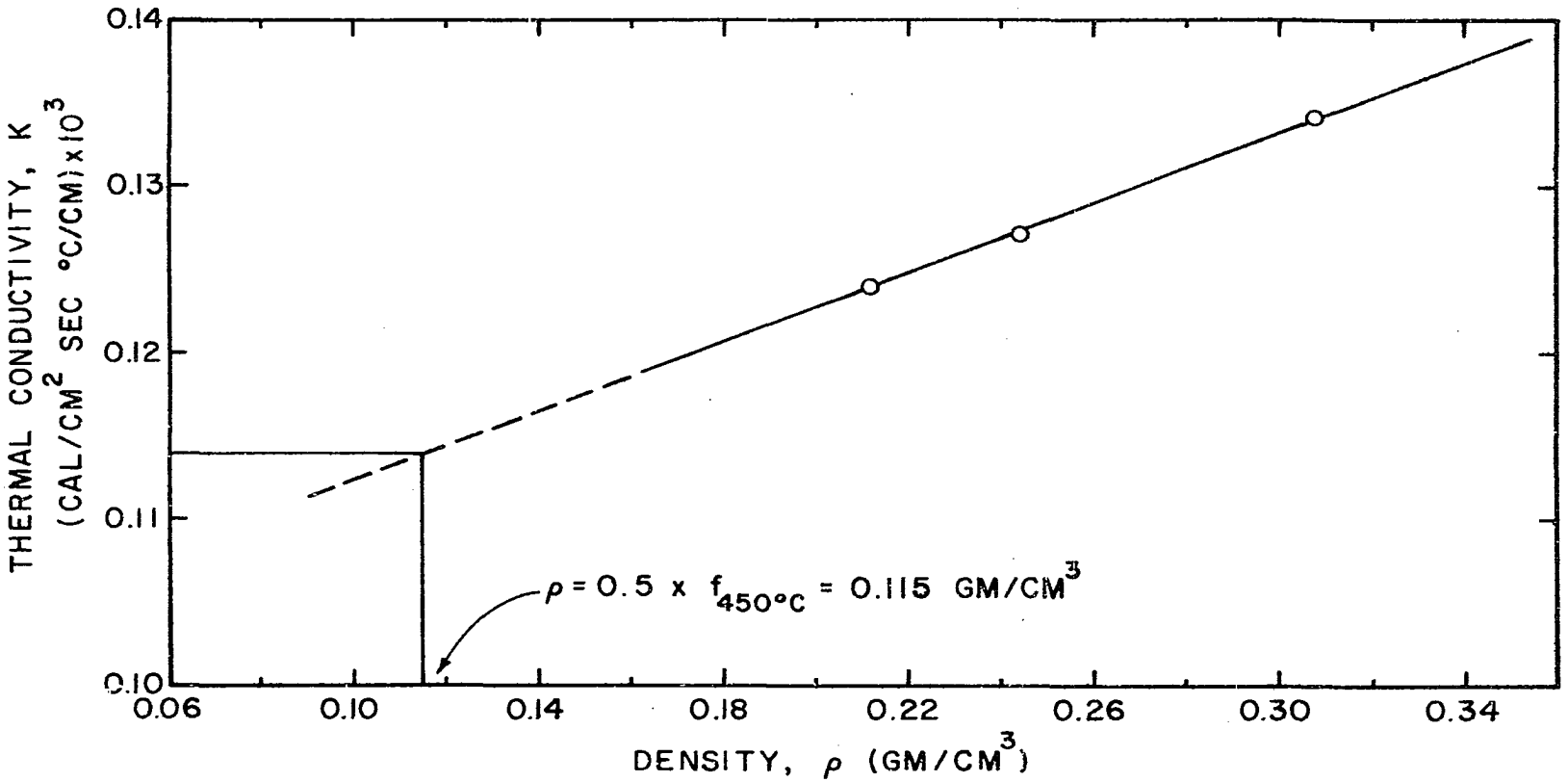


Figure V-19. Thermal Conductivity vs Density for Charcoal (From Handbook of Chemistry and Physics, 45th Ed.).

thermal diffusivity α

where $\alpha = K/\rho C$

and α = thermal diffusivity (cm^2/sec)

K = thermal conductivity (cal/cm^2 sec °C/cm)

ρ = density (gm/cm^3)

C = heat capacity (cal/gm °C)

It is a well known fact that the thermal diffusivity of a material generally exhibits a much weaker functional dependence on temperature than do its individual components, particularly K and C. This fact is usually called upon to justify the usage of an inert-constant and uniform property-model for heat transfer prediction in wood (3), as well as a variety of other materials. Therefore, in this work it was decided to determine the thermal conductivity of wood from the relation,

$$K = \alpha\rho C = \text{constant}$$

since C was known as a function of temperature (see Figure V-7) and ρ remains essentially constant at temperatures below the decomposition threshold temperature.

The equation for unsteady state heat transfer in the radial direction of an infinitely long cylindrical rod is

$$\alpha \frac{\partial^2 T}{\partial r^2} + \frac{1}{r} \frac{\partial T}{\partial r} = \frac{\partial T}{\partial t} \qquad \text{(V-2)}$$

where T = temperature, a function of r and t (°C)

r = radial position at which temperature measurement is made (cm)

t = time (sec)

α = thermal diffusivity (cm^2/sec)

The applicability of this model requires that α be constant, but it does not require constancy of K or the product ρC. The only requirement is that the ratio, $K/\rho C$ remain constant.

If the rod with radius R, initially at a uniform temperature T_i, is suddenly immersed in a fluid having a constant temperature T_a, the initial and boundary conditions are:

$$T = T_i, \quad t < 0, \quad 0 \leq r \leq R$$

$$\frac{\partial T}{\partial r} = \frac{-h}{K} (T_a - T), \quad t > 0, \quad r = R.$$

$$\frac{\partial T}{\partial r} = 0 \qquad , \quad t \geq 0, \quad r = 0 \text{ (center)}$$

The solution to Equation (V-2) is

$$\frac{T_a - T}{T_a - T_i} = \sum_{\nu=1}^{\nu=\infty} \frac{2J_1(X_\nu)}{X_\nu \left[J_o^2(X_\nu) + J_1^2(X_\nu)\right]} e^{-\left(X_\nu^2 \frac{\alpha t}{r^2}\right)} \left[J_o\left(X_\nu \frac{r}{R}\right)\right] \quad \text{(V-3)}$$

The infinite series in Equation (V-3) converges rapidly; after a short time all terms after the first become negligible (16). Equation (V-3) then reduces to the form:

$$Y = A\, e^{-bt} \quad \text{(V-4)}$$

where $Y = \dfrac{T_a - T}{T_a - T_i}$

$$A = \frac{2J_1(X_1)}{X_1\left[J_o^2(X_1) + J_1^2(X_1)\right]} \quad J_o\left(X_1 \frac{r}{R}\right)$$

and $b = \dfrac{X_1^2 \alpha}{R^2}$

which can be written as

$$\ln Y = -bt + \ln A \qquad \text{(V-5)}$$

By plotting log Y vs t and determining the slope -b, one can calculate α from Equation (V-4) if X_1 is known. X_1 is the smallest root of the transcendental equation

$$\frac{X}{(hR/K)} = \frac{J_o(X)}{J_1(X)}$$

and thus depends on the dimensionless group hR/K. However, the limiting value of X_1 as $hR/K \to \infty$ is 2.405 (16). For practical applications, if $\frac{hR}{K}$ is greater than about 100, no significant error will result from assuming $X_1 = 2.405$.

To determine α experimentally, the temperature at some point inside the cylindrical specimen is recorded as a function of time with the above described initial and boundary conditions. A plot of log Y vs t is made, and the thermal diffusivity α is calculated from the measured slope of the resulting line.

The experimental conditions required to justify usage of the above model are:

1. The rod must be long enough to eliminate end effects. It has been shown (16) that a ratio of rod length to diameter of 4 would introduce an error of only 1 part in 10,000 in an isotropic material. Even considering that the value of thermal diffusivity is on the order of two to three times as high along the grain as across the grain, a length to diameter ratio of 8 to 10 should give errors which are within the bounds of experimental accuracy.

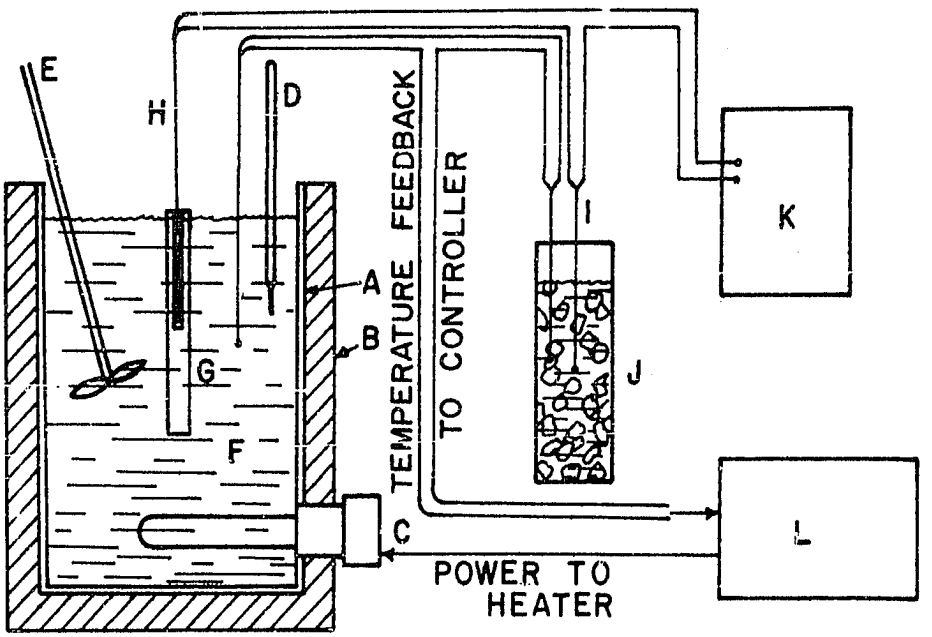
2. The rod must be at uniform temperature initially.

3. The surrounding temperature to which the sample is exposed at time t=0 must be constant.

4. The heat transfer coefficient should be high enough so that the limiting value of $X_1 = 2.405$ can be used. This requirement is a matter of practicality; the model imposes no such restriction.

It is important to note that the temperature measurement need not be made exactly in the center of the cylinder, and its exact location does not have to be known since the heating lines for all radial points are parallel.

The equipment used in the experimental determination of α is illustrated in Figure V-20. It is a direct modification of Koohyar's (36) equipment to allow different, controlled bath temperatures. It consists of an insulated two gallon bucket with a 1000 watt electrical immersion heater fitted in



A GALVANIZED BUCKET
B INSULATION
C IMMERSION HEATER
D THERMOMETER
E ELECTRICAL STIRRER
F CRISCO OIL
G SPECIMEN
H HOT JUNCTION OF THERMOCOUPLE PLACED IN SPECIMEN
I COLD JUNCTIONS OF THERMOCOUPLES PLACED IN ICE BATH
J ICE BATH
K RECORDER
L OIL BATH TEMPERATURE CONTROLLER

Figure V-20. Schematic Diagram of Thermal Diffusivity Apparatus.

the side. An electric stirrer is used to increase the fluid velocity near the surface of the sample cylinder, thus increasing the heat transfer coefficient at the sample surface. A temperature control system is used to maintain the bath temperature at any desired temperature between ambient and 250°C. The bath liquid used was common Crisco cooking oil which is relatively non viscous and easily stirred and is very stable at the temperatures involved. Iron-Constantan thermocouples were used to measure the bath temperature and also served as the feedback element to the Pyrometer Sim-Ply-Trol bath temperature controller. A Honeywell Elektronik 19 recorder was used to record the temperature of the sample, as sensed by an iron-constantan thermocouple.

The samples were pine cylinders, nominally 20.30 cm long and 1.91 cm in diameter. A hole was drilled with a 1/16 inch drill from one end to a depth of 10 cm for insertion of a Conax iron-constantan shielded thermocouple with an 18 gage grounded sheath. Before drying a sample a few drops of water were placed in the thermocouple hole to cause a slight swelling and decreased hole diameter. All samples were then dried at approximately 120°C for 24 hours to a bone dry state before their diameter and density were determined. They were then coated with an epoxy base paint ("Zynolyte" Tub and Tile Finish), which was found to be impenetrable to the oil at temperatures of 200°C and

below. After the samples were dried, the thermocouple hole diameter allowed a very snug fit when the shielded thermocouple was inserted. It is assumed that the small thickness of the eopxy coating with its relatively high thermal conductivity does not significantly affect the result obtained. After positioning the thermocouple in the specimen and registering the initial temperature, the sample was suddenly immersed in the hot oil bath, and the millivolt output of the thermocouple was continuously recorded.

Since the results of differential scanning calorimetry studies and thermal gravimetric studies indicated that no appreciable decomposition heat effects occur below 200°C, a series of 4 pine samples taken from the same board was run in the above described manner with the oil bath temperature controlled at 197 ± 1°C. A typical plot of Y vs t for sample No. 3 is shown in Figure V-21. Note that a very linear plot is obtained as predicted by the model. Table V-2 gives the calculated values of the thermal diffusivity α for all four samples and the percent deviation from the mean value.

Koohyar obtained an average value for α of 0.00177 cm^2/sec for pine samples whose average density was 0.381 gm/cm^3. Since the density was so different between the pine samples used in Koohyar's work and this work, comparison of the values of $\alpha.\rho = \frac{K}{C}$ is probably more meaningful. Thus one finds that Koohyar's value of $\alpha = 0.00177$ cm^2/sec

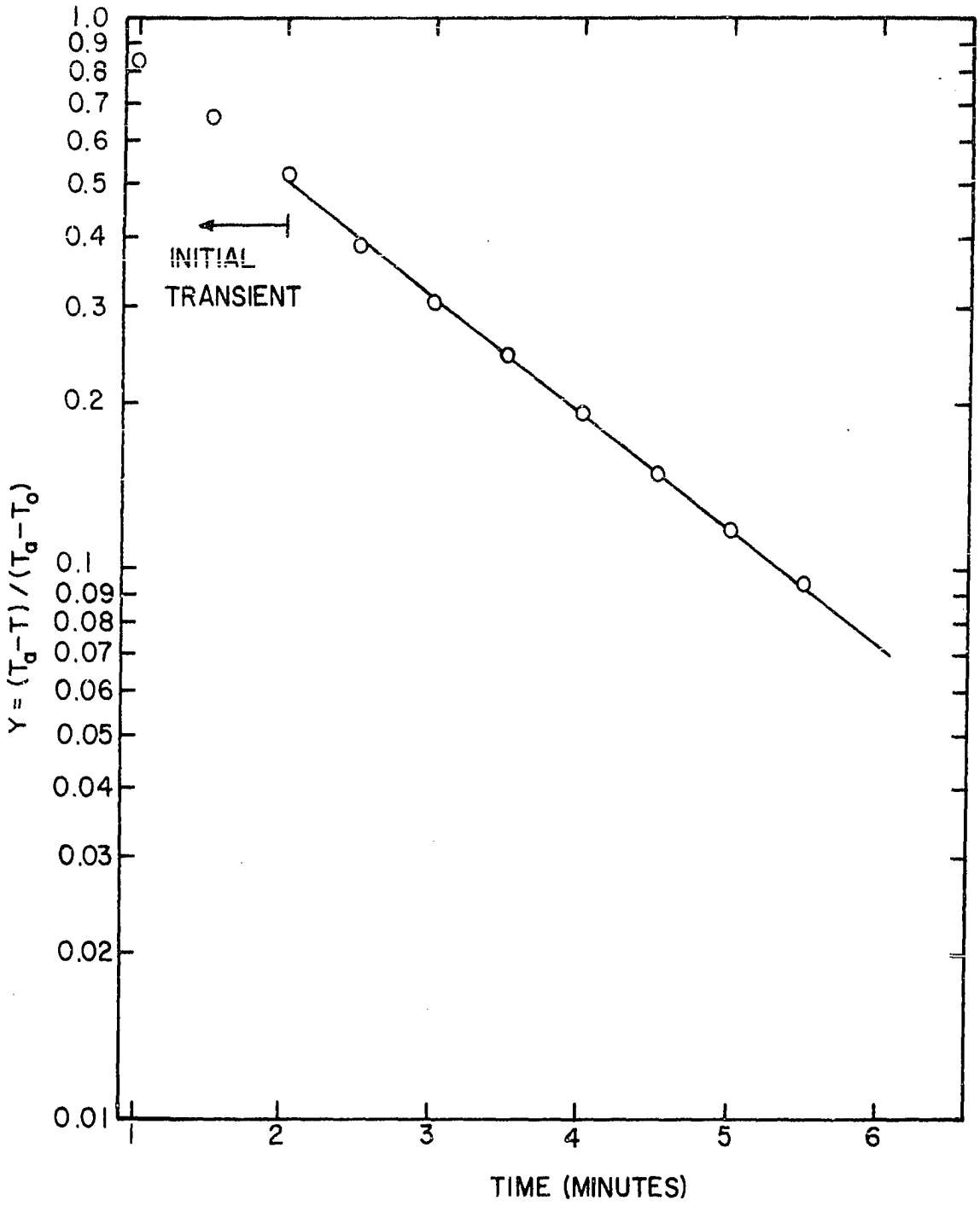


Figure V-21. Example Plot of Y vs t from Thermal Diffusivity Data.

TABLE V-2

THERMAL DIFFUSIVITY OF PINE SAMPLES
OIL BATH TEMPERATURE = 197°C

Sample	Density (gm/cm^3)	Thermal Diffusivity (cm^2/sec)	Percent Deviation from Mean	
			Density	Thermal Diffusivity
1	0.519	0.00125	1.1	2.1
2	0.523	0.00118	0.4	3.8
3	0.526	0.00124	0.2	1.9
4	0.525	0.00122	1.5	0.6
Mean	0.525	0.00122		

TABLE V-3

THERMAL DIFFUSIVITIES OF PINE SAMPLES
OIL BATH TEMPERATURE = 97°C

Sample	Density (gm/cm^3)	Thermal Diffusivity (cm^2/sec)	Percent Deviation from Mean	
			Density	Thermal Diffusivity
1	0.519	0.00136	1.1	2.9
2	0.523	0.00129	0.4	2.3
4	0.533	0.00132	1.5	0.6
Mean	0.525	0.00132		

gives K/C = 0.000674 gm/cm sec compared with K/C = 0.000610 gm/cm sec in this work. Since the heat capacity, C, (in cal/gm °C), is not a function of density, the two results indicate reasonable agreement for values of thermal conductivity. Thus, at 30°C, using values of C from Figure V-7, this work,

$$\text{Koohyar:} \quad K = C\left(\frac{K}{C}\right) = 0.37\ (0.000674)$$
$$= 0.00025\ \text{cal/cm}^2\ \text{sec °C/cm}$$
$$\text{This work:} \quad K = C\left(\frac{K}{C}\right) = 0.37\ (0.000610)$$
$$= 0.00023\ \text{cal/cm}^2\ \text{sec °C/cm}$$

One would expect on the basis of Waangard's (75) and McLean's (44) correlations to see a difference due to density that is not shown above. For example, the tabulation below shows values of K predicted by McLean's correlation and Waangard's alignment chart for the two densities in question.

Density (gm/cm^3)	Thermal conductivity, K (cal/cm^2 sec °C/cm)	
	McLean (44)	Waangard (75)
0.381	0.00024	0.00022
0.525	0.00031	0.00028

In order to see if an unknown effect had been introduced by running the samples at a bath temperature of 197°C, representing an initial heat transfer driving force of $T_a - T_i \tilde{=} 197-27 = 170$°C, as compared with an initial driving force of 97-27 = 70°C in Koohyar's experiments, the same samples run at the higher bath temperature were

rerun at an oil bath temperature of 97°C. The results are shown in Table V-3. The average value of α, and thus K, is approximately 8% higher than reported in Table V-2 for a bath temperature of 197°C. However, Koohyar found in running a much larger number of samples that variation in α was as large as 8 to 10% for different samples out of the same board and that the same samples run repeatedly gave variations as much as 4%. Thus it is difficult to attach any great significance to the difference in the values obtained between the two different bath temperatures, although the difference does appear real. Blackshear and Murty (8) have studied a similar transient method of determination of thermal diffusivity and concluded that the method is insensitive to the absolute value of the temperature at the boundary, but this author believes that additional data are necessary before this assumption can be verified.

Therefore, for temperatures up to approximately 200°C, it was decided to use the average of the above values, or $\alpha = 0.00127$ cm^2/sec.

By assuming that α is not a function of temperature over the range 40 to 200°C, one can then calculate the value of thermal conductivity at 40 and 200°C as follows:

$$K/40°C = \alpha\rho C = 0.00127\ (0.525)\ (0.380)$$
$$= 0.000253 \text{ cal/cm}^2\text{/sec °C/cm}$$

and

$$K/200°C = \alpha\rho C = 0.00127\ (0.525)\ (0.410)$$
$$= 0.000273\ cal/cm^2\ sec\ °C/cm$$

If α is assumed to remain constant up to a temperature of 240°C (only about 2% weight loss has occurred), then the predicted value of K (utilizing values for C, the heat capacity, from Figure V-7) is

$$K/240°C = \alpha\rho c = 0.00127\ (0.525)\ (0.480)$$
$$= 0.00032\ cal/cm^2\ sec\ °C/cm$$

Considering the assumptions inherent in the application of Equation V-2 and the dependence of the results on accuracy of specification of heat capacity and density, these results are in reasonable agreement with the value estimated in Figure V-18.

The thermal conductivity-temperature relationship of Figure V-18 was formulated as a first estimate for use in numerical computations using the proposed model. It was realized that considerable uncertainty existed therein, particularly in the portion of the curve above 300°C. However, in its present form the model has been written in such a way that specification of only two parameters is necessary; energy capacity and thermal conductivity. Since the energy capacity was believed to be specified with reasonable accuracy, the model can be used to "fit" the thermal conductivity by comparing predicted results with results observed by experiment. Also, since the

model in its present form does not include heat transfer due to internal convection, it is reasonable to determine an "effective" thermal conductivity in this manner which accounts for this additional mode of heat transfer. If the model, which includes only the energy capacity and an effective thermal conductivity, is capable of prediction of the transient temperature distribution and transient volatile evolution rate it should prove to be a valuable tool.

Experimental Test for Model Validation

It was desired to define and carry out an experiment in which a wood sample could be heated and partially decomposed in such a way that the boundary conditions could be specified with sufficient confidence to allow meaningful comparison between actual measured results and theoretical results computed with the proposed model. Most of the experiments of this nature which have been described in the literature have attempted to specify either the temperature of the boundary at the heated surface or the amount of radiant heat incident on the surface. Akita's method of heating specimens by immersion in a bath of molten metal is an example of the former, and measurement of incident heat has been made from several types of radiant sources including carbon arc and tungsten filament lamps (60) and flames (36). There are considerable problems associated with both of these boundary conditions. To specify the temperature of the surface, one usually relies on good contact

between the specimen surface and a known temperature surface, assuming the specimen surface temperature to be accurately approximated by the temperature of the known surface (such as the molten metal bath temperature in Akita's work, or a hot plate whose temperature is automatically controlled). Extremely good contact must be obtained. Such contact is difficult to achieve while at the same time allowing for easy removal of the gaseous decomposition products which must issue through the heated surface. In the case where the incident radiation is known, description of the boundary condition requires knowledge of the radiative heat transfer properties of the material, including reflectance, absorbtance, transmittance, emittance properties, and diathermancy. The lack of such information is well known even for materials which do not undergo state changes or decomposition. The problem is even more complicated in the case of a material like wood, where these properties change markedly during the process of heating and decomposition. Thus, it seems reasonable to believe that the uncertainties associated with the specification of boundary conditions of these types is so great that they might well result in controlling errors which would overshadow some effects which are included in the model.

A considerable amount of study was done to find a better way of specifying the boundary conditions on an

externally heated, decomposing wood specimen, resulting in the experimental configuration represented by the schematic of Figure V-22 and shown in the photograph of Figure V-23. The sample is a wood cylinder, approximately 15.3 cm in length and 4.45 cm outside diameter, with an axial hole 0.635 cm in diameter. Heat is provided at the inside surface of the wood cylinder from a single 18 gage, 80-20 nickel-chromium resistance wire. This wire size and type was chosen in conjunction with the 0.635 cm inside diameter of the wood sample cylinder to satisfy the following requirements.

1. The resistance wire type was chosen so as to minimize the temperature effect on electrical resistance. The wire used was Tophet 'A', a nominal 80-20 nickel chromium alloy containing trace amounts of other metals, including manganese, to provide increased resistance to carburizing atmospheres (manufactured by Wilbur Driver Company, Newark, New Jersey). The correction factor which must be applied to correct the resistance of the wire at 25°C for temperature is shown in Figure V-24. It should be noted that the wire can be considered to have a constant resistance, equal to its 25°C value multiplied by 1.06, over the temperature range 500°C to 1100°C with an error of less than one percent.

2. For a given power dissipation, the wire size will determine its operating temperature (the larger surface area of larger diameter wires allows a given amount of heat

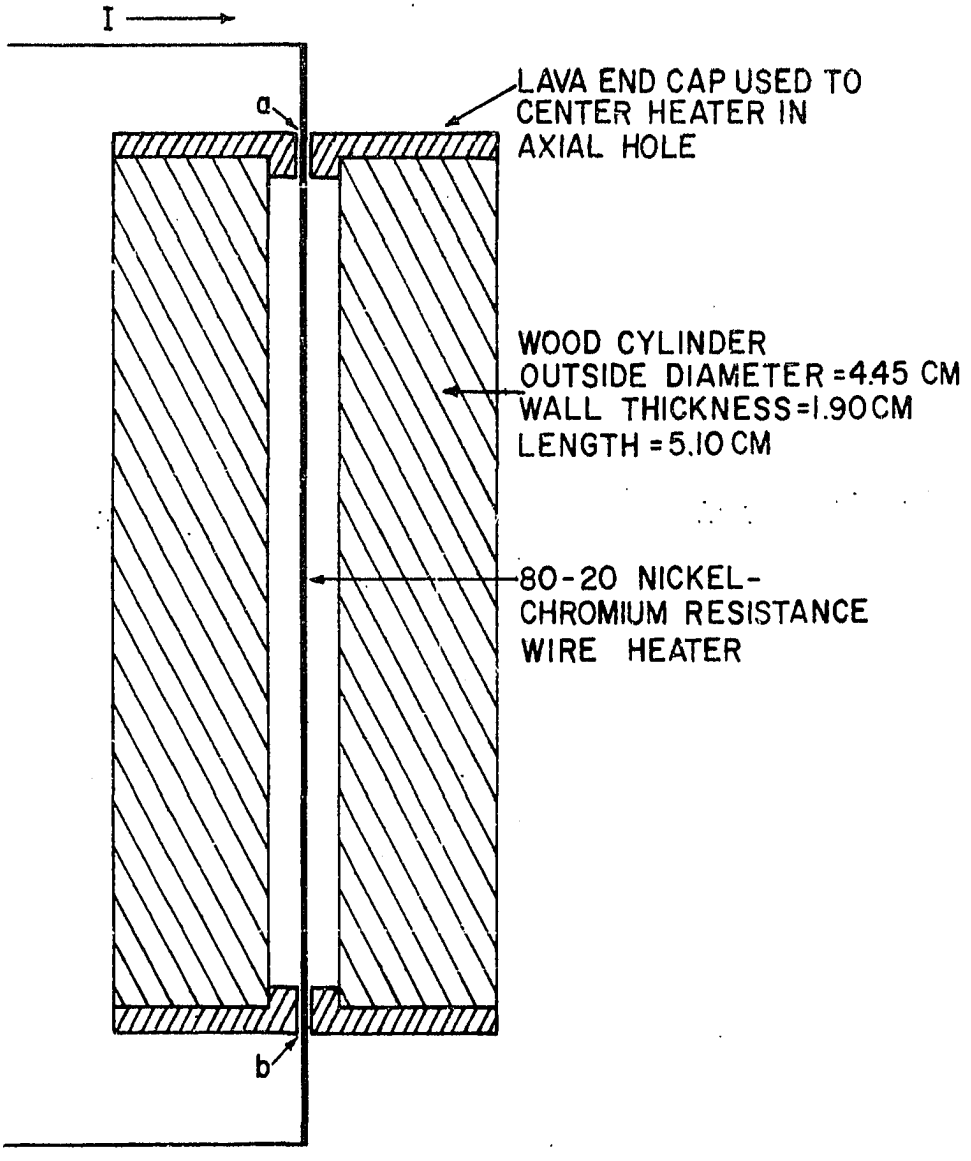


Figure V-22. Schematic of Resistance Wire Heater and Wood Cylinder.

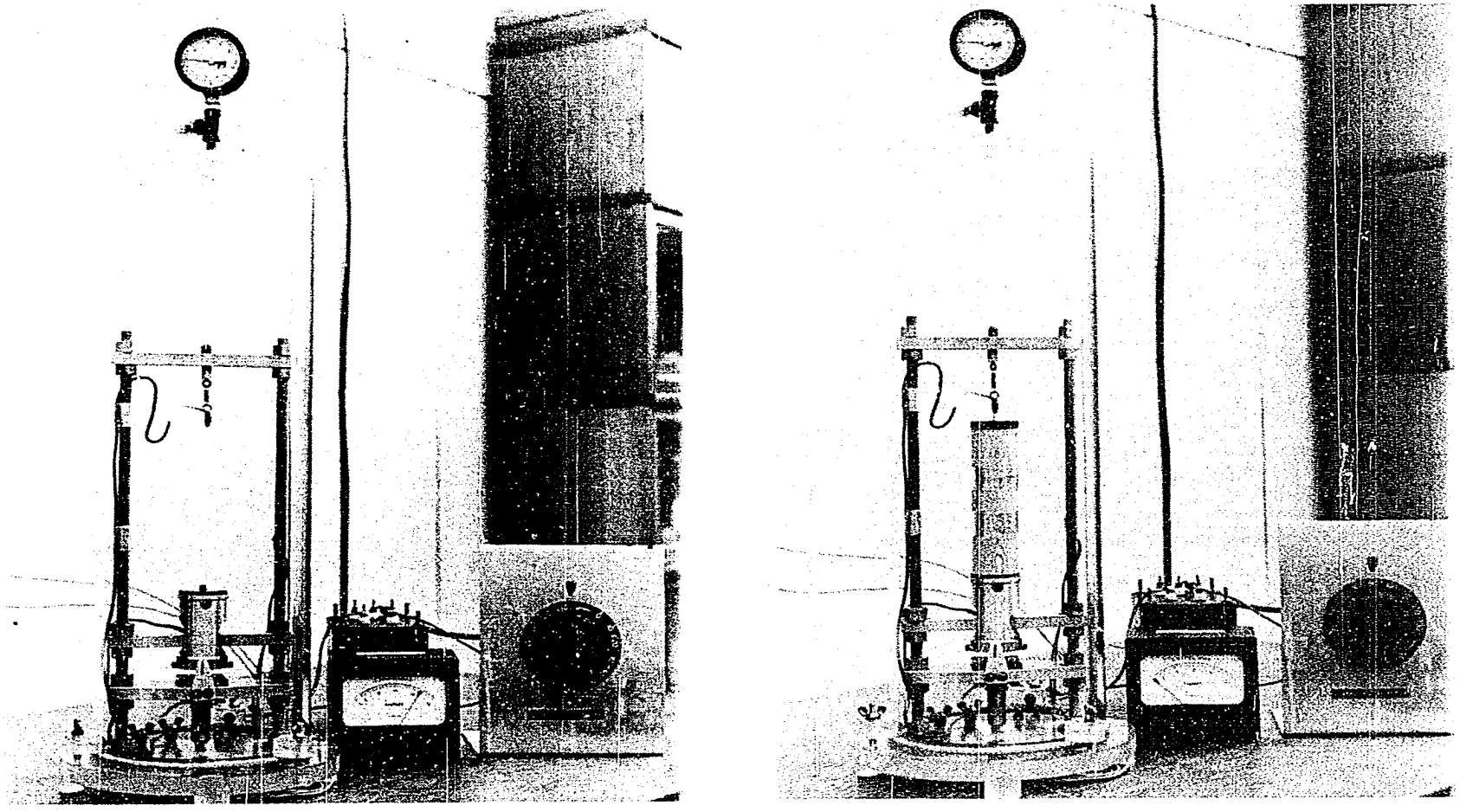


Figure V-23. Photograph of Resistance Wire Heater with and without Wood Sample in Place.

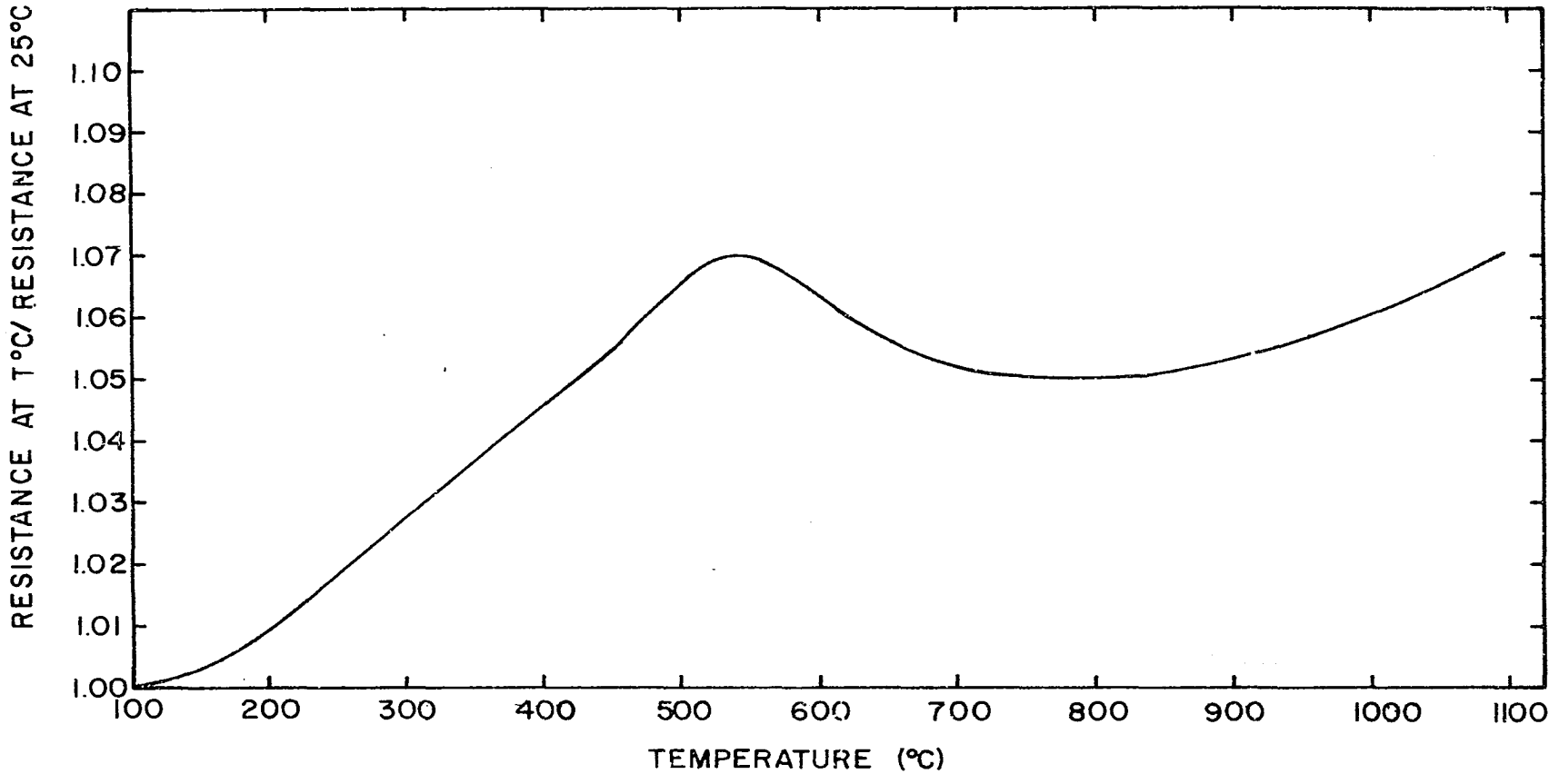


Figure V-24. Temperature Dependence of Electrical Resistance of Tophet A 80-20 Nickel-Chromium Wire.

generated in the wire to be transferred from a lower temperature than in the case of a smaller wire). The 18 gage, 0.040 inch diameter wire, when carrying 14.0 amps alternating current and operating at a temperature in the range 500-1100°C, generates heat at a rate which can be determined by application of Ohm's Law:

$$P = I^2R = (14.0)^2(R_o)(1.06)$$

where R_o = resistance at 25°C = 0.0135 ohms/cm

thus $P = (14.0)^2(0.0135)(1.06) = 2.84$ watts/cm

$= 0.68$ cal/sec-cm

It was determined that this size wire would not exceed its maximum operating temperature when operated at the levels of heat generation desired in this work. For example, generation of 0.68 cal/sec-cm of wire length will result in a heat flux at the inside surface of the wood cylinder of $\doteq 0.34$ cal/cm^2 sec if all of the heat generated in the wire is absorbed by the wood. This flux level would be sufficient to cause ignition if sufficient oxygen were present (36), and is within the operating capability of the wire in the proposed arrangement.

Reference to Figure V-22 shows that all heat transferred by the wire between points a and b is absorbed by the wood sample and the end caps or by the gas in the annulus between the wire and the inside surface of the wood specimen. It was assumed that the heat which is removed

from the wire by the gas in the annulus is a negligible amount of the total thermal energy leaving the wire, based on the following considerations and experimental evidence.

1. The ends of the wood cylinder are almost sealed by the lava plugs used to center the resistance wire; thus heat removal by natural convection is severely limited, especially in view of the small clearance ($\sim$ 0.25 cm) between the wire and the inside wood surface. Thus even if the gas in the annulus is heated to an appreciable degree, most of this heat will be transferred through the gas layer to the wood surface since very little heat can escape with the small amount of vapors exiting the hole in the lava plugs (around the resistance wire).

2. At the temperatures of operation of the wire in these experiments, the primary means of heat transfer from the wire is assumed to be radiative. Since the attentuation of thermal radiation by the vapors in a 0.25 cm path length can be neglected, most of the heat generated within the wire will be transferred directly to the wood surface by radiation. This assumption can be partially verified by measuring the temperature of the wire with a given amount of current passing through it when the wire is in the open air and when it is in a container which is evacuated. If the heat removal from the wire when exposed to the open air is due to any appreciable extent to convective and conductive heat transfer, the wire should operate at a measurably

higher temperature when in a vacuum (at the same power level). The wire temperature was measured with an optical pyrometer by viewing the wire through the Plexiglas enclosure, first with nitrogen passing through the enclosure, and then with the enclosure evacuated to less than 25 millimeters of mercury. In both cases a current of 18.3 amperes alternating current was maintained in the wire. The optical pyrometer used was a Pyro Micro-Optical Pyrometer manufactured by the Pyrometer Instrument Co., Inc., Bergenfield, New Jersey. The instrument has a claimed reproducibility of ± 3°C. The measured temperature of the wire (assuming an emissivity of 1.0) was 1850 ± 10°C in a vacuum and 1800 ± 10°C in an essentially still, nitrogen atmosphere. Since the space between the wire and the cylindrical Plexiglas container was about 9 cm as compared with a space of 0.25 cm between the wire surface and the wood sample during a run, (thus providing for a greatly enhanced convective cooling capability over that present in a wood sample run), the results indicate that the heat flux can be considered purely radiative, without much error. However, even that portion of heat which is absorbed by the gas in the annular space during a run could be expected to give up a major portion of its heat to the inside wood sample surface due to the limitation on flow rate of gases out the end cap holes.

Strong end effects due to transfer of heat from the wire directly to the lava end caps and from the wood underneath the caps to the caps would be expected so that in order to specify the boundary conditions accurately for the entire 15.3 cm length wood specimen, boundary conditions taking these effects into account would have to be specified at both ends of the cylinder. These end boundary conditions would be difficult to specify with a high degree of accuracy. The problem can be considerably simplified by considering only the center 5.1 cm section of the wood sample. Assuming the electrical heat generation rate to be constant and uniform along the wire's length, one can specify the heat flux at the inside surface of the wood sample and let the two 5.1 cm sections on either end "absorb" the end effects. In such a case a boundary condition of no heat flux can be made at the top and bottom of the 5.1 cm center section of the wood sample. The outside of the cylinder can be assumed to transfer heat to the surrounding atmosphere according to Newton's law of cooling,

$$- K\frac{\partial T}{\partial r}\bigg|_{r_o = \text{outside radius}} = h_c(T_s - T_a)$$

where K = thermal conductivity (cal/cm^2 sec °C/cm)

h_c = heat transfer coefficient (cal/cm^2 sec °C)

T_s = temperature of outside surface (°C)

T_a = temperature of ambient (°C)

Figure V-25 shows a schematic of a section of cylindrical symmetry of the 5.1 cm long central portion of the 15.3 cm long cylinder used for model validation studies, with the boundary conditions used in the numerical solution to Equation IV-6.

The zero-flux boundary conditions at the ends of the 5.1 cm long central test section are justified by the absorption of the end effects in the two inch wood sections on the ends, resulting effectively in one-dimensional, radial heat flow in the center test section. The boundary condition at the outside radial surface of the cylinder was assumed to be described by Newton's law of cooling. The heat transfer coefficient h_c was estimated as follows. In all runs, the sample and its resistance wire heat source were totally enclosed in a sealed Plexiglas container purged with dry nitrogen at a very slow flow rate. Flow of nitrogen through the enclosure served to sweep away gaseous decompposition products. Since the nitrogen velocity was low past the sample surface, it was assumed that a natural convection heat transfer coefficient was applicable. This heat transfer coefficient was calculated using the Saunders and Weise correlation (43):

$$\frac{h_c L}{k_f} = 0.59 \left[\frac{L^3 \rho_f^2 g \beta_f \Delta t}{\mu_f^2} \left(\frac{C_p \mu}{k} \right)_f \right]^{0.25} \qquad \text{(V-6)}$$

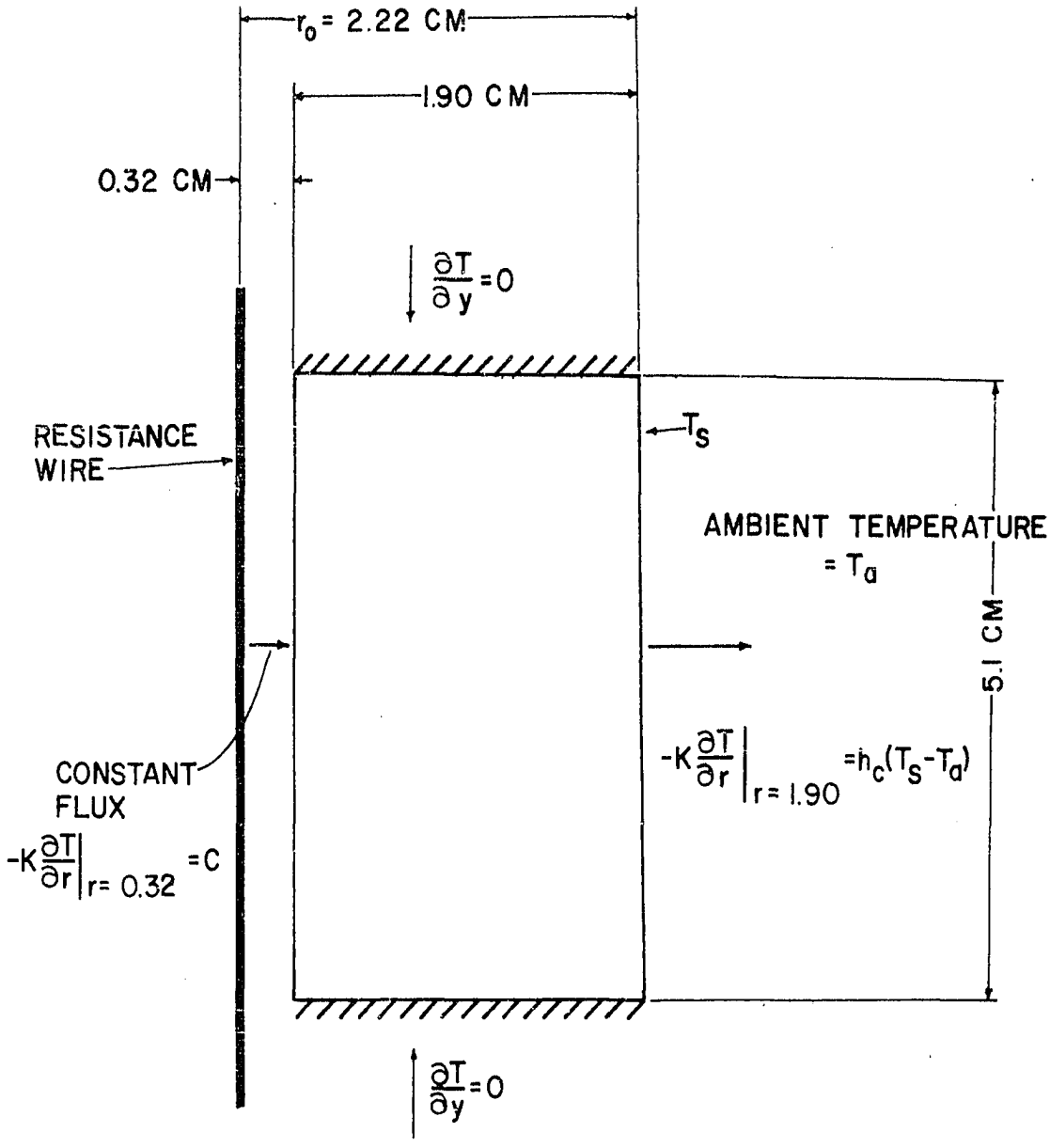


Figure V-25. Schematic of Section of Cylindrical Symmetry of Center Test Specimen.

A mean film temperature of 66°C was assumed for specification of thermal and physical properties of nitrogen at atmospheric pressure. Thus for nitrogen around the cylinder:

ρ_f = density (0.00108 gm/cm^3)

μ_f = viscosity (0.00019 gm/cm sec)

C_p = specific heat (0.25 cal/gm °C

k_f = thermal conductivity (0.0000691) cal/cm^2 sec °C/cm)

β_f = coefficient of volumetric expansion (0.00367)

L = length of cylinder (15.3 cm)

ΔT = temperature driving force, assumed (67°C)

h_c = heat transfer coefficient (cal/cm^2 sec °C)

Equation V-6 then gives

$$\frac{h_c L}{k_f} = 0.59 \left[3.36 \times 10^7\right]^{0.25}$$

and $h_c = 0.00021$ cal/cm^2 sec °C

As suggested previously, the heat flux at the inside surface of the wood cylinder was determined by assuming that all of the heat generated in the 5.1 cm center section of the resistance wire was absorbed uniformly by the inside surface of the central wood test specimen. In relation to this assumption, several important advantages accrue from the experimental design chosen. The thermal mass of the wire itself is very small so that its temperature response is rapid. This effect can best be

illustrated by writing a transient heat balance on a unit length of the wire. Let the heat generated per unit length of wire be considered a constant, Q. At a given constant current this assumption is valid for operating temperatures from 500°C to 1200°C since the resistance of the wire is effectively independent of temperature in that range. Let the heat transferred from the wire per unit length be $\alpha(T_{ws} - T_s)$ where T_{ws} is the wire surface temperature, T_s is the temperature of the heat sink (here assumed to be the wood surface temperature), and α is a heat transfer coefficient which includes all operative modes of heat transfer (α of course is a strong function of T here, but for purposes of this illustration, let it be considered constant). Let C equal the heat capacity of the wire in cal/°C. Assuming the temperature gradient in the wire to be negligible so that the unit length of wire can be described as a lumped parameter system, a transient heat balance gives

$$Q - \alpha(T_{ws} - T_s) = C \frac{dT_{ws}}{dt} \qquad \text{(V-7)}$$

Rearranging, $\frac{C}{\alpha} \frac{dT_{ws}}{dt} + T_{ws} = Q/\alpha + T_s$

or $$\tau \frac{dT_{ws}}{dt} + T_{ws} = Q/\alpha + T_s \qquad \text{(V-8)}$$

where $\tau = C/\alpha$ can be considered as a first order time

constant for the system. Assume that at t = 0, $T_{ws} = T_s$ and Q = 0. Laplace Transformation of Equation V-8 then yields

$$(\tau S + 1)\ T_{ws}\ (S) = \frac{1}{\alpha}\ Q(S) + T_s(S)$$

or
$$T_{ws}\ (S) = \frac{Q(S)}{\alpha(\tau S + 1)} + \frac{T_s(S)}{\tau S + 1} \qquad \text{(V-9)}$$

This transformed differential equation describes the transient response of the wire's surface temperature to changes in both the electrical heat generation rate and the exterior heat sink temperature. Thus for changes only in Q, the electrical heat generation rate, the equation reduces to

$$\frac{T_{ws}(S)}{Q(S)} = \frac{1}{\alpha(\tau S + 1)} \qquad \text{(V-10)}$$

while for heat sink temperature changes only,

$$\frac{T_{ws}(S)}{T_s(S)} = \frac{1}{\tau S + 1} \qquad \text{(V-11)}$$

Now consider what happens when at time t = 0, a current is suddenly passed through the resistance wire. Initially, of course, the wire temperature will respond to this heat generation and will rise to a level which

provides sufficient heat transfer potential to allow the heat generated in the wire to be transferred to the surroundings. However, as the heat is transferred to the wood specimen, its temperature rises, so that the wire temperature must in turn continually rise in order for the wire to transfer the heat which is being generated at a constant rate. One can think of this process as a natural feedback situation; the wire temperature changes in response to the increase of the wood surface temperature. The important fact is that the amount of heat transferred from the wire to the wood surface is dependent on their respective temperatures and not directly on the heat generation rate. Thus, if one hopes to determine the heat flux at the surface of the wood specimen by calculating the heat generation rate in the wire, it must be assumed that the temperature response of the wire is sufficiently fast to allow neglect of the transient heat accumulation in the wire itself. This response speed is measured by the magnitude of the time constant $\tau = \frac{C}{\alpha}$, which is directly proportional to the heat capacity of the wire per unit length. For the 18 gage wire used, the heat capacity per centimeter of length is approximately 0.01 cal/°C. Thus if α is moderately large, which it can be expected to be when the wire temperature is high, say above 500°C, the time constant is very small. Hence the wire can be expected to change its temperature rapidly enough to assume that regardless of its

necessary increase throughout the process of heating the wood specimen, the flux from the wire can be considered a constant value equal to the rate of heat generated internally. A measure of the response speed of the heating wire can be obtained by observing the time required for the wire to come to its steady state operating temperature after a step change is made in the internal heat generation rate (by simply turning on the current through the wire). Based on a definition of the first order time constant as the amount of time required for the temperature to achieve 63% of its final steady state value in response to a step change in the internal heat generation rate, the time constant was conservatively estimated by visual observation to be about 6 seconds. Since the heating times for wood samples herein ranged from 4 to 8 minutes the response capability of the wire appears sufficient to justify the assumption of a constant heat flux at the inside surface of the wood cylinder.

Also, it has been noted in the section on previous work that Williams (80) has shown that pine samples are effectively opaque to radiation emitted from a black body at 2000°K or below. The nickel-chromium wire used in this work melts at a temperature of approximately 1250°C, and thus was always operating at a somewhat lower temperature. Therefore it can be safely assumed that the major portion of its radiation has a wavelength in the infrared region

and is therefore absorbed at the surface of the wood specimen, so that diathermancy need not be considered. Such would not necessarily be the case with some other types of heat sources such as carbon arc or tungsten filament lamps.

In all experiments conducted herein the current in the wire was maintained at 14.0 amperes, resulting in a heat generation per unit length of wire of

$$P = I^2R = (14.0)^2(0.0135)$$
$$= 2.84 \text{ watts/cm}$$
$$= 0.68 \text{ cal/sec cm}$$

Assuming this heat to be absorbed uniformly by the inside surface of the wood test specimen, the rate of transfer of heat to the inside surface of the wood cylinder is then

$$\frac{0.68 \text{ cal/sec cm length}}{2.0 \text{ cm}^2\text{/cm length}}$$
$$= 0.34 \text{ cal/cm}^2 \text{ sec}$$

Utilizing these boundary conditions along with the measured energy capacity vs temperature (DSC data) and estimated thermal conductivity vs temperature relations presented in the preceding sections of this chapter, the system of Equations (IV-7) was solved to predict the transient temperature distribution in the wood cylinder.

For use in the computations, the energy capacity curve was extrapolated to higher temperatures by assuming that the value of the energy capacity remains constant at a

value of 0.9 cal/gm °C (based on original weight) at temperatures beyond 450°C.

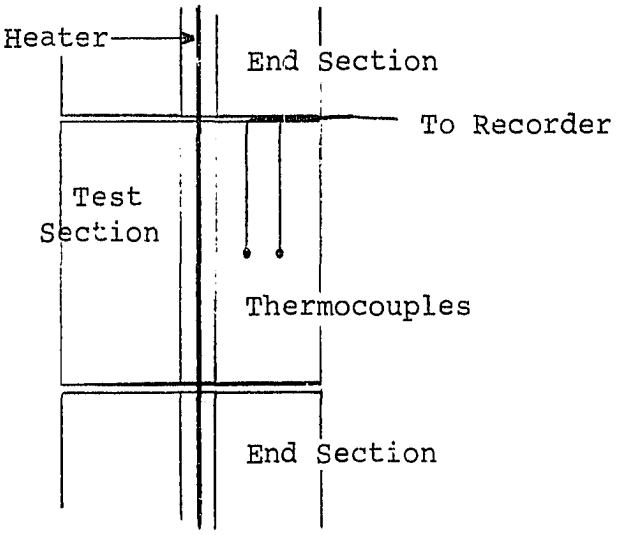
As discussed in Chapter IV, the method used for solution of this system of first order, non-linear, differential equations is based on a variant of the Peaceman-Rachford alternating direction, implicit, iterative methods and is described in Hashemi's thesis (26). Since at each time level in the solution, one obtains the temperature of the mesh regions (i,j), it is a straighforward procedure to multiply the volume of each mesh region by the percent weight loss at the temperature of the mesh regions, and by summing over all of the mesh regions, to compute the percent weight loss of the entire sample as a function of time. The percent weight loss as a function of temperature can be obtained directly from the thermogravimetric data which were presented in Figure V-10.

To provide an experimental check on the validity of the computed results, the actual temperatures obtained at two radial positions in the central wood cylinder test section as a function of time and the total weight loss of the test section during a run were measured. Although the primary objective of the computations was the prediction of weight loss (i.e. volatile product evolution) rates as a function of time, some temperature measurements were desirable to check the validity of the predicted temperature profiles. In this work it was decided to make temperature

measurements at two radial positions which were far enough removed from the heated surface to be outside the region of thermal decomposition. It was felt that measured temperatures in the uncharred region would provide a better check on the validity of the thermal conductivity values used in the computations than would measurements in the char region. In addition, it is believed that measurements of temperatures can be made with considerably greater accuracy in the uncharred region than in the charred region. The temperature gradients in the region of char formation are very steep, so that knowledge of exact location of temperature measurement becomes critical. Since the char front may move inward a distance of only 0.5 cm or so, and the temperature drop over this region may be several hundred degrees centigrade, accurate measurement becomes rather uncertain due to the problem of exact specification of the location. Additional uncertainties are present if the thermocouples are in a region where decomposition is occurring, and accompanying volatile product flow patterns are present.

Fine wire (36 gage) chromel-alumel thermocouples were imbedded in holes drilled parallel to the cylinder's axis with a No. 72 drill, at the selected radial positions, to a depth of approximately 2.5 cm. The individual thermocouple wires were insulated with a Teflon coating which is resistant to temperatures of 260°C. The thermocouple wires were led out between the center test section and

the end "guard" section as shown below.



With this arrangement, the thermocouple lead wires are lying along an isothermal surface for a distance of approximately one inch from the bead location, thus minimizing conduction of heat through the thermocouple leads which would otherwise result in measurement error. The thermocouple voltages were continuously recorded by a two channel Honeywell Electronik 19 Recorder.

Pine samples were used in this portion of the study. Cylinders of pine 15.3 cm long and 4.45 cm in diameter were cut on a lathe. These cylinders were cut into 5.1 cm long sections and each section was drilled axially with a ¼ inch drill. After the thermocouple wells were drilled and the thermocouples were inserted, a few drops of water were inserted into each thermocouple well with a hypodermic syringe. This moisture caused the wood to swell slightly, resulting in a tight fit of the thermocouples. The test section, with thermocouples in place, and the end guard

sections were then dried for approximately 20 hours in an oven maintained at 110 ± 5°C. After drying, the test section was accurately weighed, and the test section and end sections were fitted together in their original, uncut, orientation and taped together with Permacel aluminum reflecting tape around the joints. Care was taken to insure that the axial hole was aligned in all three sections. Small lava end caps were used to center the resistance wire in the center of the axial hole as shown in Figure V-22. The sample assembly was then covered with the Plexiglas enclosure shown in Figure V-23. The enclosure was evacuated to a pressure of less than 1 inch of mercury and then purged with a low flow rate of dry nitrogen.

A run was started by closing a switch which allowed 14.0 amps of alternating current to flow through the resistance wire. The current was measured with a Simpson 0-25 amp AC ammeter (± 4% accuracy). The temperatures at the two radial positions were continuously recorded. The current to the heater was turned off at the end of the run. Runs with total heating times of 8 minutes down to 4 minutes were made. After allowing the sample to cool, the center test section was weighed to determine the weight of volatile products evolved.

After weighing the center section it was cut in half for examination of the char front. A typical sample section appearance is shown in Figure V-26. It should be

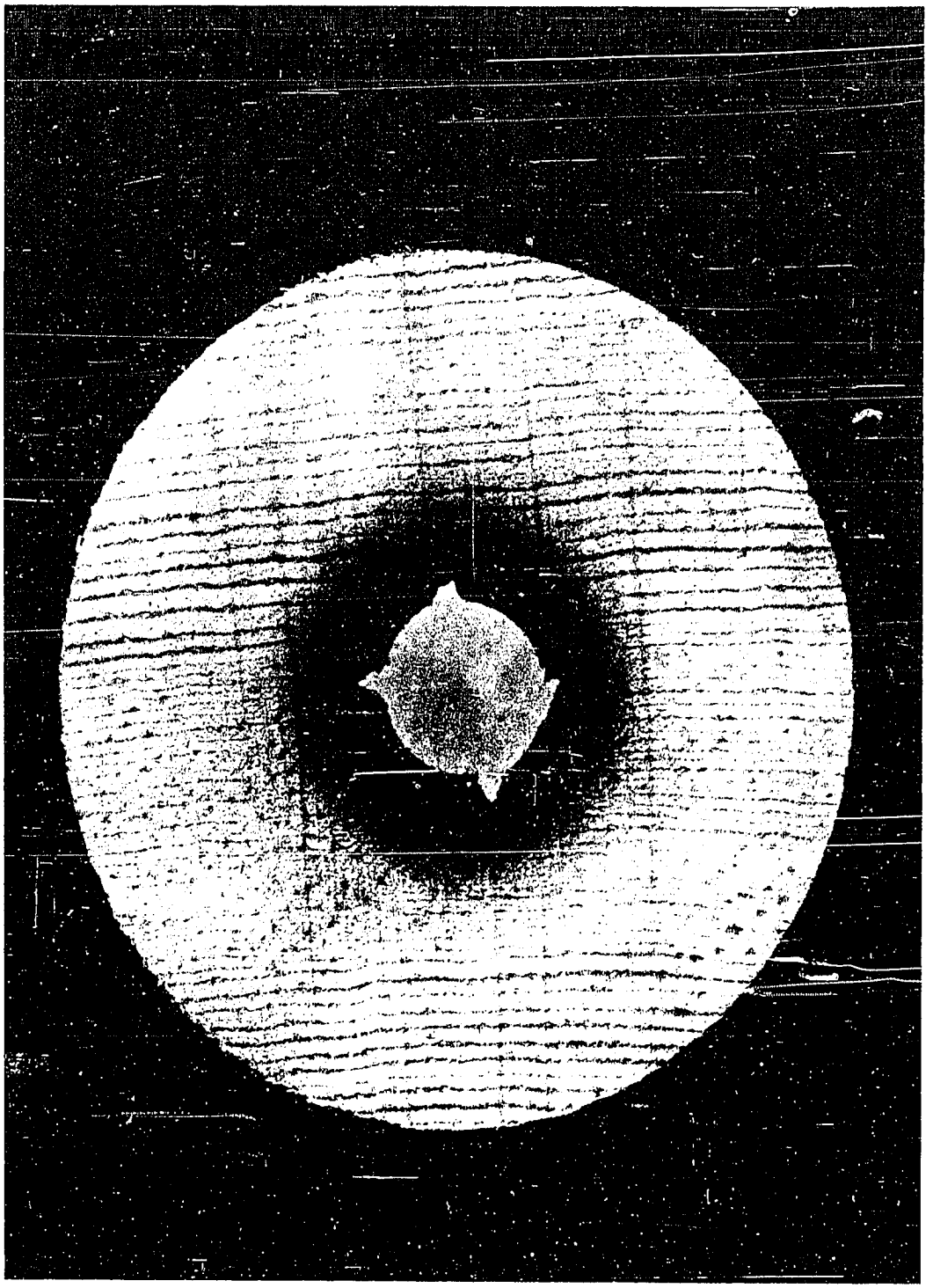


Figure V-26. Photograph of Cross Section of Pine Test Cylinder after Completion of Run.

noted that a very sharp char boundary is evident and that the outside boundary of the char region is circular. From examination of the energy content curve of Figure V-7 and the differential thermal gravimetric curve of Figure V-15, it seems reasonable to characterize the sharp char boundary by a temperature of about 390°C, the temperature at which the peak heat effect and rate of weight loss occurs. Thus by locating the position of this sharp char front and by observation of the temperatures measured with thermocouples, it is possible to check the shape and magnitude of the computed temperature profile.

An initial computer run was made to check the predicted transient temperature distributions. It was evident that some adjustment was necessary in the values of the thermal conductivity used in the computation since the computed temperatures were about 15% too low in the uncharred region and appeared too high near the surface. Several computer runs were made to test the effect of different "effective" thermal conductivity vs temperature relations. This thermal conductivity vs temperature specification was adjusted until satisfactory agreement was obtained between the computed temperatures and thermocouple measurements and the temperature estimated at the sharp char front. The thermal conductivity vs temperature relation which gave satisfactory agreement is shown in Figure V-27. Figure V-28 shows the computed temperature profile in the

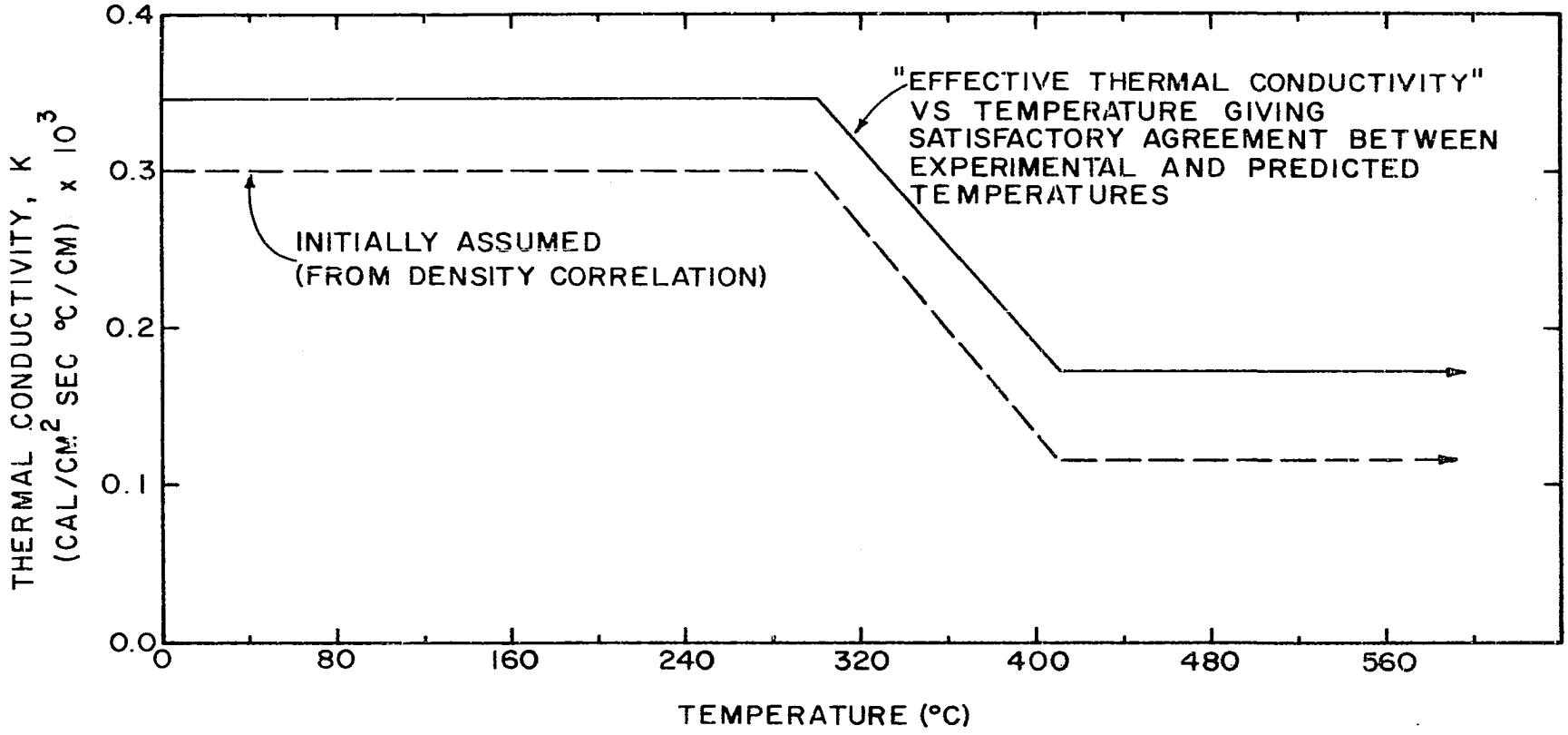


Figure V-27. Effective Thermal Conductivity vs Temperature Relationship Giving Satisfactory Agreement Between Predicted and Measured Temperatures.

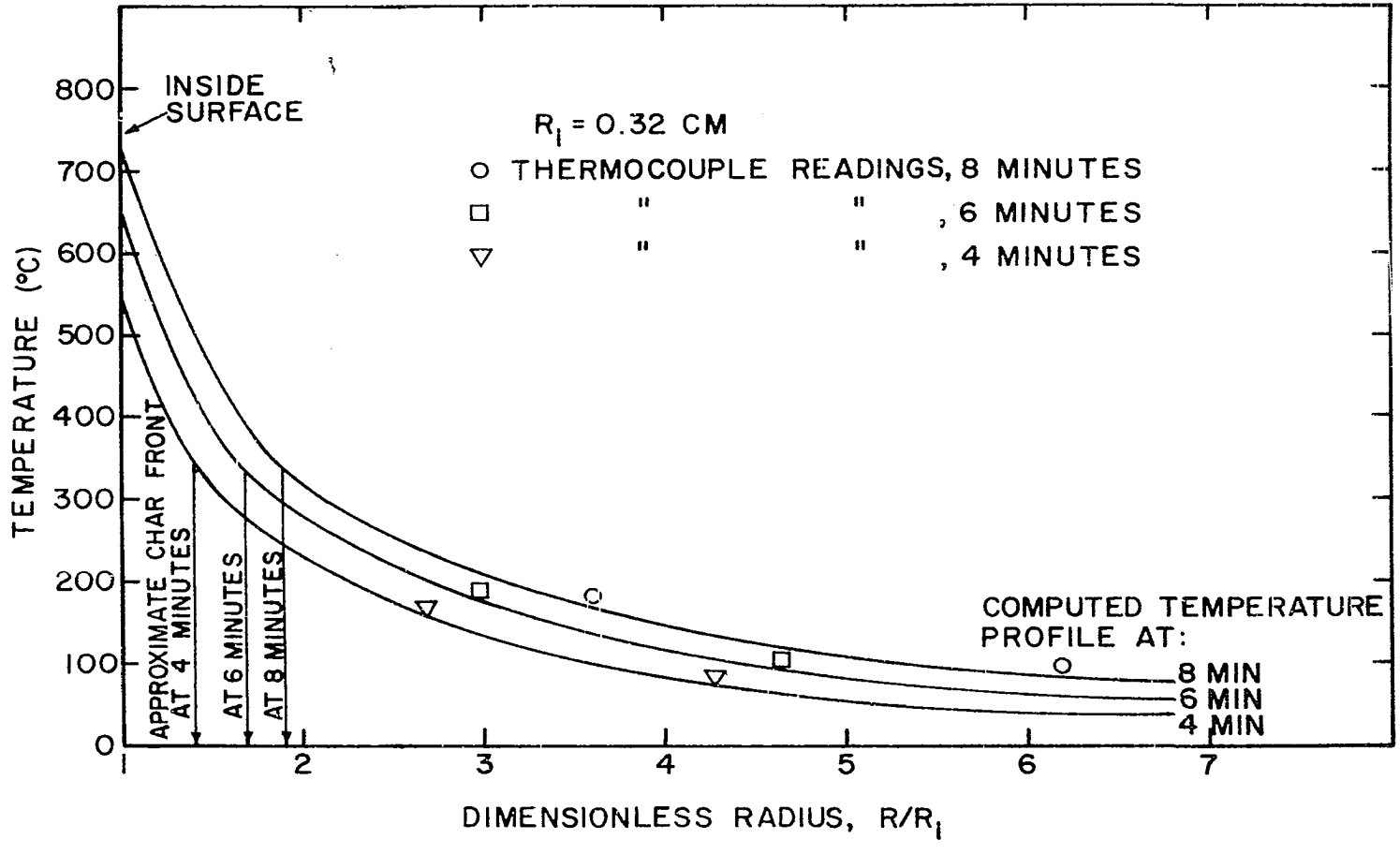


Figure V-28. Comparison of Predicted and Measured Temperature Profiles.

wood cylinder at t=4 minutes, 6 minutes, and 8 minutes compared with temperatures measured by the thermocouples and by specification of the location of the char front. Since the location of the char front is largely dependent on observation of degree of darkness, and since by prior experimentation it was determined that darkening begins at a temperature of about 250°C (when weight loss begins to become appreciable) it is thought that the temperature of the char front shown in Figure V-26 may have been as low as 350°C.

Figure V-29 shows the comparison of computed vs thermocouple measured temperatures at two radial positions as a function of time for the 8 minute run. Figure V-30 shows similar comparisons of results for a 6 minute heater run and Figure V-31 shows the same comparisons for a 4 minute run. Figure V-32 shows the predicted total weight loss of the test section vs time as compared with the weight loss measurements made at the ends of 8 minute, 6 minute, and 4 minute runs.

Reference to Figures V-29 through V-31 shows quite good agreement between predicted and observed temperatures for heating times up to about three minutes. For heating times greater than three minutes, the difference between predicted and observed temperatures becomes somewhat larger, although not excessive ($< 12\%$). As shown in Figures V-28 through V-31, the predicted temperatures at longer times

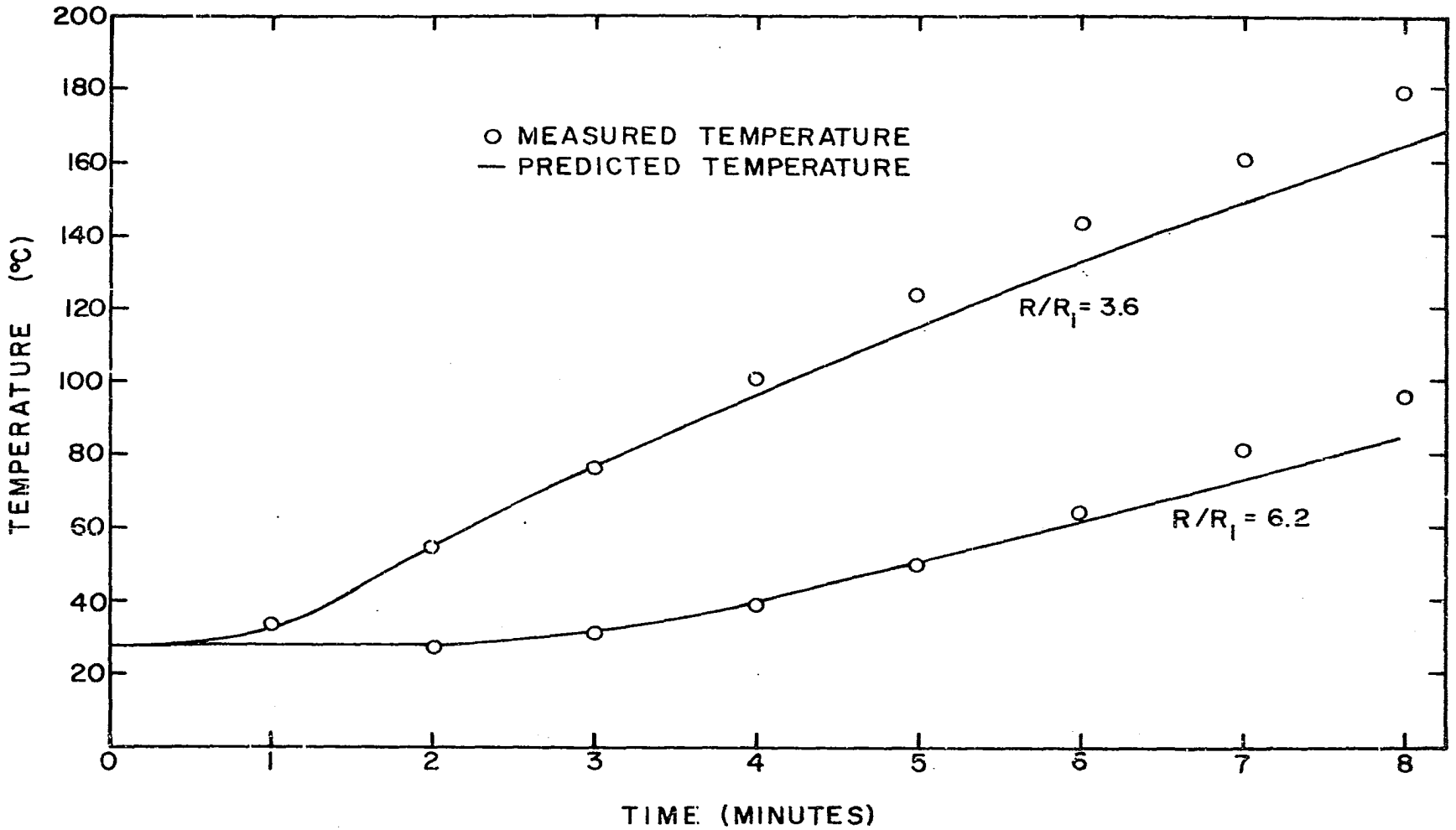


Figure V-29. Comparison of Measured and Predicted Temperature vs Time at Two Radial Positions for Eight Minute Run.

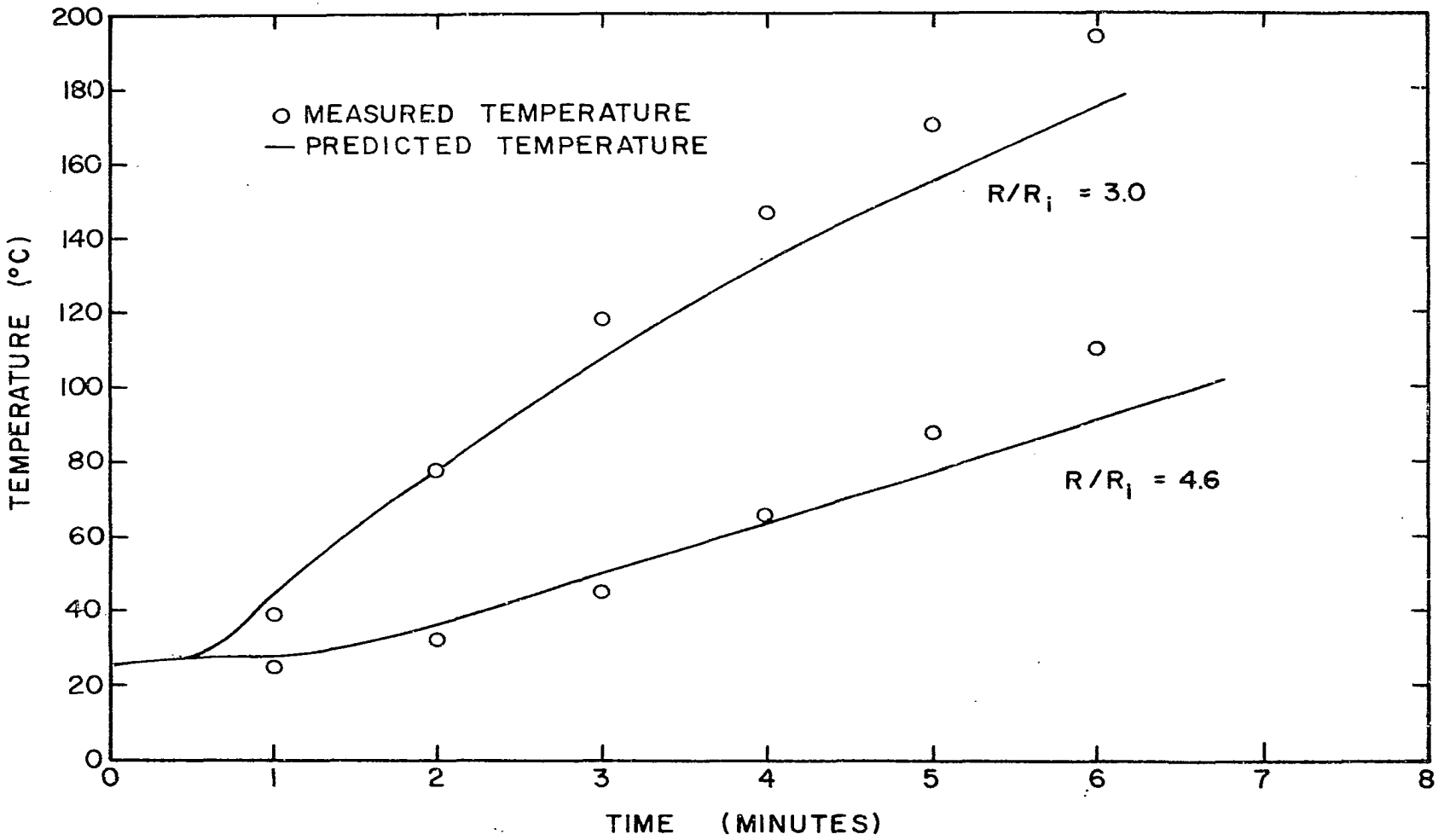


Figure V-30. Comparison of Measured and Predicted Temperature vs Time at Two Radial Positions for Six Minute Run.

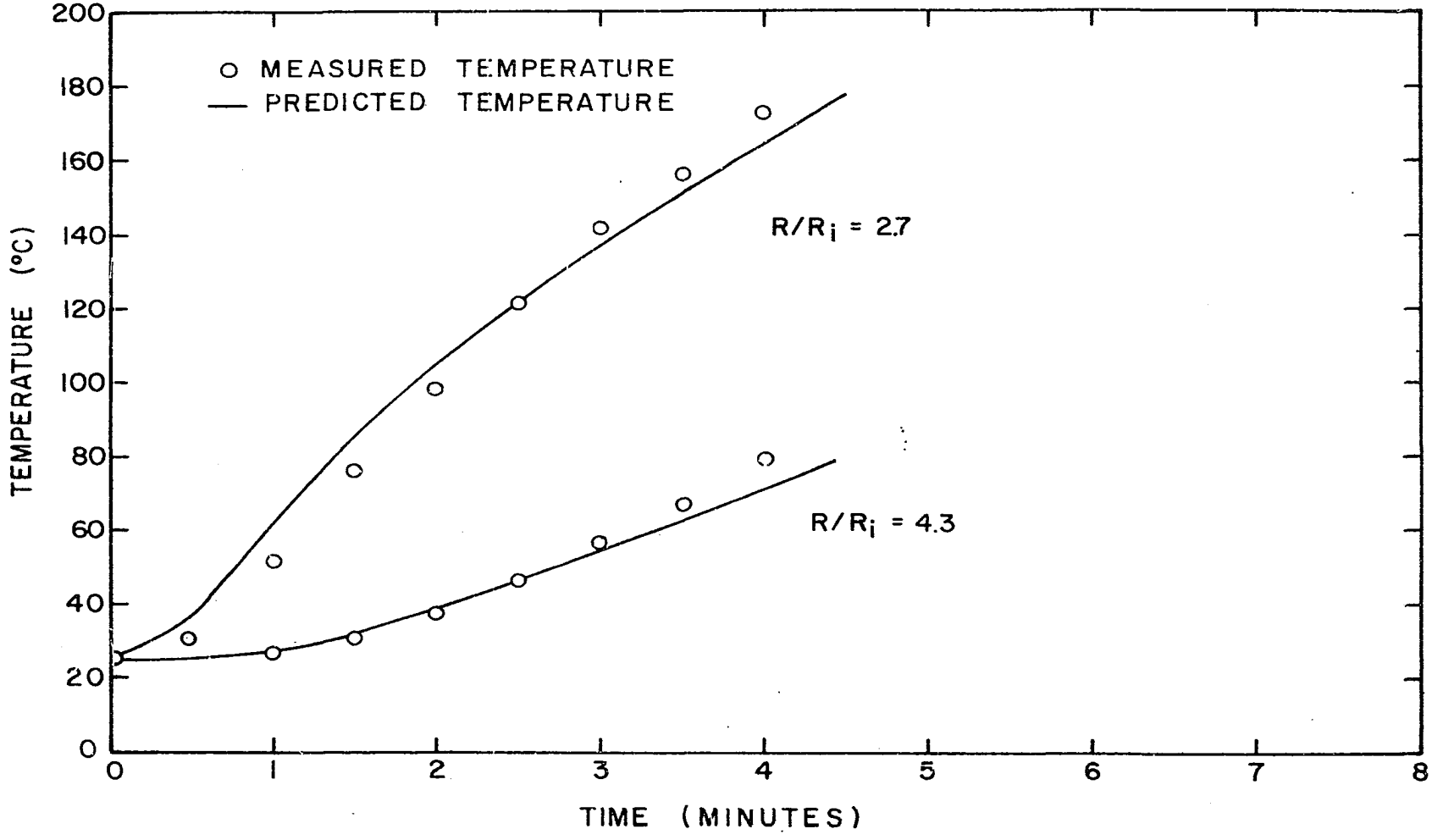


Figure V-31. Comparison of Measured and Predicted Temperature vs Time at Two Radial Positions for Four Minute Run.

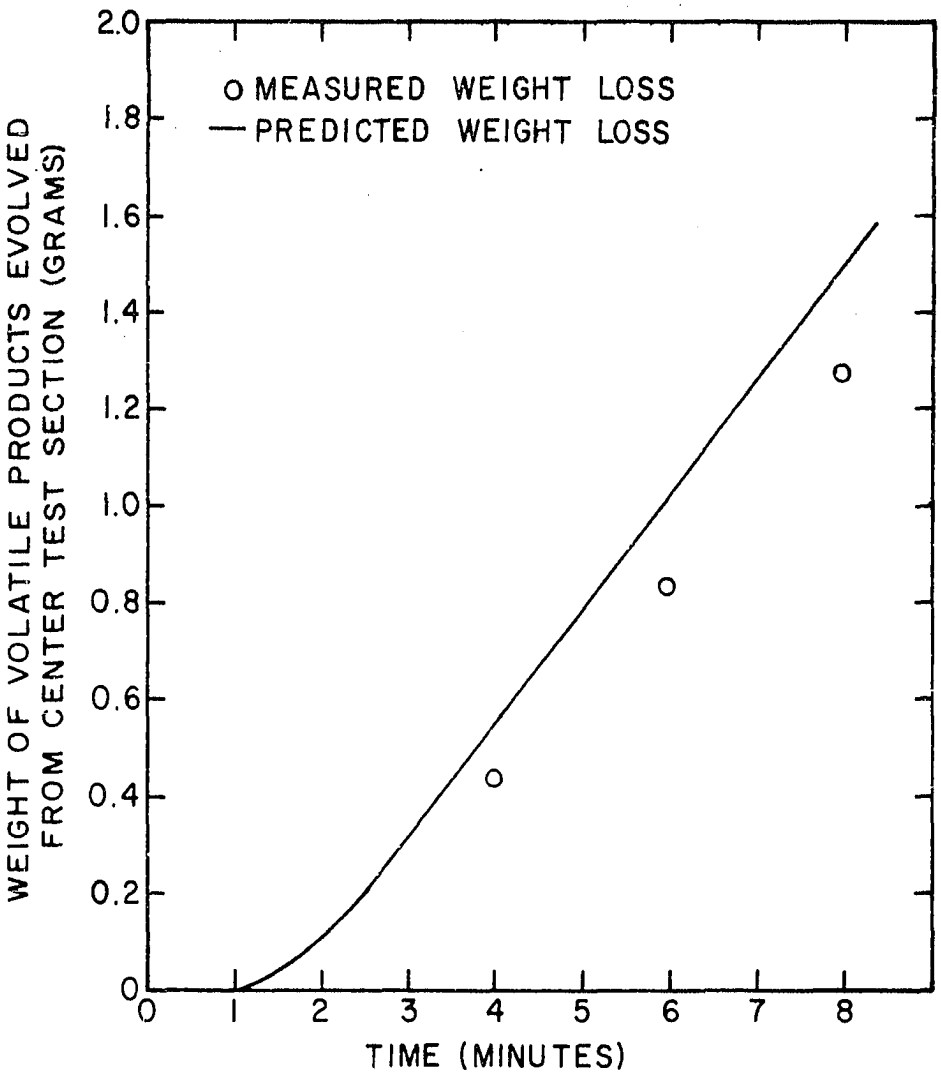


Figure V-32. Measured vs Predicted Weight Loss of Pine Test Section.

were in all cases lower than the observed values. However, considering experimental errors in specifying boundary conditions and in the thermocouple temperature measurements, and the limitations imposed by the model, the agreement is considered good.

The predicted mass losses were in all cases higher than the observed values ($\sim$15%), as shown in Figure V-32. It seems likely that this difference may be attributable to the neglect of time dependence of weight loss and this will be discussed in more detail in Chapter VI. However, the predicted mass losses are also considered to be satisfactory, within the limitations imposed by the model and experimental errors.

CHAPTER VI

DISCUSSION OF RESULTS

Since several of the approaches taken to the solution of this problem are thought to be original ones, there are relatively few direct comparisons which can be made between some of the results reported herein and results obtained by previous investigators.

To this author's knowledge, no previous attempts have been made to measure the "energy capacity" of a material, which includes both sensible energy and decomposition energy effects. Since both effects are lumped into the present measurement technique, it is necessary to separate them in order to allow comparison with results of previous investigators. Reference to Figure VI-1 indicates how the energy capacity curve for pine wood might reasonably be separated into a sensible heat component and a decomposition heat effect component. Thermogravimetric weight loss data (Figure V-10) indicates that weight loss (thus decomposition) of pine and oak wood is essentially zero at temperatures below 200°C, and can be considered complete at temperatures above about 430°C. Thus at temperatures below 200°C and above about

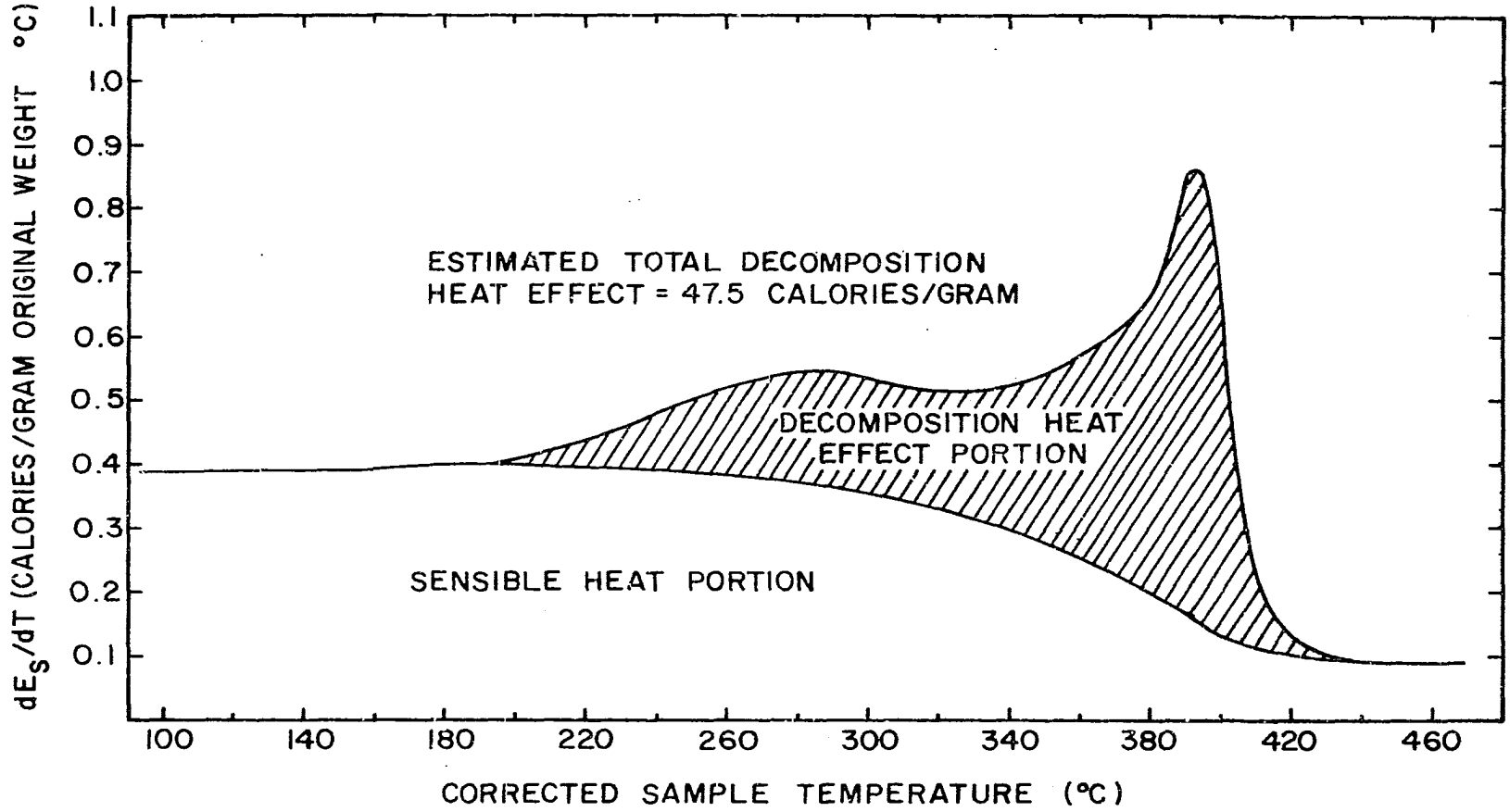


Figure VI-1. "Energy Capacity" of Pine Wood as a Function of Temperature in Nitrogen Atmosphere (Based on Original Non-Decomposed Sample Weight), Showing Sensible Heat and Decomposition Effect Regions.

430°C, the "energy capacity" as shown in Figure VI-1 is simply the sensible heat capacity of non-decomposing wood and wood char respectively. The energy capacity of non-decomposed wood is in good agreement with values reported in the literature. The energy capacity of the charred residue (above 430°C) based on its actual weight, is about 0.36 cal/gm°C. This value is in good agreement with values reported for the specific heat of charcoal at the same temperature by Widell (79) in Figure II-13. Note that the energy capacity, expressed on the basis of the original non-decomposed weight, levels off at a value of about 0.09 cal/gm°C, or about 23% of the energy capacity of the non-decomposed wood, at temperatures above 430°C. This result seems to be in excellent agreement with the fact that the weight of solid material remaining, as determined from the thermogravimetric data of Figure V-10, levels off at temperatures above about 430°C to approximately the same percentage of its original weight. By assuming the sensible heat portion of the energy capacity to be proportional to the amount of non-decomposed material left, the value of the energy capacity at 200°C can be multiplied by the per cent weight remaining at a given temperature to arrive at an estimate of the sensible heat portion as a function of temperature, as shown in Figure VI-1. By measuring the area of the energy capacity curve

lying above this sensible heat portion, one can estimate the amount of energy involved due to thermal decomposition. The shaded area in Figure VI-1 represents an endothermic heat sink due to wood pyrolysis of 47.5 cal/gm of original dry wood. This value is about half of the value (88 ± 3.6 cal/gm) reported by Tang (69) for α-cellulose and measured by means of a "standard" DTA technique. As discussed in the section on previous work, most other investigators have estimated the internal primary heat effect due to decomposition to be exothermic.

Further evidence substantiating the accuracy of the energy capacity curves can be seen by plotting the decomposition heat effect (as determined above) for pine vs temperature. The decomposition heat effect can be read directly from Figure VI-1 as the difference between the energy capacity curve and the estimated sensible heat curve. Figure VI-2 gives the results of such a plot, compared with data replotted from the differential thermal gravimetric curve of Figure V-15. Note that the curves begin at essentially the same temperature, have the same qualitative shape, end in the same temperature range, and show excellent agreement between the temperatures at which the peaks occur. Simultaneous (with respect to temperature) appearance of these two peaks simply means that the maximum rate of heat absorbtion by the decomposition process occurs at the maximum rate

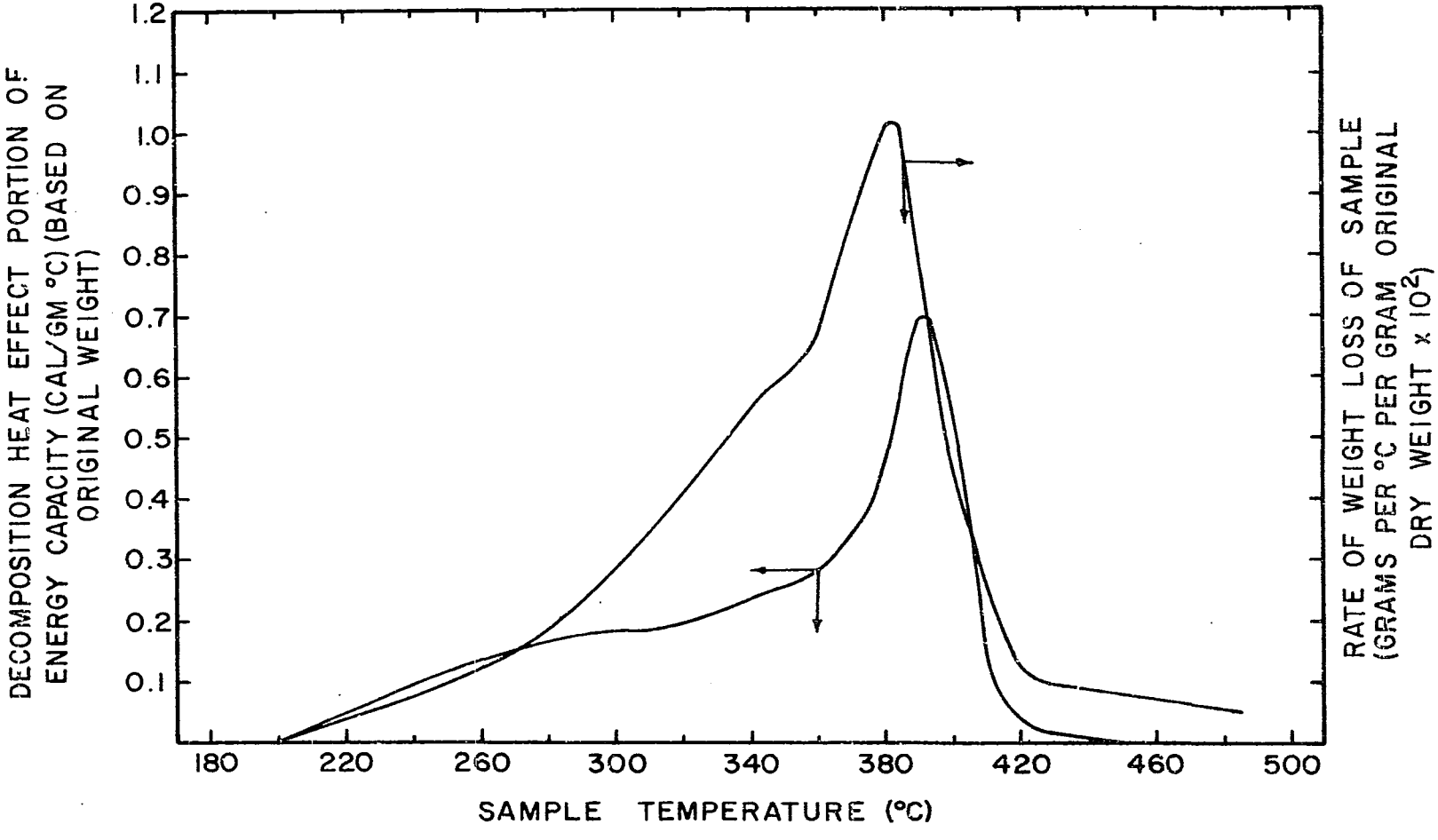


Figure VI-2. Comparison of Decomposition Heat Effect with Rate of Weight Loss of Pine Wood as a Function of Temperature.

of weight loss. Experimental agreement between the temperatures at which these two peaks occur, in spite of the fact that the two measurements are made by independent methods, is considered excellent evidence of the accuracy of temperature specification in both measurements. Note also that a constant ratio between the magnitudes of the two curves would indicate that the assumption of a constant heat absorption per unit weight of material decomposed is valid. Such a constant ratio is not strictly indicated; however, it is rather difficult to attach a great significance to this variance in view of the uncertainties in the measurement techniques arising from resolution capability and accuracy of the differentiation process by which the rate of weight loss curve is determined.

To this author's knowledge, this study is the first to present data which allows a check on the validity of the assumption of a constant decomposition heat effect per unit weight of wood decomposed. This assumption is of course a basic one in the models proposed by previous investigators. Since the volatile products which are formed at different temperatures would be expected to be different, the assumption of constancy of heat effect per unit weight evolved does not seem to be theoretically justified. However the results shown in Figure VI-2, in view of the uncertainties involved, indicate that such an assumption may be tenable. No such assumption is necessary,

of course, in the model used in this work.

It is interesting to note that the differences which were apparent between the energy capacity curves of oak and pine woods were also apparent in the weight loss and rate of weight loss curves. For example, the peak temperature in the oak energy capacity curve was about 12°C lower than that for the pine energy capacity curve. About the same difference was noted between peak temperatures in the rate of weight loss curves. Also, the DTG curve for oak showed a plateau in the rate of weight loss in the temperature range 300°C-340°C, the same temperature range in which the energy capacity curve indicates a temporary decrease. When the energy capacity curve for oak is divided into its sensible heat and decomposition heat effect regions in the same way as was done for pine, the result is shown in Figure VI-3. The shaded area represents an endothermic heat effect of 26.6 cal/gm. Figure VI-4 shows the comparison of the decomposition heat effect of oak with its rate of weight loss (DTG) vs temperature behavior, again indicating at least qualitative similarity.

The primary reason for making thermogravimetric weight loss measurements at different heating rates was to gain some insight into the importance of history dependence in the wood heating-decomposition process. It was postulated that this dependence could be studied

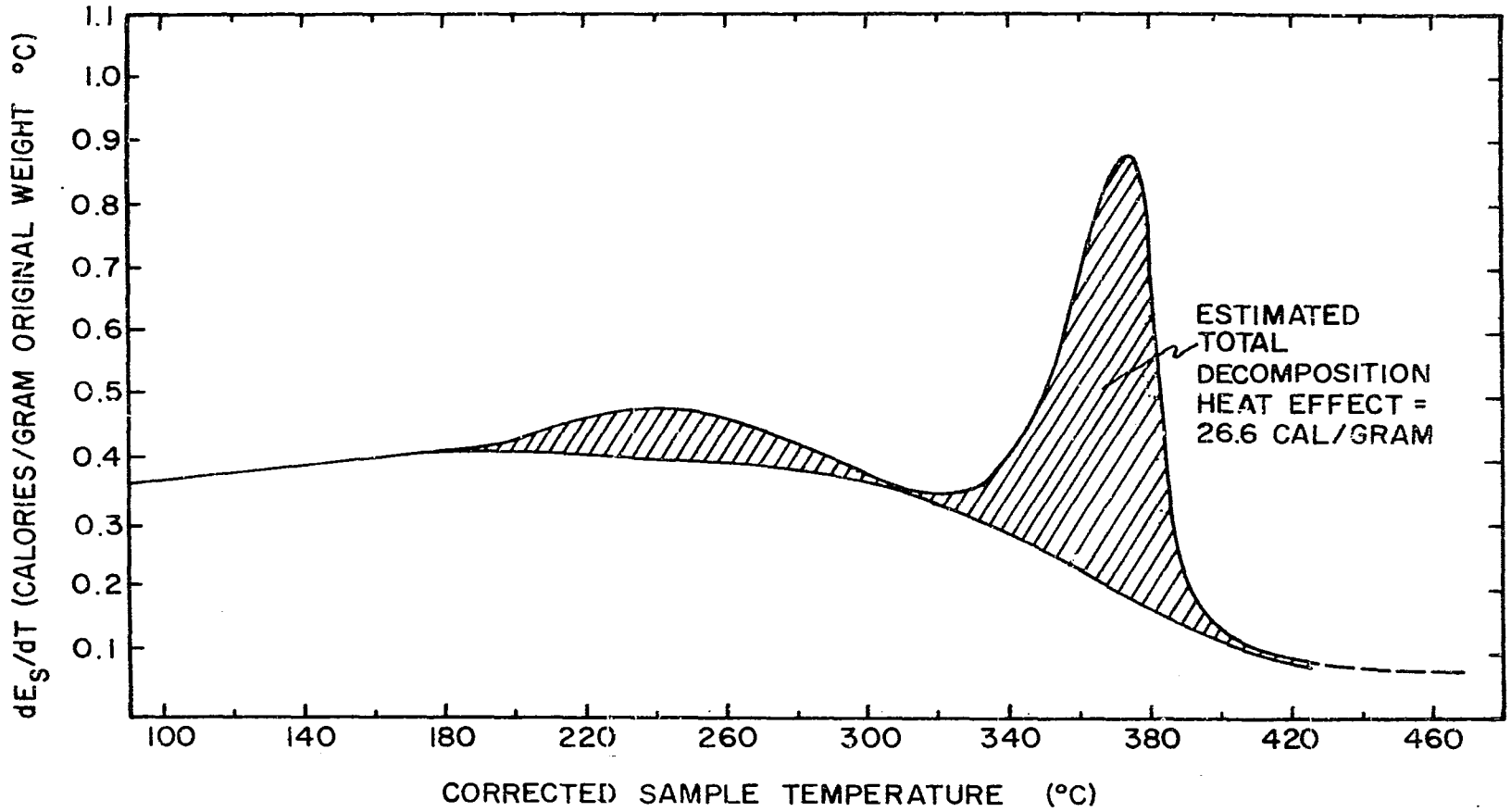


Figure VI-3. "Energy Capacity" of Oak Wood as a Function of Temperature in Nitrogen Atmosphere (Based on Original, Non-Decomposed Sample Weight), Showing Estimated Sensible Heat and Decomposition Heat Effect Regions.

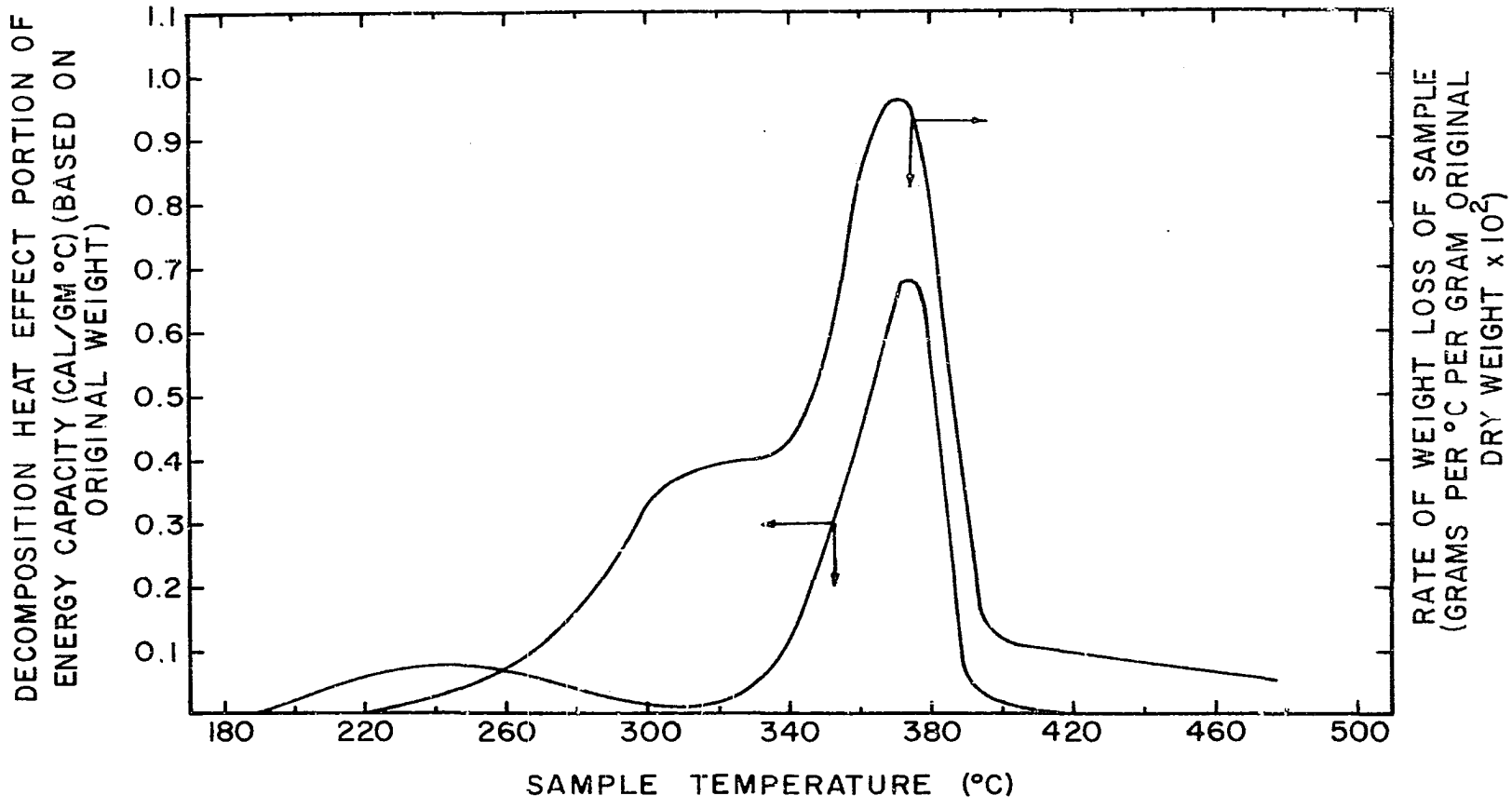


Figure VI-4. Comparison of Decomposition Heat Effect with Rate of Weight Loss of Oak Wood as a Function of Temperature.

by making weight loss measurements at different heating rates instead of making calorimetric measurements at different heating rates. Such a procedure is much simpler due to the considerable problems involved in calorimetric measurements at higher heating rates. The DSC-1B instrument has an upper scan speed limit of 80° C/, which itself is not considered practical by this author for measurements of the type made in this study. However, the thermogravimetric analysis equipment, which has a very high resolution capability and a temperature calibration procedure which allows independent temperature calibration at different heating rates, is ideally suited for such purposes.

As would be expected, the curves of weight loss vs temperature were shifted to the right at higher heating rates. However, in view of the fact that the difference in rates of heating was a factor of 8 (from 20°C to 160°C), the shift is not considered to be too important. There is also some uncertainty as to how much of this observed shift is due to measurement error. This uncertainty is apparent in the difference between the effects of rates of heating on pine vs oak wood. Figure V-14 seems to indicate less time dependence for oak than was observed for pine in Figure V-13 (i.e. less shift to the right at higher heating rates). Therefore some doubt remains as to the absolute magnitude of the shift observed. The

main uncertainty, which is characteristic of TGA measurements, is thought to be in the accuracy of temperature measurement. When one considers the magnitude of the thermal lags which were obtained at the higher heating rates, as indicated in the temperature calibration curves of Figure V-12, in conjunction with the differences in thermal properties between the wood samples and the metal magnetic temperature standards, there is some reason to suspect that some of the observed shift is due to experimental error.

The final value of weight remaining was decreased slightly in all cases at higher heating rates, in agreement with the experience of previous investigators.

In this author's opinion, the amount of shift observed is not large enough to negate the applicability of a model which does not include history dependence effects, at least in applications where the rates of heating are not greater than 160°C/min. In the experiments for model validation the maximum rates of heating, which occurred at the surface, were within this range.

Both the energy capacity data and thermal gravimetric weight loss data used in computations with the proposed model were measured at heating rates of 20°C/min. It seems desirable to use thermal gravimetric data which is determined at the same heating rate used for measurement of energy capacity for the following reason. Since

it is expected that higher heating rates result in a shift of both curves toward higher temperatures, such a simultaneous shift would serve to cancel out some of the error in predicted weight losses which might be expected to result from neglect of the effect of time dependence (rate of heating).

In summary, the agreement between data obtained from differential scanning calorimetry measurements and thermogravimetric and differential thermogravimetric analysis are in good agreement and indicate that no gross errors are present. The absolute accuracy of the energy capacity vs temperature relation is thought to be amply demonstrated in the substantial agreement obtained from the model validation experiments.

It was noted that to obtain good agreement between observed temperatures and temperatures computed with the proposed model, some adjustment was necessary in the values used for thermal conductivity. The final thermal conductivity vs temperature relation which gave reasonably accurate prediction of both transient temperature distributions and transient volatile product evolution rates was presented in Figure V-24.

Several observations can be made about this thermal conductivity-temperature relation. First, the thermal conductivity of uncharred wood, which gave good agreement between predicted and observed results, was a value of

0.00035 cal/cm^2 sec °C/cm, assumed to be constant over the temperature range from 25°C to 310°C. The value predicted for the thermal conductivity of wood at a temperature of about 40°C by McLean, for wood of this density, is 0.00030 cal/cm^2 sec °C/cm. Since one expects some increase in the thermal conductivity of wood with temperature (at least for temperatures below those at which decomposition results) an average value of 0.00035 cal/cm^2 sec °C/cm for temperatures below 310°C is a reasonable one, in good agreement with the available literature values at lower temperatures. As for the value of 0.00017 cal/cm^2 sec °C/cm for temperatures above 410°C, that is, for the totally charred region, there is no information available which allows an independent check on its accuracy. The difficulty in measuring the thermal conductivity of the charred region at the temperatures in question are considerable. First of all, in order to have any confidence in the measurements obtained in a thermal conductivity experiment for use in this problem measurements would have to be made on the charred material at the temperatures in question, that is above 400°C. Since at these temperatures, the material has lost almost 80% of its original weight, it has very little mechanical strength, and the preparation of specimens would be very difficult. Also, the results of these experiments indicate a rather large dimensional change in the char region. It can be seen in

Figure V-26 that cracks are apparent in the char region of the samples after cooling. These cracks are the result of shrinkage. However, it is believed that the shrinkage, and the resultant cracks, occurred as the sample was cooling, and not during the heating process.

Such shrinkage during heating apparently did not occur in the experiments made by Blackshear and Murty (8) on pressed cellulose cylinders. Reference to their measurements of density vs temperature by x-ray methods (see Chapter II, this thesis, for discussion) indicated densities at temperatures above 400°C (after completion of charring) which were about 25% of their original value. Since the results of previous investigators indicate that the per cent weight of cellulose remaining at temperatures above 400°C is also about 20 to 25%, Blackshear and Murty's results indicate that no shrinkage occurred during the heating-decomposition process.

Also, it is thought that the position of the char front would be affected by the formation of large cracks such as those shown in Figure V-23, if they were present during the heating process, since the radial symmetry of the resistance to heat flow would be altered. However, the char fronts appeared very symmetrical and in fact appeared to be exactly circular. (Incidentally, this fact is also offered as extremely good evidence that there is no difference between thermal conductivities in pine

wood in the radial and tangential transverse directions.)

In view of this crack formation, which is thought to be the result of cooling, one would have to char a sample and make a thermal conductivity measurement of the charred region before the sample was allowed to cool, if a meaningful conductivity measurement is to be obtained. The problems involved in designing an experiment which would allow such a procedure, although probably possible, are indeed formidable. Such experiments were not within the scope of the present work.

Several other observations should be made concerning the specification of an "effective" thermal conductivity of the char region during decomposition. The "effective" conductivity of the char region, when decomposition products are flowing through its interstices on their way to the surface, may be significantly different from its value when no gases fill the interstices. It is a generally accepted fact that the low thermal conductivity of any insulating material (such as wood, or charred wood) is due to the presence of an extremely large number of void spaces in the solid matrix. Thus the ability of heat to be conducted through these voids appears to be the controlling factor which determines the materials effective thermal conductivity rather than the thermal conductivity of the <u>solid</u> material. At room temperatures the thermal conductivity of pore spaces can

be considered negligible compared to solids but that may not be the case at all at high temperatures (33). At high temperatures, heat transfer across pore spaces may take place by convection, gas conduction, or thermal radiation.

Thus, the value of 0.00017 cal/cm^2 sec °C/cm for "effective" thermal conductivity at temperatures above 410°C, although higher than the value of 0.00011 cal/cm^2 sec °C/cm predicted by the conductivity density correlation, does not seem unreasonable since the original estimate did not include any effects due to temperature or the presence of gases in the char interstices. Both these effects would indicate an increase in the effective thermal conductivity. More accurate specification of the thermal conductivity than that used herein will have to be done by experiments designed to allow control of all of these factors which effect the conduction of heat in wood char at high temperatures.

Considering the uncertainty in extrapolation of the energy capacity to temperatures higher than 450°C, the neglect of time dependence of the decomposition process, and the assumption of constancy of sample dimensions during the decomposition process; the agreement between predicted and observed temperatures and weight losses is considered satisfactory.

CHAPTER VII

SUMMARY AND CONCLUSIONS

A differential scanning calorimetric technique, based on an approach used for measurement of specific heat of inert materials, has been applied to the measurement of the "energy capacity" of dry wood, which includes both sensible heat and decomposition heat effects. The results of these measurements show good agreement with previously available data for heat capacity of non-decomposed wood and completely charred wood residue. The decomposition heat effects, as evidenced in the energy capacity curves, show striking correlation with thermal gravimetric and differential thermal gravimetric data, also taken in this study.

Differential scanning calorimetry data on the thermal decomposition of dry pine and oak wood in an inert atmosphere of nitrogen show the net internal heat effect due to decomposition to be endothermic.

The history dependence, or time dependence, of the decomposition of pine and oak wood has been studied using dynamic thermal gravimetry. The thermal decomposition weight loss behavior as a function of temperature was studied at heating rates varying from 20 °C/min to 160 °C/min. The

results indicate, at least for the rates considered herein, that the time dependence may not be as great as has been suggested by previous investigators, and that for such rates, the application of a heat transfer-thermal decomposition model which neglects dependence on rate of heating is defensible.

A mathematical model, developed at this laboratory for computer solution of heat transfer problems involving change of phase heat effects, has been used in conjunction with the energy capacity data and thermal gravimetric weight loss data to predict the transient temperature distribution and volatile product evolution rates in an externally heated wood specimen. For use in the model, the thermal conductivity was expressed as a function of the local density. This local density was specified as a function of temperature by using thermal gravimetric weight loss data and assuming constancy of the sample's exterior dimensions during the heating-decomposition process. The present model includes primary decomposition heat effects but does not account for internal convective heat effects, history dependence of the decomposition process, or secondary pyrolytic effects.

The model was tested by comparison of predicted results with temperature and weight loss measurements made on a large wood specimen with an experimental technique specifically designed to allow accurate description of boundary conditions. The method utilizes a fast-response

electrical heating element positioned in an axial hole through a wood cylinder. The design allows for specification of a constant heat flux at the cylindrical specimen's inside surface, and it has operating characteristics which preclude diathermancy effects.

Although some adjustment was necessary in the thermal conductivity vs temperature relation used, to obtain agreement between predicted and measured temperatures and weight losses, the final thermal conductivity relations used were reasonable and in agreement with expected results. With such an "effective thermal conductivity" the model gave reasonable predictions of both temperature and weight loss data.

LITERATURE CITED

1. Akita, K., "Studies on the Mechanism of Ignition of Wood," Report of Fire Research Institute of Japan, No. 9 (1959), 1-44, 51-54, 77-83, 99-105.

2. Arseneau, D. F., "The Differential Thermal Analysis of Wood," Canadian Journal of Chemistry, 39 (1961), 1915-1919.

3. Bamford, C. H., J. Crank, and D. H. Malan, "The Combustion of Wood, Part 1," Proc. of Cambridge Phil. Soc., 42 (1946), 166.

4. Barrall, E. M. and L. B. Rogers, "Differential Thermal Analysis of Organic Compounds - The Effect of Diluting Agents," Analytical Chemistry, 34, No. 9 (Aug. 1962), 1106-1111.

5. Barrall, E. M. and L. B. Rogers,"Differential Thermal Analysis of Organic Compounds - Effect of Geometry and Operating Variables," ibid, 1101-1105.

6. Barshad, I., "Temperature and Heat of Reaction Calibration of the Differential Thermal Analysis Apparatus," American Mineralogist, 37 (1952), 667-694.

7. Berg, L. G., I. N. Lepeshkov, and N. B. Bodaleva, "Quantitative Analysis of Natural Salts by the Thermographic Method," Compt. Rend. Acad. Sci., S.S.S.R., 31 (1941), 577-580.

8. Blackshear, Perry L., Kanuary Murty, and Jay Matthews, "Some Research Pertaining to the Problem of Predicting the Burning Rate of Cellulosic Fuels," Tech. Rpt. No. 3, OCD contract No. OS-62-89 with University of Minnesota Institute of Technology, Minneapolis, Minn., (Aug. 30, 1965).

9. Boersma, S. L., "A Theory of Differential Thermal Analysis and New Methods of Measurement and Interpretation," Journal of the American Ceramic Society, 38, No. 8 (1955), 281-284.

10. Bowes, P. C., "Estimates of the Rate of Heat Evolution and Activation Energies for a Stage in the Ignition of Some Woods and Fibreboard," Fire Research Note No. 266/1956, Fire Research Station, Boreham Woods, Herts. (September, 1956).

11. Bowes, P. C. and S. E. Townsend, "Ignition of Combustible Dusts on Hot Surfaces," British Journal of Applied Physics, 13 (1962), 105.

12. Brenden, J. J., "Effect of Fire - Retardant and Other Inorganic Salts on Pyrolysis Products of Ponderosa Pine," Forest Products Journal, (February 1965), 69-72.

13. Broido, A., "Thermogravimetric and Differential Thermal Analysis of Potassium Bicarbonate Contaminated Cellulose," WSCI Paper No. 66-20, 1966 Spring Meeting, Western States Section, The Combustion Institute, Denver Research Institute (April 1966).

14. Browne, F. L. and J. J. Brenden, "Heat of Combustion of the Volatile Pyrolysis Products of Fire Retardant Treated Ponderosa Pine," U.S. Forest Service Research Paper No. FPL 19 (Dec. 1964).

15. Browne, F. L. and W. K. Tang, "Thermogravimetric and Differential Thermal Analysis of Wood and Wood Treated with Organic Salts During Pyrolysis," Fire Research Abstracts and Reviews, 4, No. 3.

16. Chung, Paul K. and M. L. Jackson, "Thermal Diffusivity of Low Conductivity Materials," Industrial and Engineering Chemistry, 46, No. 12 (1954), 2563-2566.

17. Coats, A. W. and J. P. Redfern, "Thermogravimetric Analysis - A Review," The Analyst, 88 (1963), 906-924.

18. Domansky, Radislov and Frantisek Rendos, "Zum Studium der Pyrolysis des Holzes and seiner Komponenten," Holz als Roh- und - Werkstoff, 20 (1962), 473-476.

19. Dunlap, Frederick, "The Specific Heat of Wood," U.S. Dept. of Agriculture, Forest Service Bulletin No. 110 (1912).

20. Eichner, H. W., "Basic Research on the Pyrolysis of Wood," Forest Products Journal (April 1962).

21. Eyraud, C., "Apparatus for Differential Heat Analysis," Compt. Rend., 238 (1954), 1511-1512.

22. Frank-Kamenetskii, D. A., Diffusion and Heat Exchange in Chemical Kinetics, Princeton University Press (1955).

23. Ginnings, D. C. and G. T. Furukawa, "Heat Capacity Standards for the Range 14 to 1200°K," Journal of the American Chemical Society, 75 (1953), 522-527.

24. Goos, A. W., "The Thermal Decomposition of Wood," Chapter 20 in Wood Chemistry, Vol. II, A.C.S. Nomograph Series No. 97, Second Edition, New York: Reinhold Publishing Company (1952).

25. Griffiths, Ezer and G. W. Kaye, "The Measurement of Thermal Conductivity," Proceedings of the Royal Society of London, Series A, 104 (1923), 71-98.

26. Hashemi, H. T., "Heat Conduction with Change of Phase," Ph. D. Dissertation, University of Oklahoma (1965).

27. Hauser, R. E., B. S. Thesis, N.Y. State College of Ceramics (1953).

28. Hawley, L. F., Chapter 19 in Wood Chemistry, Vol. II, A.C.S. Nomograph Series No. 97, Second Edition, New York, Reinhold Publishing Company (1952).

29. Heinrich, H. J. and B. Kaesche - Krisher, "Contributions to the Explanation of Self-Ignition of Wood," Brennstoff - Chemie, 43, No. 5, 142-148.

30. Iskhakov, Kh. A., "Thermogravimetric Investigations of Wood," Gidroliz i. Lesokhim, Prom 10 (8) (1957), 18-19.

31. Jakob, Max, Heat Transfer Vol 1, New York: John Wiley and Sons, Inc. (1949), 275-278.

32. Keylworth, R. and N. Christoph, "Constributions to the Study of Thermal Decomposition of Wood by Means of Differential Thermal Analysis," Deutscher Verband Fur Material Prufung (DVM), 2, No. 8 (20 Aug 1960), 281-288.

33. Kingery, W. D., Property Measurements at High Temperatures, New York: John Wiley and Sons, Inc. (1959).

34. Klason, Peter, "Theory of the Dry Distillation of Wood," I. Jour. Prakt. Chem., 90 (1914), 413-447.

35. Kollman, F., Technologie des Holzes und der Holzwerkstoffs, Vol. 1, Second Edition, Berlin: Julius Springer (1936).

36. Koohyar, Ameer, The Ignition of Wood by Flame Radiation, Ph.D. Dissertation, University of Oklahoma (1967).

37. Kracek, F. C., "The Polymorphism of Potassium Nitrate," Journal of Physical Chemistry, 34 (1930), 225-247.

38. Kronig, R. and Snoodijk, "Determination of Heats of Transformation in Ceramic Materials," Applied Science Research, A3 (1953), 27-30.

39. Kujiria, T. and T. Akahira, "Effect of Temperature on the Deterioration of Fibrous Insulating Materials," Scientific Papers of the Institute of Physical and Chemical Research (Tokyo), 2, 223-252.

40. Kulp, J. L. and A. F. Trites, "Differential Thermal Analysis of Natural Hydrous Ferric Oxides," American Mineralogist, 36 (1951), 23-24.

41. Lawrence, E. K., "Analytical Study of Flame Initiation," S. M. Thesis, Chemical Engineering MIT (1952).

42. Madersky, S. L., V. E. Hart, and S. Straus, "Pyrolysis of Cellulose in a Vacuum," Journal of Research NBS, 60 (1956), 343-54.

43. McAdams, W. H., Heat Transmission, New York: McGraw Hill (1954), 173-174.

44. Maclean, J. D., "Thermal Conductivity of Wood," Heating, Piping and Air Conditioning (July 1940), 459-464.

45. Maclean, J. D., "Rate of Disintegration of Wood Under Different Heating Conditions," American Wood Preserver's Association Proceedings, 47, (1951), 155-169.

46. McNaughton, G. C., "Ignition and Charring Temperature of Wood," Wood Products, 50, No. 2, 21-22.

47. Martin, S., "Thermal Radiation Damage to Cellulosic Materials - I - Wood," U.S. Naval Radiological Defense Laboratory R & D Technical Report USNRDL-TR-102-NS081-001 (10 Feb 1956).

48. Mitchell, R. L., R. M. Seborg, and M. A. Millett, "Effect of Heat on the Properties and Chemical Composition of Douglas Fir Wood and its Major Components," Journal of Forest Products Research Society, 3 (1953), 38-42, 72-73.

49. Morita, H. and H. M. Rice, Analytical Chemistry, 27 (1955), 336.

50. O'Neil, M. J., "The Analysis of a Temperature Controlled Scanning Calorimeter," Analytical Chemistry, 36, No. 7 (June 1964), 1233-1238.

51. Othmer, D. F. and W. F. Schurig, "Destructive Distillation of Maple Wood," Industrial and Engineering Chemistry, 33, No. 2 (1941), 188.

52. Richtmyer, R. D. and K. W. Morton, Difference Methods for Initial Value Problems, Second Edition, New York: Interscience Publishers (1967).

53. Roberts, A. F. and G. Clough, "Thermal Decomposition of Wood in an Inert Atmosphere," Fire Research Abstracts and Reviews, 4, No. 3, 177-179.

54. Rogers, R. N. and E. D. Morris, Jr., "Determination of Emissivities with a Differential Scanning Calorimeter," Analytical Chemistry, 38, No. 3 (March 1966), 410-412.

55. Rowley, F. B., "The Heat Conductivity of Wood at Climatic Temperature Differences," Transactions American Soc. of Heating and Ventilating Engineers, 39 (1933), 313-323.

56. Sabatier, I. G., "Measurement of the Heats of Transformation by Differential Thermal Analysis," Bull. Soc. Franc. Mineral, 77 (1954), 953-968.

57. Sandermann, W. and Hans Augustin, "Chemische Untersuchungen uber die Thermische Fersetzung of Holz Erste Metteilung: Stand der Forschung, Zwerte Metteilung: Unterschungen mit Hilfe der DTA," Holz als Roh - und - Werkstoff, 21 (1963), 305-315.

58. Schwiete, H. E. and G. Ziegler, "Theory and Application of Dynamic Difference Calorimetry," Ber. Deut. Keram. Ges., 35 (1958), 193-204.

59. Sergeeva, V. N. and A. Vaivads, "Thermographic Study of Pyrolysis of Wood and its Consituents," Latvijas PSR Finatnu Akad. Vestis, No. 9 (1954), 103.

60. Simms, D. L., "On the Pilot Ignition of Wood by Radiation," Combustion and Flame, 7 (1963), 253.

61. Smothers, W. J. and Yao Chiang, Handbook of Differential Thermal Analysis, New York: Chemical Publishing Company (1966).

62. Soule, J. L., "Quantitative Interpretation of Differential Thermal Analysis," Journal of Phys. Radium, 13 (1952), 516-520.

63. Speil, S., L. H. Berkelhamer, J. A. Pask, and B. Davis, U.S. Bureau of Mines Technical Papers, 664 (1945).

64. Squire, W. and C. Foster, "A Mathematical Study of the Mechanism of Wood Burning," NBS Contract CST-362 with Southwest Research Institute, Tech. Prog. Rpt. No. 1 (1961).

65. Stamm, Alfred J., "Thermal Degradation of Wood and Cellulose," Industrial and Engineering Chemistry, 48 (1956), 413-417.

66. Tang, W. K., "Effect of Inorganic Salts on Pyrolysis of Wood, Alpha-Cellulose, and Lignin," U.S. Forest Service Research Paper, FPL 71 (January 1967).

67. Tang, W. K., "Study of the Effect of Chemical Treatment on the Thermal Decomposition of Wood," Forest Products Laboratory Report (1960).

68. Tang, W. K., "The Effect of Inorganic Salts on Pyrolysis, Ignition, and Combustion of Wood, Alpha-Cellulose, and Lignin," Ph. D. Dissertation, University of Wisconsin (1964).

69. Tang, W. K., and W. K. Neill, "Effect of Flame Retardants on Pyrolysis and Combustion of α-Cellulose," Journal of Polymer Science: Part C, 6 (1964), 65-81.

70. Tsang, N. F., "Quantitative Differential Thermal Analysis," Chapter 5 in Handbook of Differential Thermal Analysis, New York: Chemical Publishing Company, Inc. (1966).

71. Thermal Analysis Newsletter, No. 3, Analytical Division Perkin-Elmer Corporation, Norwalk, Conn.

72. Tyulpanov, R. S., "Study and Estimation of Thermal Decomposition of Wood," Gidroliz i. Lesokhim, Prom 10 (6), (1957), 13-14

73. Vassallo, D. A. and J. C. Harden, "Precise Phase Transition Measurements of Organic Materials by Differential Thermal Analysis," Analytical Chemistry, 34 (1962), 132.

74. Vold, M. J., Analytical Chemistry, 21 (1949), 683.

75. Waangard, F. F., "Transverse Heat Conductivity of Wood," Heating, Piping, and Air Conditioning (July 1940, 459-464.

76. Waangard, F. F., "The Transverse Heat Conductivity of Wood," Ph. D. Thesis, New York State College of Forestry (1939).

77. Weatherford, W. D. Jr., D. M. Sheppard, and M. L. Valtierra, "An Experimental and Mathematical Study of the Mechanism of Wood Ignition," NBS Contract CST-1102 with Southwest Research Institute, Final Report (November 1965).

78. Wendlandt, Wesley W., Thermal Methods of Analysis, New York: Interscience Publishers, a Division of John Wiley and Sons (1964).

79. Widell, Torsten, "Thermal Investigations into Carbonization of Wood," Acta Polytechnica, Chemical and Metallurgical Series, 1, No. 6 (1949), 35.

80. Williams, C. C., "Damage Initiation in Organic Materials Exposed to High Intensity Thermal Radiation," Sc. D. Thesis, Chemical Engineering, MIT (1953).

81. Wittels, Mark, "The Differential Thermal Analyzer as a Microcalorimeter," American Mineralogist, 36 (1951), 615.

82. Wright, R. H. and A. M. Hayward, "Kinetics of the Thermal Decomposition of Wood," Canadian Journal of Technology, 29, No. 12 (Dec. 1951), 503-510.